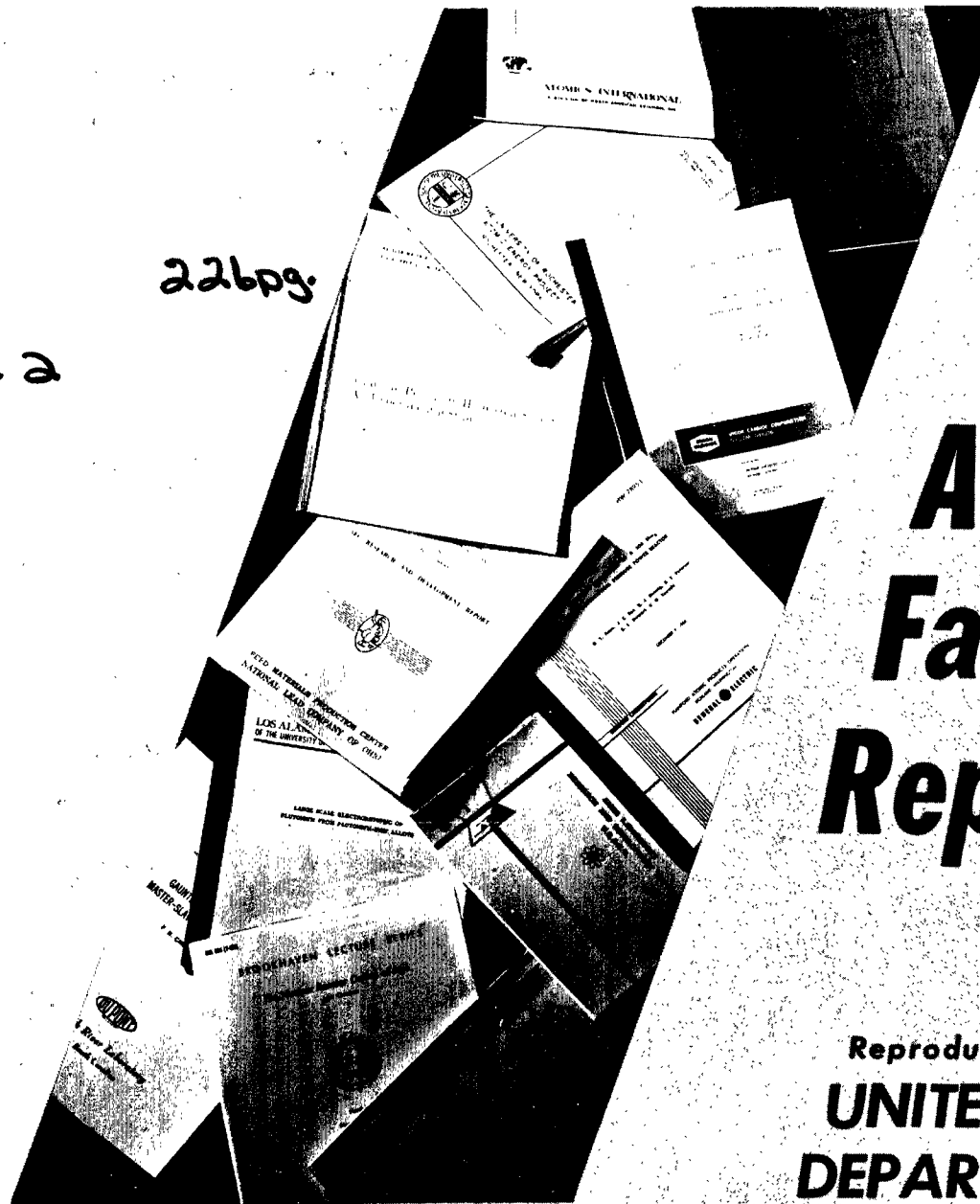


N40-4645 Del. 2

226pg.

39820



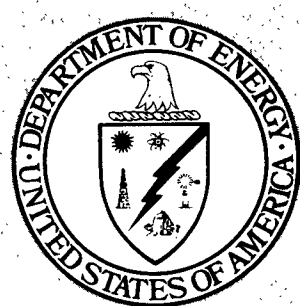
A Facsimile Report

Reproduced by

**UNITED STATES
DEPARTMENT OF ENERGY**

Technical Information Center

P. O. Box 62 Oak Ridge, TN 37830



	<u>CONTENTS</u>	Page
ACKNOWLEDGEMENTS		iv
ILLUSTRATIONS		v
ABSTRACT		vi
CHAPTER 1 INTRODUCTION		1
CHAPTER 2 CASTLE TESTS		5
2.1 Bravo		6
2.2 Romeo		9
2.3 Koon		11
2.4 Union		12
2.5 Yankee		12
2.6 Nectar		15
CHAPTER 3 WORLD-WIDE FALLOUT		19
3.1 Castle Total		19
3.2 Totals for Individual Tests		19
3.3 Comparison With Total Beta Yield		23
3.4 Meteorological Interpretation		33
3.5 Maximum Activity at Individual Stations		34
CHAPTER 4 SPECIAL OBSERVATIONS		38
APPENDIX A MAPS OF DAILY FALLOUT		39
REFERENCES		228

ACKNOWLEDGEMENTS

The work reported on here was performed under the direction of Dr. Lester Machta, Chief, Special Projects Section, Scientific Services Division, U. S. Weather Bureau. The monitoring program was established by the Health and Safety Laboratory, New York Operations Office, Atomic Energy Commission, Merril Eisenbud, Director, and that office provided the radiological data. Mr. Daniel E. Lynch of the Health and Safety Laboratory served as coordinator of the program.

Many helpful suggestions were received from colleagues in the Special Projects Section, D. Lee Harris, Kenneth M. Nagler, Francis Pooler, Jr., and Leo R. Quenneville. The staff of this section performed the laborious and painstaking plotting of data and preparation of the finished manuscript.

ILLUSTRATIONS

	Page
1.1 Fallout Monitoring Network, Pacific Hemisphere	2
1.2 Fallout Monitoring Network, Atlantic Hemisphere.	3
2.1 Winds Aloft for Castle Events.	7
2.2 Meteorological Trajectories for Burst No. 1, Bravo	8
2.3 Meteorological Trajectories for Burst No. 2, Romeo	10
2.4 Meteorological Trajectories for Burst No. 3, Koon.	13
2.5 Meteorological Trajectories for Burst No. 4, Union	14
2.6 Meteorological Trajectories for Burst No. 5, Yankee. . . .	16
2.7 Meteorological Trajectories for Burst No. 6, Nectar. . . .	17
3.1 Total Fallout From Castle Series as of July 1, 1954, Pacific Hemisphere .	20
3.2 Total Fallout From Castle Series as of July 1, 1954, Atlantic Hemisphere.	21
3.3 Total Fallout From Bravo, Pacific Hemisphere	24
3.4 Total Fallout From Bravo, Atlantic Hemisphere.	25
3.5 Total Fallout From Romeo. Pacific Hemisphere	26
3.6 Total Fallout From Romeo, Atlantic Hemisphere.	27
3.7 Total Fallout From Union, Pacific Hemisphere	28
3.8 Total Fallout From Union, Atlantic Hemisphere.	29
3.9 Total Fallout From Yankees, Pacific Hemisphere.	30
3.10 Total Fallout From Yankee, Atlantic Hemisphere	31
3.11 Total Fallout From Nectar.	32
3.12 Maximum Activity on Sampling Day at Individual Stations, Pacific Hemisphere .	36
3.13 Maximum Activity on Sampling Day at Individual Stations, Atlantic Hemisphere.	37
A.1 - A.186 Radioactive Fallout in the 24-hour Periods Begin- ning February 28 - May 31, 1954.	40-225
A.187 - A.188 Average Daily Fallout During Month of June, 1954. .	226-227

ABSTRACT

A world-wide network of gummed film stations was established to monitor fallout following Operation Castle. Although meteorological data were poor, a general connection of tropospheric flow patterns with observed fallout was evident. There was a tendency for debris to remain in tropical latitudes, with incursions into the temperate regions associated with meteorological disturbances of the predominantly zonal flow. As the season advanced, such incursions became more evident. Outside of the tropics, the southwestern United States received the greatest total fallout, about five times that received in Japan.

The maximum fallout on any day at an individual station in the United States, corrected to sampling day, was 200,000 d/m².

It is concluded that the probability of early fallout in inhabited regions would be reduced by holding Pacific test series in the winter months.

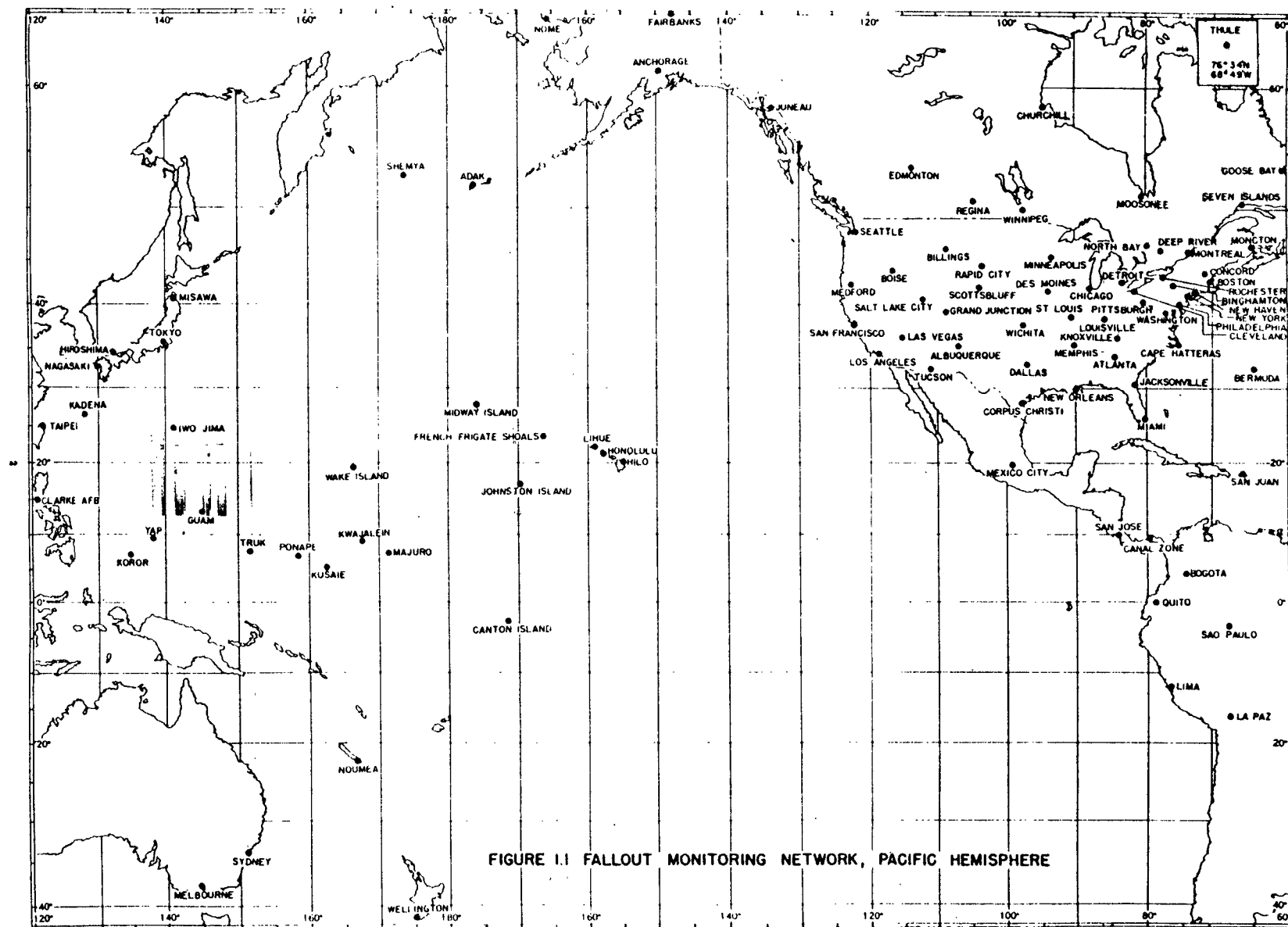
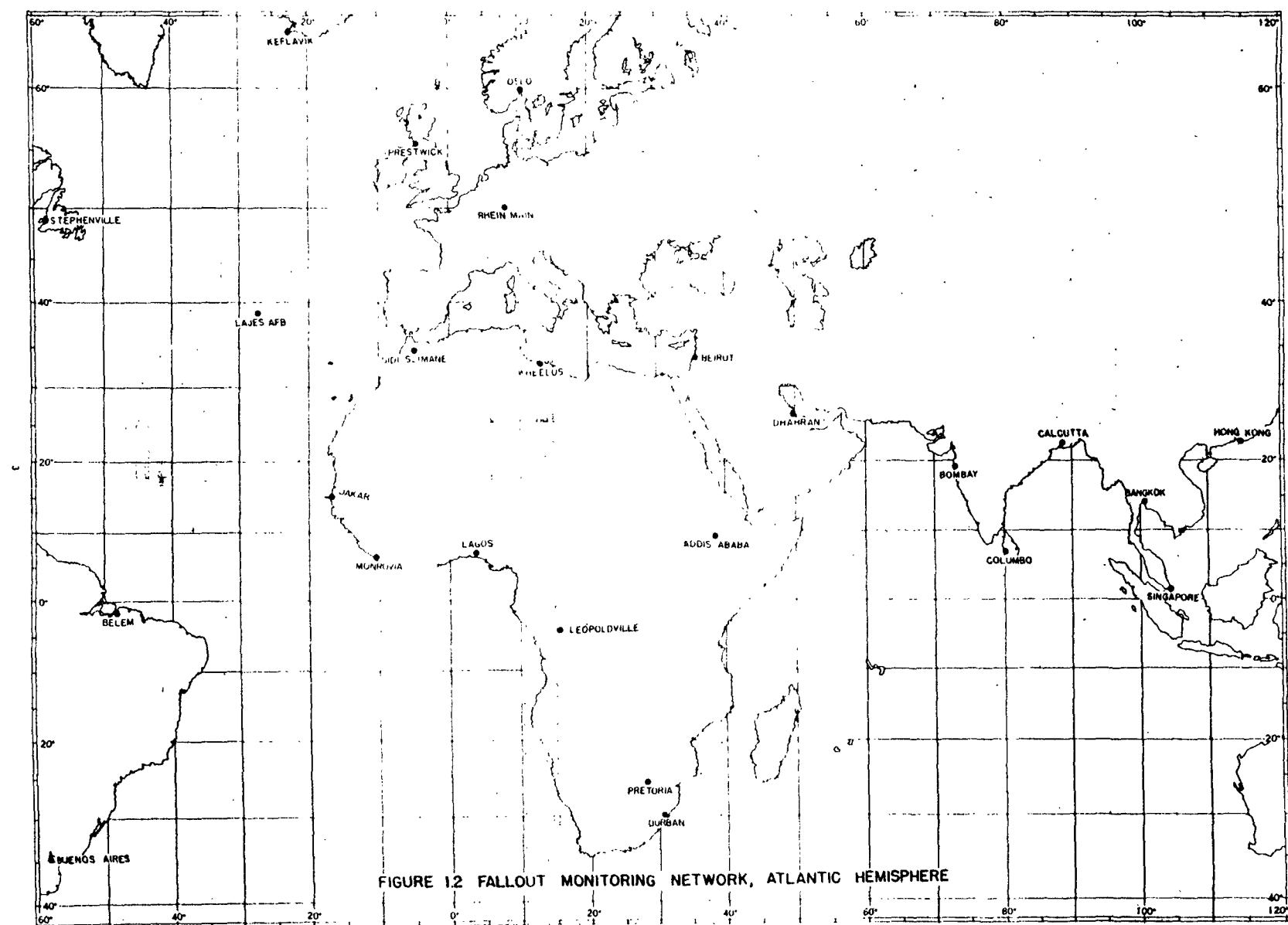


FIGURE 1.1 FALLOUT MONITORING NETWORK, PACIFIC HEMISPHERE



indications that the arbitrary system was in error, the activity was reassigned to the appropriate burst. In the case of observations in the Pacific and adjoining regions, it was usually possible to determine the burst responsible for the activity from an examination of the trajectories of the debris in conjunction with observed increases in radioactivity. Elsewhere in the world, it was ordinarily necessary to use the arbitrarily assigned burst. All maps of daily fallout values indicate the burst assignment used in computing the decay correction. Unless otherwise indicated, all radioactivity is reported in units of disintegrations per minute per square foot of gummed film, decayed to 100 days after the day of the burst. The $t^{-1.2}$ law for the decay of fission product activity has been used throughout.

The maps of daily fallout include only the data from the land stations, since there is considerable uncertainty in the ship data. The locations of the ships were imperfectly known and the procedures for avoiding cross-contamination of samples in handling and mailing, particularly on ships exposed to heavy fallout at some time during their voyage, were not adequate. The ship data were utilized in the drawing of isolines of activity on the fallout maps and in the interpretation of the land station data.

CHAPTER 2

CASTLE TESTS

The bursts of the Castle series are given in Table 2.1.

Table 2.1. Castle Test Series

Burst No.	Code name	Date 1954	Time GCT	Yield Total (MT)
1	Bravo	Feb. 28	1845	15
2	Romeo	Mar. 26	1830	
3	Koon	Apr. 6	1820	
4	Union	Apr. 25	1810	
5	Yankee	May 4	1810	
6	Nectar	May 13	1820	

The first burst was detonated on Bikini Atoll, the succeeding four from barges in the Bikini lagoon and the last on Enewetak Atoll.

most of the radioactive clouds created in the Castle series extended to very great heights, and the greater part of the cloud in levels beyond the reach of routine meteorological observations. For this reason, it has been impossible to prepare adequate meteorological trajectories to determine the path of the debris at various levels. The network of upper air observing stations in the tropics is extremely sparse at best, and wind reports at levels above 40,000 feet are virtually nonexistent, with the exception of a few from stations in the Marshall Islands and adjacent areas established especially for this test series. Even at these stations, the highest observations rarely extend above 100,000 ft.

The meteorological trajectories for the various bursts cannot, therefore, be computed at levels above 40,000 ft. and are doubtful even at lower levels. All trajectories given in this report were computed by personnel of the Air Weather Service (SUPA Branch) and are prepared for the 850-mb. (5,000-ft.), 700-mb. (10,000-ft.), 500-mb. (18,000-ft.), 300-mb. (30,000-ft.), and 200-mb. (40,000-ft.), levels only.

The temperature soundings for all of the Castle bursts were very similar in their major features. There were no pronounced inversions in the lower layers (except for an inversion at about 7,000 feet during Romeo). The air was quite moist up to about 5,000 feet, and somewhat drier above, with fairly steep lapse rates in the upper troposphere. The tropopause was between 48,000 and 54,000 feet with very stable lapse rates in the lower stratosphere above. The winds obtained from observations made at or near each of the shots are shown in Figure 2.1.

2.1 BRAVO

The first burst of the Castle series, Bravo, was detonated from a coral reef in Bikini Atoll on 1845 GCT, February 28, 1954. The resulting cloud of radioactive debris reached to ~~feet~~ feet.

The tropopause at this time was at about 54,000 feet,

The low-level easterly trades extended to about 6,000 feet, with light westerly winds increasing with altitude to a maximum of about 40 knots at 35-40,000 feet, extending to the base of the stratosphere. Easterly winds prevailed throughout the stratosphere to the highest altitude reached by the meteorological observations, about 100,000 feet. Winds at this level were easterly at about 50 knots.

Trajectories of the lower parts of the cloud are shown in Figure 2.2, but unfortunately, no trajectories can be constructed for the higher levels. Available evidence to about 100,000 feet (observations in the Marshalls and at Guam) indicates general easterly winds in the lower stratosphere, so that this portion of the cloud moved toward the Phillipines. No observations to indicate the movement of the cloud above 100,000 feet are available. However, it is likely that easterly winds prevailed at these levels.

The daily fallout maps for the period following the Bravo test are particularly interesting in that the background of fission product activity from previous tests was negligible and the succeeding burst did not occur until 26 days later, so that the progression of areas of fallout from day to day is more easily seen.

SECRET

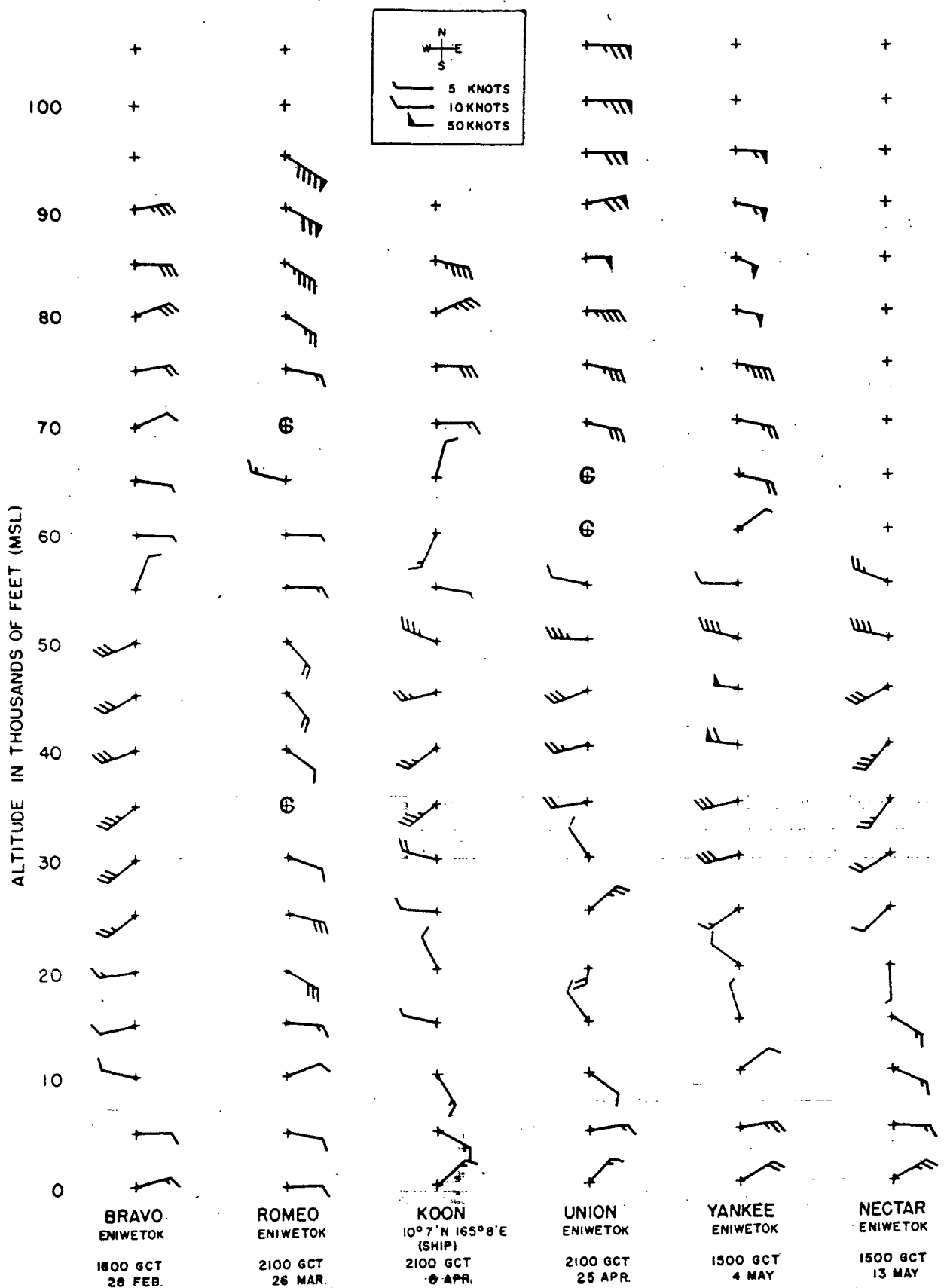


FIGURE 2.1 WINDS ALOFT FOR CASTLE EVENTS

~~SECRET~~

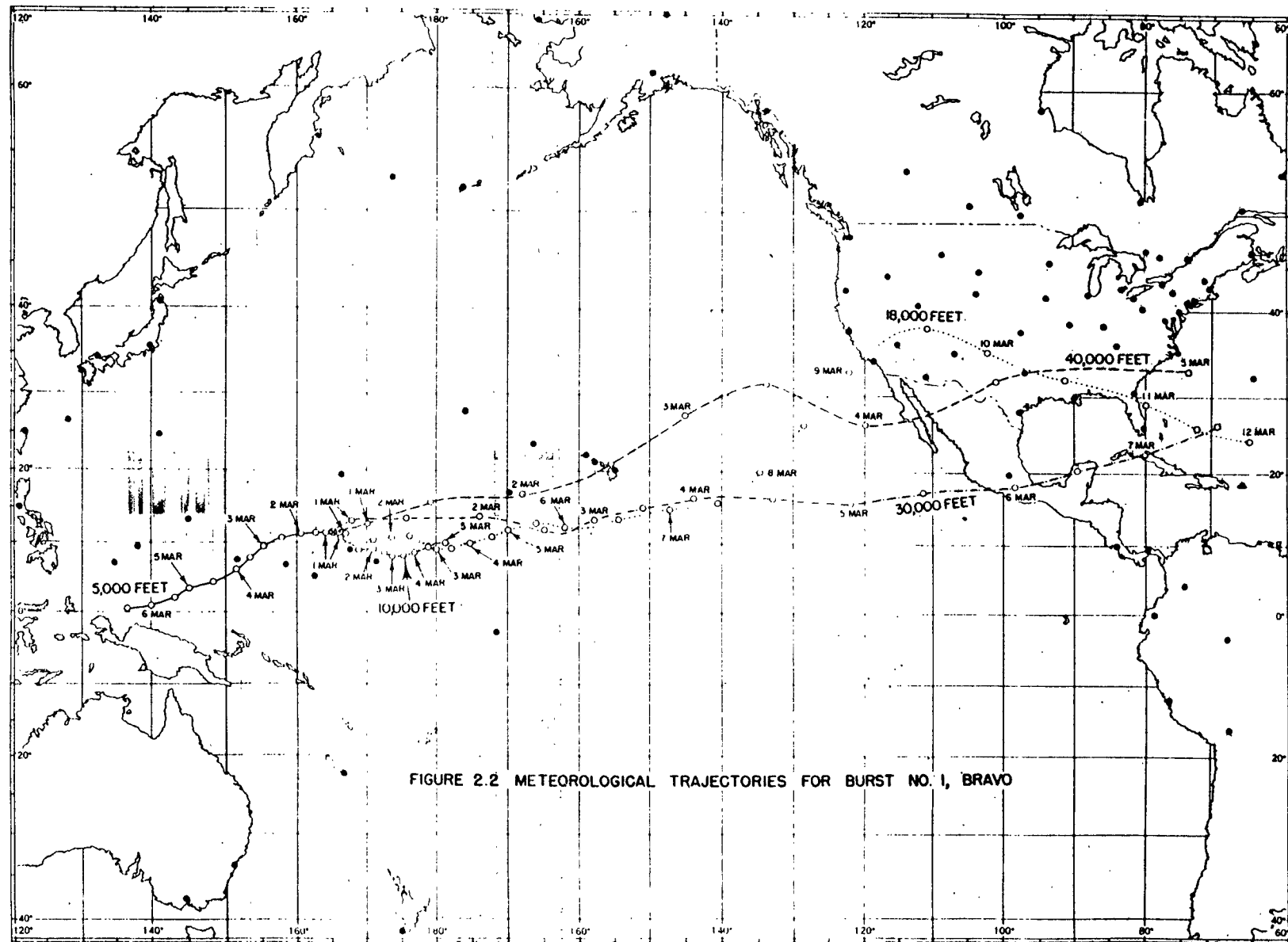


FIGURE 2.2 METEOROLOGICAL TRAJECTORIES FOR BURST NO. 1, BRAVO

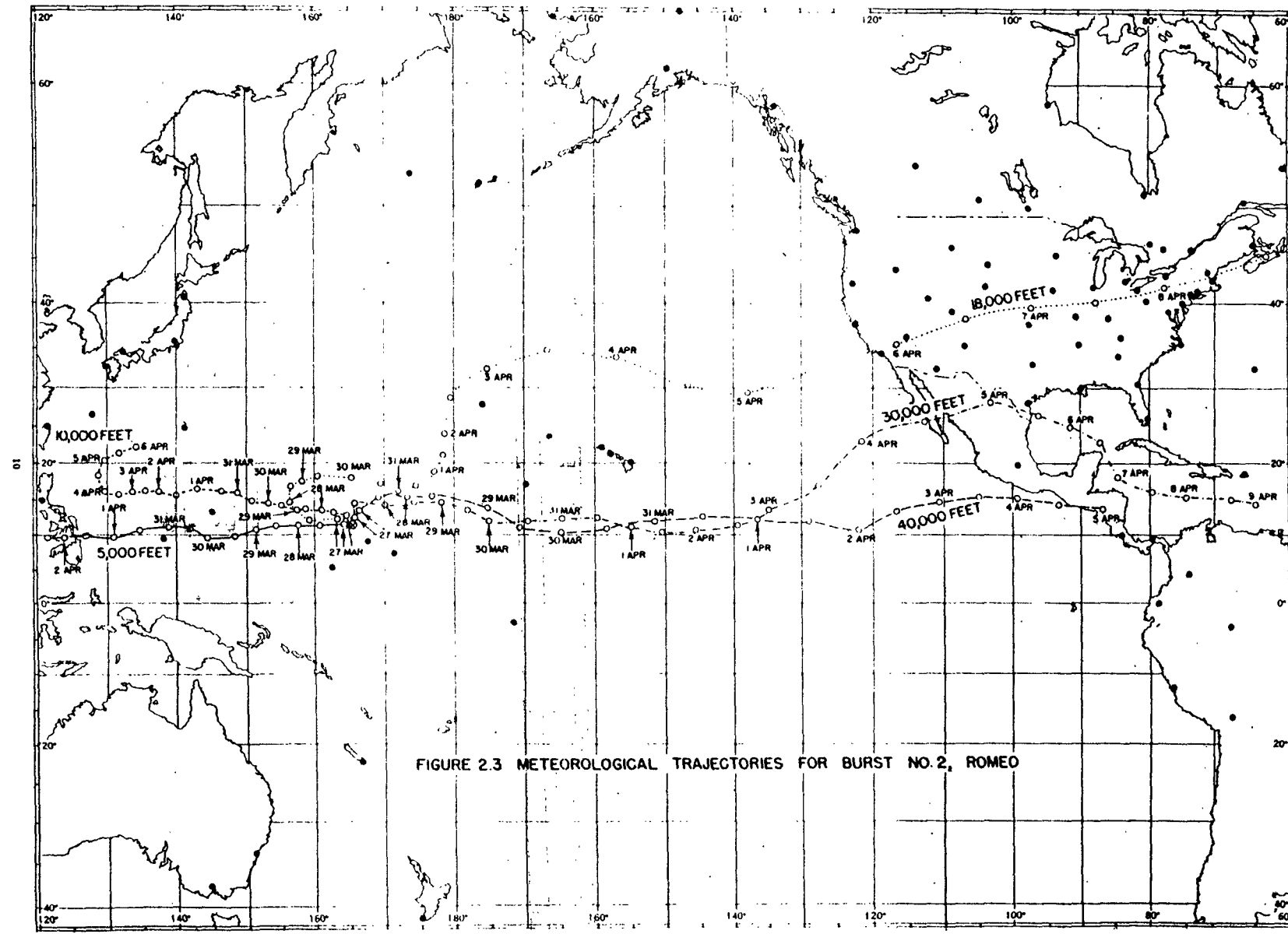
The eastward moving debris reached the Americas on March 7 and 8, indicating an average west wind of about 40 knots, in good agreement with the few wind observations available in the upper troposphere. Although the progression of debris to the west appears to be in good agreement with the 5,000-foot trajectory, indicating that the transport occurred in the trade wind layers, it is entirely possible that stratospheric debris moving with the upper level easterlies contributed to this fallout also.

The most striking fact which emerges from a study of the fallout in the period following the Bravo test is the tendency for the debris to remain in the tropical latitudes. By far the largest amounts of fallout occurred in the latitude band from 10°S to 20°N, with occasional excursions into the more temperate latitudes of each hemisphere, particularly in the Americas. An example of this can be seen in the southwestern United States in the period beginning March 15. At this time, a deep low pressure system extending through most of the troposphere was located just off the west coast, with strong southwesterly winds over the southwestern states. This depression moved slowly eastward so that by March 18th, the southwesterly winds were over the Mississippi Valley. An examination of the fallout maps reveals that fallout during this period was associated with the southwesterly winds, which carried debris from the tropical regions. It is significant that this fallout was independent of precipitation. The highest fallout values occurred during the first three days of the period when there was no precipitation, and even on the 18th, when there were several stations reporting precipitation, the fallout occurred in the region dominated by the southwesterly winds and was not closely associated with the existence of precipitation. A somewhat similar series of events occurred in the period March 21-25, although precipitation was more widespread in this case and may have had more influence on the observed fallout patterns.

2.2 Romeo

The second burst of the Castle series, Romeo,
was detonated
from a barge at 1830 GCT, March 26, 1951.

The wind observations associated with this burst showed light easterly winds at virtually all levels increasing in speed above 80,000 feet to a maximum of 92 knots from the SE at the top of the highest observation, 95,000 feet. Although the trajectories (Figure 2.3) at all levels in the troposphere moved westward initially, the 30,000- and 40,000-foot trajectories curved northward



and then eastward within a very short time. The lowest levels continued westward and the 18,000-foot trajectory appeared to curve back towards the United States on the 28th, although the meteorological data is uncertain. Winds in the stratosphere up to the level of the top of the cloud were probably from the east, carrying most of the mushroom westward.

Although almost a month elapsed between the first and second bursts of the Castle series, enough debris from the first burst was present to seriously interfere with attempts to trace the progress of the second cloud by an examination of fallout data. For example, an increase in deposited activity occurred at some stations in Central and South America on March 31 and April 1, several days before the meteorological trajectories would indicate the arrival of debris. It is not certain if this is due to the complete lack of meteorological observations in the Eastern Pacific and the winds were really stronger than assumed, or that the debris was actually from the Bravo burst. (Note: Since all fallout data is extrapolated to 100 days after the assigned burst, values assigned to different bursts cannot be compared directly. The extrapolation factor depends both on the day of the burst and on the day the sample was counted. For the areas mentioned in this paragraph, values assigned to burst 2 would have to be increased by about a factor of three if the debris were assigned to burst 1).

By April 2nd and 3rd increases in activity are evident along the Gulf Coast of the United States and certainly by the 4th and 5th there is good evidence that debris from this burst has arrived over the United States. Again, as when fresh Bravo debris was present, fallout seemed to occur irrespective of the occurrence of precipitation.

The progression of debris westward from the test site appears to have been more rapid than indicated by the low-level trajectories at 5,000 and 10,000 feet, at least for the first few days following the burst. Whether the arrival of debris at Yap and Koror on March 29 is a result of transport of material westward in the stratospheric easterlies or in faster-than-observed low-level trades is not certain. Again, as with Bravo debris, there was a marked tendency for the fallout to occur in the tropical areas, with occasional incursions into the United States.

2.3 KOON

Koon, the third burst of the series

was detonated at
Bikini at 1820 GCT, April 6, 1954, but cloudy conditions prevented

accurate observations of the character of the cloud.

The winds were easterly to 5,000 feet, light southerly above to about 30,000 feet, becoming westerly about 30-40 knots to the tropopause. Because of large amounts of fallout from the second burst, which occurred eleven days earlier, it was impossible to trace the history of the debris from Koon. According to the meteorological trajectories (Figure 2.4), the lowest layers moved westward, the mid-tropospheric portion milled about to the north of the Marshalls for many days and the upper portion moved eastward, remaining south of the Hawaiian Islands, reaching the southwestern states on April 13. No fallout station reported debris which can be definitely assigned to this burst, although it is likely that some of the activity assigned to Romeo is a mixture of debris from the two bursts. No fallout has been assigned to Koon in this report.

2.4 UNION

The fourth test of the series, Union, detonated at Bikini at 1810 GCT, April 25, 1954.

The wind pattern was typical, easterly trades in the lower levels, light winds above, becoming westerly near the tropopause, and strong easterlies above 70,000 feet. Trajectories of this burst are shown in Figure 2.5. If the 30,000- and 40,000-foot trajectories are correct, very little fallout was evident from these levels, since no debris was detected in Mexico or along the Gulf coast until May 5 or later. Fallout at Medford, Ore., on May 2 and in the western states on the following days is in good agreement with the 18,000-foot meteorological trajectory. It is very possible that the lack of meteorological data resulted in erroneous trajectories at 30,000 and 40,000 feet, since debris arriving in Central and South America on May 5 was most likely transported at these levels. Fallout to the west of Bikini seemed to be in good agreement with the trajectories. It should be noted that even though a month had elapsed since the last burst, considerable fallout is occurring throughout the tropics and it is by no means certain that the debris assigned to Union is not from an earlier burst, or that some of the activity assumed to be from Romeo is not actually from Union.

2.5 YANKEE

Yankee, the fifth burst of the series, was detonated from Bikini at 1810 GCT, May 4, 1954.

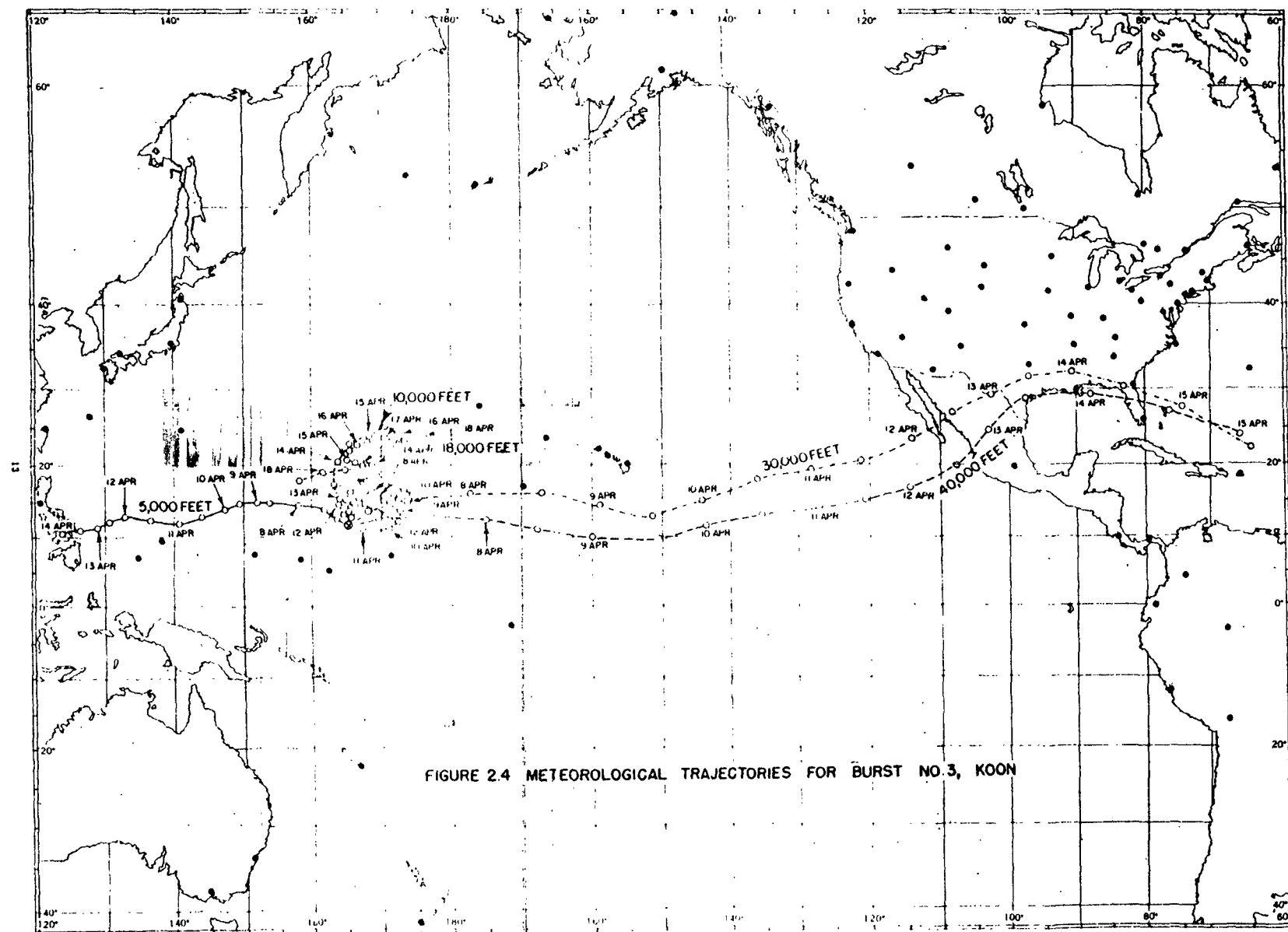
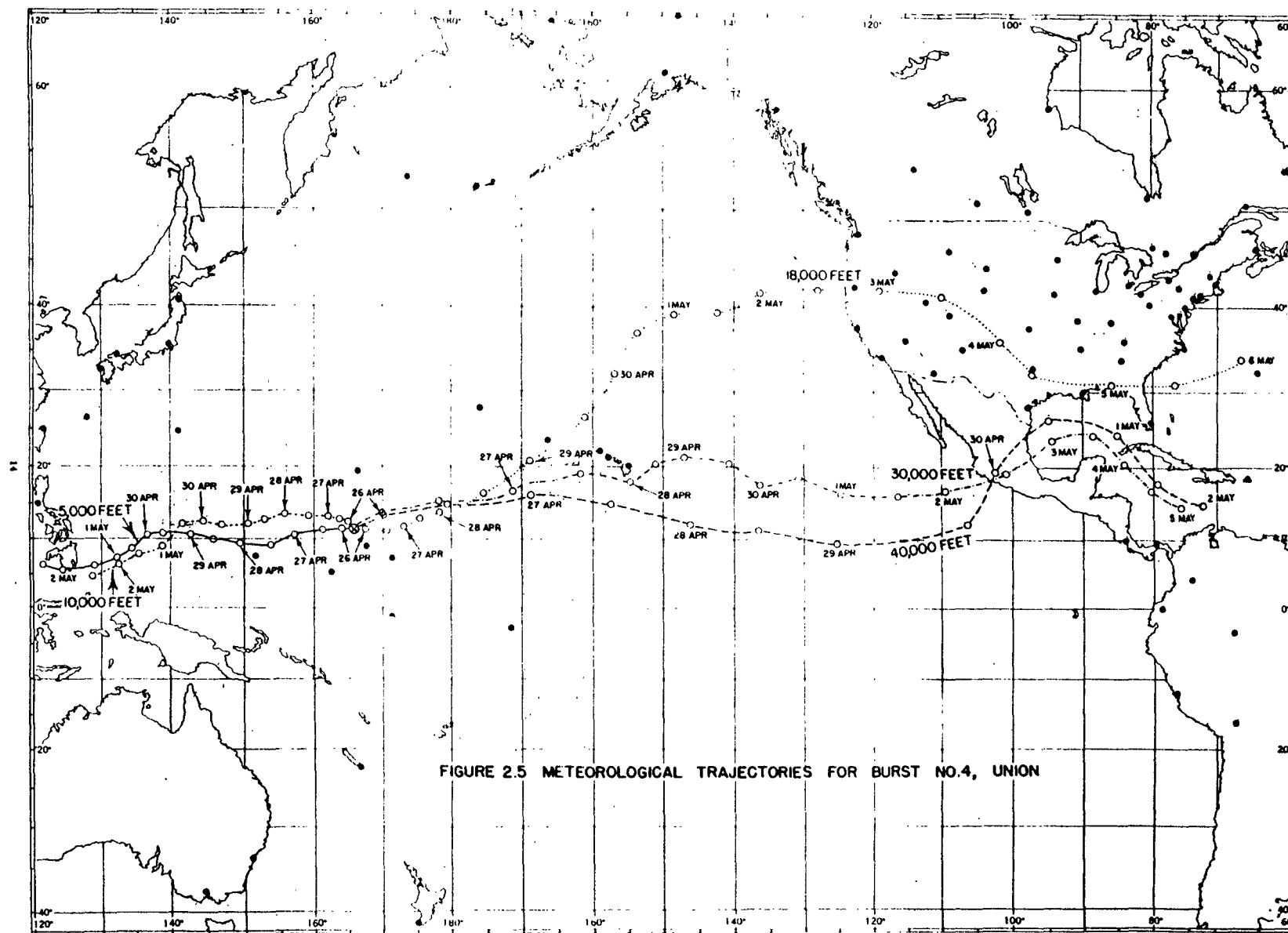


FIGURE 2.4 METEOROLOGICAL TRAJECTORIES FOR BURST NO. 3, KONO



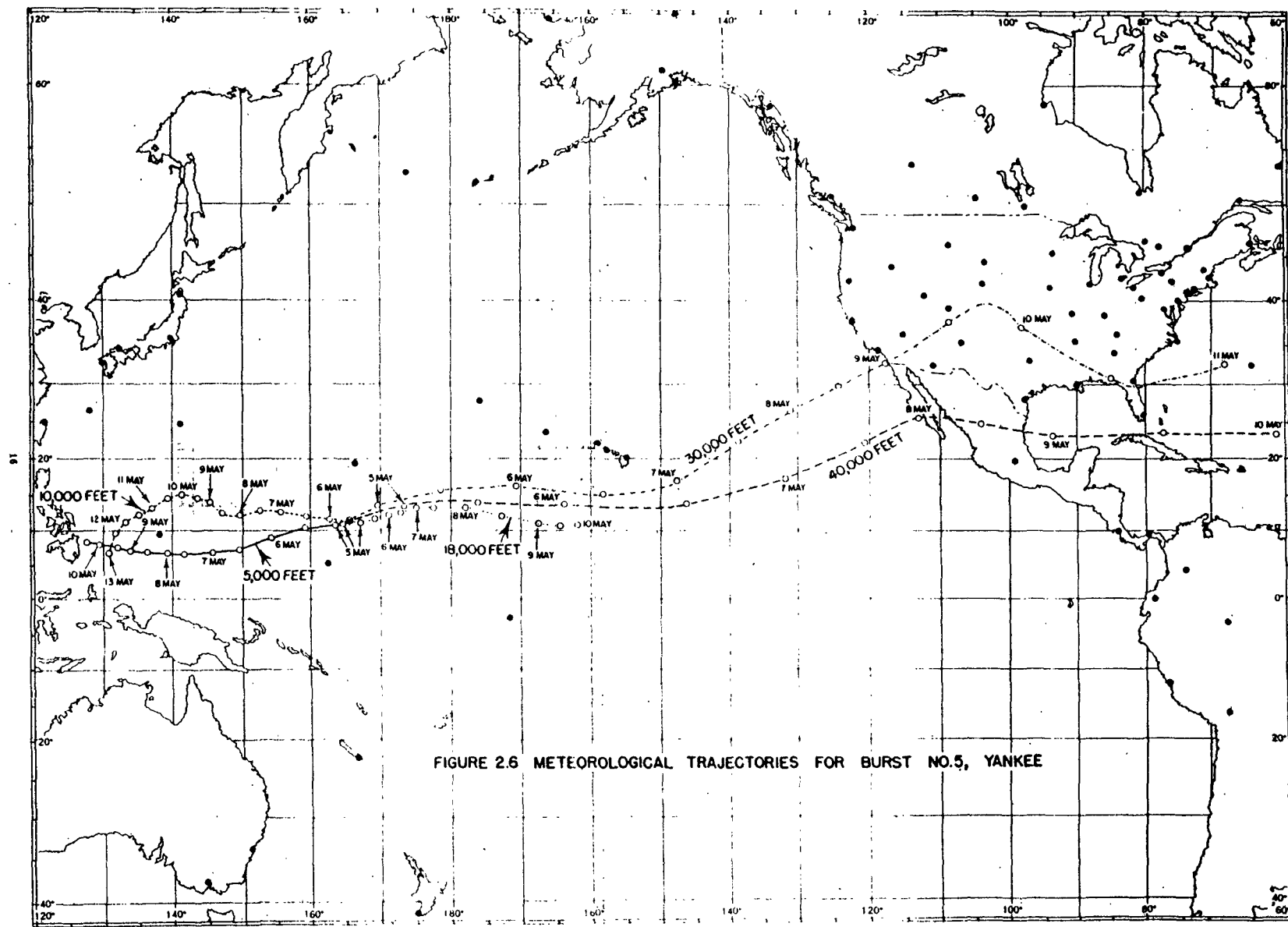
Although the winds, in general, were similar to those of the previous bursts, the westerly winds just below the tropopause attained higher speeds than had occurred during the previous tests, 55 to 65 knots at 40,000 feet. Trajectories are shown in Figure 2.6. Debris reached Mexico City on May 8, and fallout was widespread over the western plains states and the Rockies by May 9. Fallout from this burst continued over the western half of the United States (with the exception of the Pacific Coast) in significant amounts for a period of more than a week. The fallout from Yankee in this region exceeded, by almost an order of magnitude, the fallout from any of the other tests of the series. The westward moving debris appeared to proceed faster than indicated by the low-level trades, reaching Koror by May 6 and Singapore by May 9. Again, it is very possible that high-level easterlies carried the debris, since the 25-30 knot winds required are somewhat faster than expected in the trades of the Western Pacific.

2.6 NECTAR

The last test of the series, Nectar, was the only burst detonated from Enewetak. It occurred at 1820 GCT, May 13, 1954,

The resulting cloud reached 70,000 feet. The easterly winds extended to 20,000 feet, with light westerlies above to the base of the stratosphere. The trajectories from this burst (Figure 2.7) began with a slightly greater component towards the north than for the previous bursts.

Since Yankee and Nectar were separated by only nine days, it is virtually impossible to distinguish between debris from the two bursts. An attempt to separate the two sources of debris was made for the first week following Nectar, but was not attempted beyond this time. Daily fallout maps for the remainder of the month, May 22-31, are given with all data extrapolated to 100 days after Nectar because of the arbitrary system of burst assignment used. However, it is likely that the major portion of the fallout reported on these days originated from Yankee. To convert the reported activity to 100 days after Yankee, assuming the debris originating from Yankee, the values given on the maps should be increased by about 30-40%.



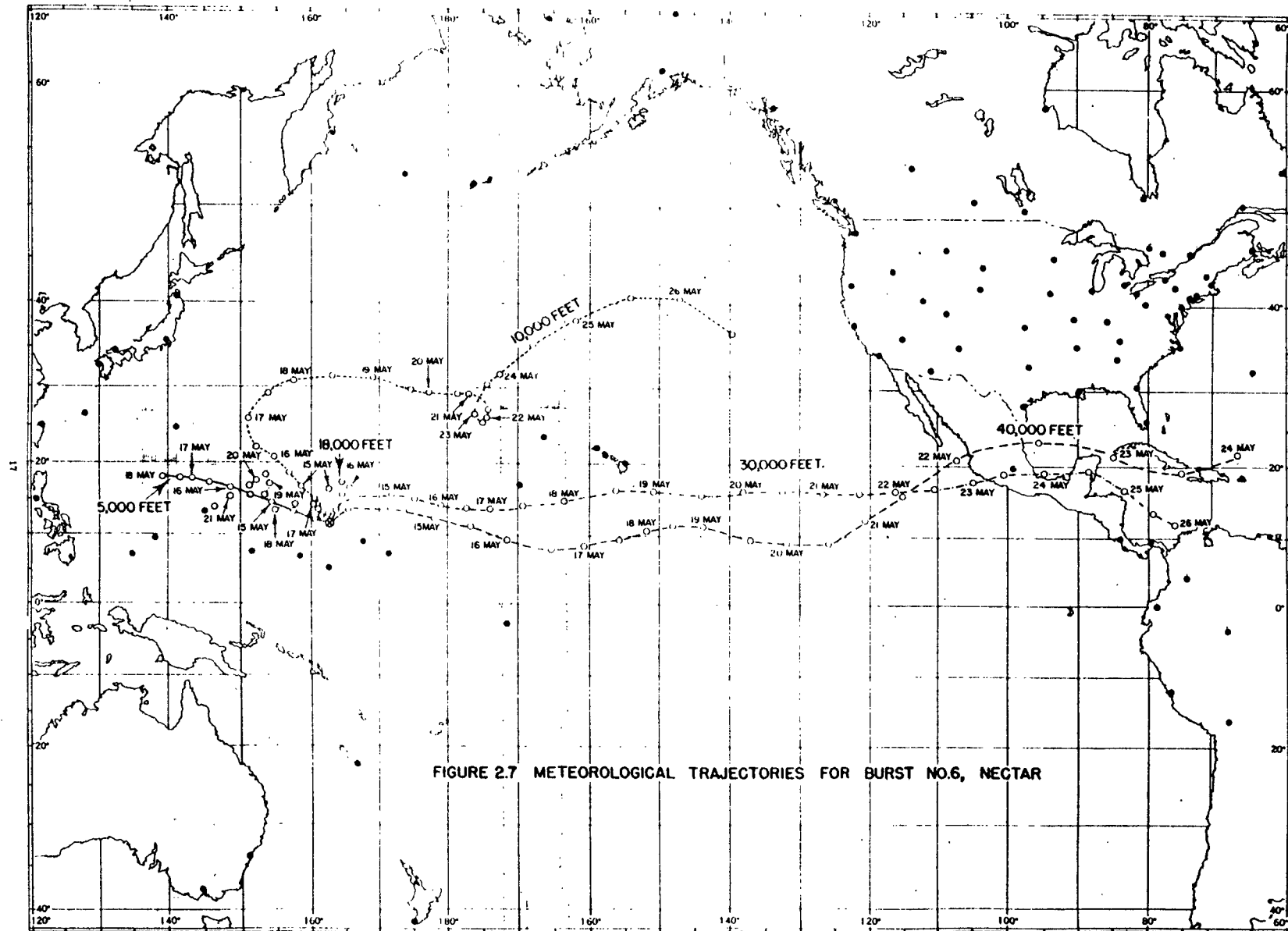


FIGURE 2.7 METEOROLOGICAL TRAJECTORIES FOR BURST NO.6, NECTAR

To conserve space, daily fallout maps for the month of June are not shown. Rather, a map showing the average daily fallout for the month is given, together with the number of days for which data was available at each station. Again, the extrapolator is based on Nectar, and activity is shown at 100 days after burst. It is also likely that the major portion of the fallout in June originated from Yankee and all values should be increased by about 25% to give values at 100 days after Yankee.

Although the discussion of the transport of debris in the atmosphere has been confined to essentially horizontal trajectories, the actual paths of individual radioactive particles are complex, three-dimensional phenomena, influenced by the fall velocities of the particles, atmospheric turbulence, rain scavenging and orographic effects.

CHAPTER 3

TOTAL WORLD-WIDE FALLOUT

3.1 CASTLE TOTAL

The total world-wide fallout from each of the Castle tests (except Koon) and from the whole series has been computed on the basis of results from the monitoring network. Since none of the stations were located immediately downwind of the test area so as to experience fallout in the first day or two following a detonation, it is apparent that by far the largest fraction of the fallout, the "close-in" fallout, has not been measured.

A composite map for the complete series, showing the total of all fallout occurring through June 30, 1954, and decayed to July 1, 1954, is shown in Figures 3.1 and 3.2. These maps contain the cumulative total of all debris deposited on the network from February 28 through June 30, 1954. The debris was extrapolated to July 1 on the basis of the burst assignments indicated in Appendix A (except for fallout occurring after May 21, which was reextrapolated to Yankee, see Section 2.6).

Isolines of activity were interpolated between stations and the average fallout for the world was computed, by numerical integration, to be $919\frac{1}{4}$ d/m/ft² for a total of 22.73 megacuries.

3.2 TOTALS FOR INDIVIDUAL TESTS

To obtain the total fallout due to each of the individual tests, the following procedure, was used. At each station, all fallout assigned to the given burst, as indicated on the maps of Appendix A, was summed, and the total fallout values, in d/m/ft² at 100 days after burst, were entered on a map. (For these computations, fallout occurring after May 21 was not considered, since there was some doubt as to burst assignment.) In the event that data were missing for an occasional day at a given station, the missing values were estimated by interpolation. If data were missing for a number of days, the sum was entered in parentheses and indicated as a lower limit of activity. Isolines of activity were drawn and the total fallout computed by numerical integration.

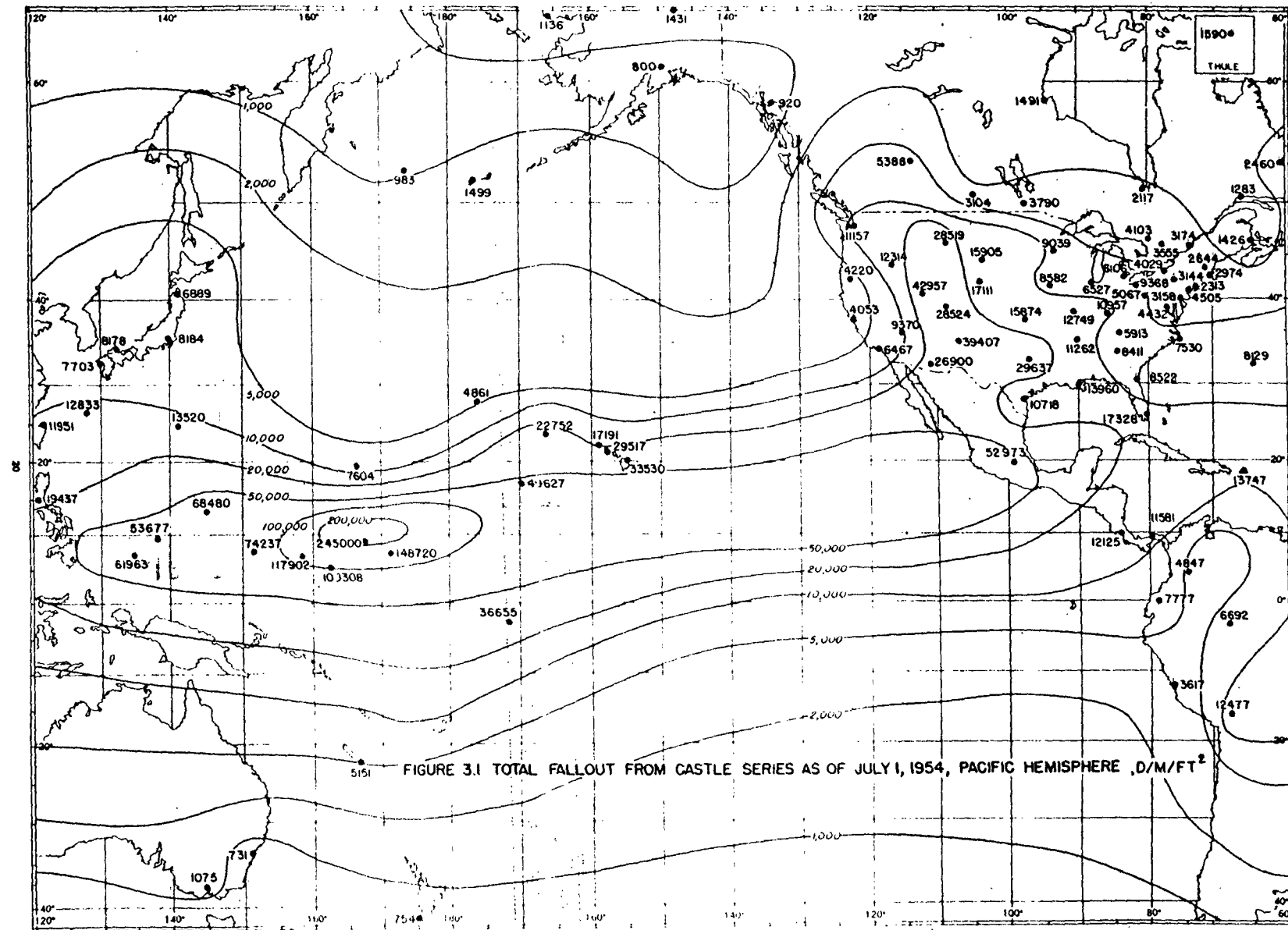


FIGURE 3.1 TOTAL FALLOUT FROM CASTLE SERIES AS OF JULY 1, 1954, PACIFIC

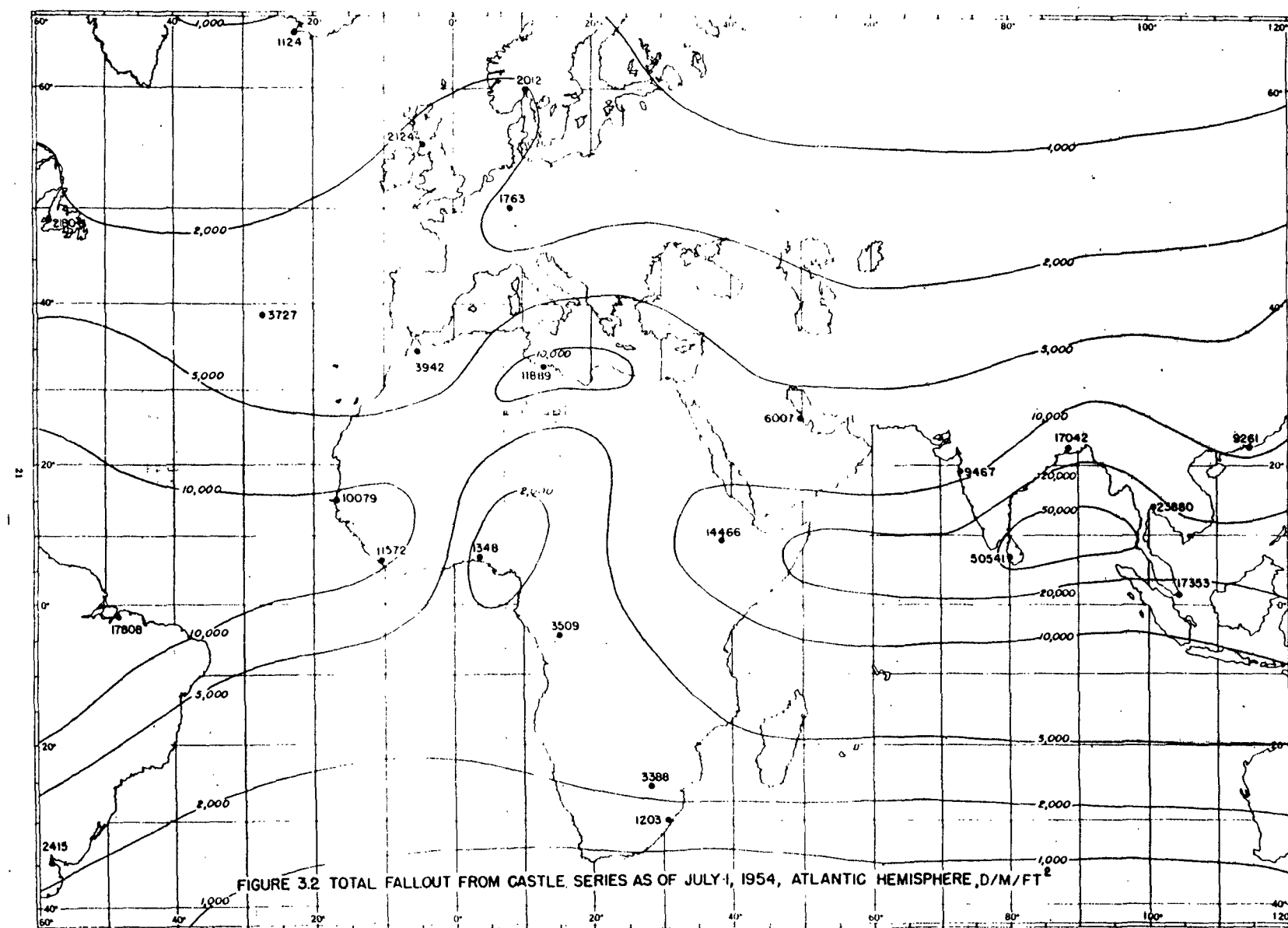


FIGURE 3.2 TOTAL FALLOUT FROM CASTLE SERIES AS OF JULY 1, 1954, ATLANTIC HEMISPHERE, D/M/FT²

It is not appropriate to compare the results from the various tests without first considering the time periods between tests. For example, fallout from Bravo was not masked by later debris for about a month in the region of tests, and could be identified for an even longer period in regions remote from the test site. On the other hand, Union debris was quickly overshadowed by fallout from Yankee, which occurred nine days later.

The world-wide distribution of fallout from Bravo is shown in Figures 3.3 and 3.4. Assigned to the burst was all fallout from the period from February 28 to April 5, 1954, with the exception of debris in a limited area which was determined to be from Romeo (See Appendix A). The average activity of this fallout, corrected to 100 days after burst, was $1937 \text{ d/m}^2\text{ft}^2$, for a total fallout of 4.79 megacuries, or 3.74 megacuries as of July 1, 1954.

Figures 3.5 and 3.6 show the total Romeo fallout from the time of the bursts through May 3, 1954. The world-wide average activity at 100 days after burst was $1445 \text{ d/m}^2\text{ft}^2$ for a total of 3.57 megacuries, or 3.71 megacuries on July 1. No debris was assigned to the third burst, Koon.

Fallout from Union (Figures 3.7 and 3.8) covers the period through May 12, a somewhat shorter period than the first two bursts, since Yankee was detonated only nine days after Union. The world-wide average fallout was $284 \text{ d/m}^2\text{ft}^2$ at 100 days after burst for a total of 0.70 megacuries, or 1.13 megacuries on July 1.

Yankee cumulative results are given in Figures 3.9 and 3.10. Debris was specifically attributed to this burst through May 21. However, much of the fallout which occurred beyond this period also originated from Yankee so that the total fallout is undoubtedly much greater than the values given. Through May 21, Yankee fallout averaged $1219 \text{ d/m}^2\text{ft}^2$, for a total of 3.01 megacuries at 100 days after burst. Corrected to July 1, 1954, this value becomes 5.78 megacuries.

Nectar fallout is shown in Figure 3.11. Since this burst followed the Yankee burst by only nine days, debris from Nectar is identifiable as such only for a few days and in the region near the test area. This fallout from Nectar amounts to a world-wide average of $81 \text{ d/m}^2\text{ft}^2$, or 0.20 megacuries, at 100 days after burst, 0.47 megacuries on July 1, 1954.

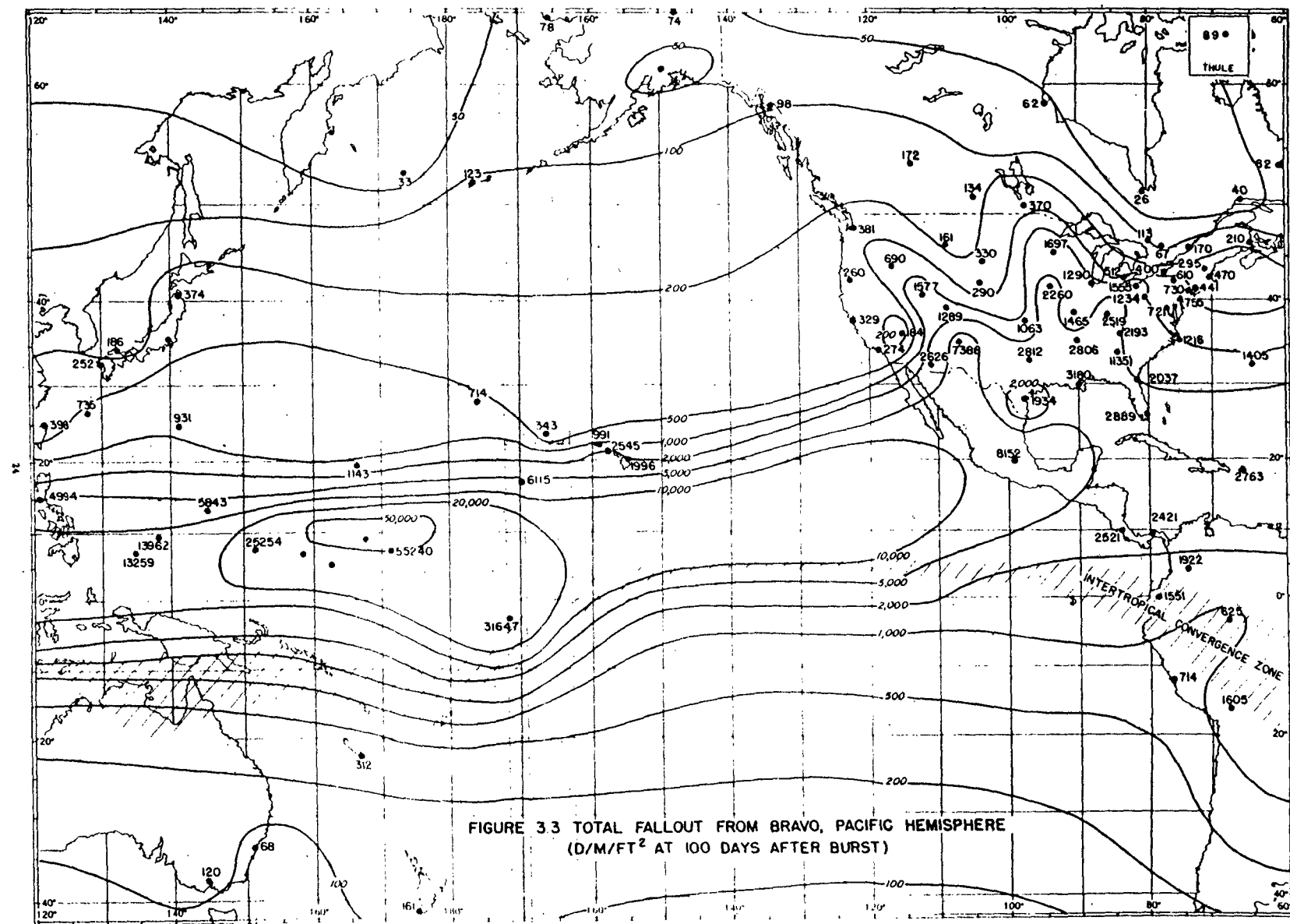
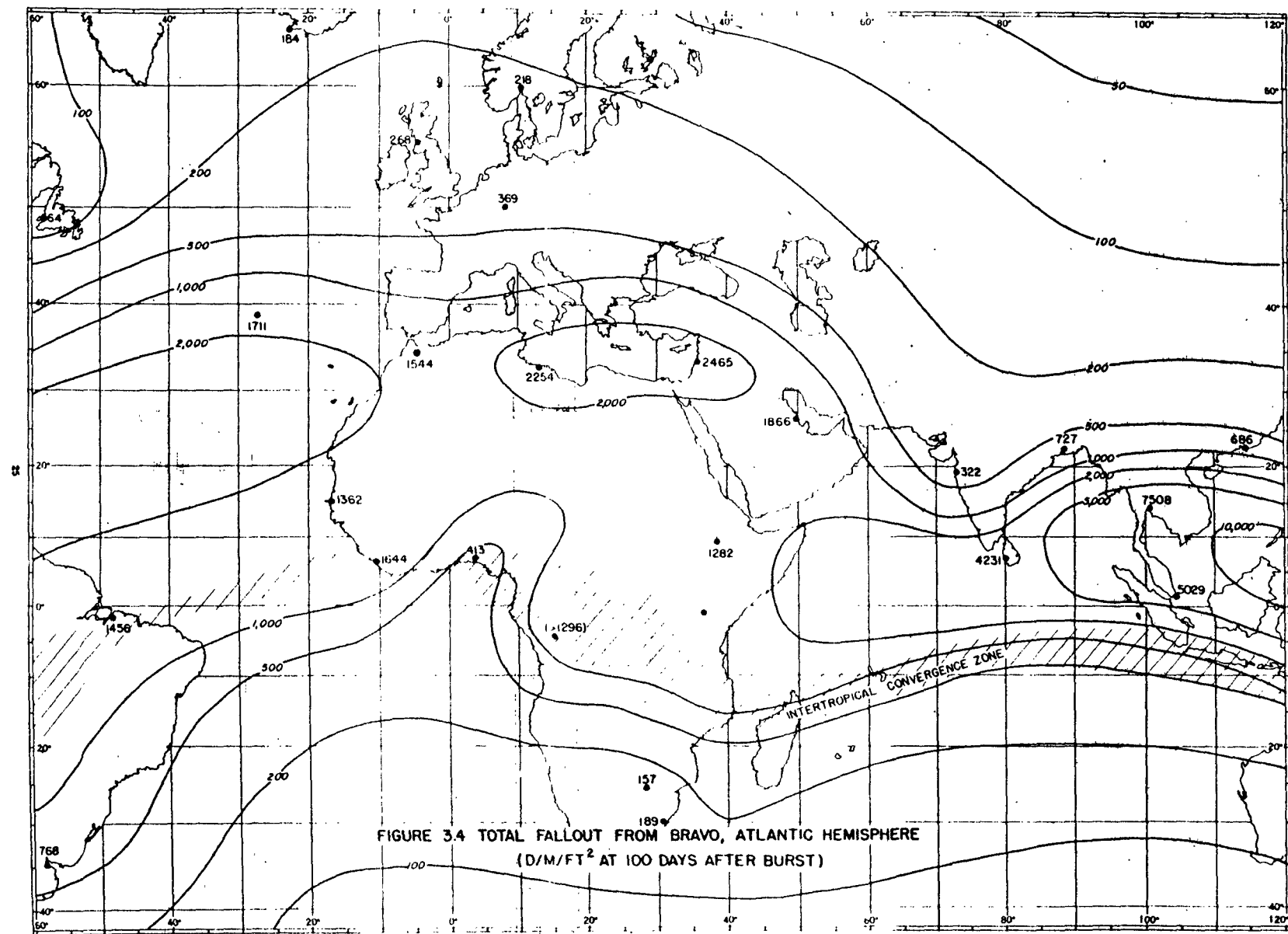
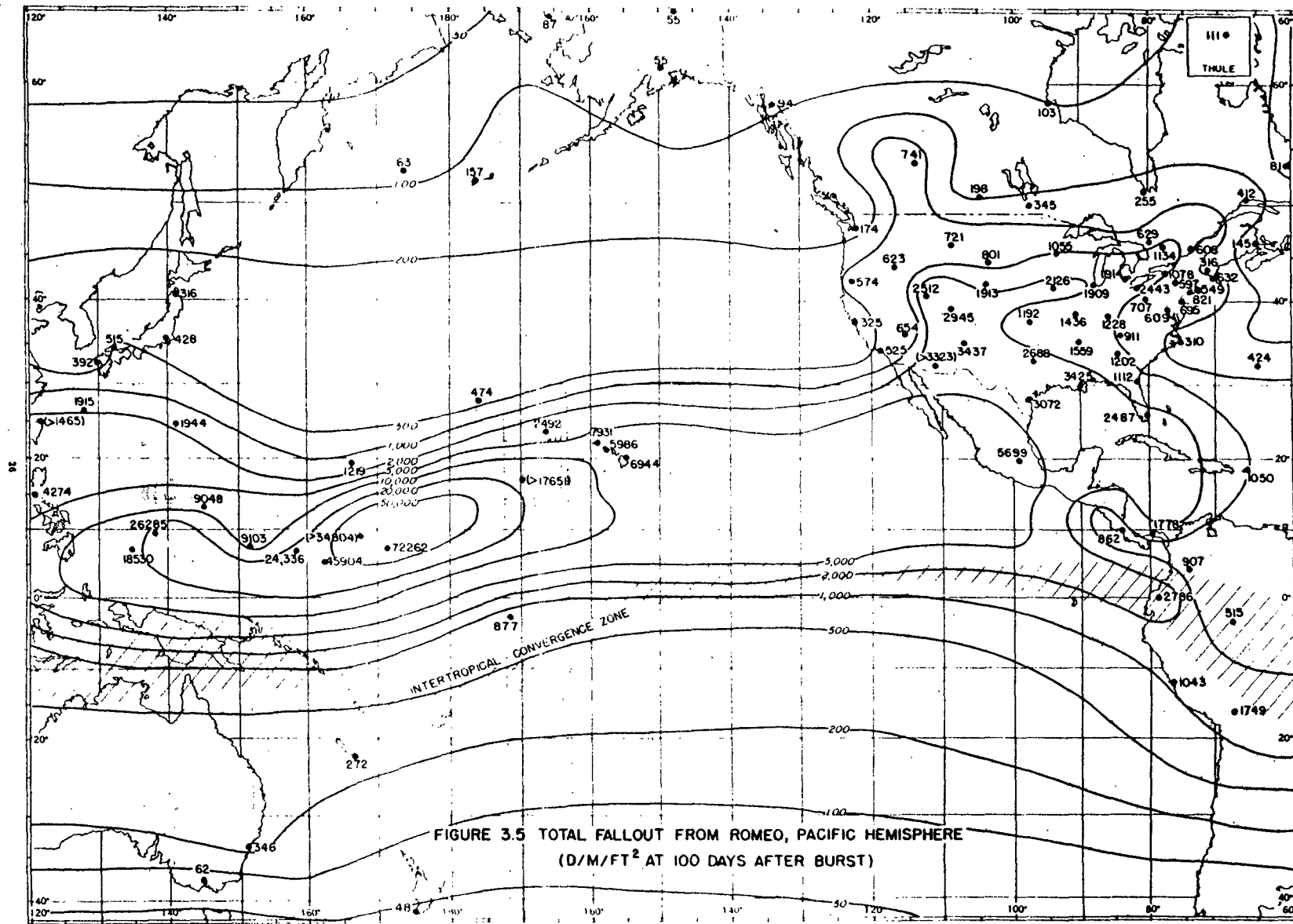
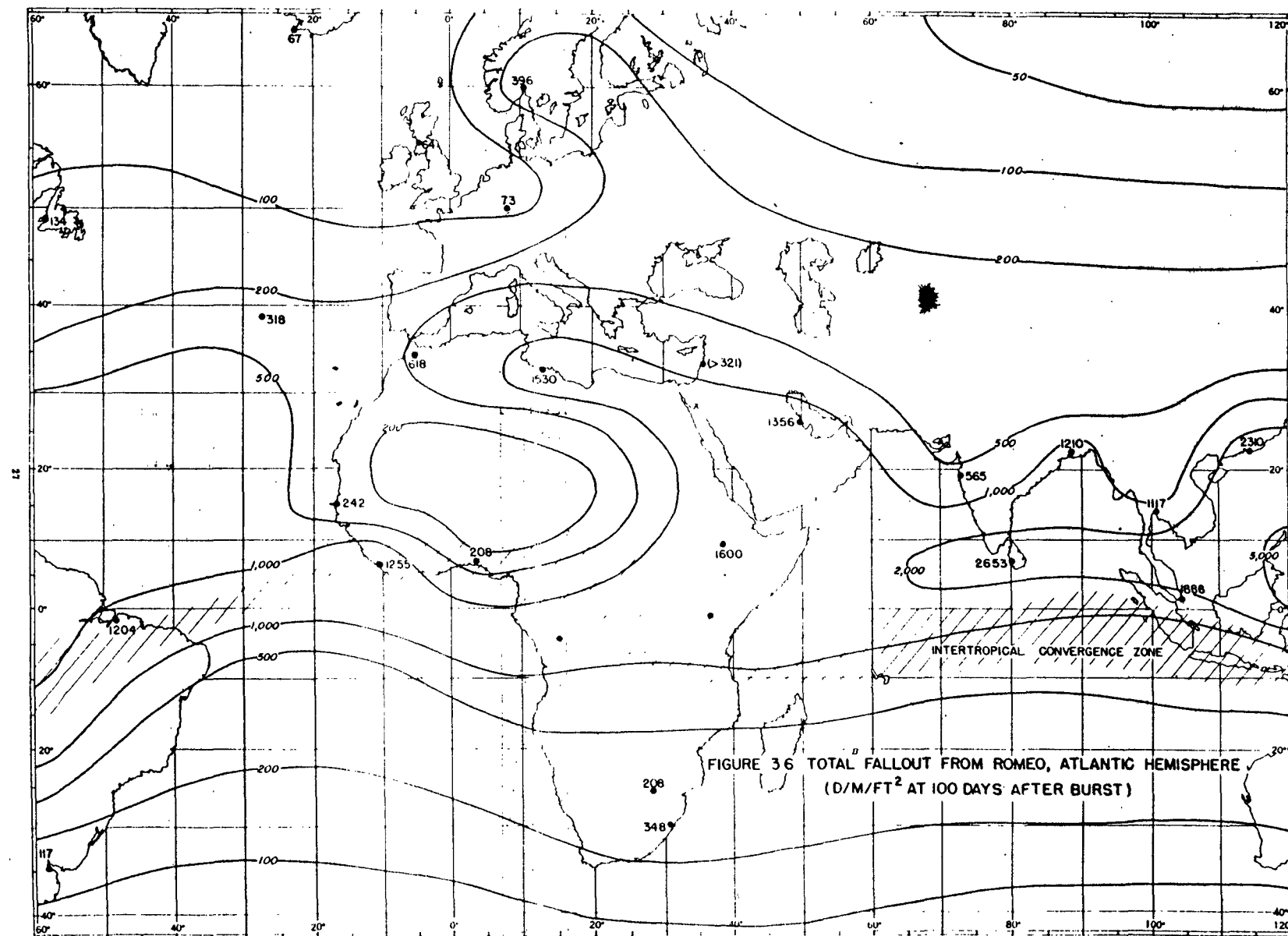


FIGURE 3.3 TOTAL FALLOUT FROM BRAVO, PACIFIC HEMISPHERE
($\text{d/m}^2 \text{ft}^2$ AT 100 DAYS AFTER BURST)







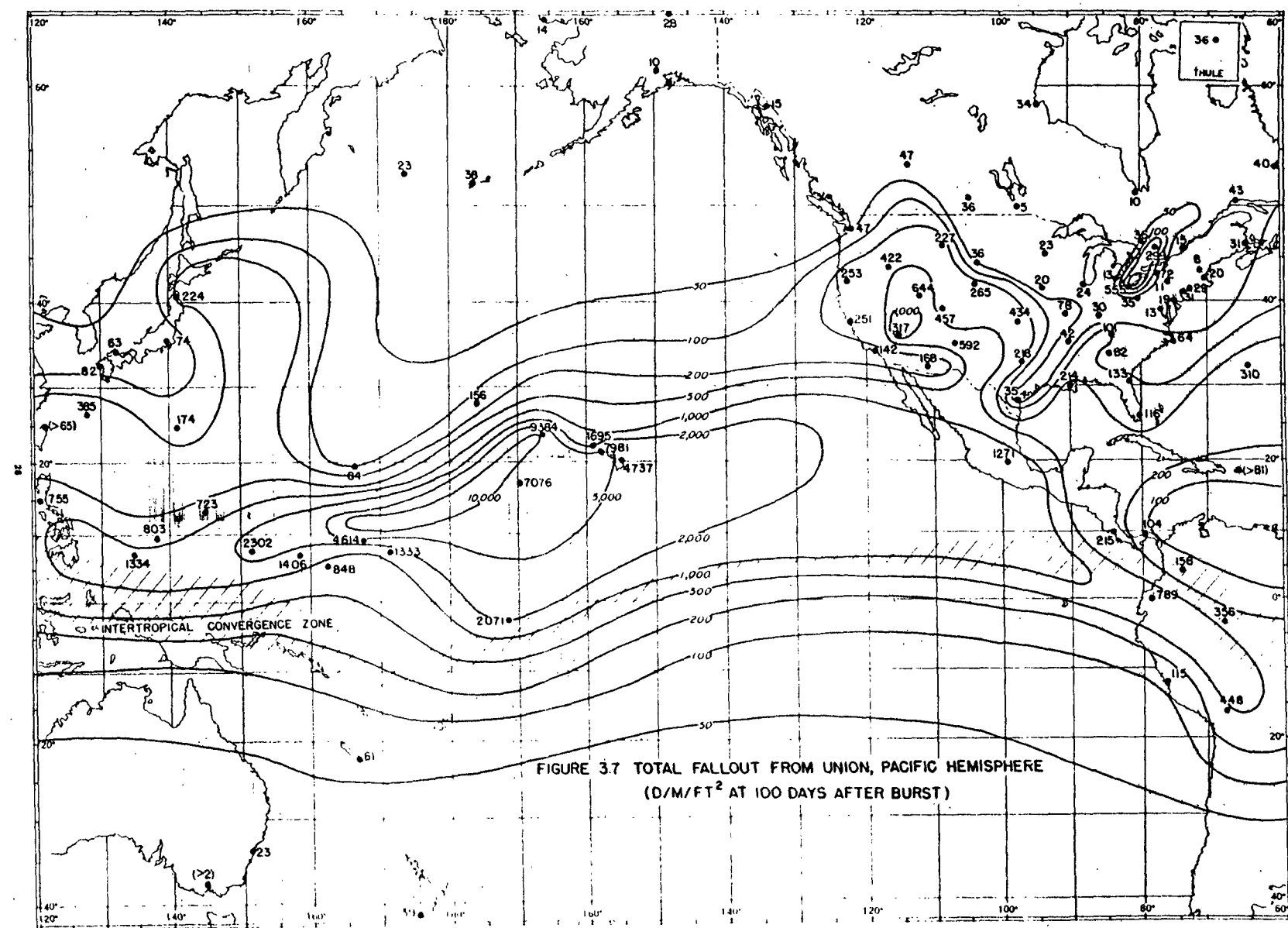
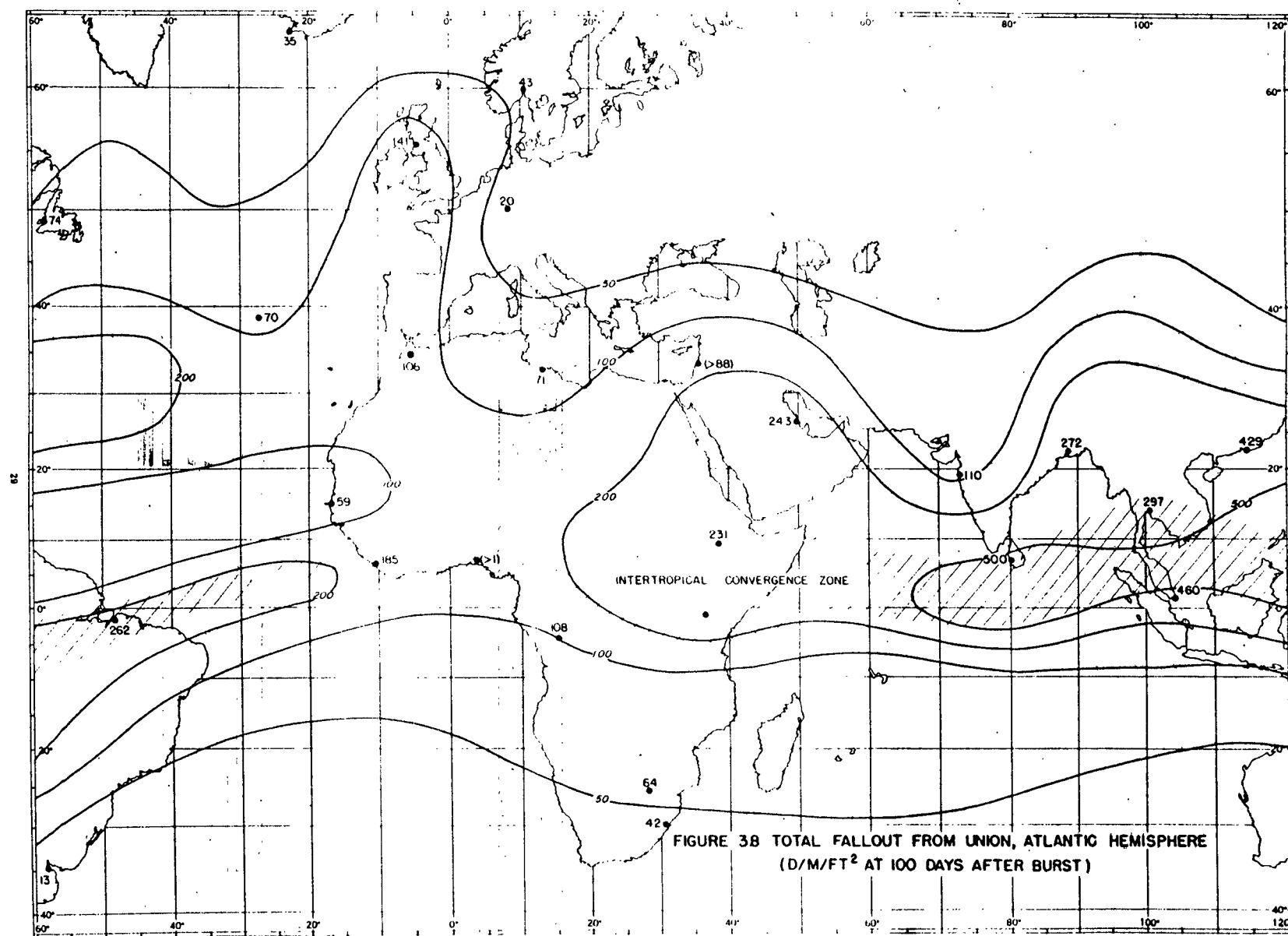
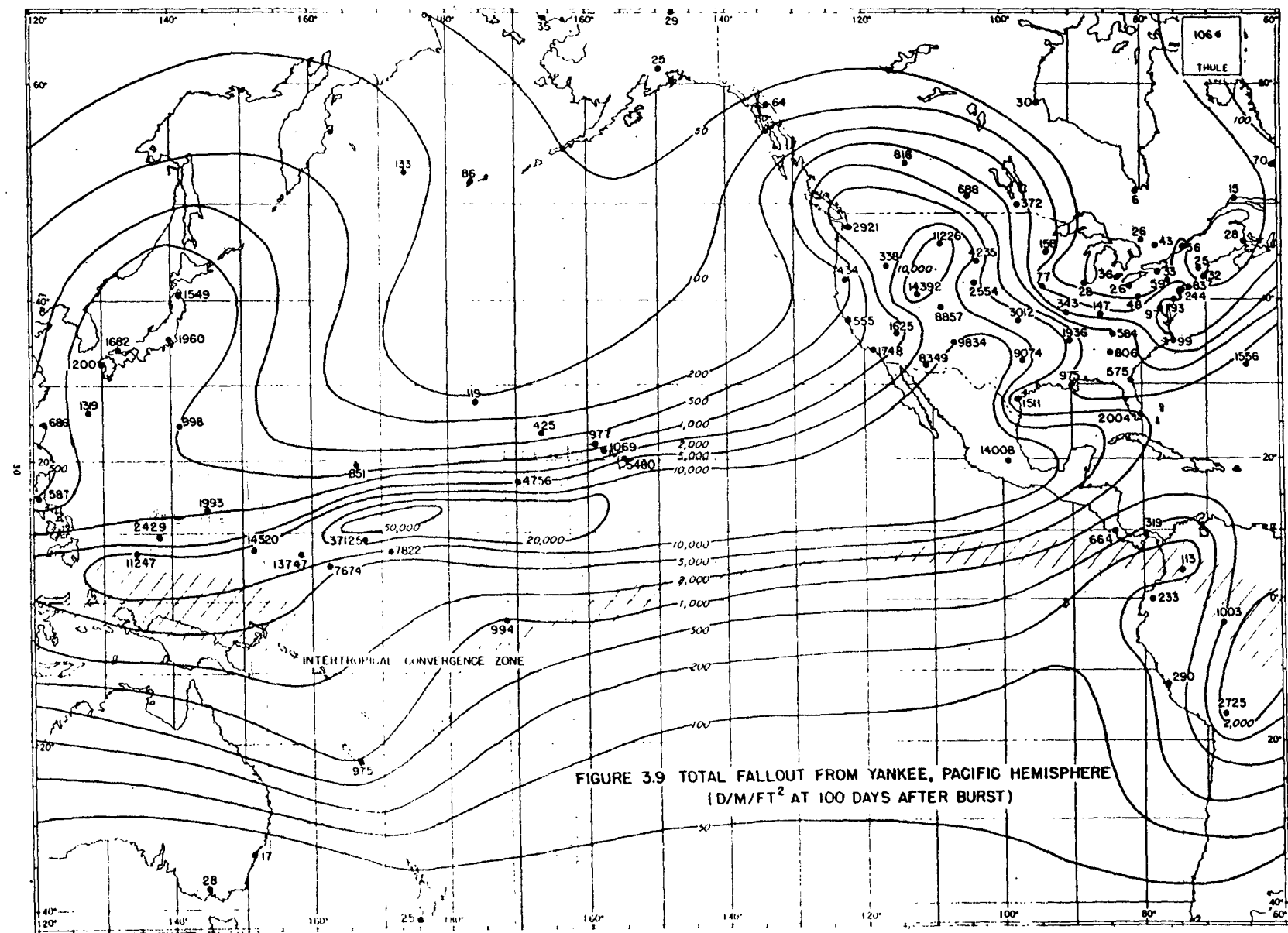
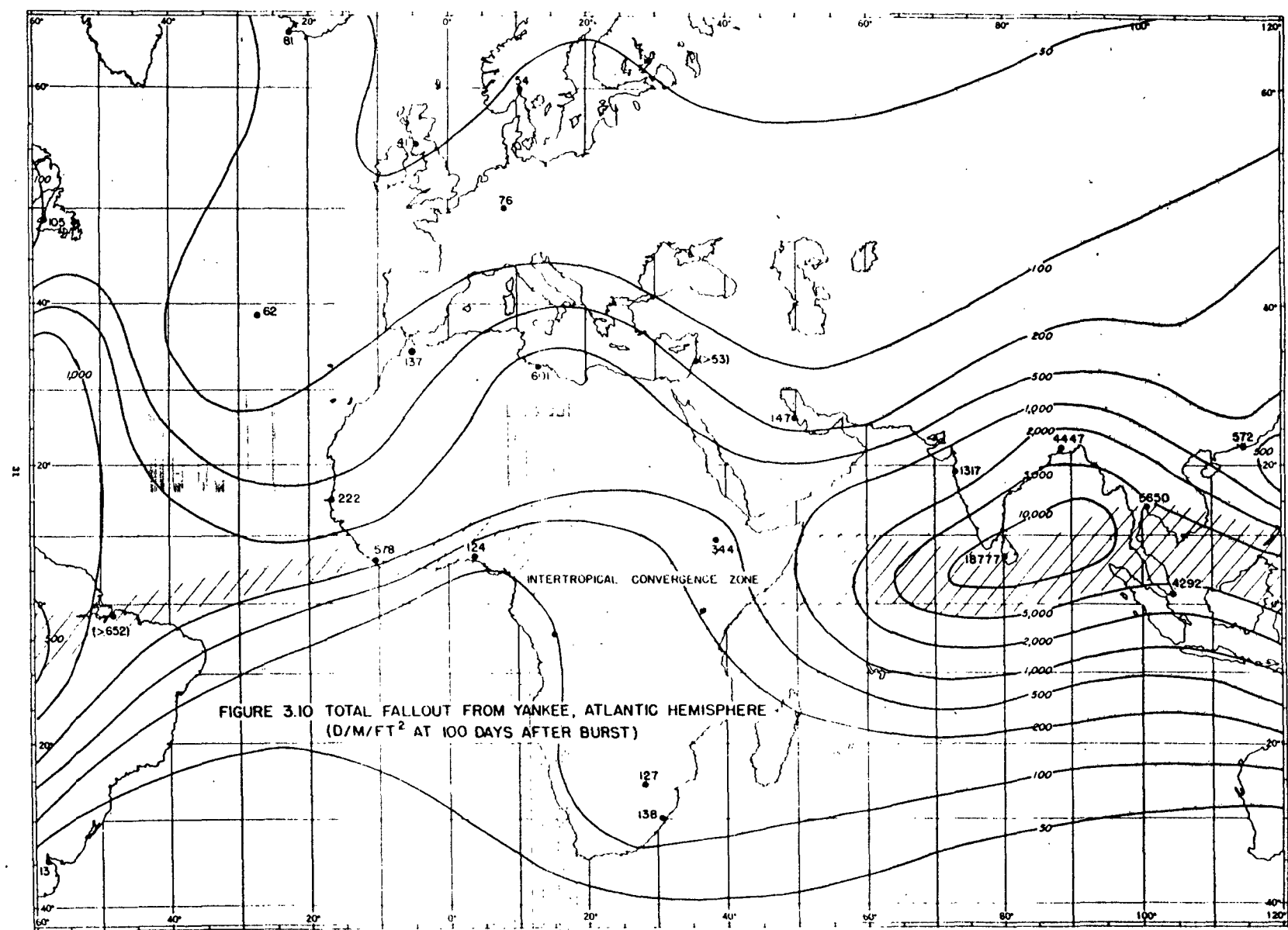
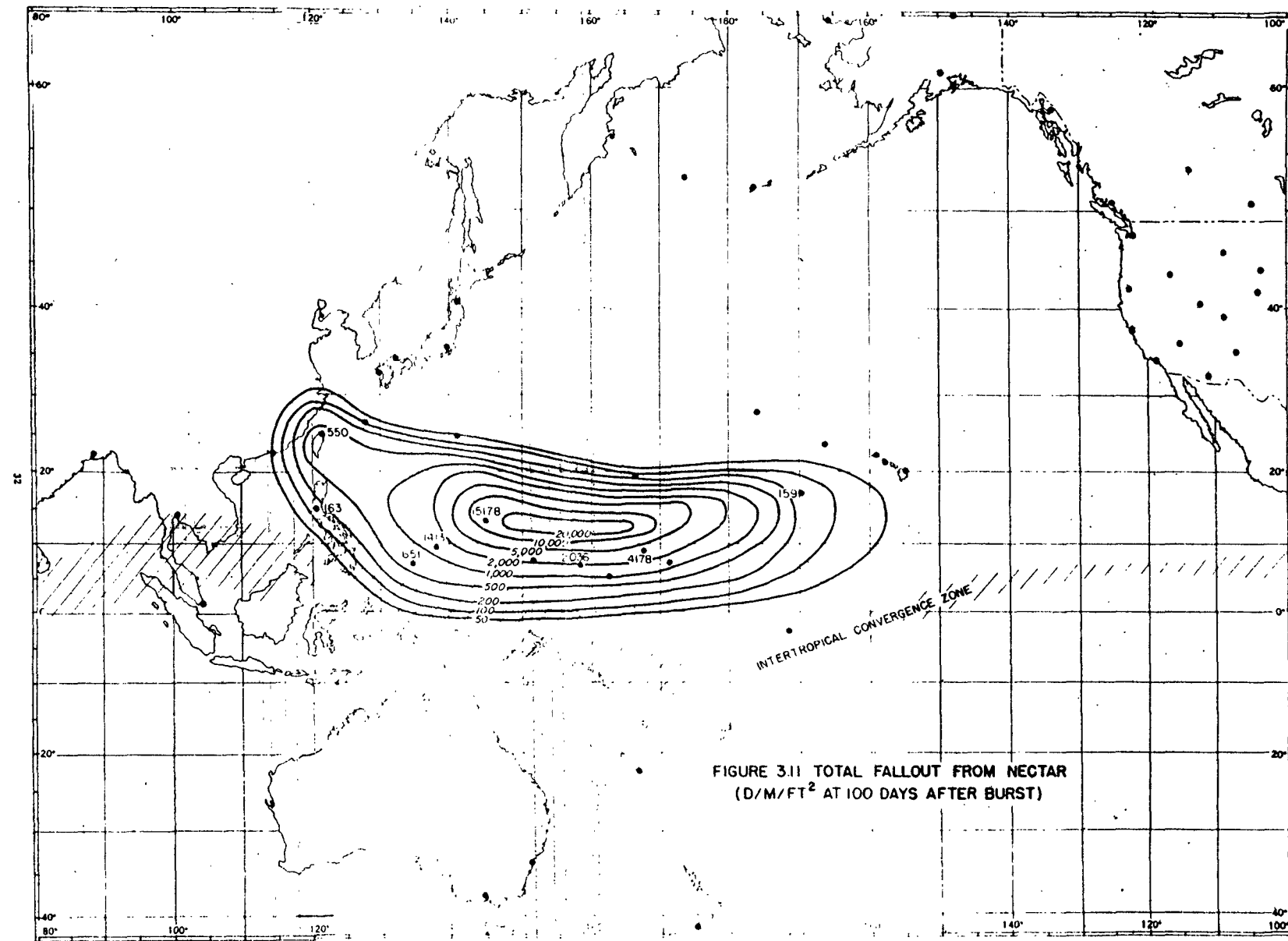


FIGURE 3.7 TOTAL FALLOUT FROM UNION, PACIFIC HEMISPHERE
($\text{D}/\text{M}/\text{FT}^2$ AT 100 DAYS AFTER BURST)









The small percentage of total debris accounted for by the observing network is somewhat puzzling. Although it must be assumed that a large fraction of the active debris was deposited in the vicinity of the test site, it is also true that the shortcomings of the gummed film technique, which have been discussed in previous reports, may be responsible for the effect noted.

3.4 METEOROLOGICAL INTERPRETATION

The total fallout from the Bravo test (Figures 3.3 and 3.4) clearly show the tendency for the major activity to remain near the source latitude.

There seems to be no evidence that debris was carried northward around the western side of the Pacific high-pressure cell. Almost no fallout occurred in Japan, and very little on Iwo Jima from the Bravo test,

The difference between the two tests is a result of the seasonal difference in the location and intensity of the western cell of the Pacific high. This cell is almost non-existent, in the mean, during the winter and

early spring, when the Aleutian lows are farther south. As the western cell of the Pacific high intensifies, more debris can be carried toward the north, so that by the time of the Yankee test (Figures 3.9 and 3.10), in early May, a larger fraction of the fallout occurred in Japan. Presumably, tests in the summer and early fall would result in the greatest contamination of the Japanese Islands, while winter tests would result in the least. Also during the winter months, precipitation in Japan is at a minimum except for a narrow zone on the western slopes. For most of Japan, maximum rainfall occurs during the warm season, with the heaviest rains in June and September.

Similarly, in other inhabited regions likely to be most affected by relatively early fallout, Mexico and Central America to the east and the Phillipines to the west of the test area, the dry season occurs in the winter and the rainiest in the warmer months, so that here too, fallout would be at a minimum for winter tests as compared to other seasons.

3.5 MAXIMUM ACTIVITY AT INDIVIDUAL STATIONS

The highest fallout reported on sampling day on an individual gummed film at each of the stations of the network is shown in Figures 3.12 and 3.13, together with the burst responsible (figure in parentheses), the number of days after burst that the fallout occurred and the precipitation observed. All activity values are in $\text{d}/\text{m}^2/\text{ft}^2$ corrected to sampling day. As can be seen, the fifth burst, Yankee, was responsible for the highest activity at most of the stations. This is a result not only of the fact that Yankee had the highest fission yield of any of the devices tested, but also because of the meteorological conditions associated with this burst. The high tropospheric westerlies were faster, resulting in a more rapid transport of debris towards the Americas. In addition, the winds in the eastern Pacific were from the west southwest, resulting in the passage of fresh debris over the southwestern and southern states.

On the western side of the Pacific, the normal seasonal increase in intensity of the western portion of the Pacific high-pressure cell and the retreat of the Aleutian low resulted in the transport of Yankee debris towards the Japanese Islands in the lower levels, although the direct trajectories at these levels moved generally eastward.

SECRET

Activity in excess of 200,000 d/m/ft² on sampling day occurred at two stations in the United States following the Yankee burst (Billings, Mont., and Salt Lake City, Utah) and was a result of dry fallout at Salt Lake City and with rain at Billings. These values exceed by an order of magnitude the maximum fallout reported at any of the Japanese stations and are larger than the maximum values reported at many of the Pacific Islands much closer to the Pacific Proving Ground. (It should be noted that it is likely that Kusae, Ponape and Kwajalein received their maximum activity following the Bravo burst; however, these stations did not start gummed film observations until about two weeks after this burst and the values given probably do not represent the maximum fallout for the Castle series.)

SECRET

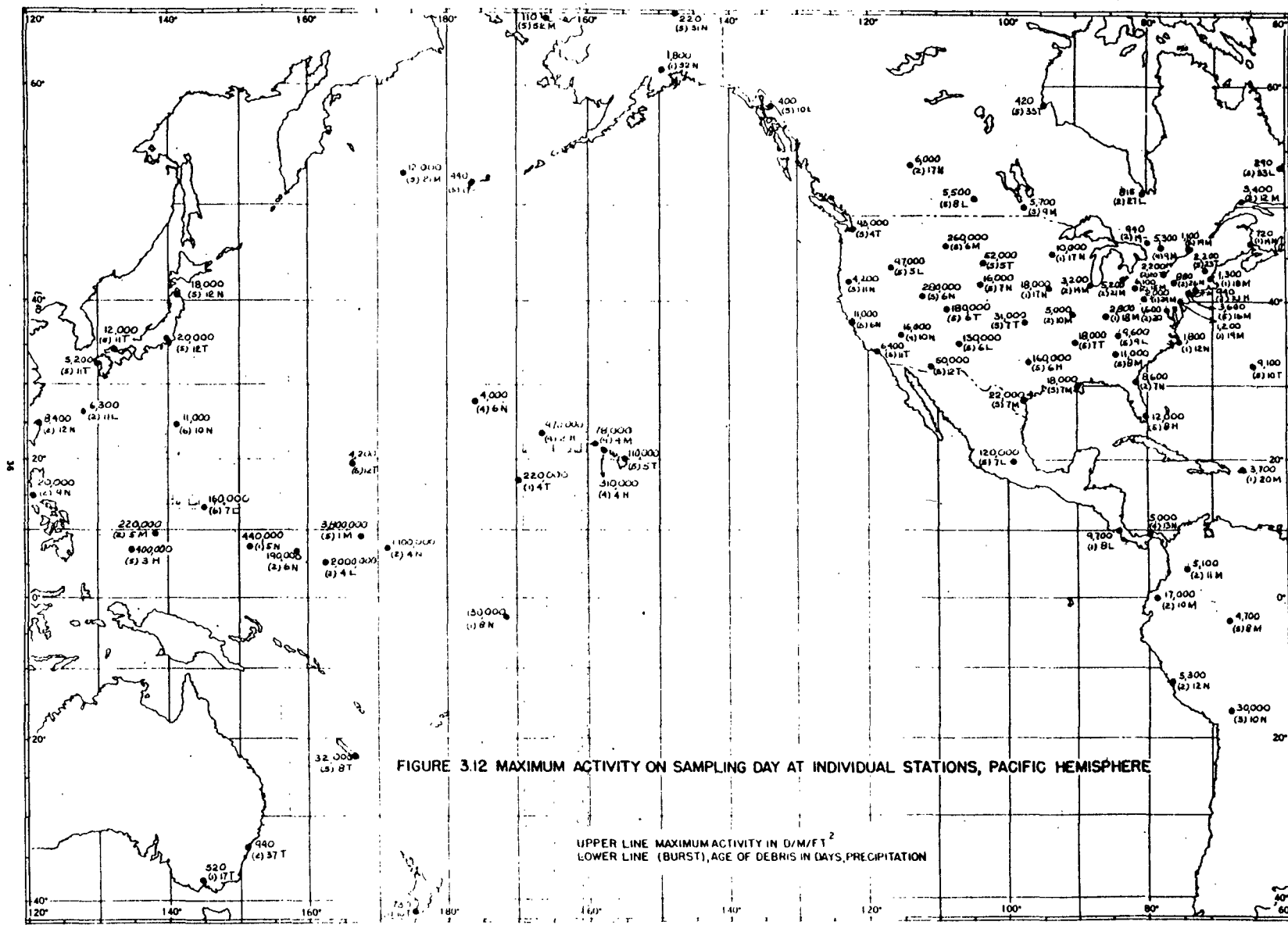
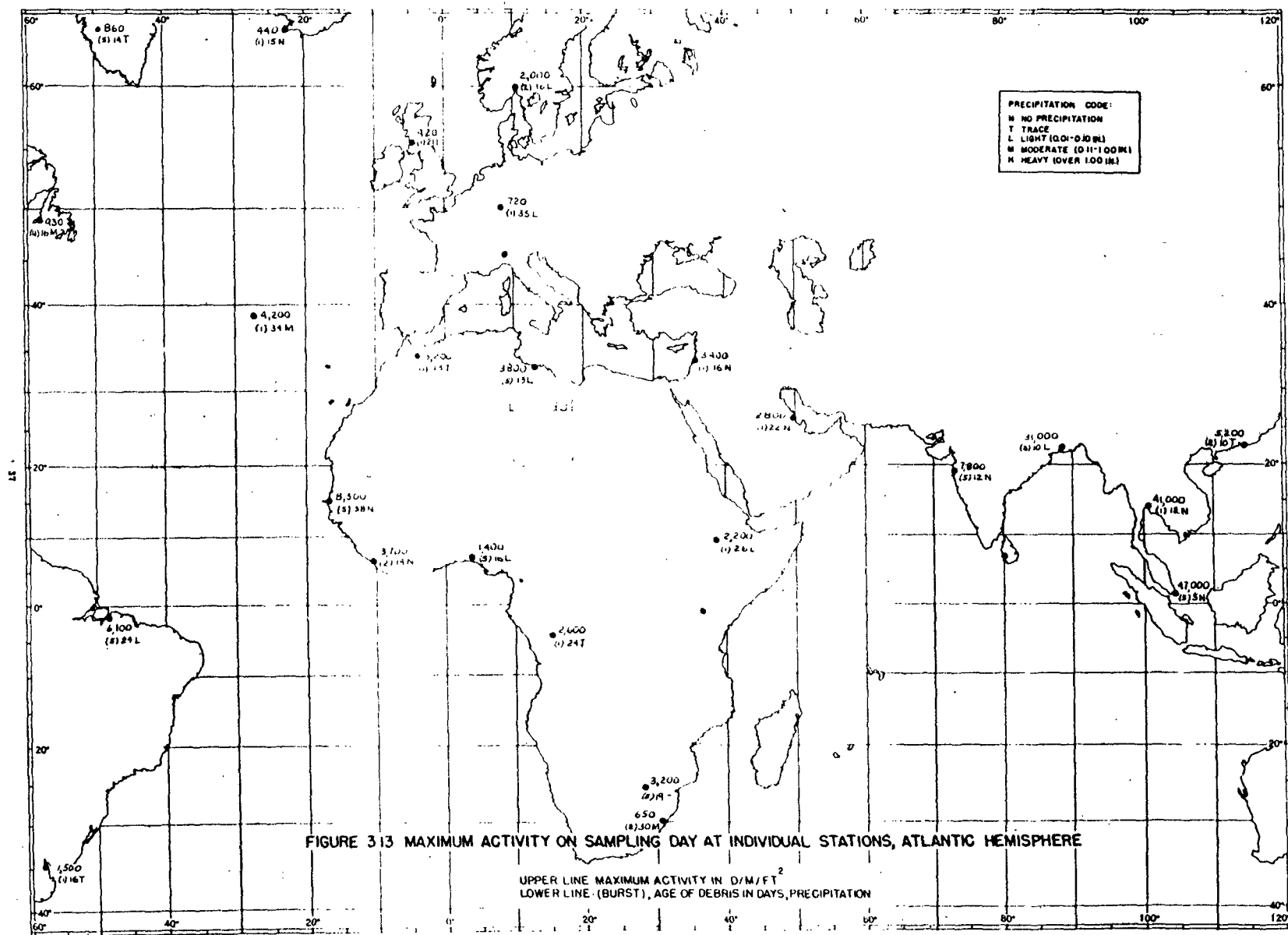


FIGURE 3.12 MAXIMUM ACTIVITY ON SAMPLING DAY AT INDIVIDUAL STATIONS, PACIFIC HEMISPHERE

UPPER LINE MAXIMUM ACTIVITY IN D/M/FT²
LOWER LINE (BURST), AGE OF DEBRIS IN DAYS, PRECIPITATION



CHAPTER 4

SPECIAL OBSERVATIONS

A series of special gummed film collections were made on Ponape, in the Caroline Islands. In addition to the regular gummed film observations, (which were made at 0030 GCT daily at Ponape), a gummed film stand was placed near the windward shore of the island to attempt to sample air unaffected by local dust sources. No significant differences were found. Another gummed film stand was placed near the regular stands, but the film was changed at 12-hour intervals, in the morning and evening. On 11 days with heavy fallout, the film exposed during the daytime hours collected about 50% more activity than did the film exposed during the night hours, despite the fact that precipitation was about equally distributed in the two periods. This may be a result of the nocturnal stabilization of the very lowest layers of the atmosphere which inhibited the deposition of debris from turbulent eddies, although diurnal variations in the vertical temperature lapse rate are small on a 13 $\frac{1}{4}$ -square-mile island in the trade wind belt.

To investigate the denosition of debris due to rainfall, rainwater samples were collected by a 30-inch diameter funnel (4.9 ft^2) coincident with the exposure of the 24-hour films. The collected water was filtered at the end of each observation period and the filter sent to New York, for analysis. On the nine days with the heaviest fallout at Ponape, the total collection on the rain filters averaged 56% as much activity as on the one-square-foot gummed film. During the month of June, when fallout was relatively light, the rain filters collected twice as much activity as the gummed film. This is again indicative of the importance of the rainout process in bringing old debris (and presumably smaller particles) to the ground.

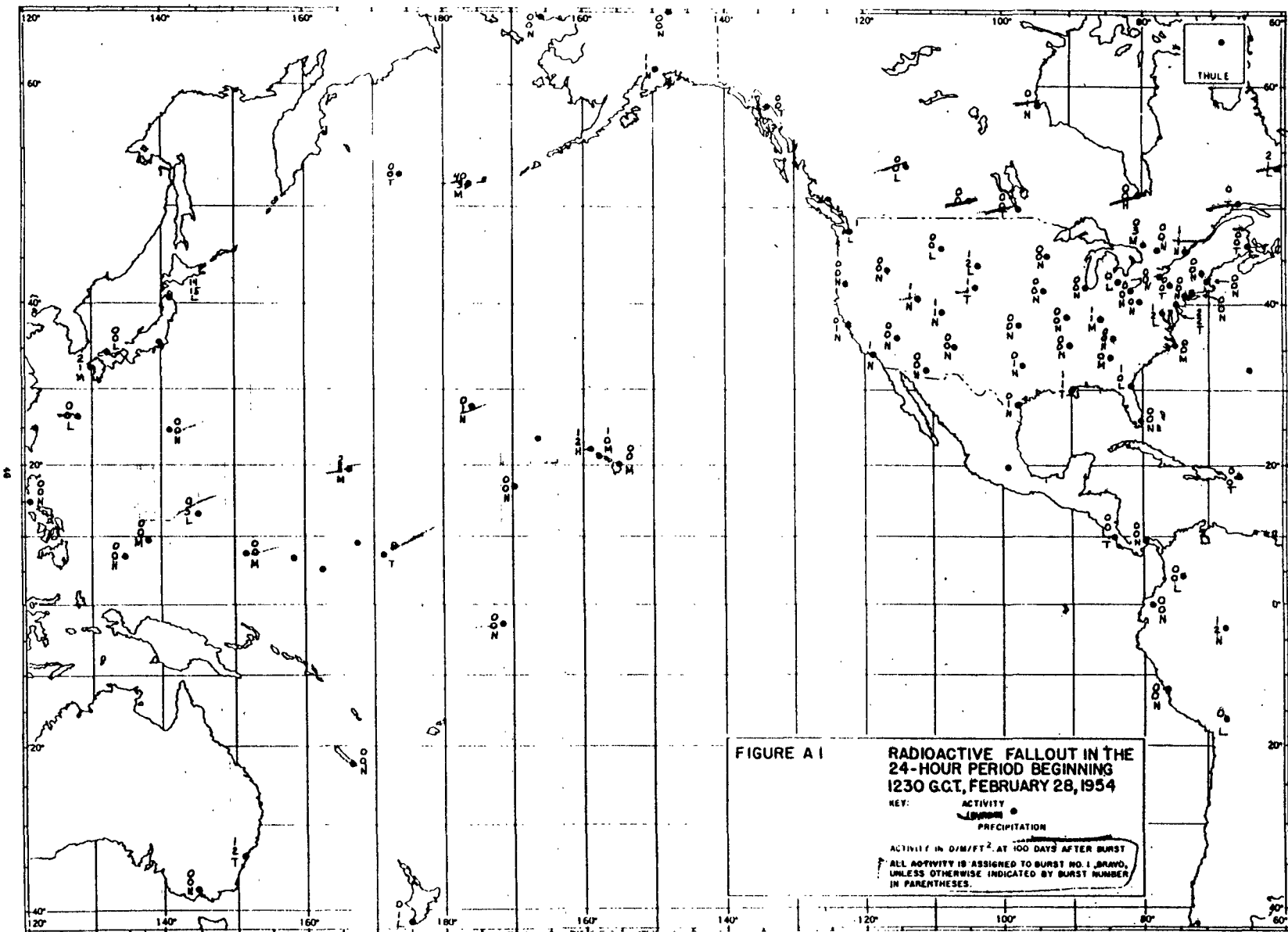
APPENDIX A

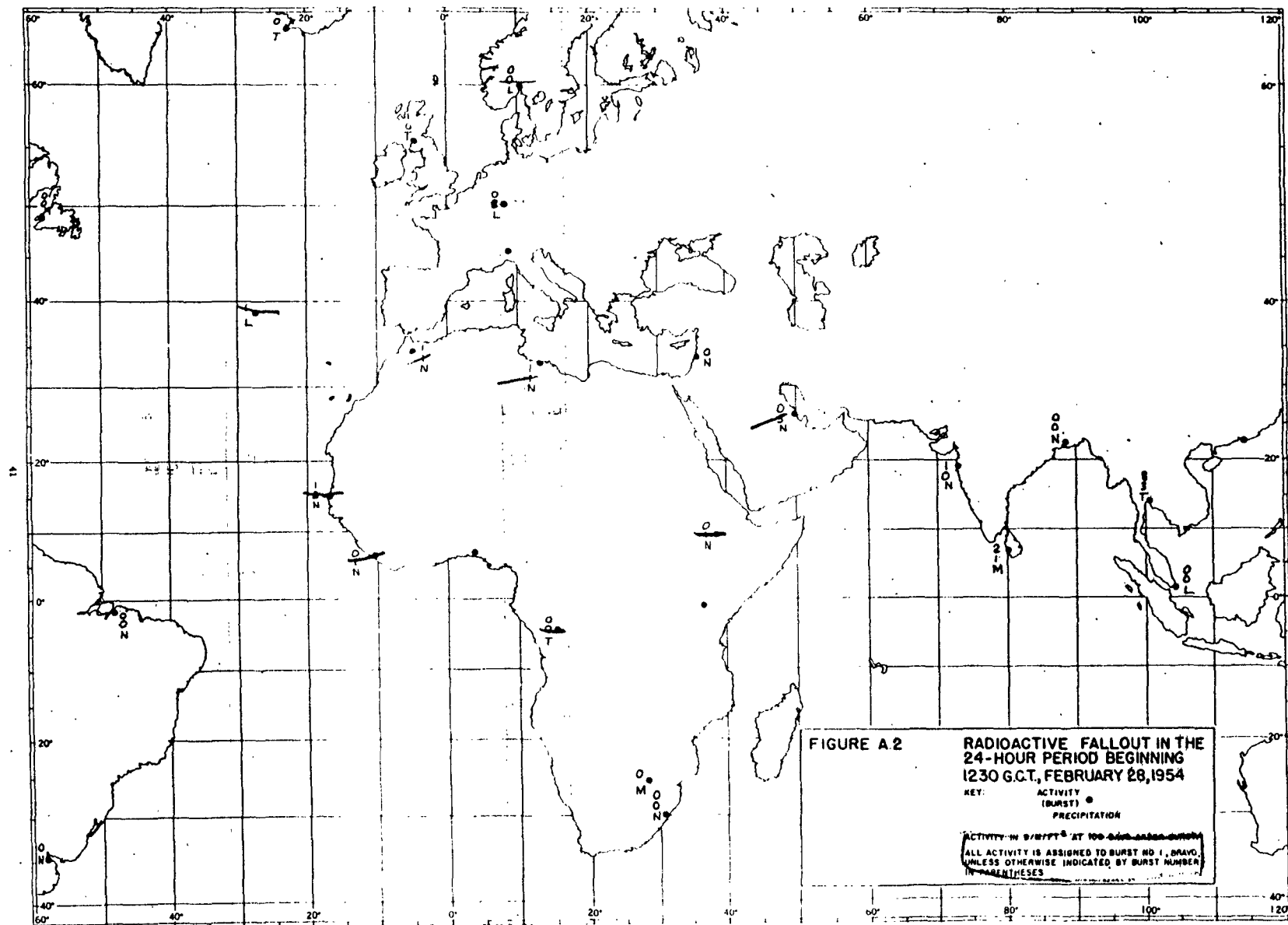
MAPS OF DAILY FALLOUT

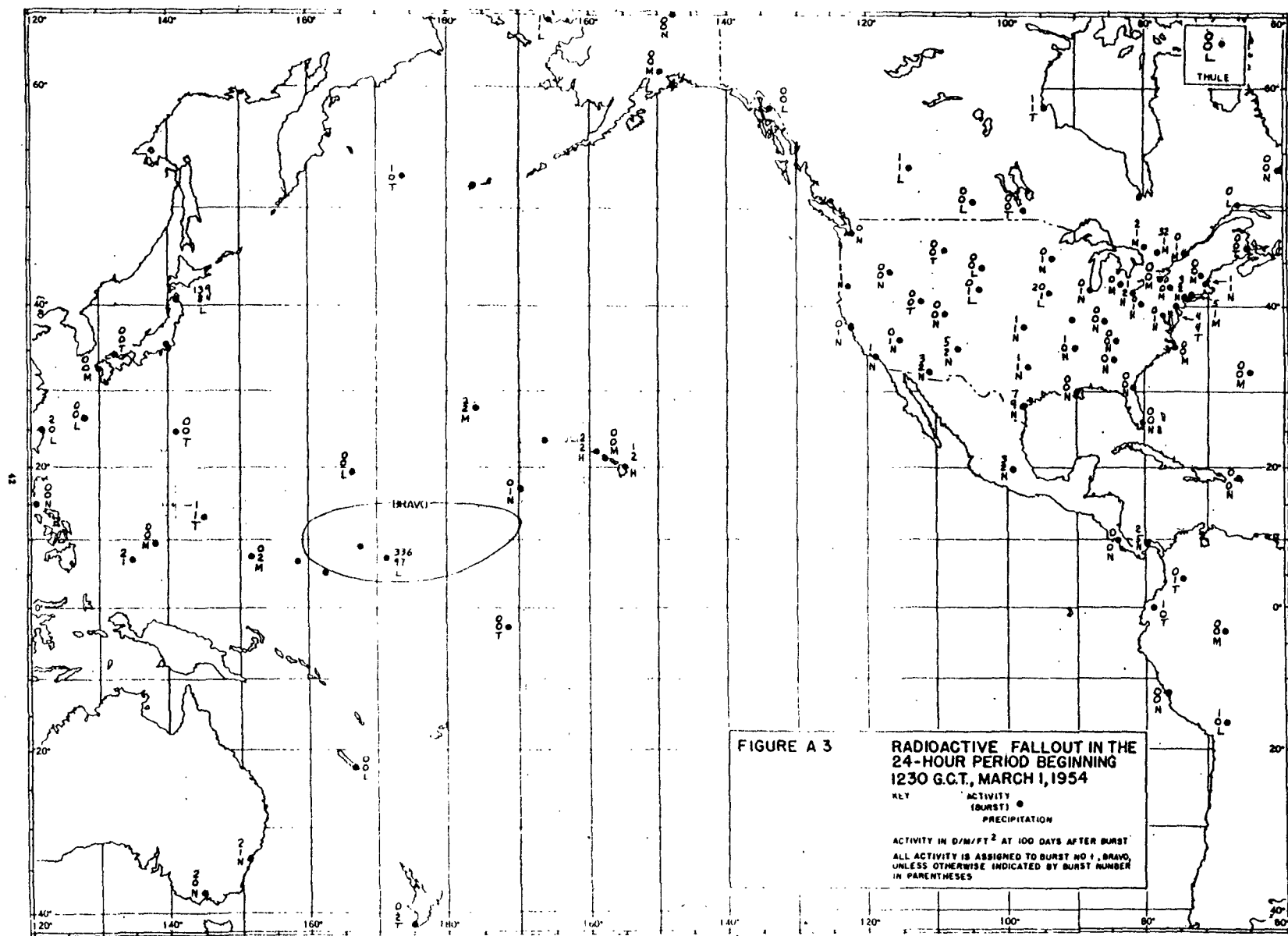
Maps showing the daily fallout on the monitoring network from February 28 to May 31, 1954, and the average daily fallout during the month of June, 1954, are appended. All values of radioactivity are in d/m collected on a square foot of gummed film in a day, extrapolated to 100 days after the burst. In most cases, two films were exposed simultaneously and the values for each are shown. The burst to which the debris was assigned for extrapolation purposes is indicated on each map. (See sec. 2.6 with reference to burst assignments after May 21.)

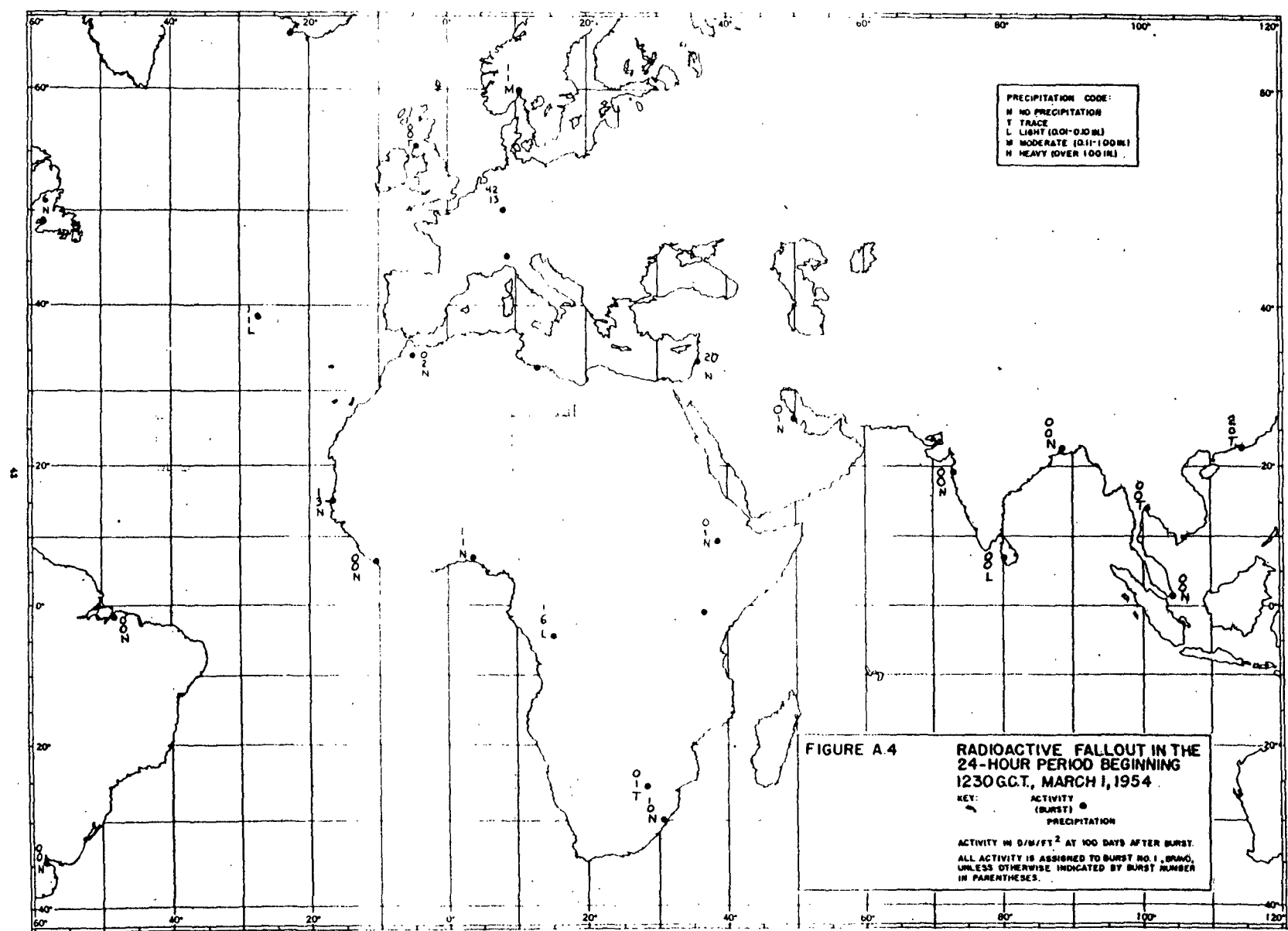
Lines delineating the areas of significant fallout (over 100 d/m²/ft²/day extrapolated to 100 days after burst), labelled with the event believed responsible for the fallout, are shown. The lines are dashed in areas of greatest uncertainty.

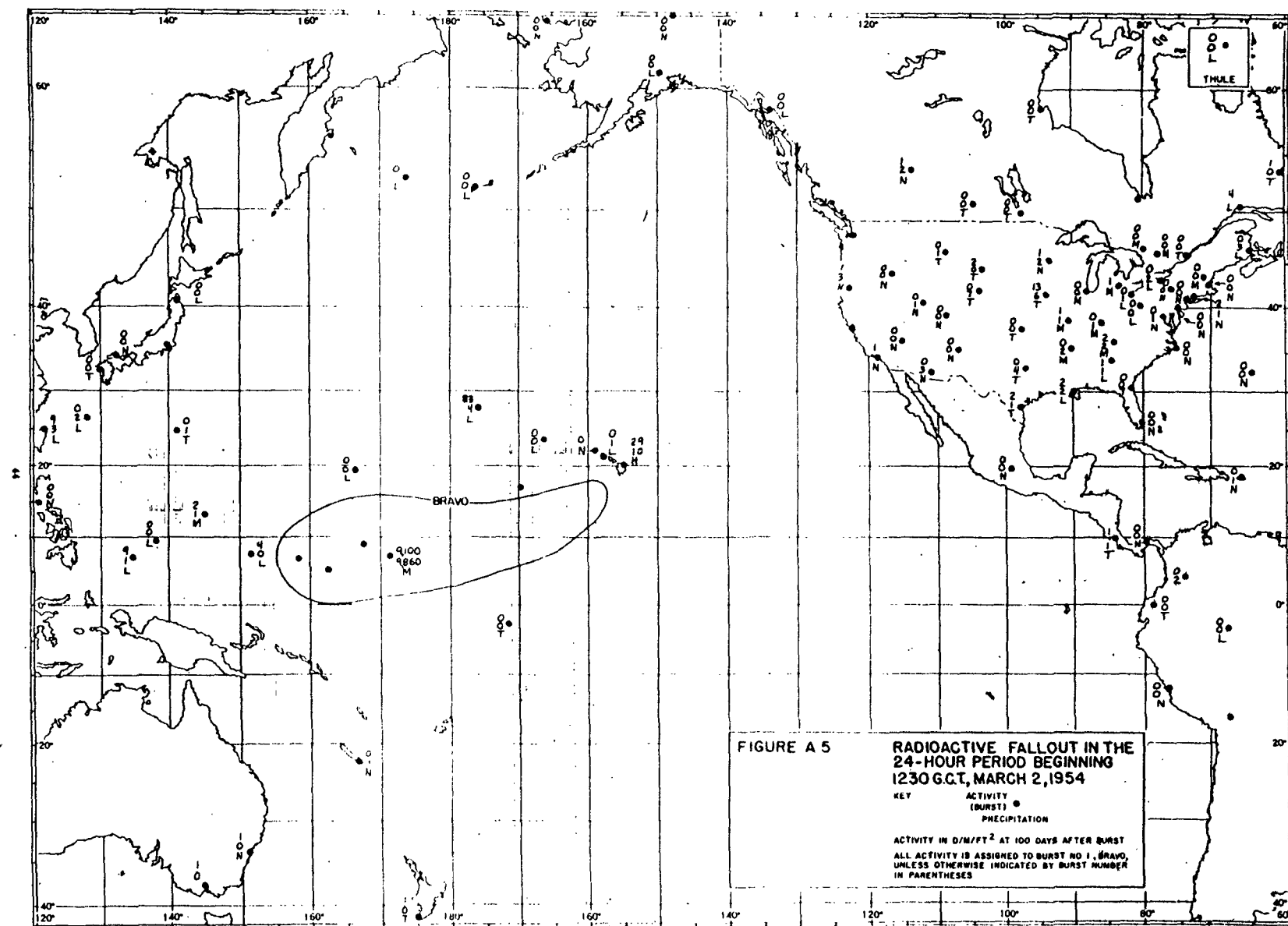
The precipitation which fell during each sampling period is shown in accordance with the code given on the maps. Snow has been reduced to its water equivalent.

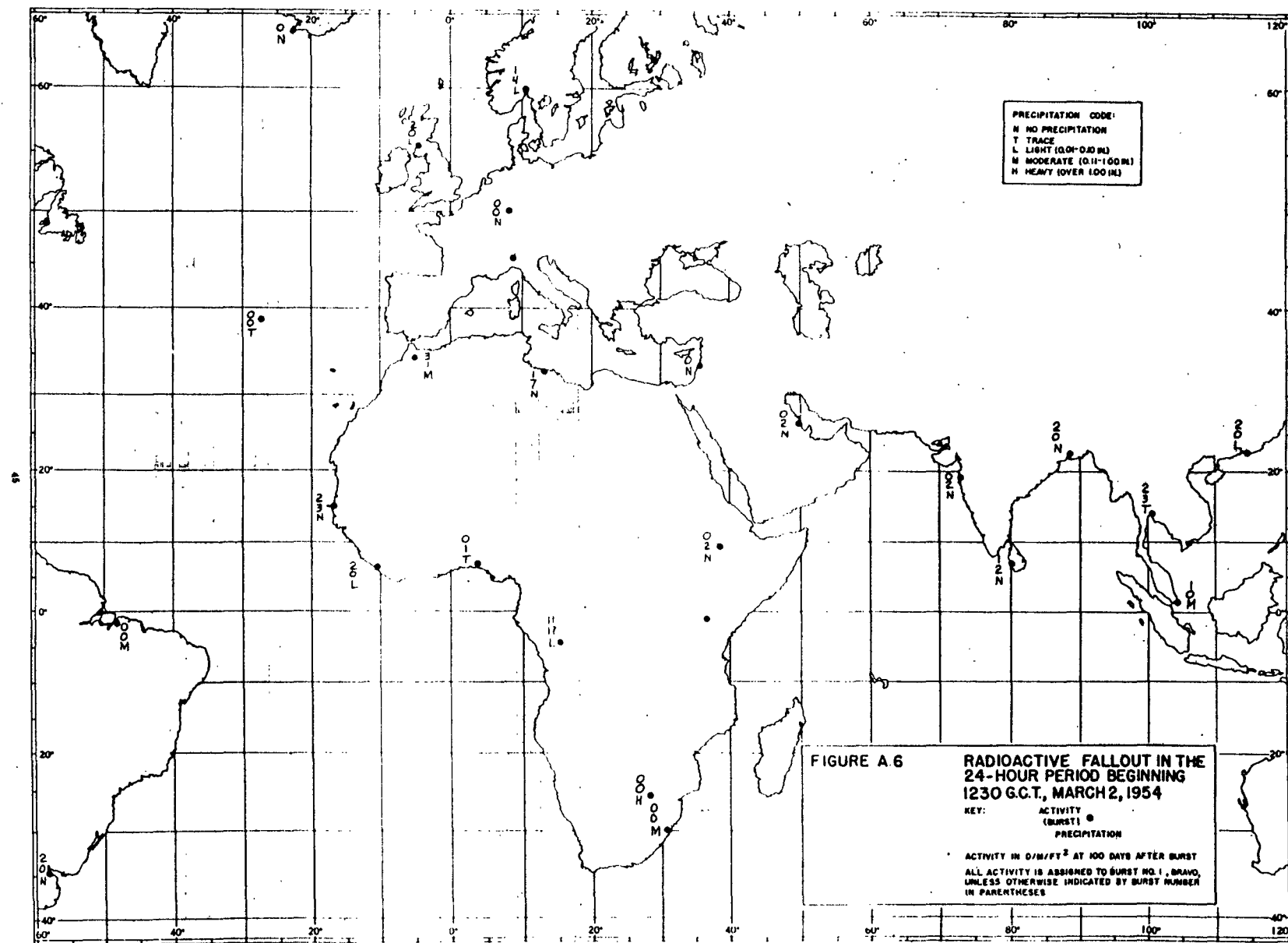


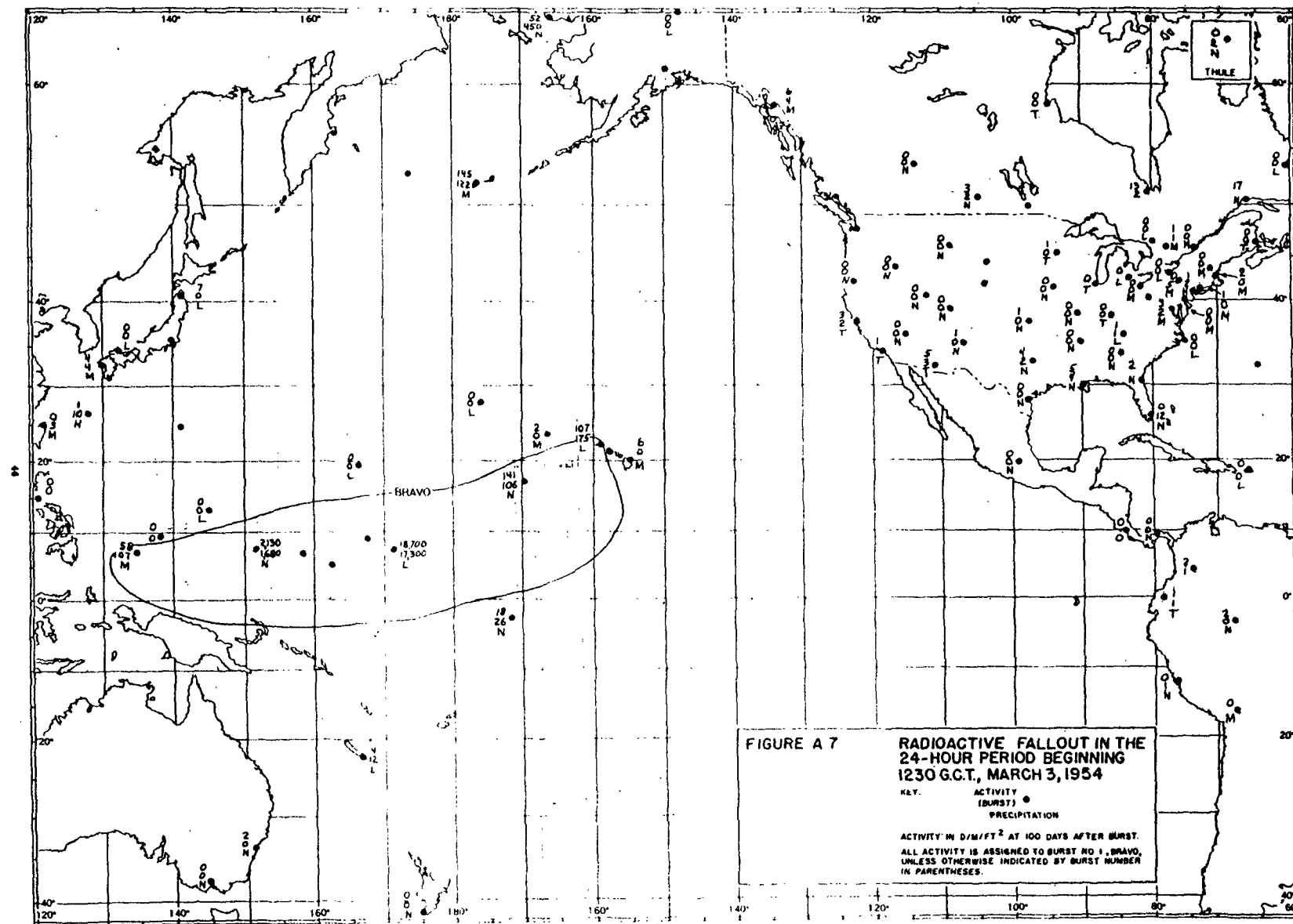


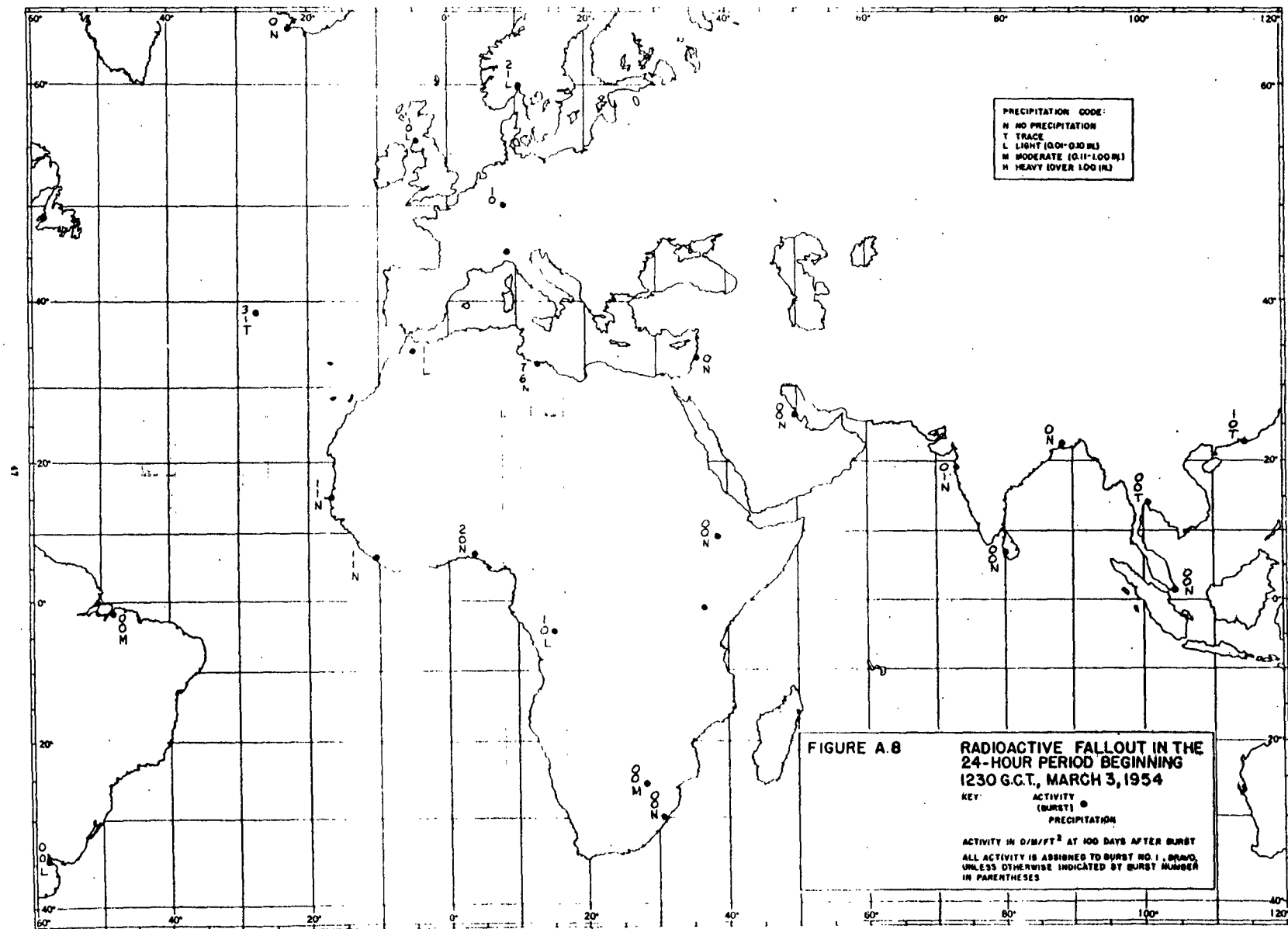


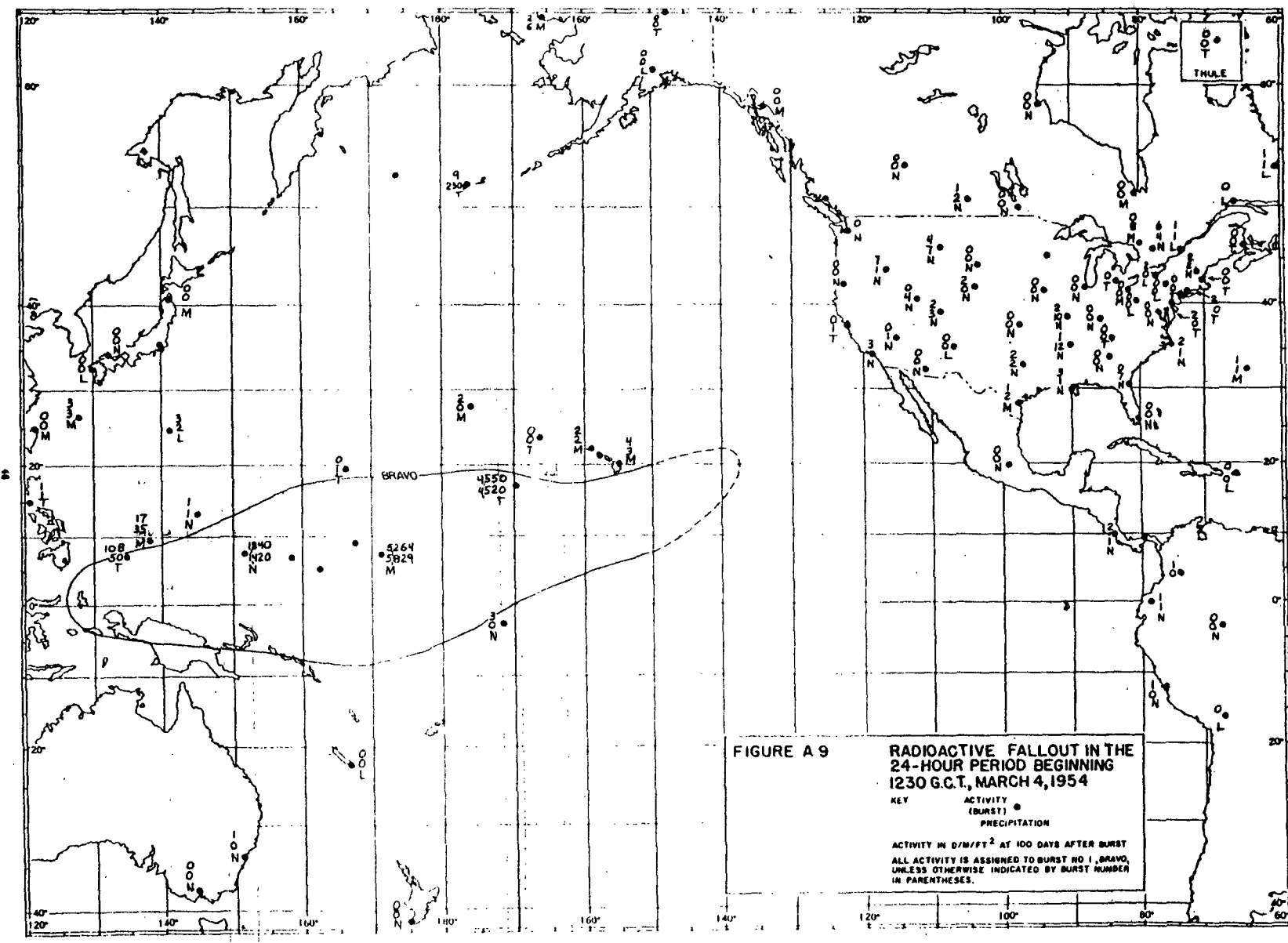


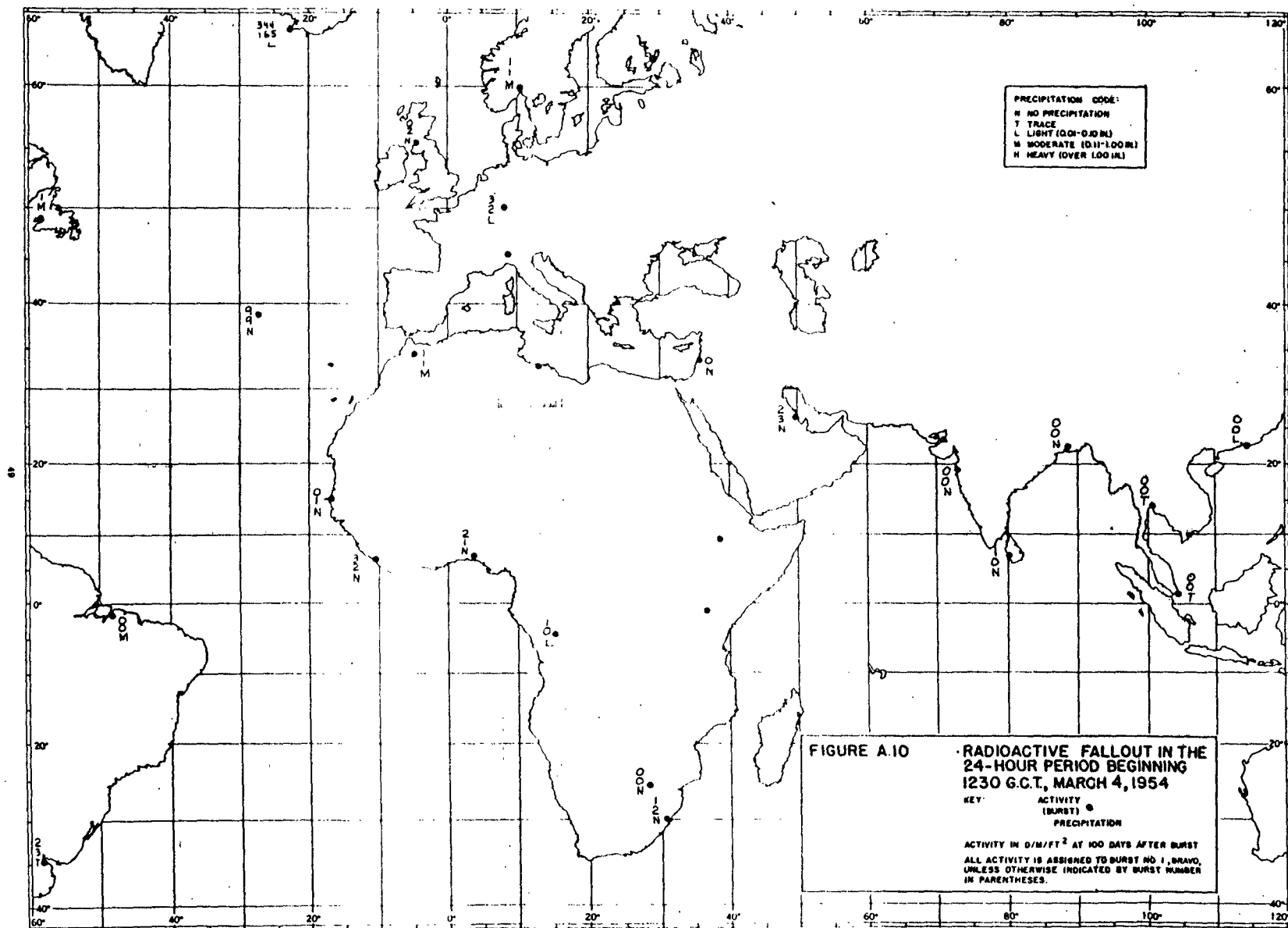


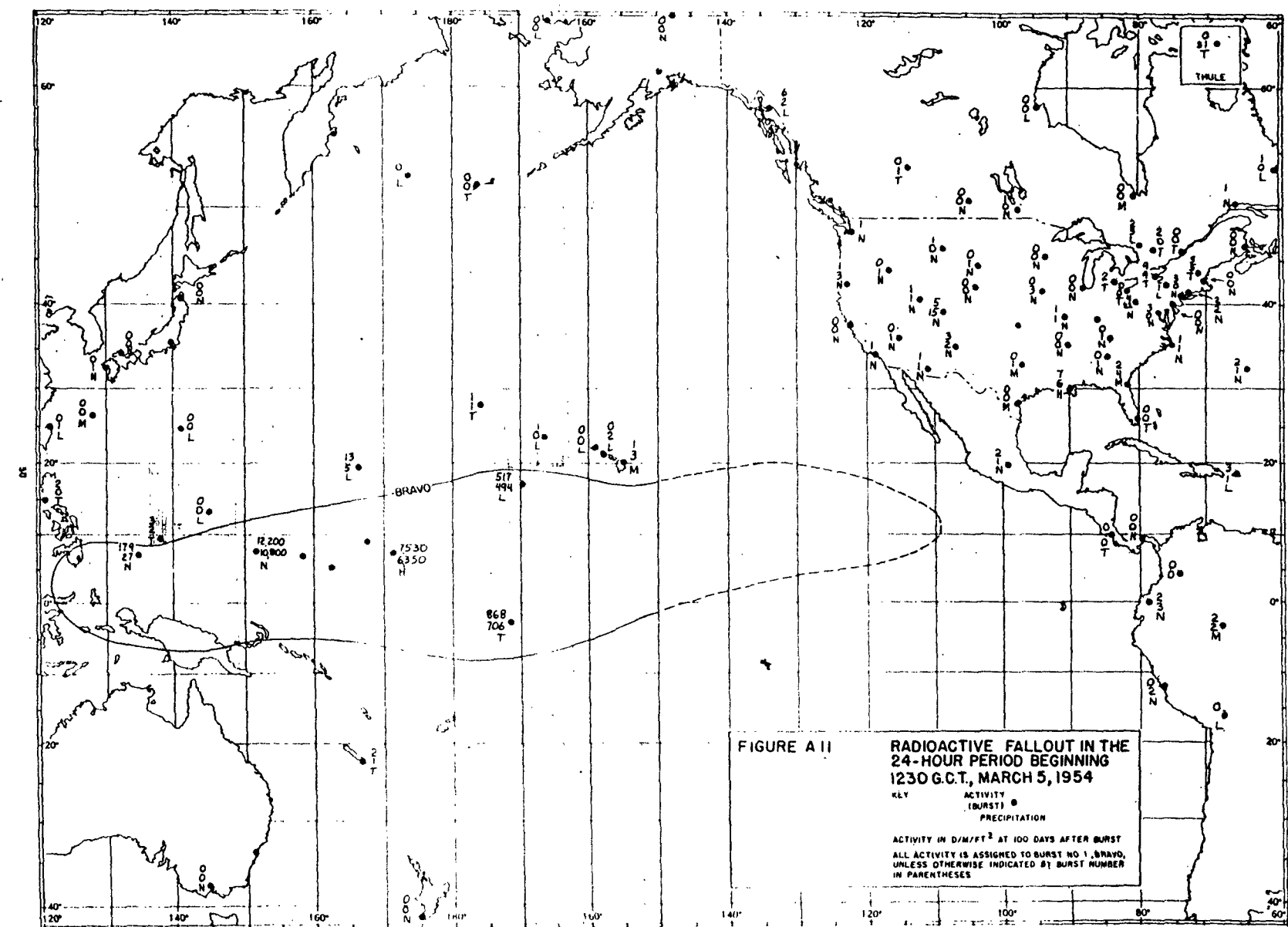


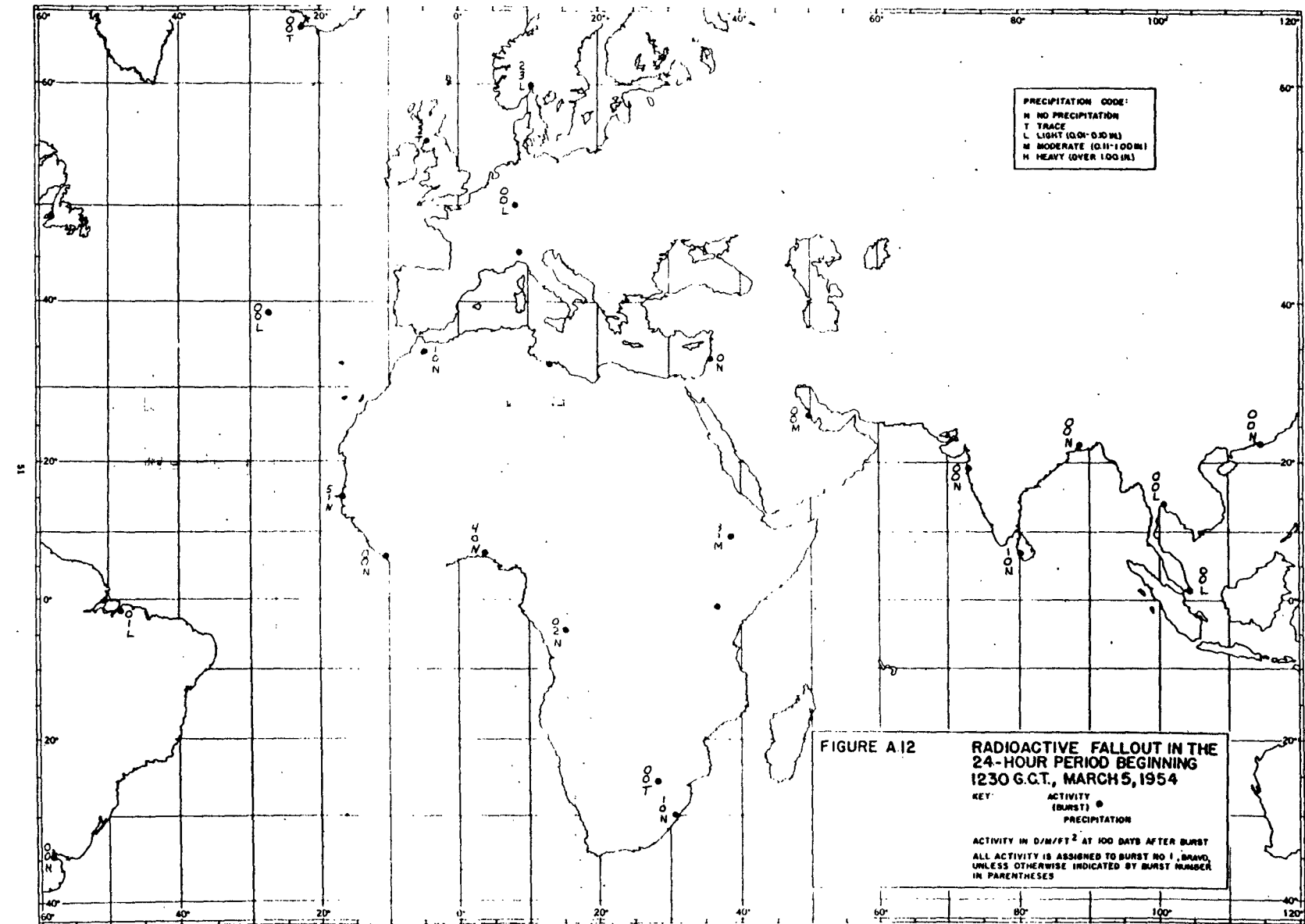


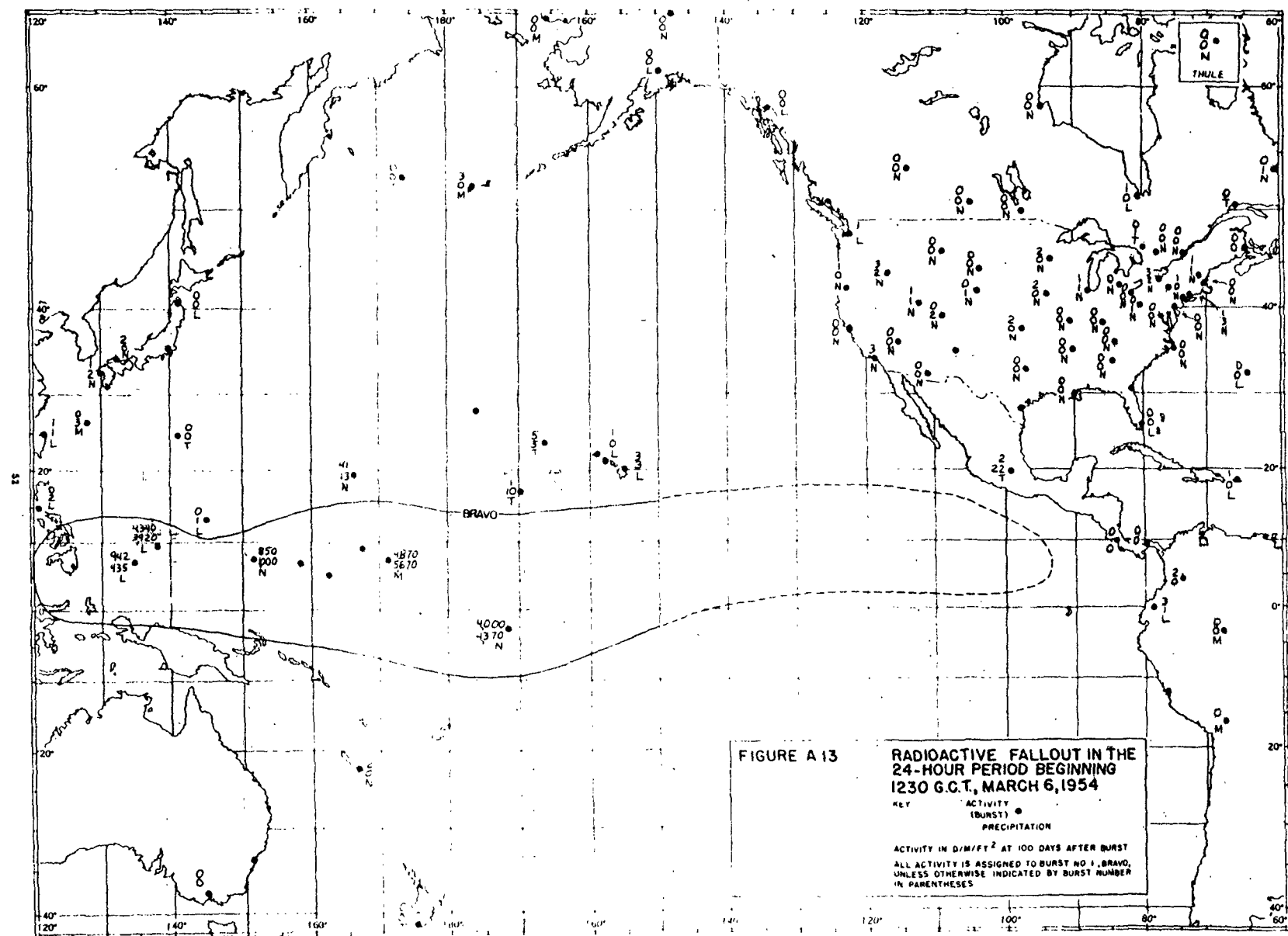


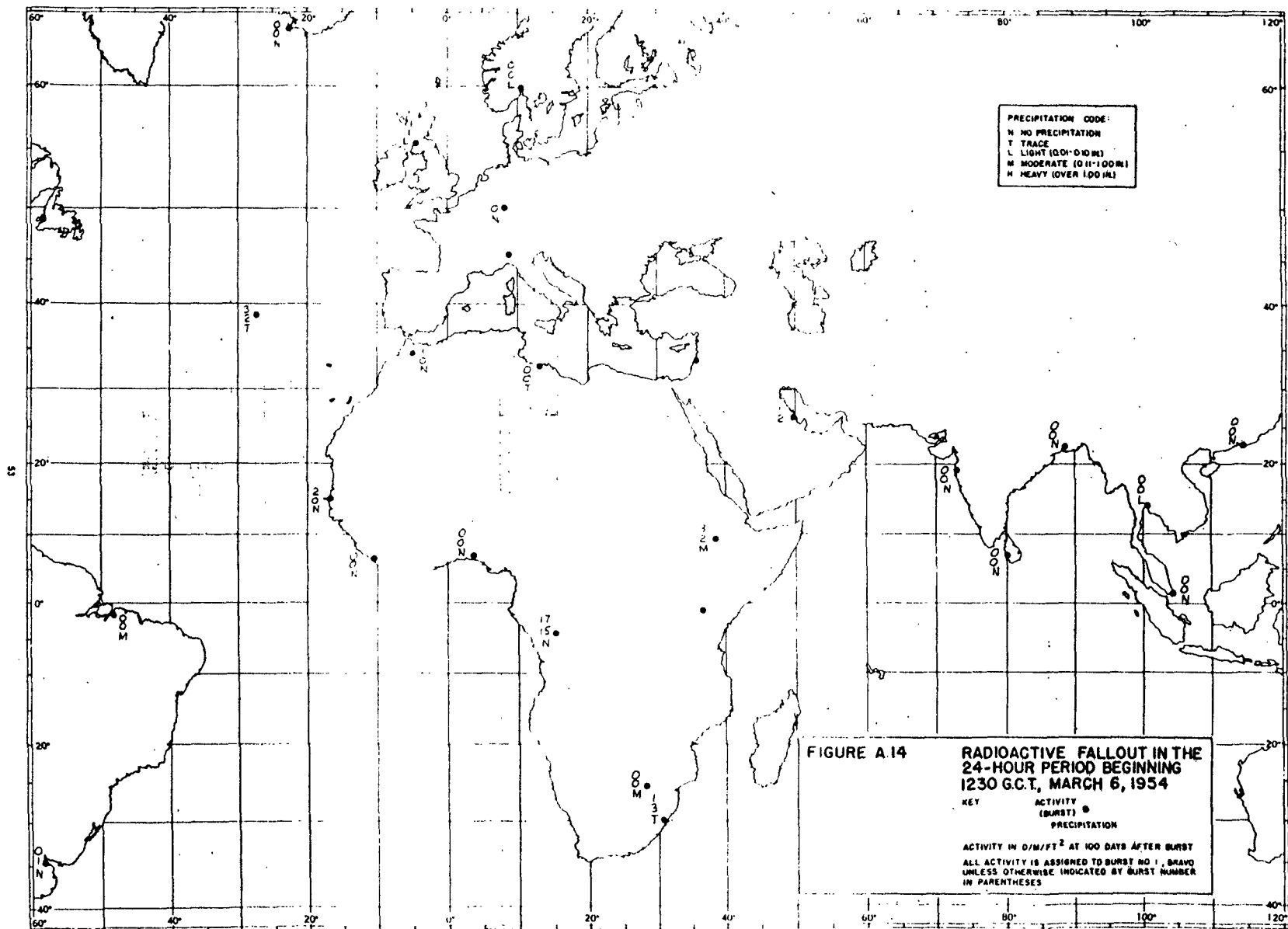












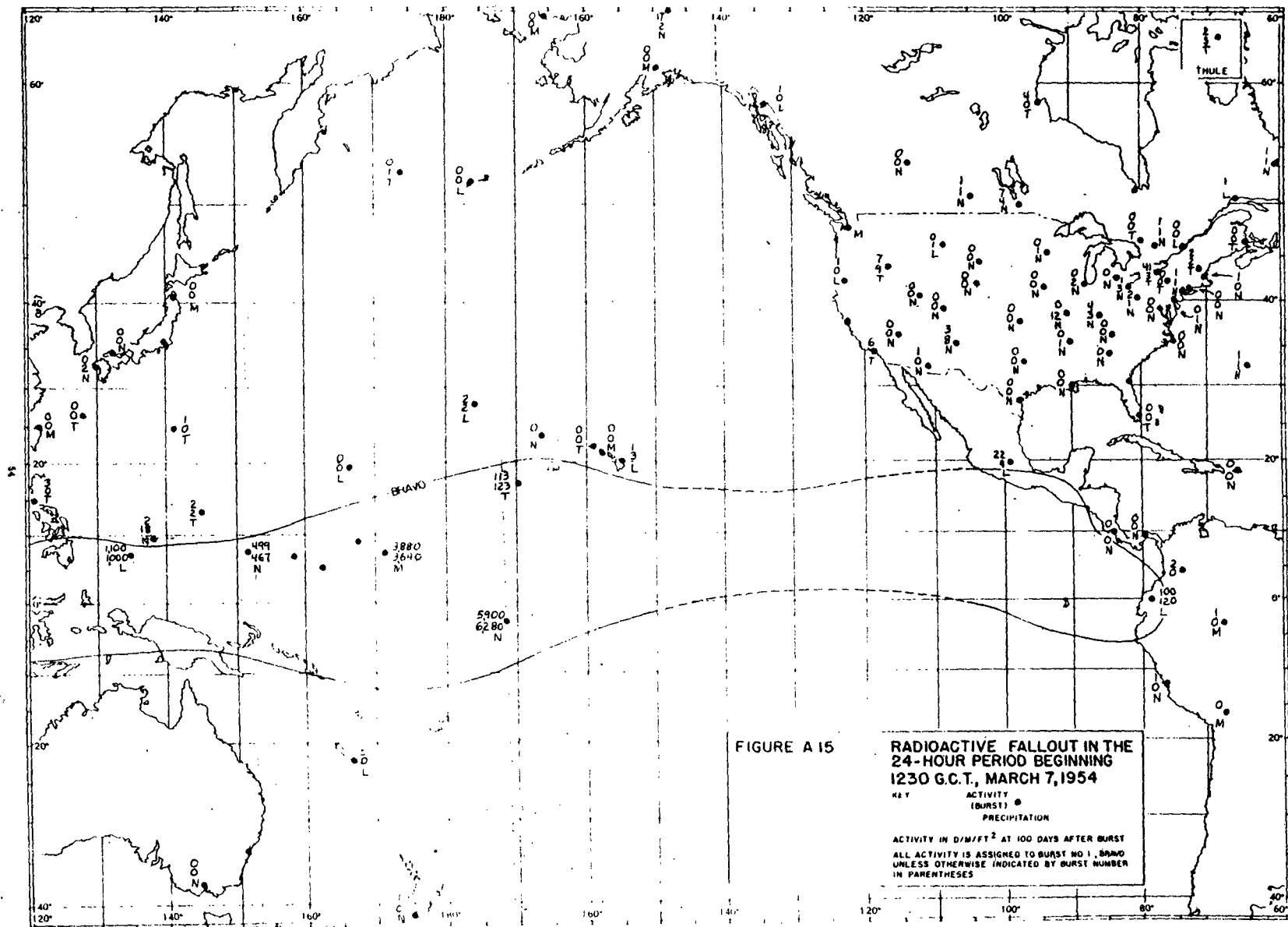
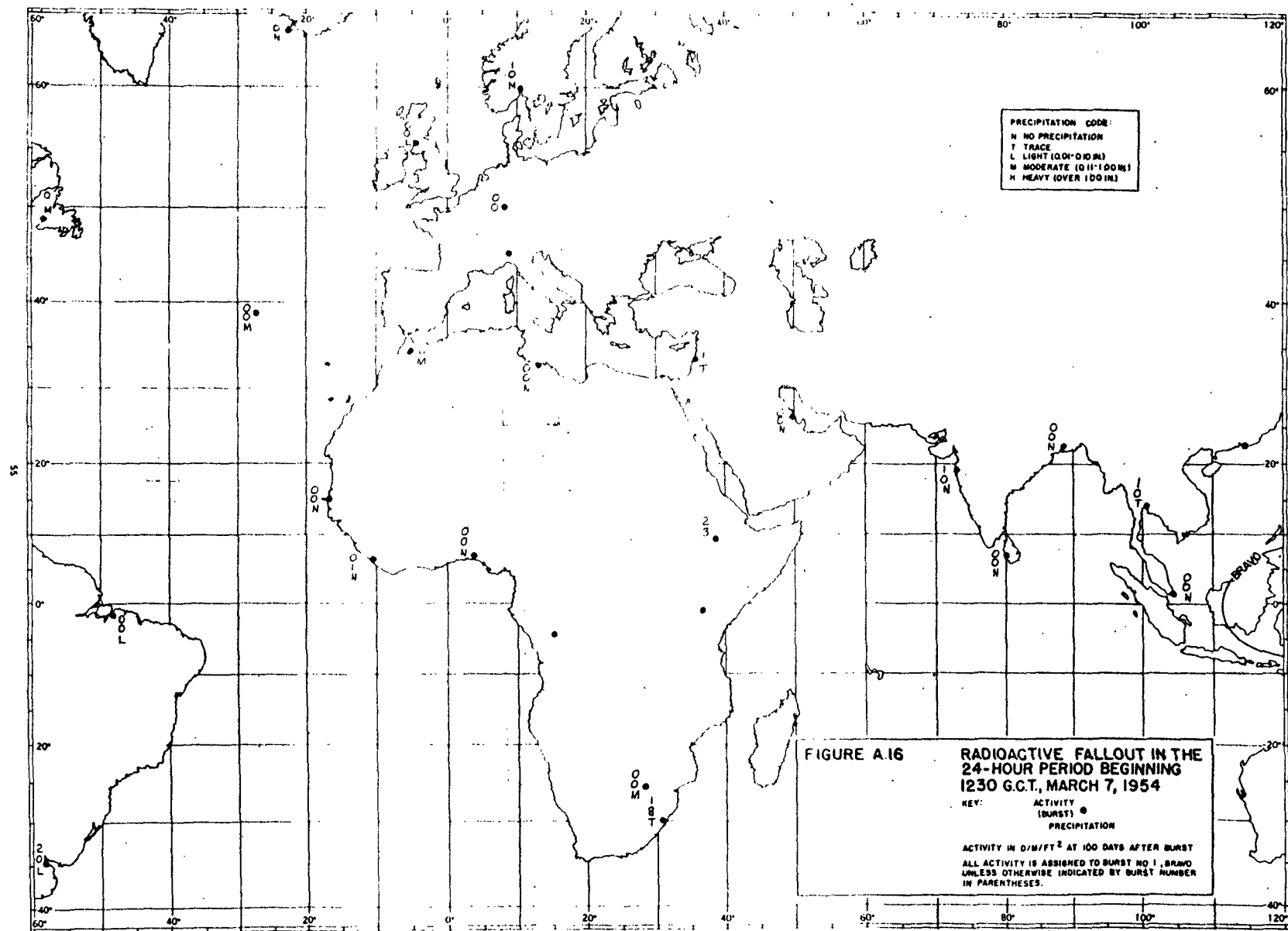


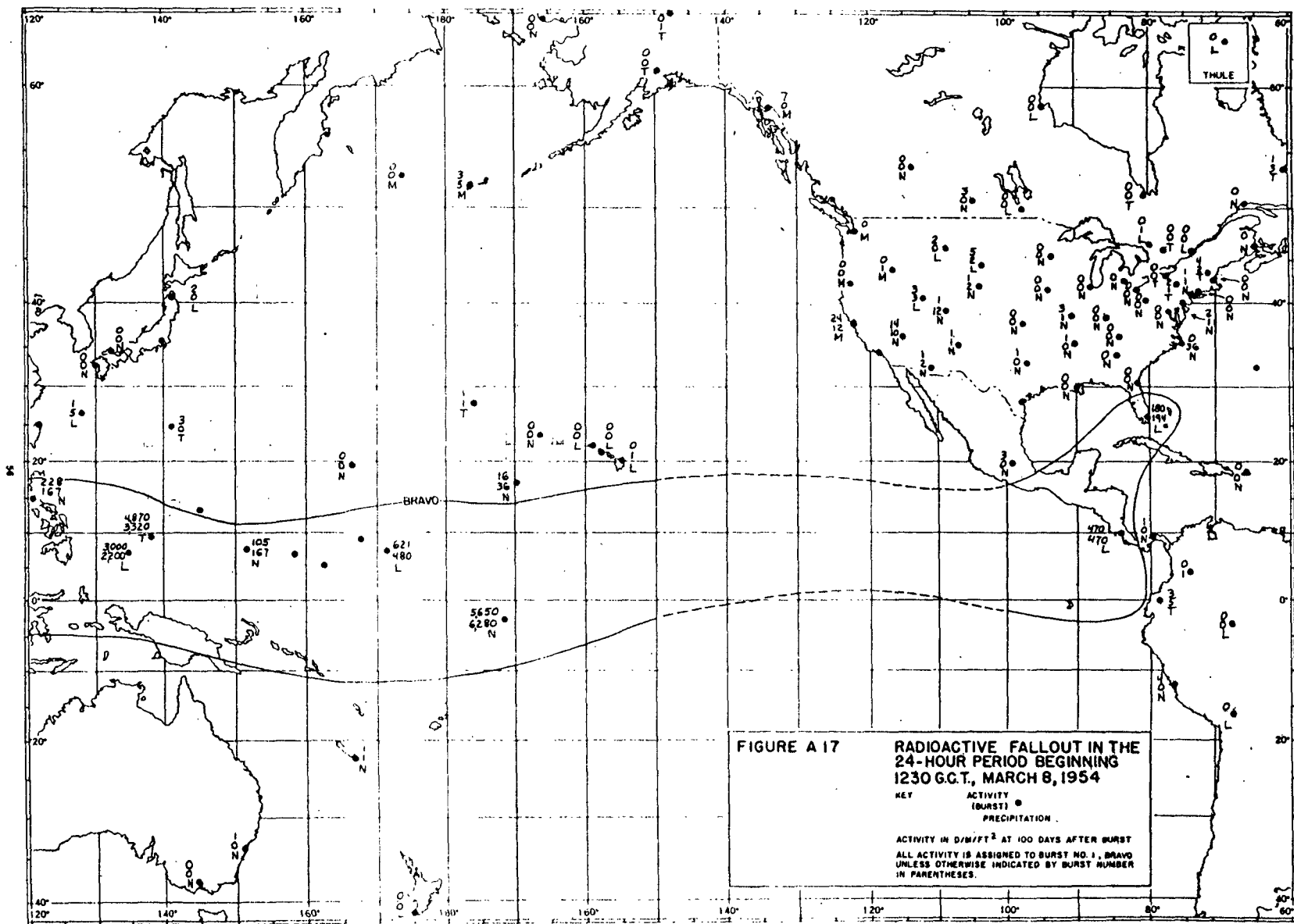
FIGURE A 15

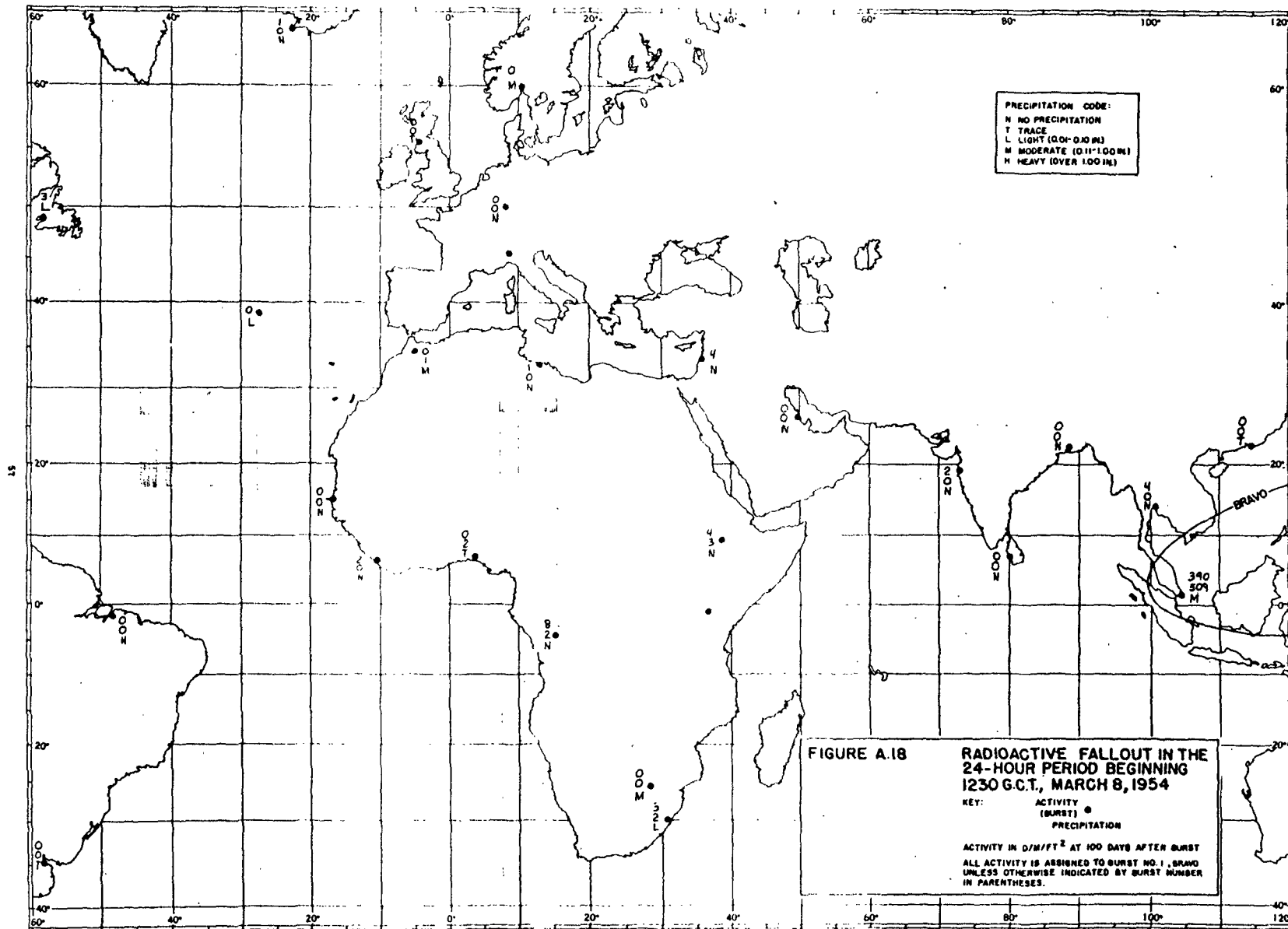
RADIOACTIVE FALLOUT IN THE
24-HOUR PERIOD BEGINNING
1230 G.C.T., MARCH 7, 1954

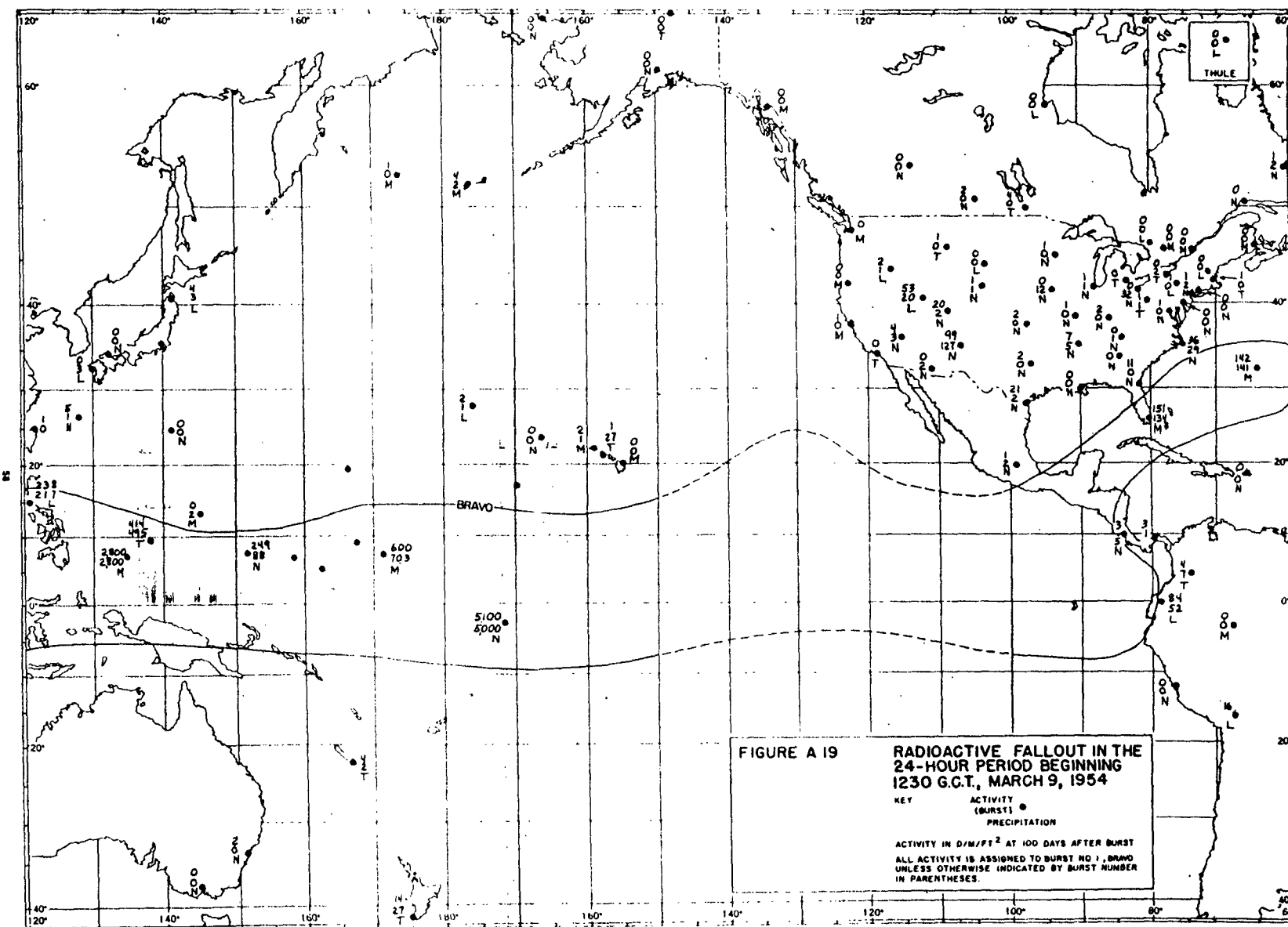
KEY
ACTIVITY
(BURST) •
PRECIPITATION

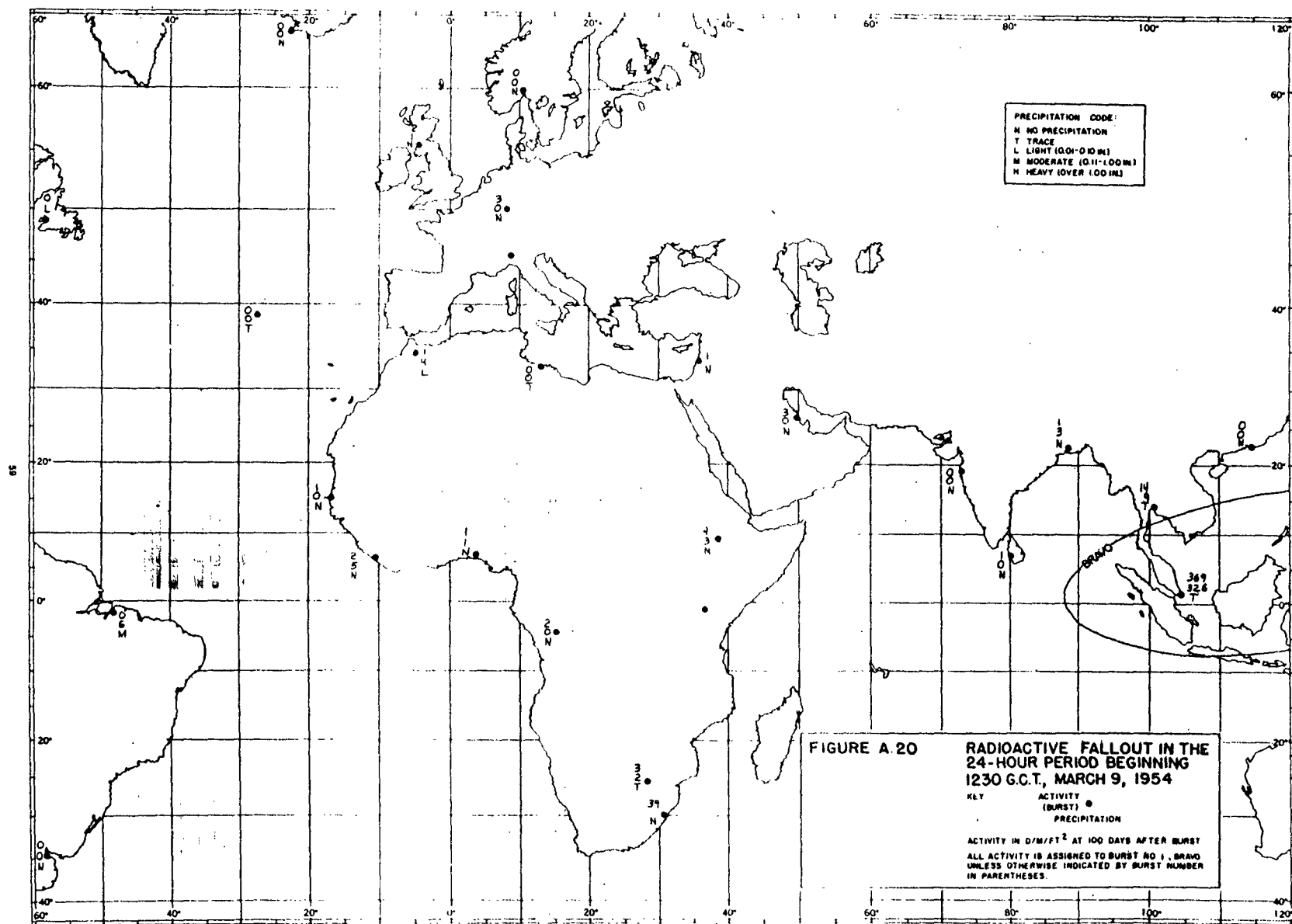
ACTIVITY IN D/M/FT² AT 100 DAYS AFTER BURST
ALL ACTIVITY IS ASSIGNED TO BURST NO. 1, BAND
UNLESS OTHERWISE INDICATED BY BURST NUMBER
IN PARENTHESES











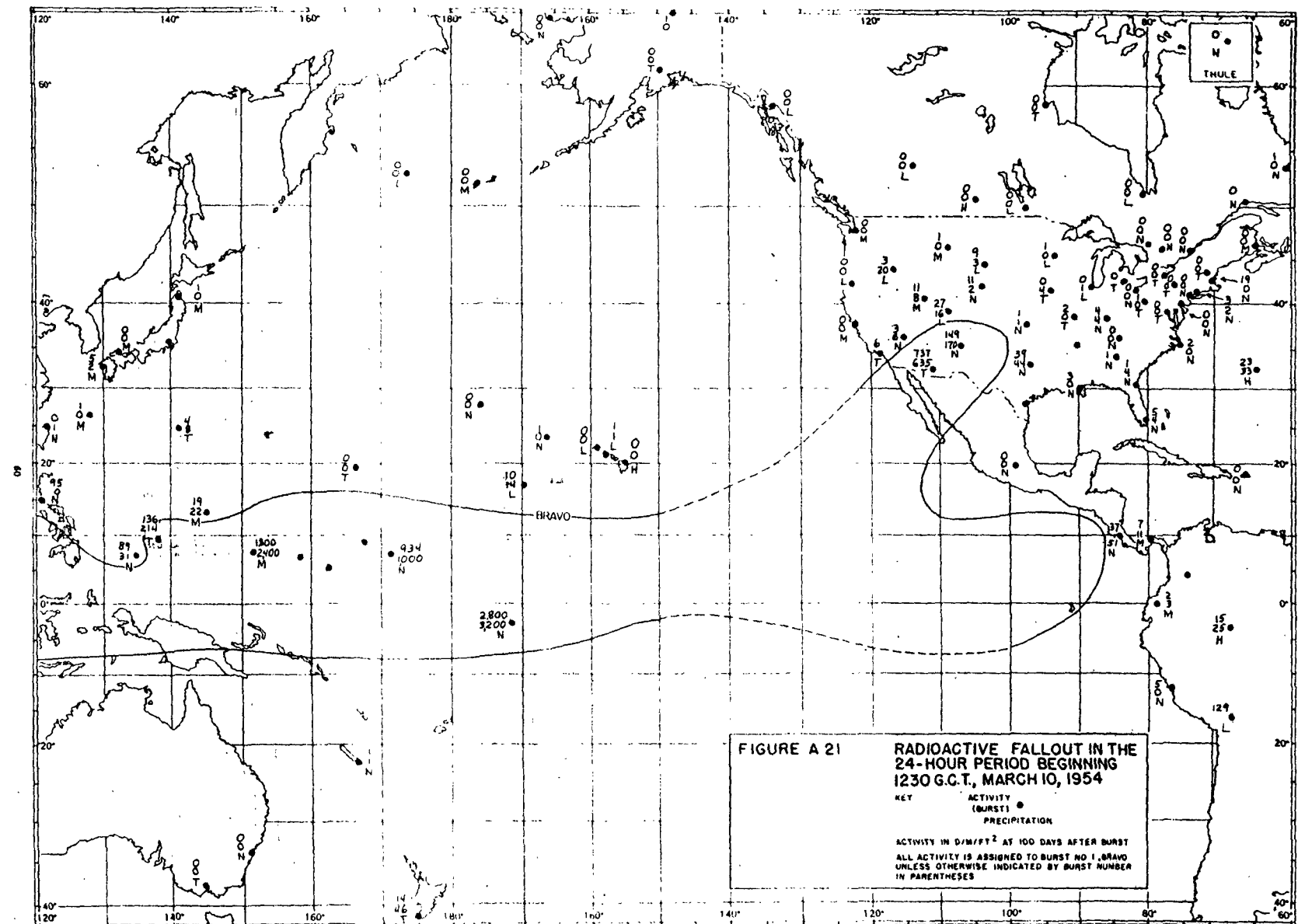
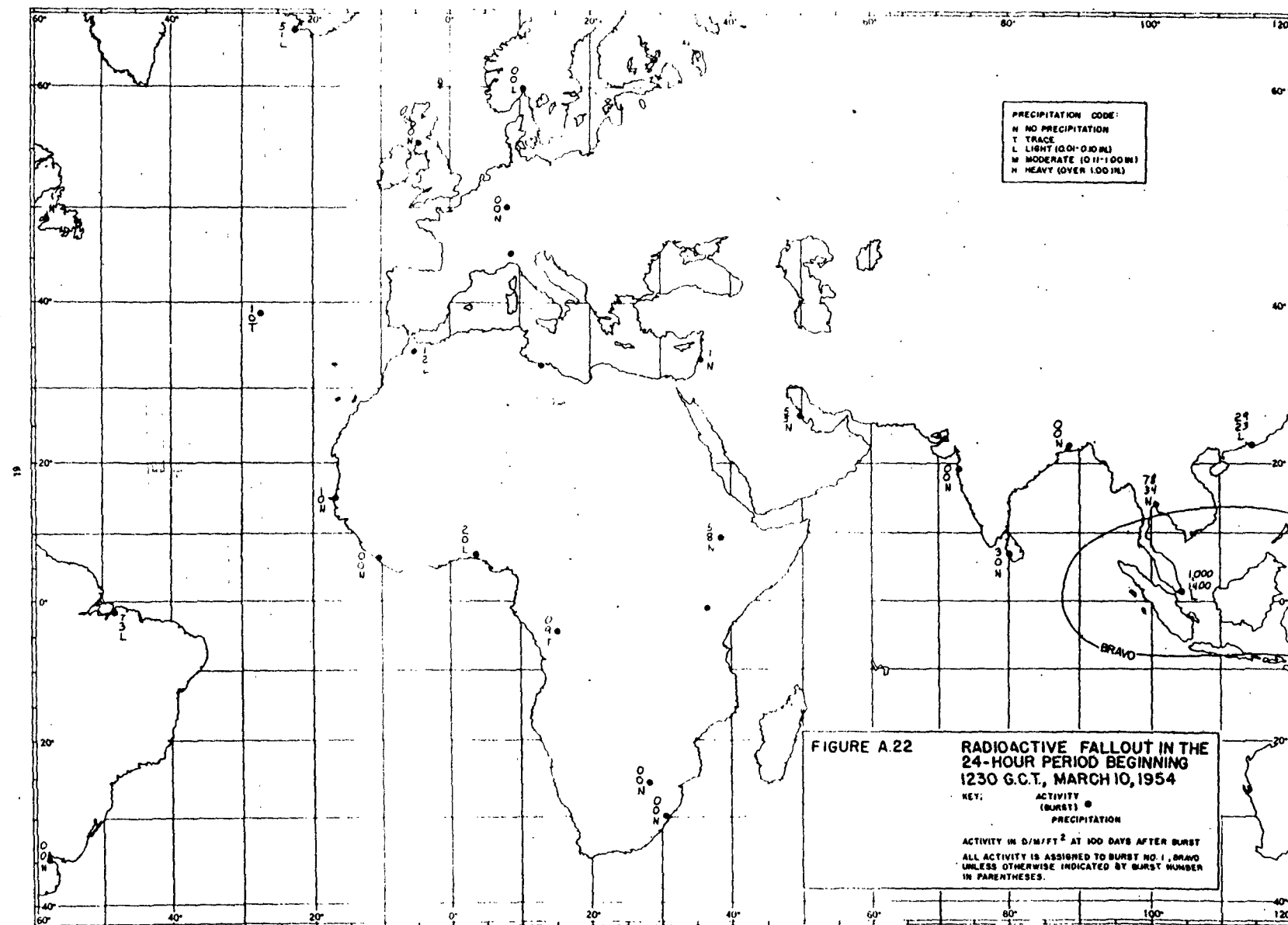
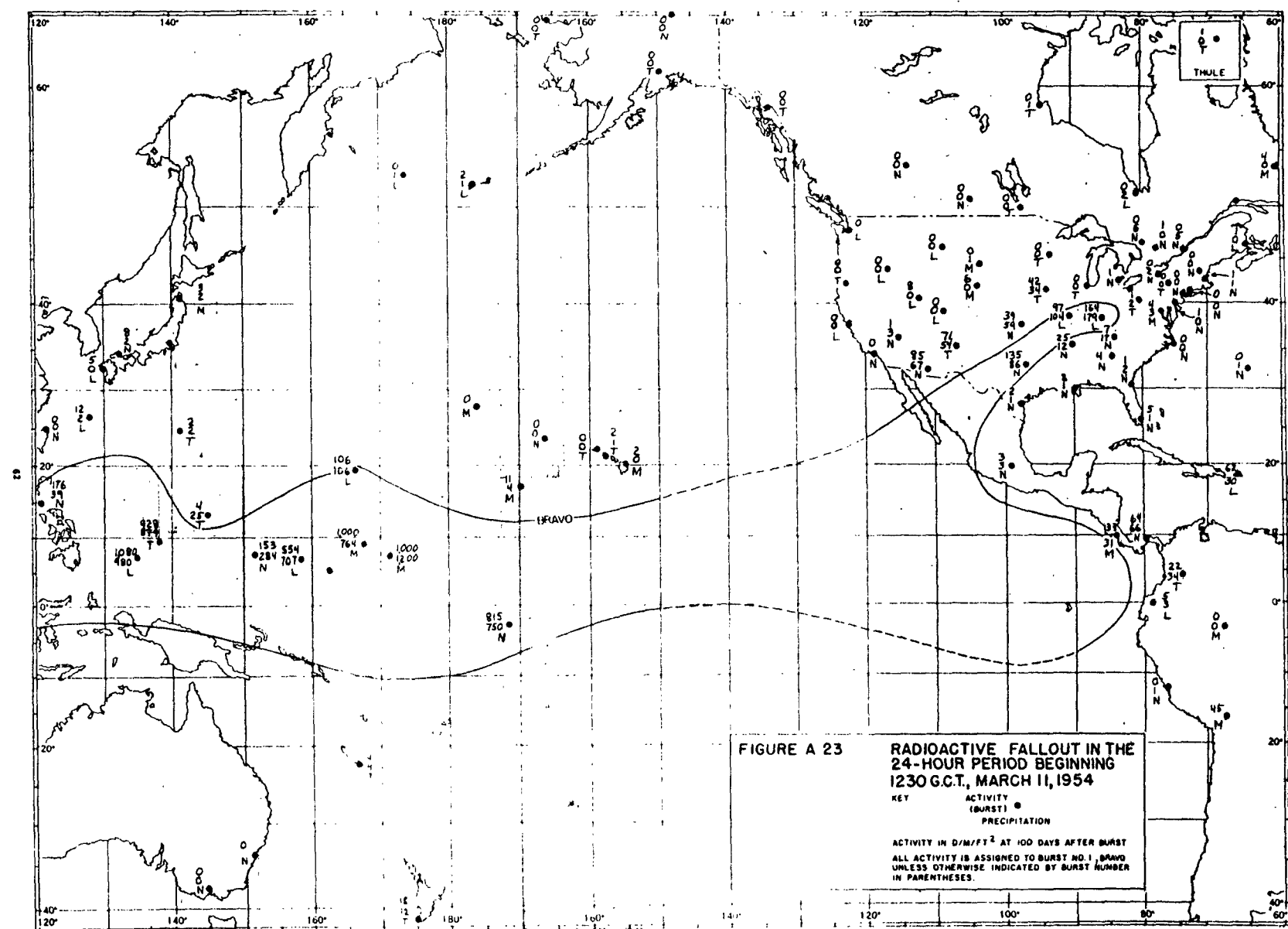
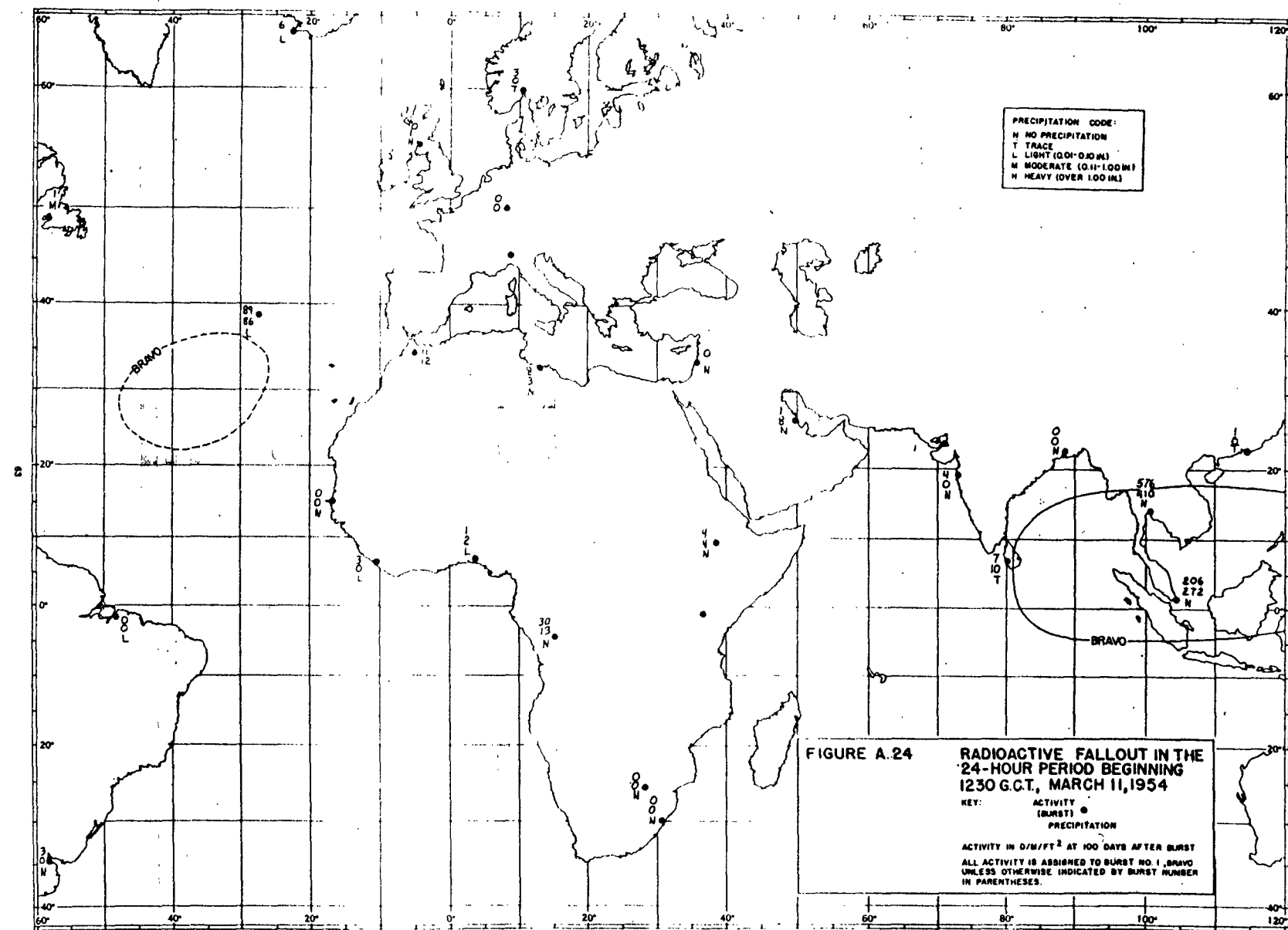
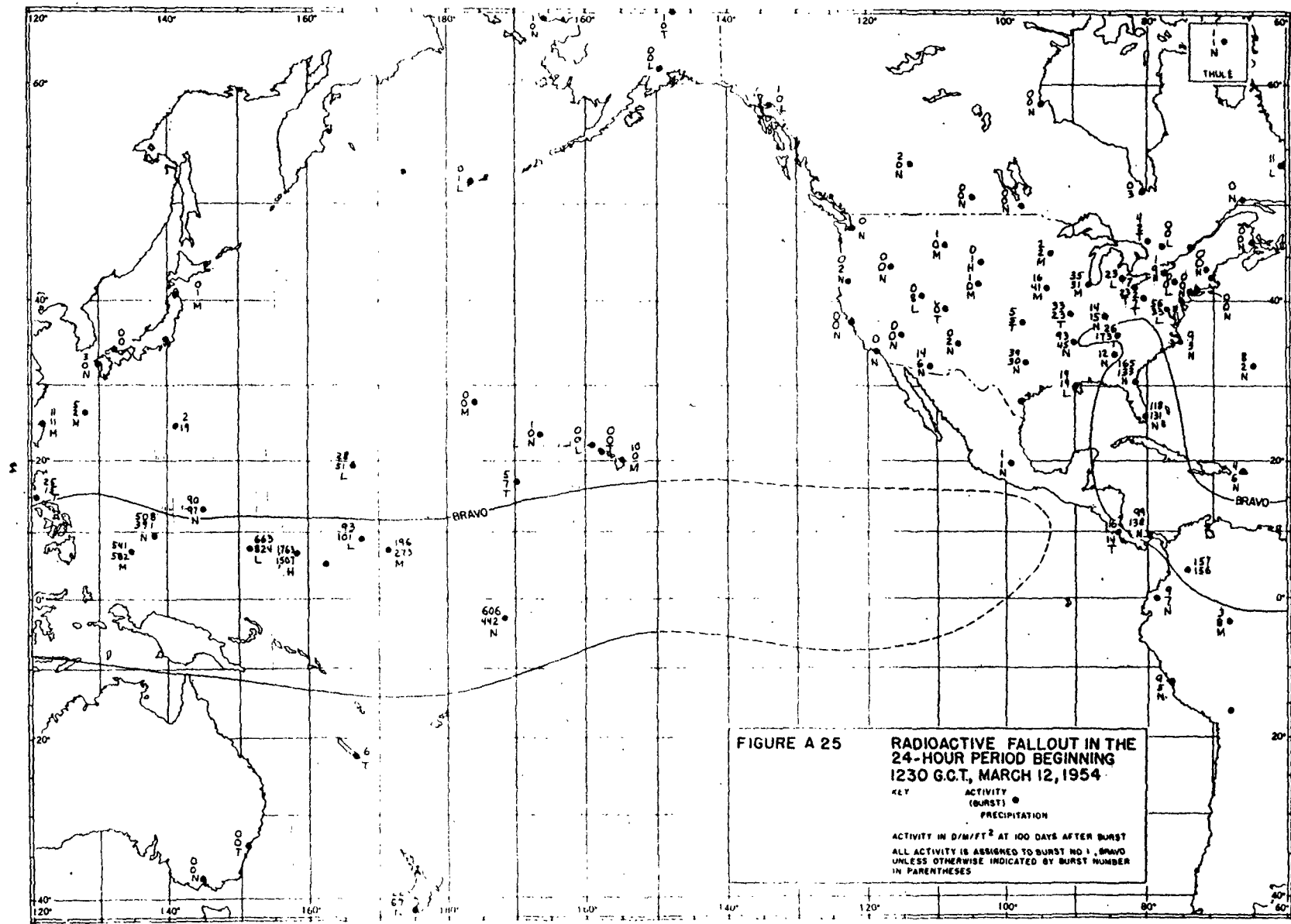


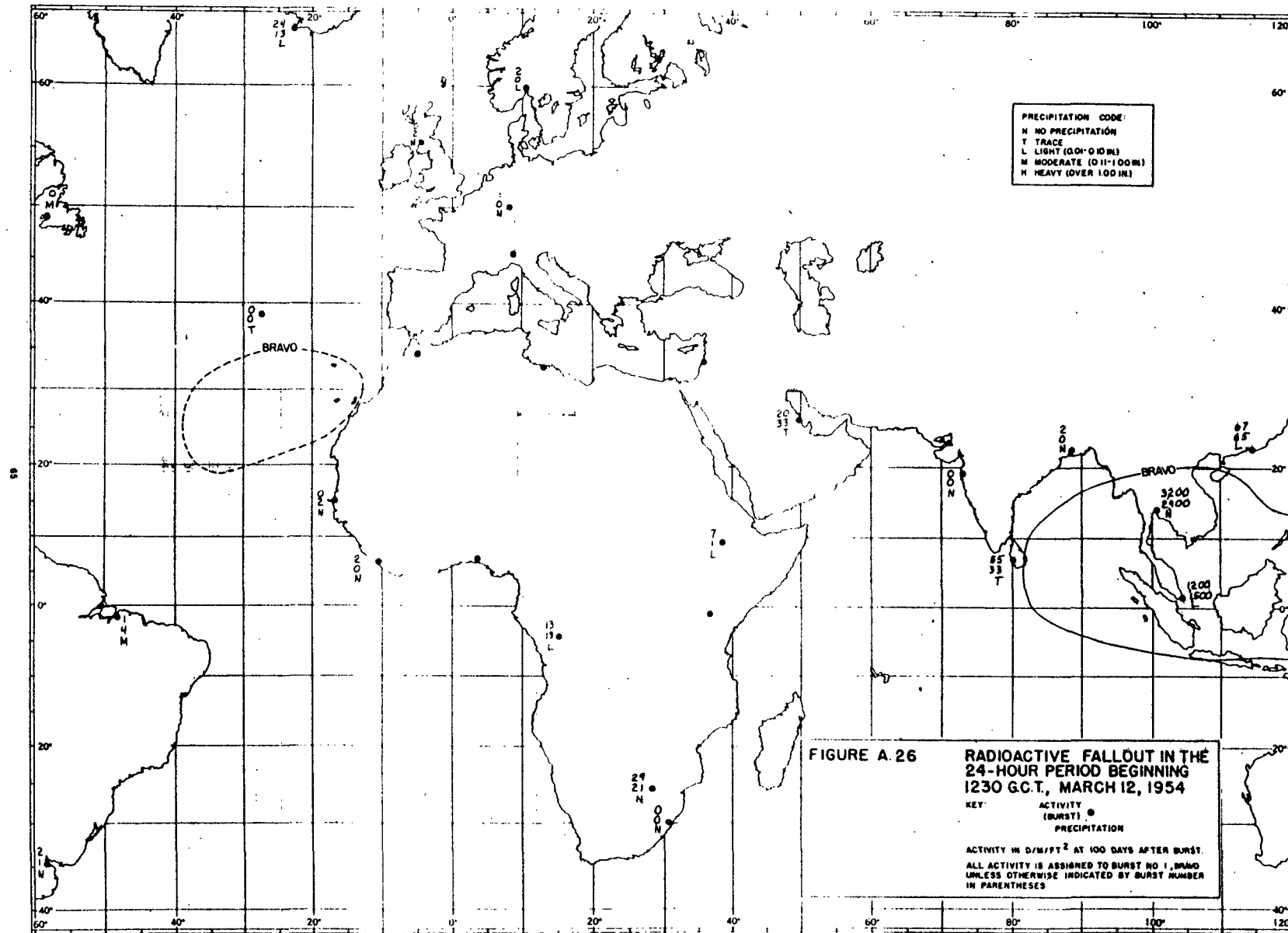
FIGURE A 21 **RADIOACTIVE FALLOUT IN THE
24-HOUR PERIOD BEGINNING
1230 G.C.T., MARCH 10, 1954**

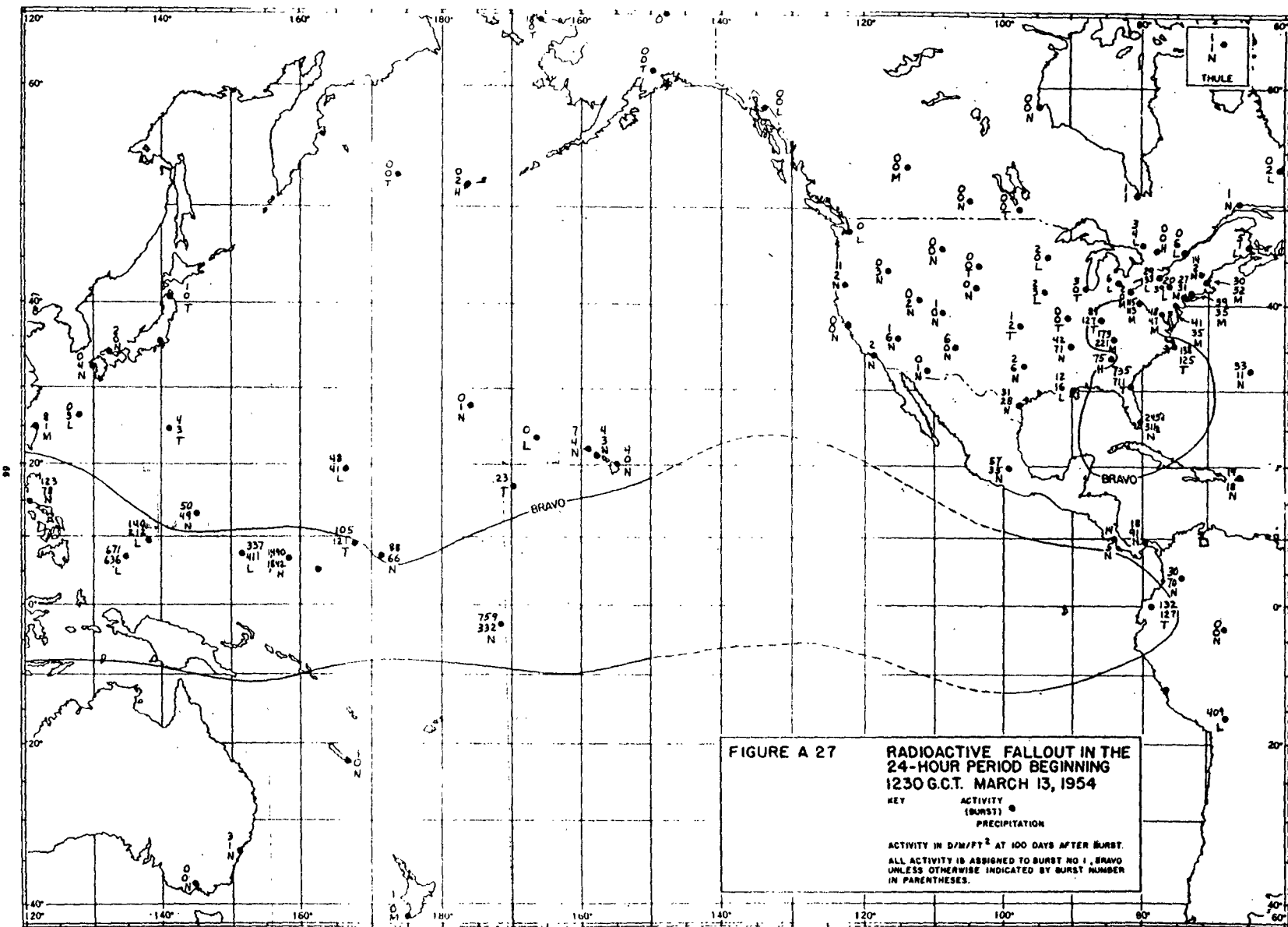


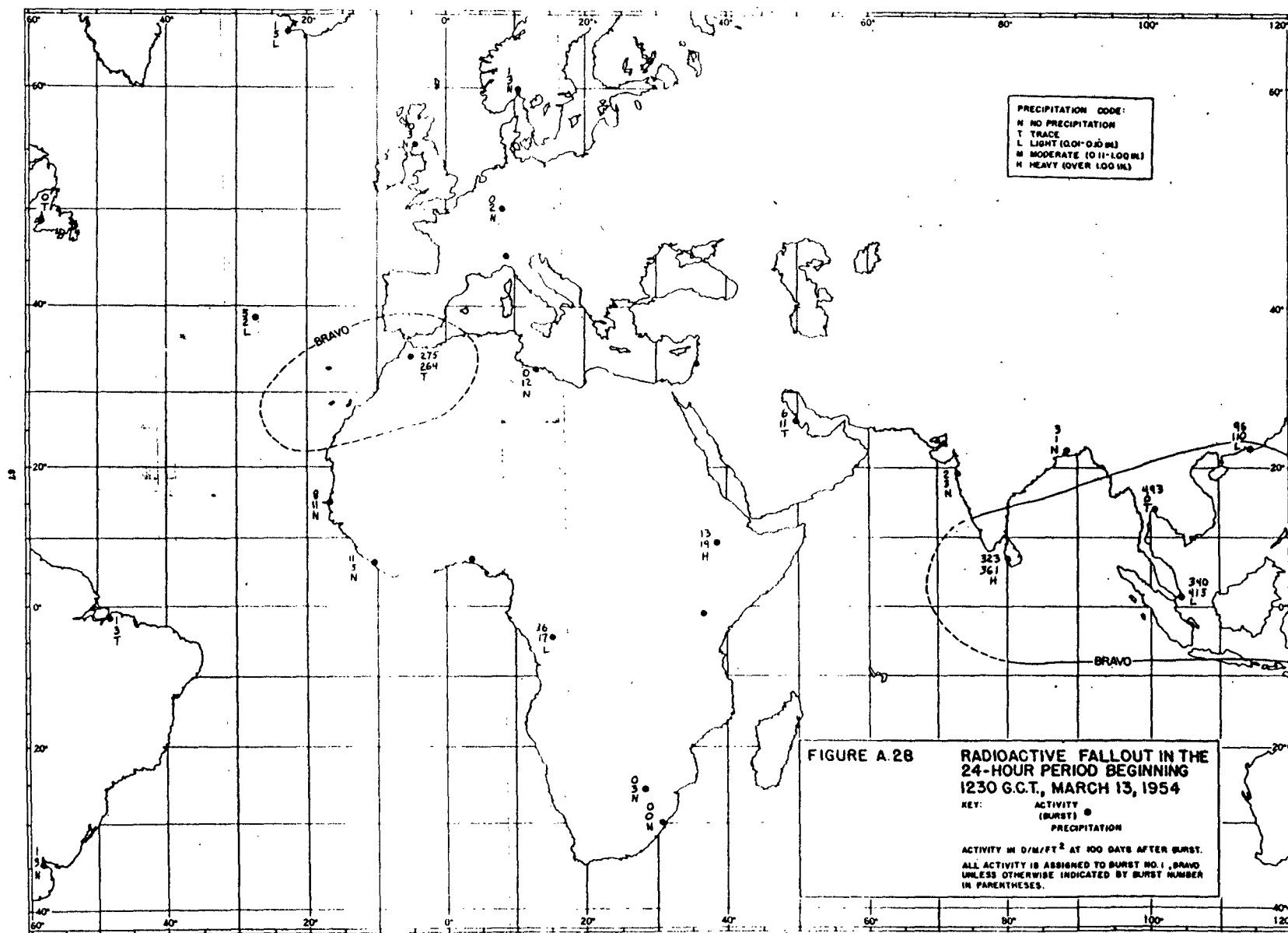












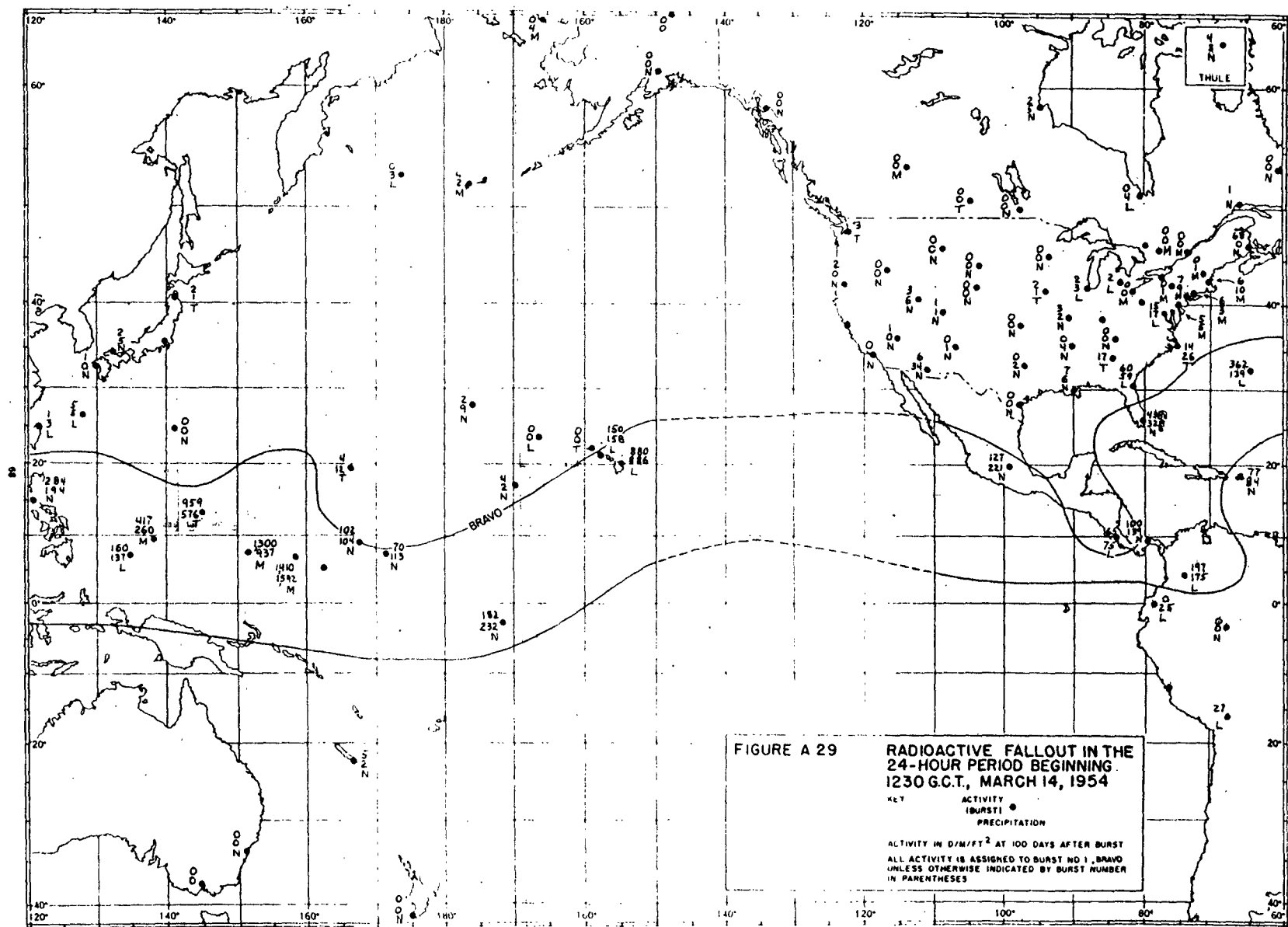
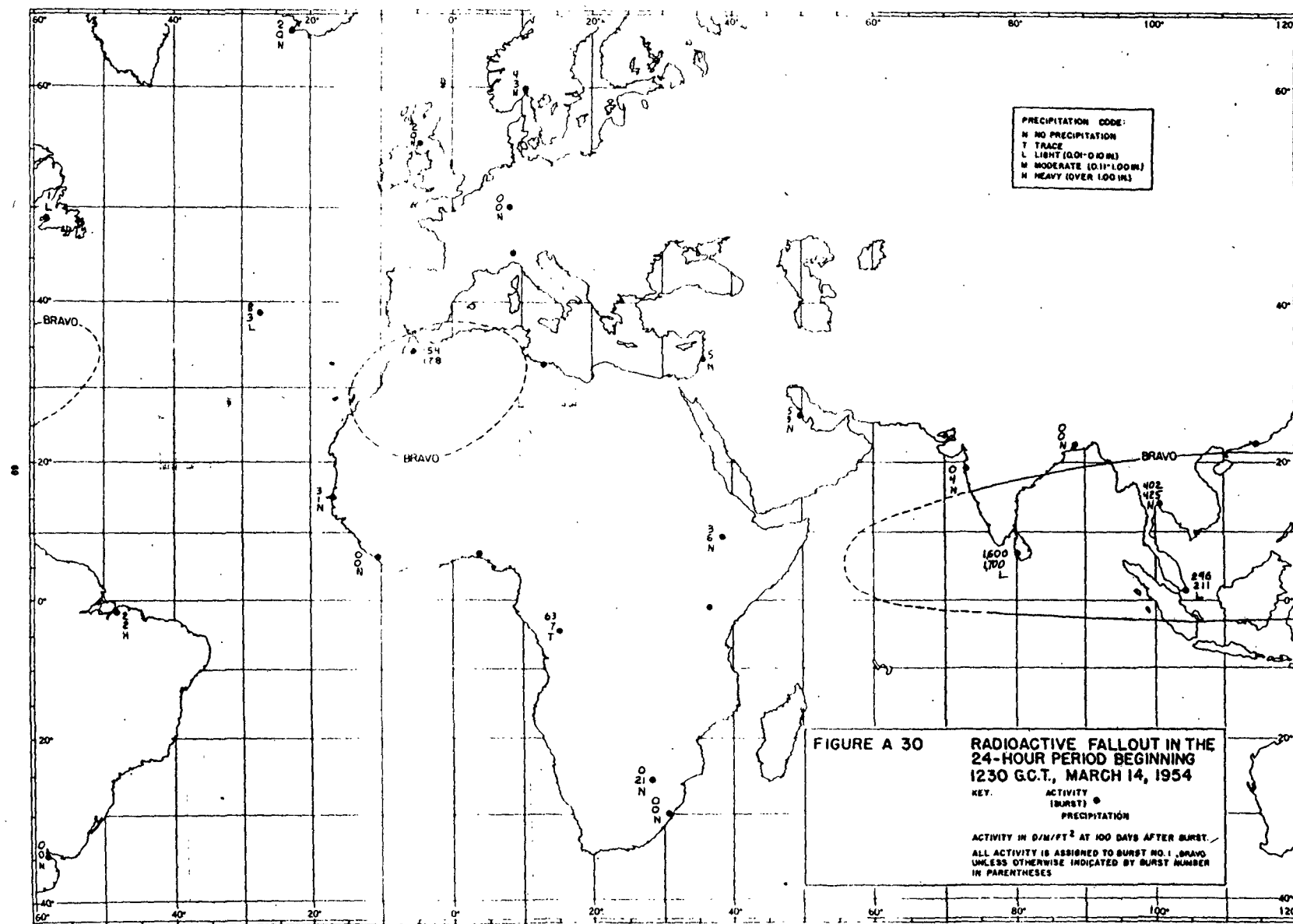


FIGURE A 29
RADIOACTIVE FALLOUT IN THE
24-HOUR PERIOD BEGINNING
1230 G.C.T., MARCH 14, 1954

$\mu\text{R}/\text{hr}$ ACTIVITY
BURST PRECIPITATION

ACTIVITY IN $\mu\text{R}/\text{hr}$ AT 100 DAYS AFTER BURST
ALL ACTIVITY IS ASSIGNED TO BURST NO 1, BRAVO
UNLESS OTHERWISE INDICATED BY BURST NUMBER
IN PARENTHESES



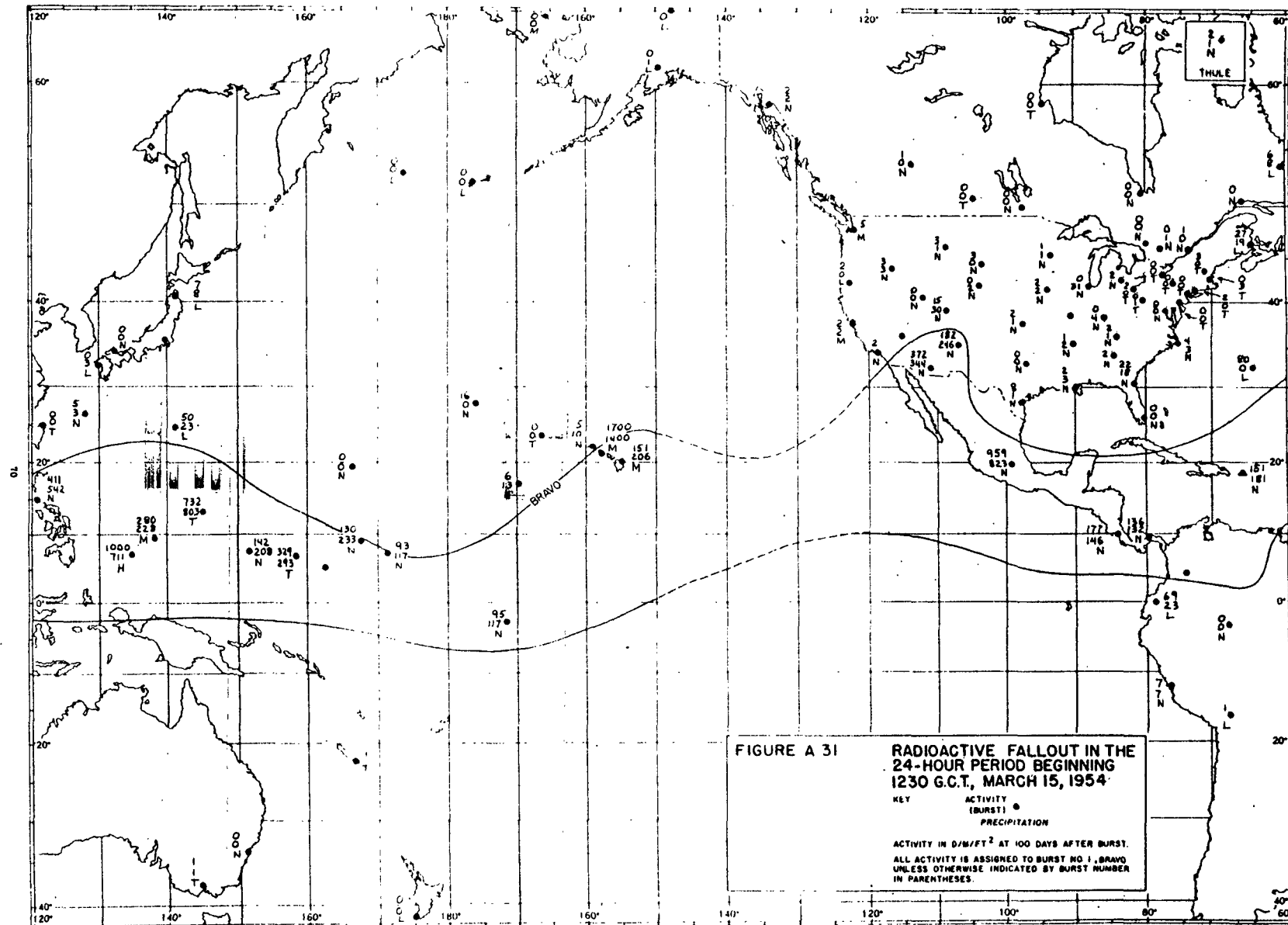
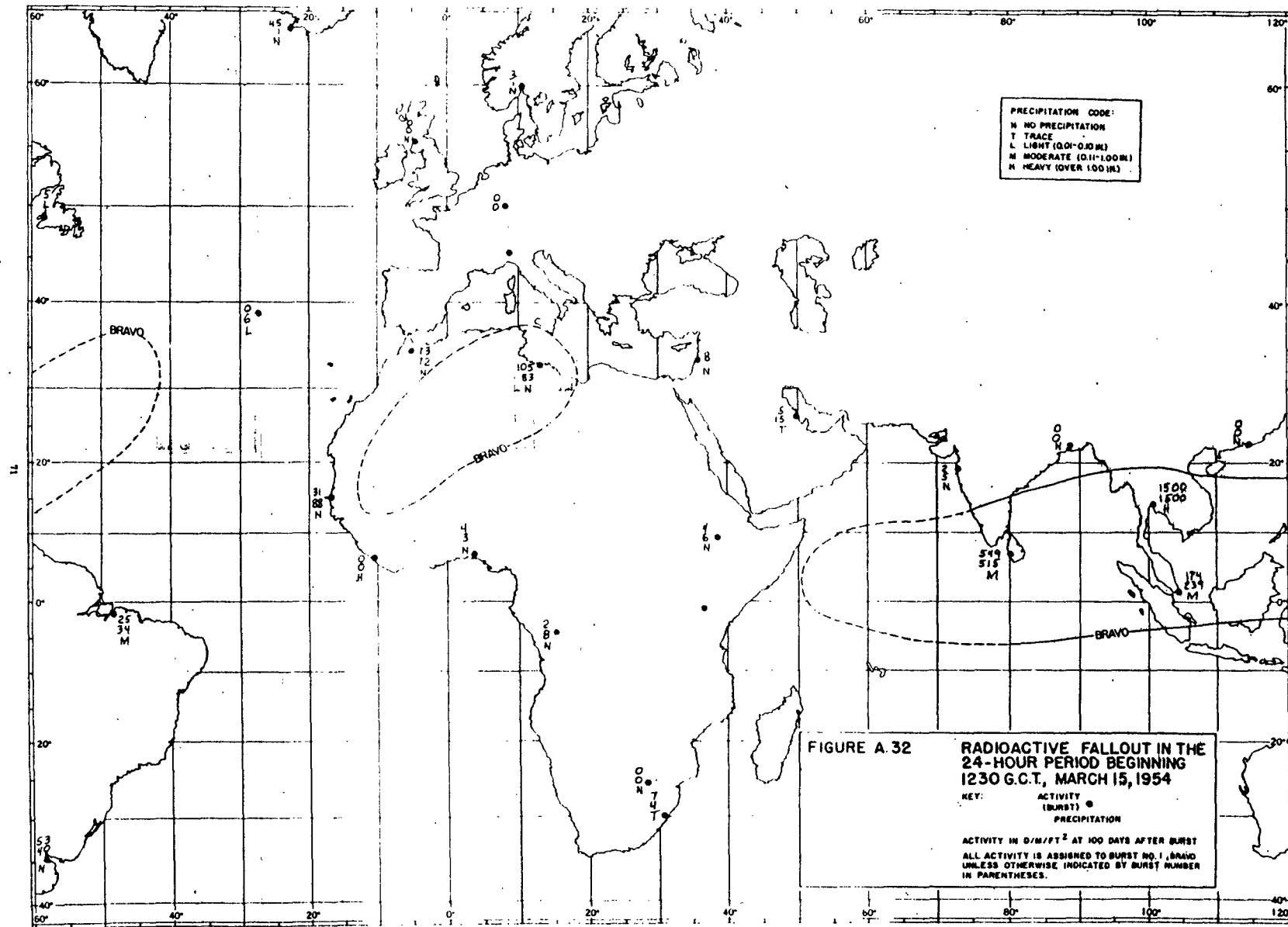


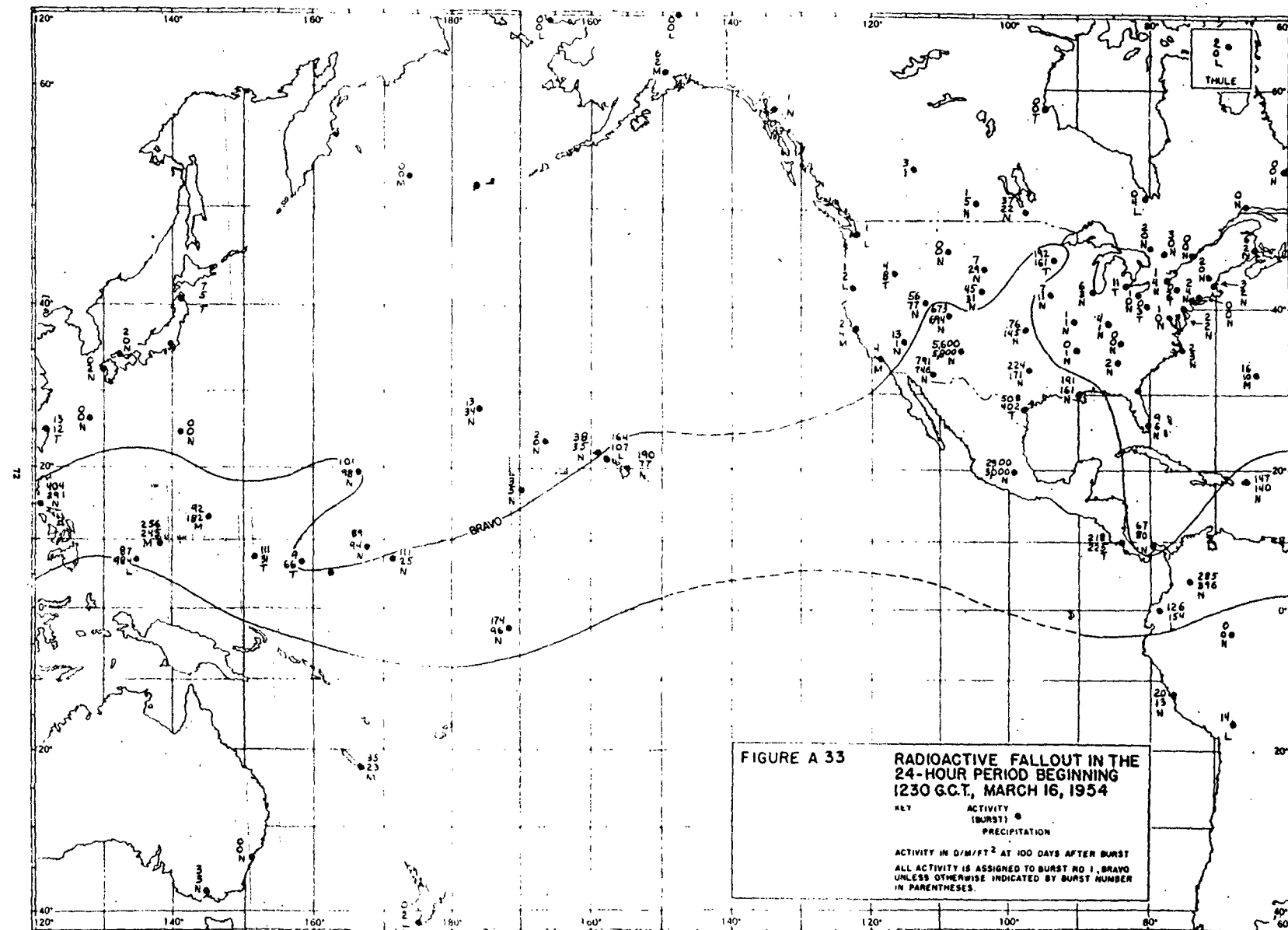
FIGURE A 31

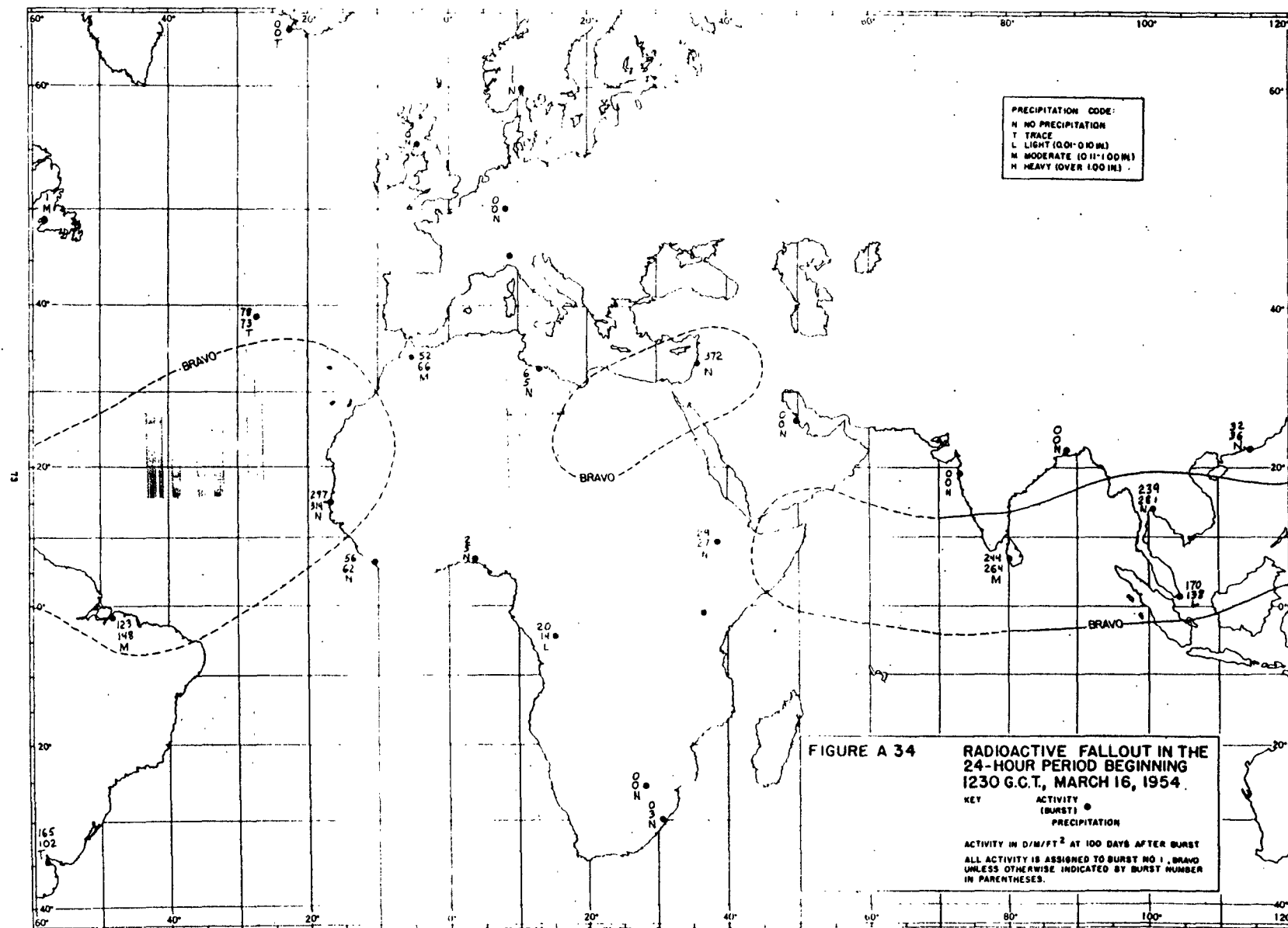
RADIOACTIVE FALLOUT IN THE
24-HOUR PERIOD BEGINNING
1230 G.C.T., MARCH 15, 1954

KEY ACTIVITY
(BURST) ●
PRECIPITATION

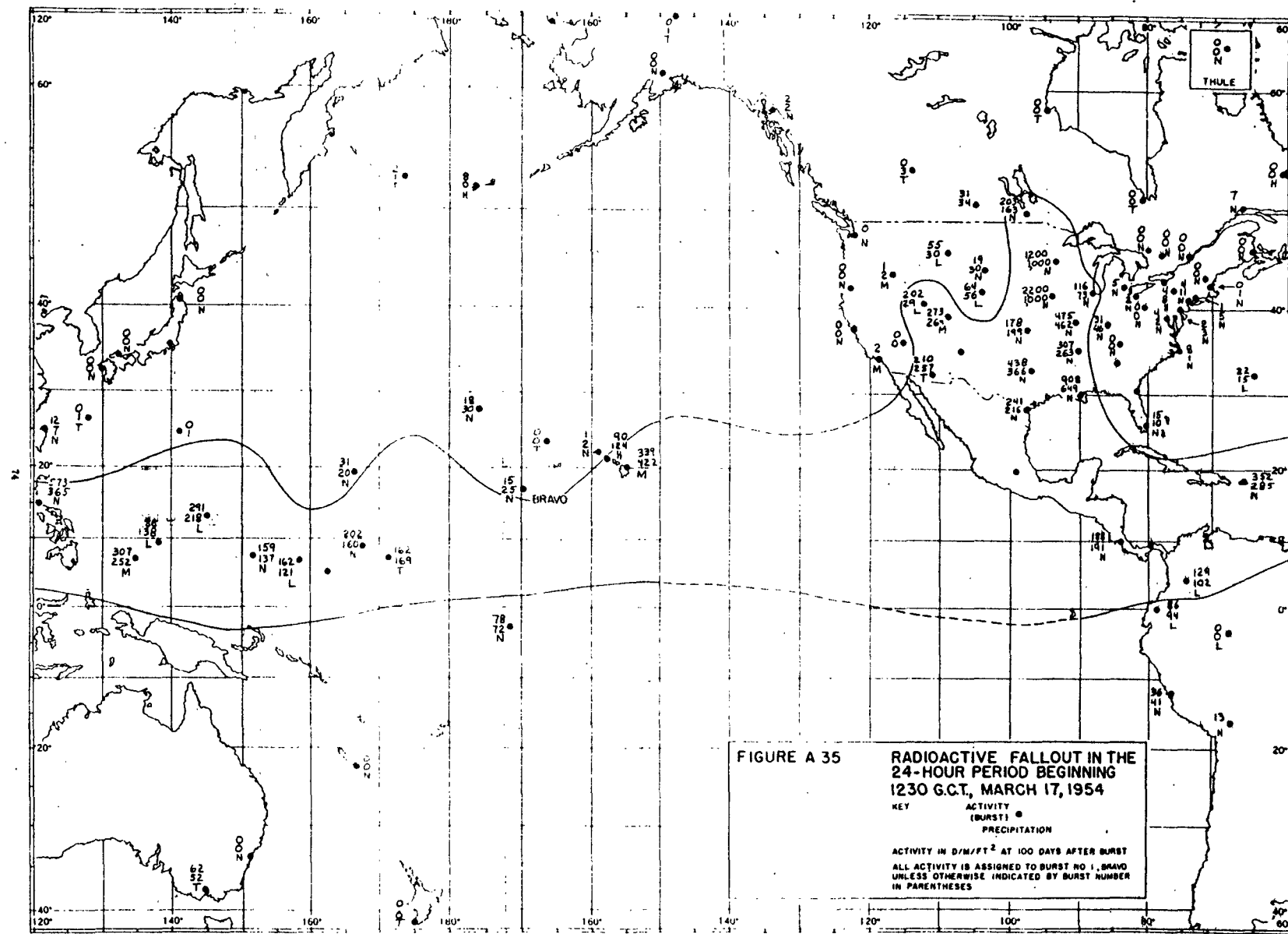
ACTIVITY IN $\mu\text{R}/\text{HR}$ AT 100 DAYS AFTER BURST.
ALL ACTIVITY IS ASSIGNED TO BURST NO. 1, BRAVO
UNLESS OTHERWISE INDICATED BY BURST NUMBER
IN PARENTHESES.

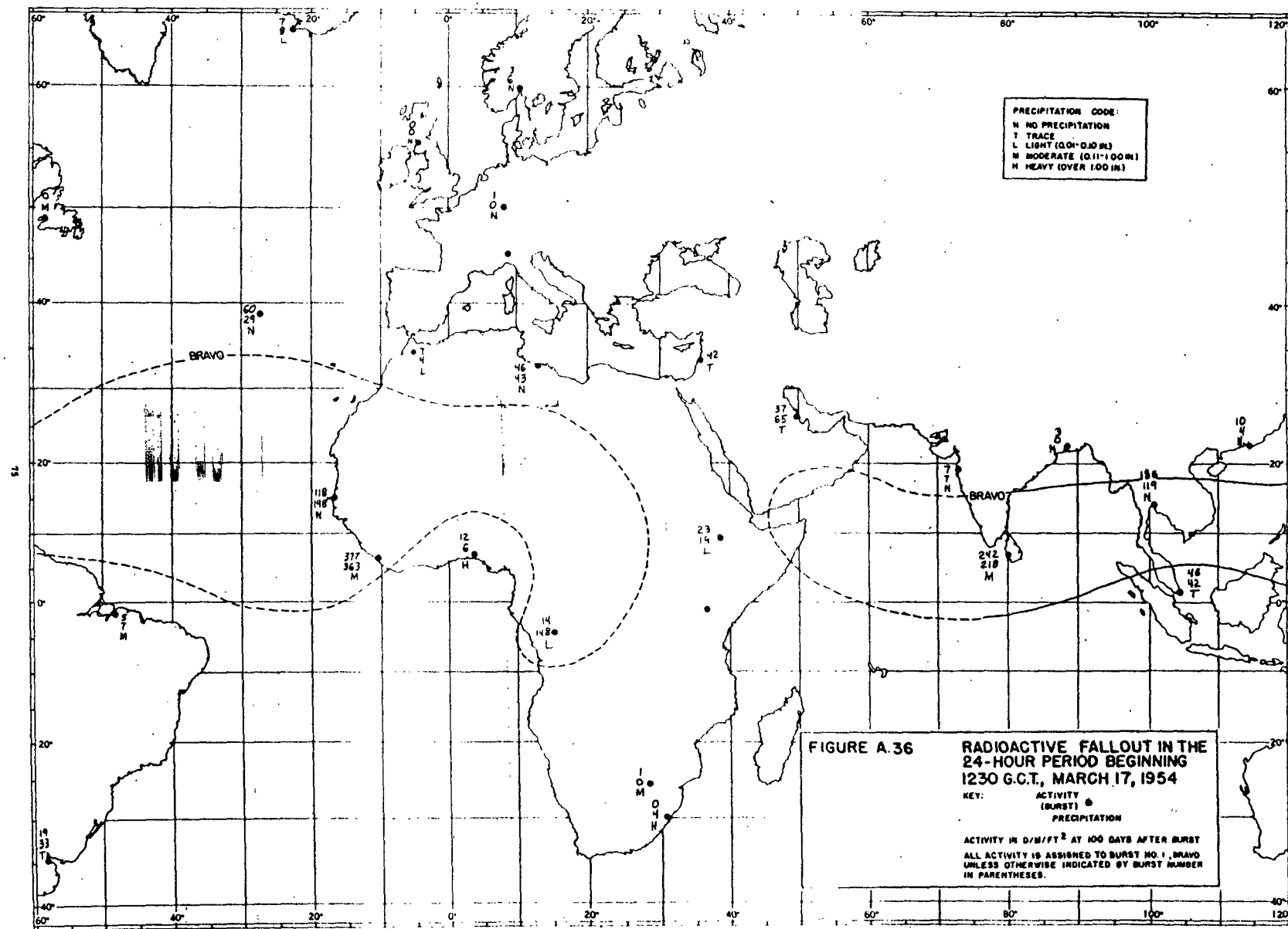




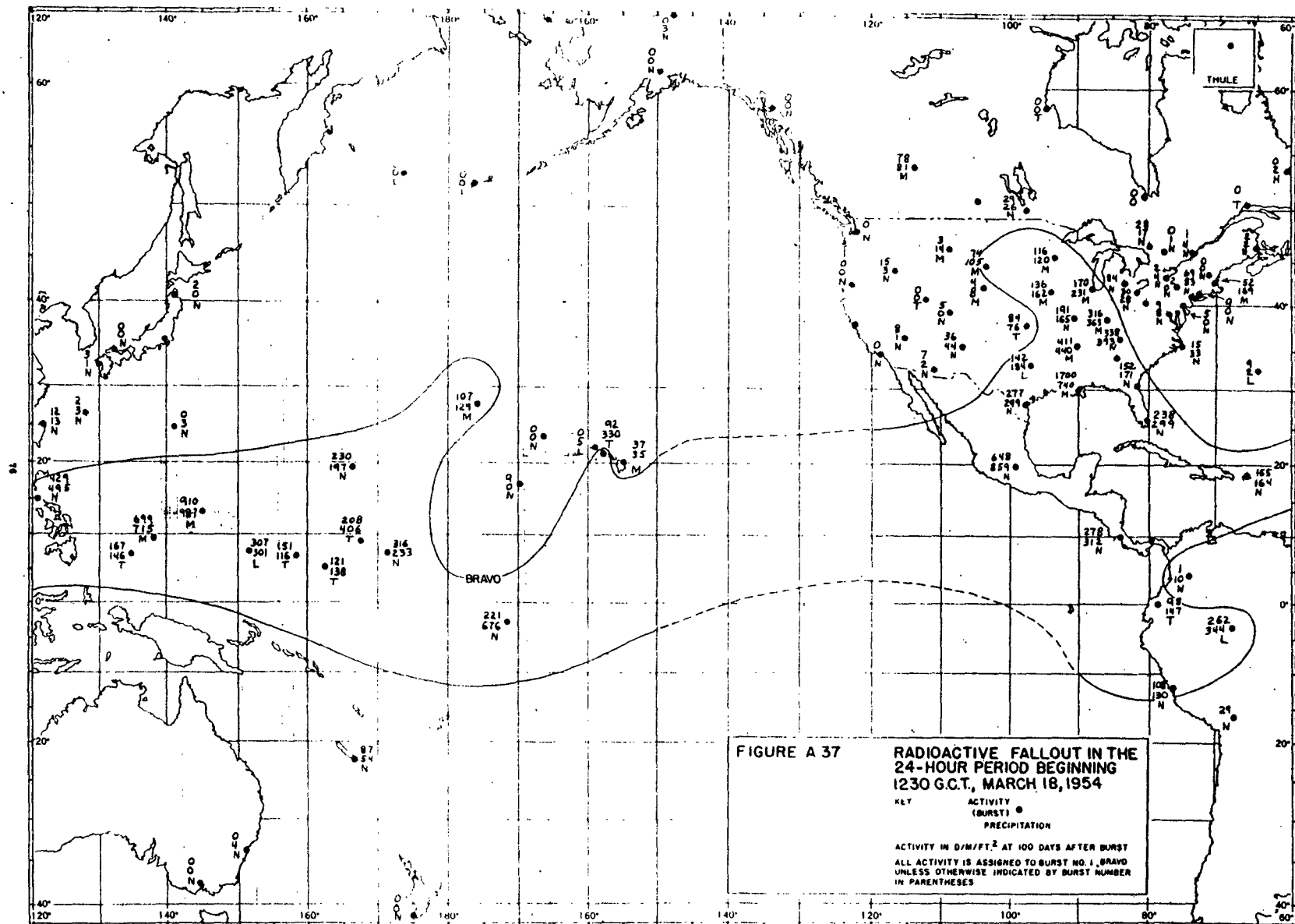


**FIGURE A 34 RADIOACTIVE FALLOUT IN THE
24-HOUR PERIOD BEGINNING
1230 G.C.T., MARCH 16, 1954.**





**FIGURE A.36 RADIOACTIVE FALLOUT IN THE
24-HOUR PERIOD BEGINNING
1230 G.C.T., MARCH 17, 1954**



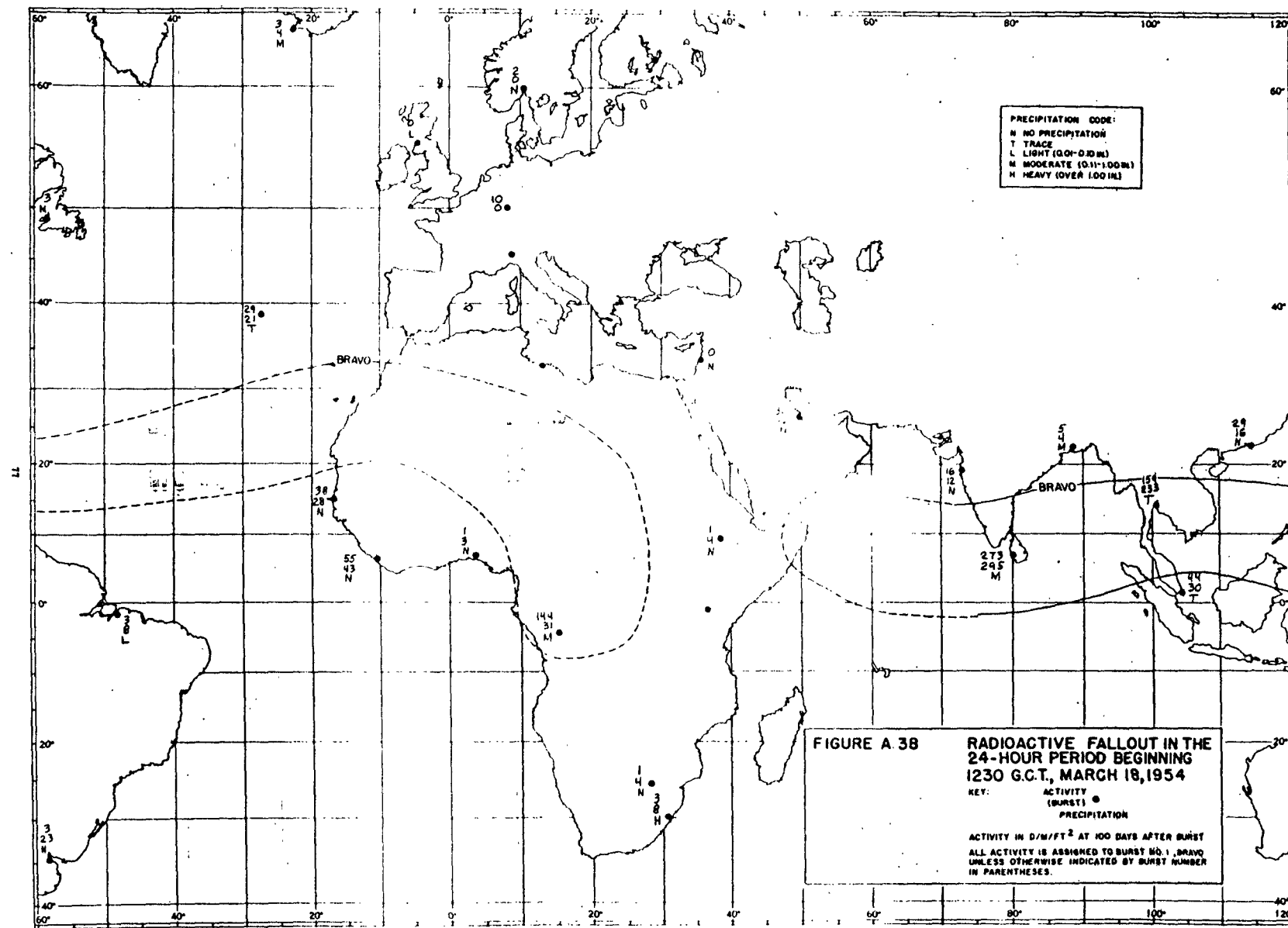


FIGURE A.38 **RADIOACTIVE FALLOUT IN THE
24-HOUR PERIOD BEGINNING
1230 G.C.T., MARCH 18, 1954**

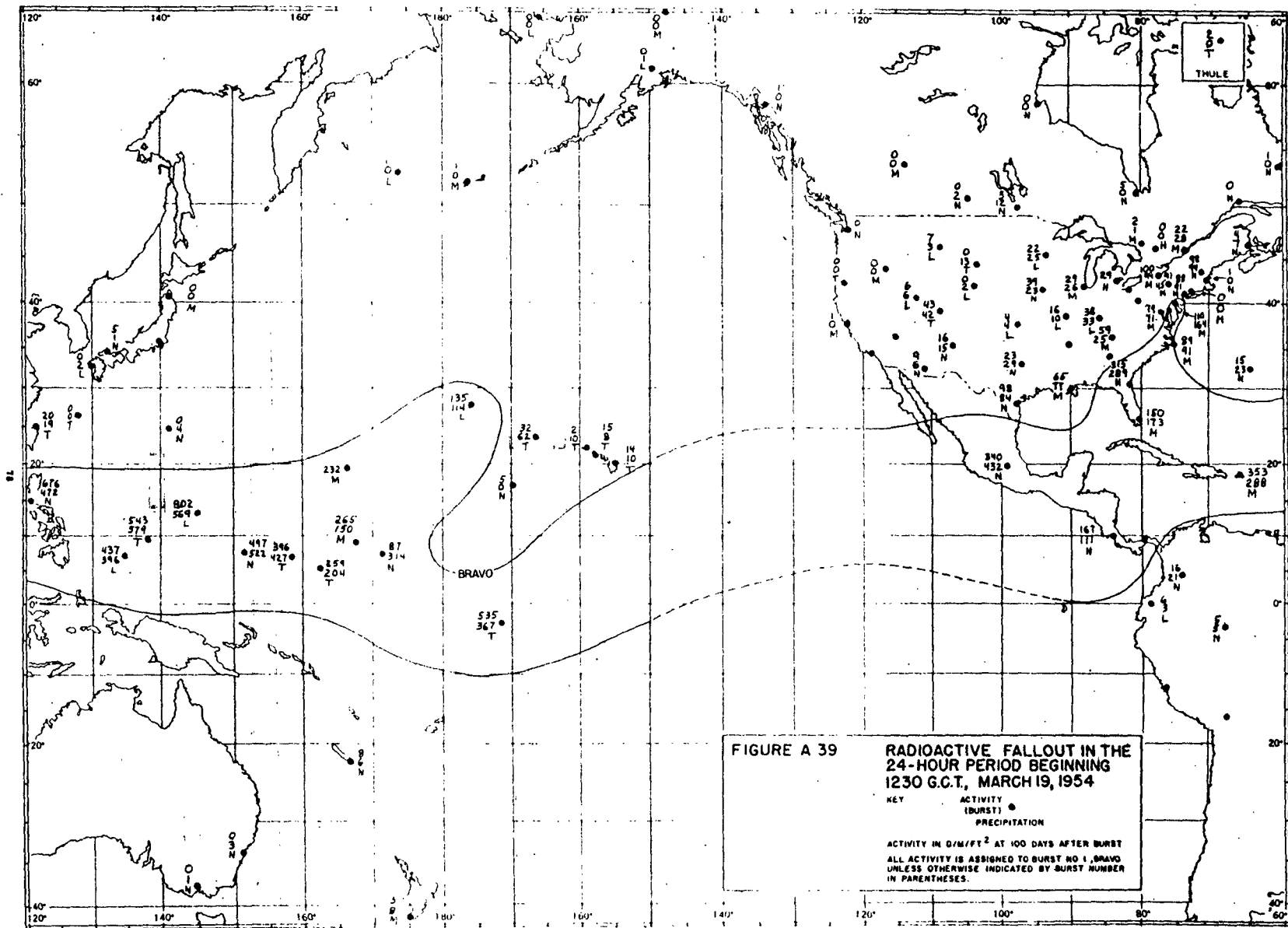
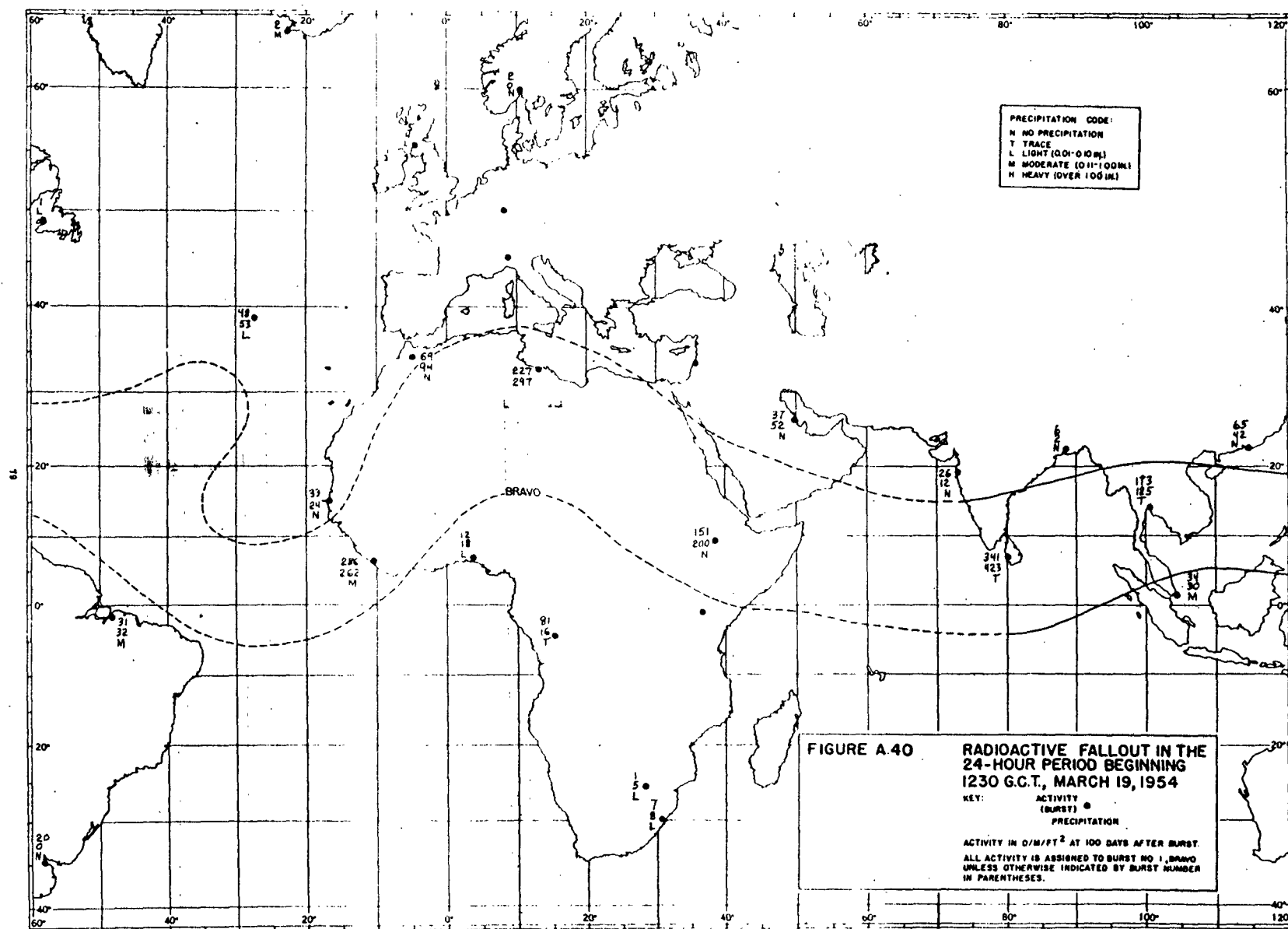


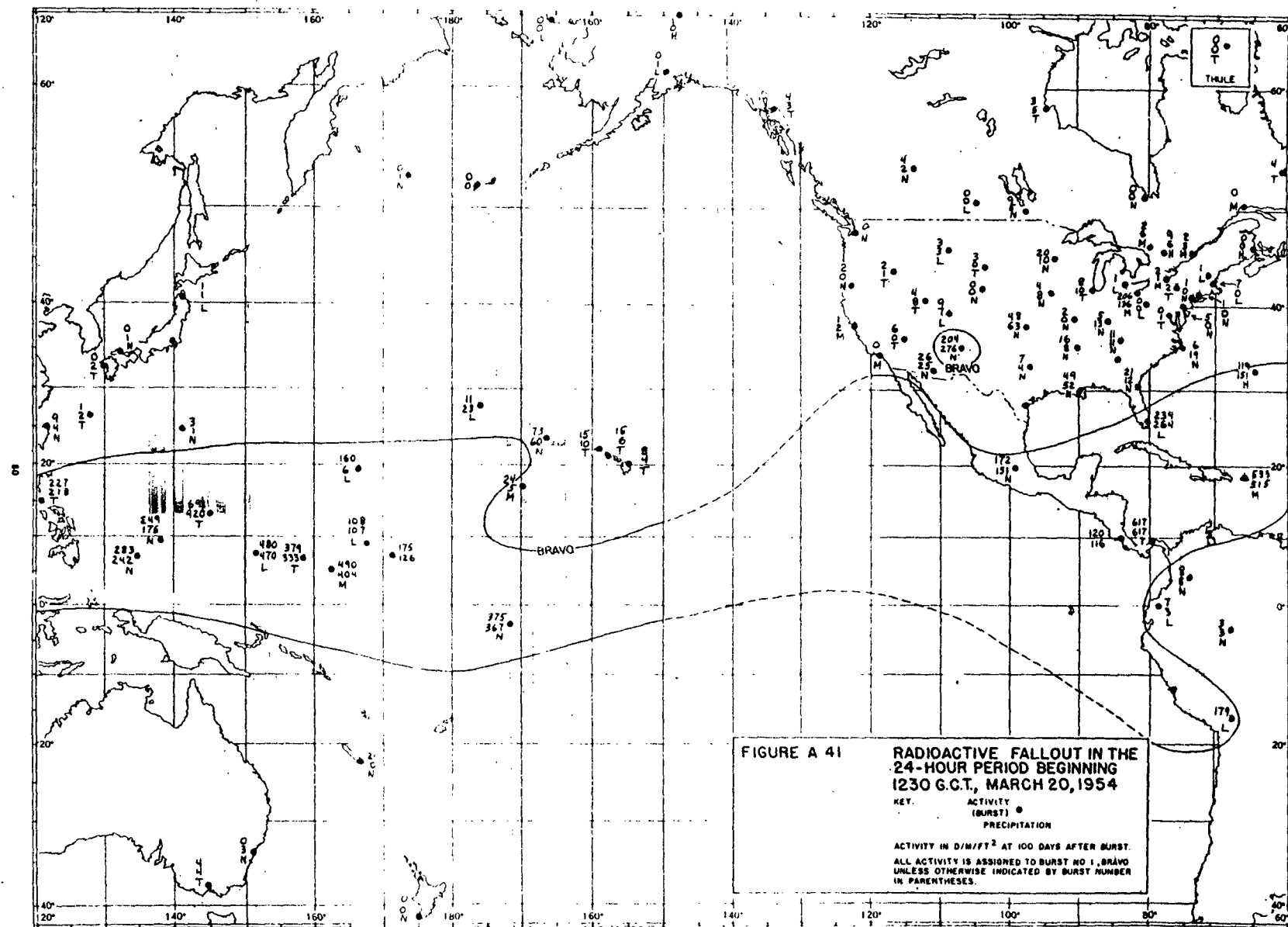
FIGURE A 39

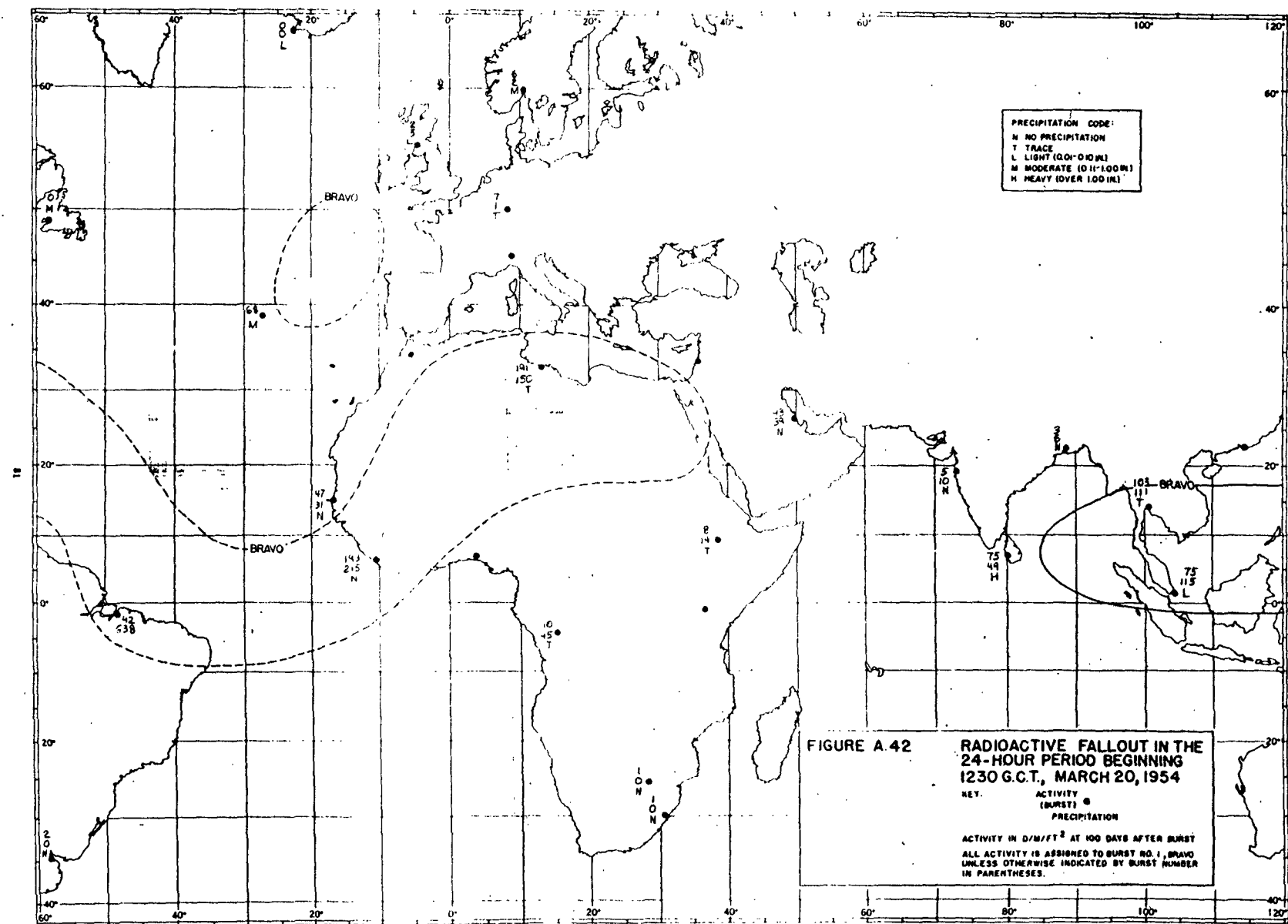
RADIOACTIVE FALLOUT IN THE
24-HOUR PERIOD BEGINNING
1230 G.C.T., MARCH 19, 1954

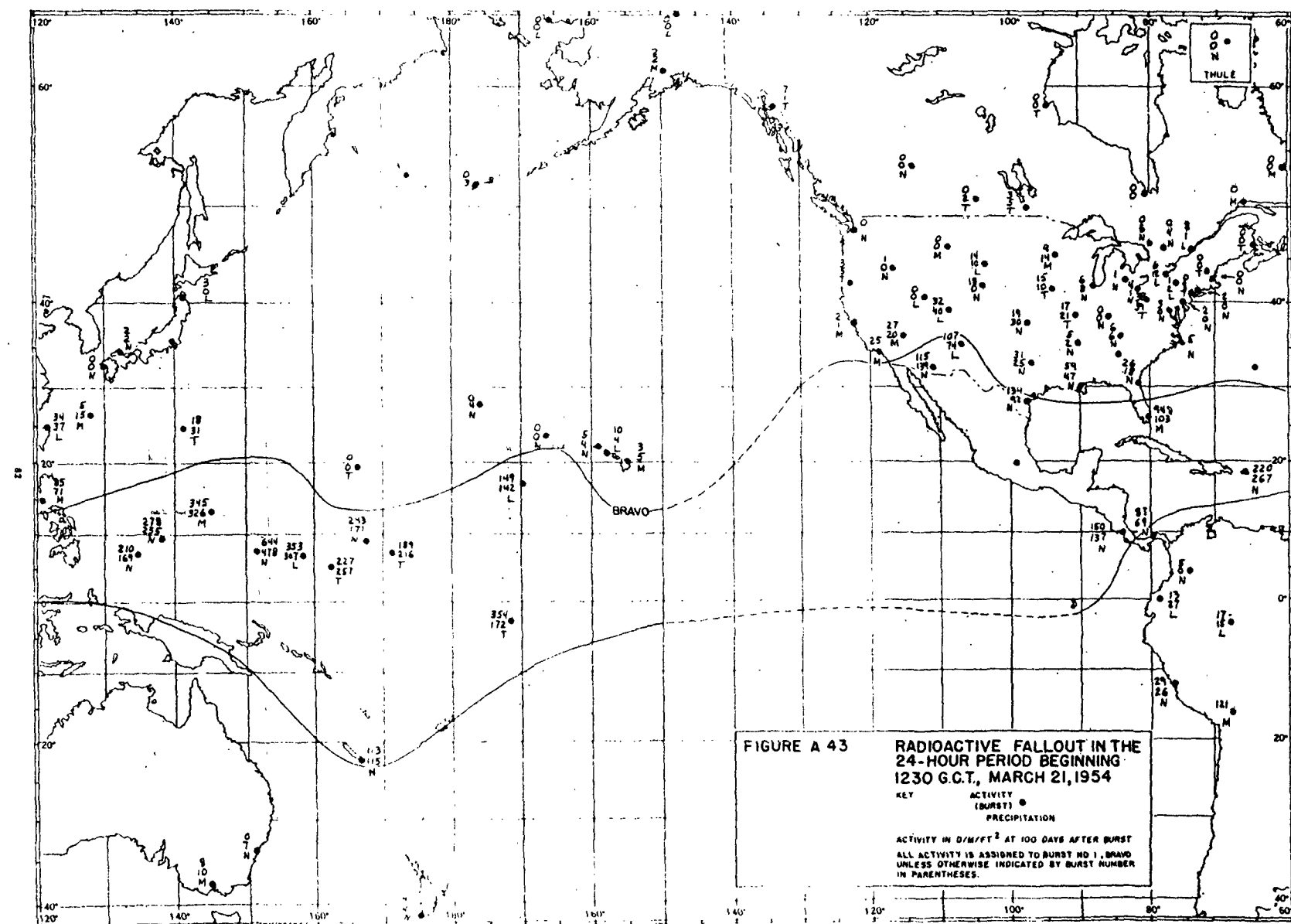
KEY ACTIVITY
(BURST) ●
PRECIPITATION

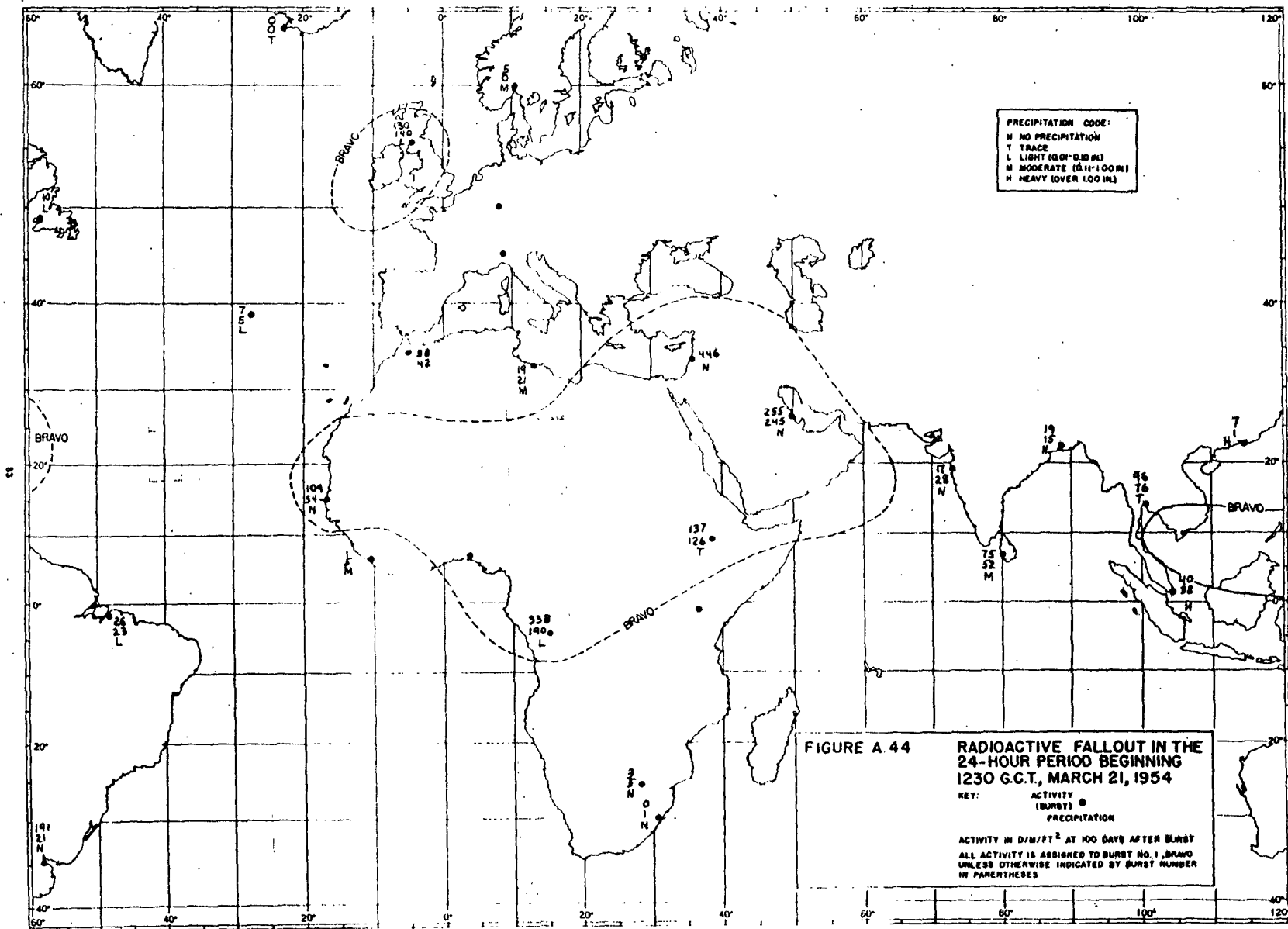
ACTIVITY IN D/M² FT² AT 100 DAYS AFTER BURST
ALL ACTIVITY IS ASSIGNED TO BURST NO 1, BRAVO
UNLESS OTHERWISE INDICATED BY BURST NUMBER
IN PARENTHESES.

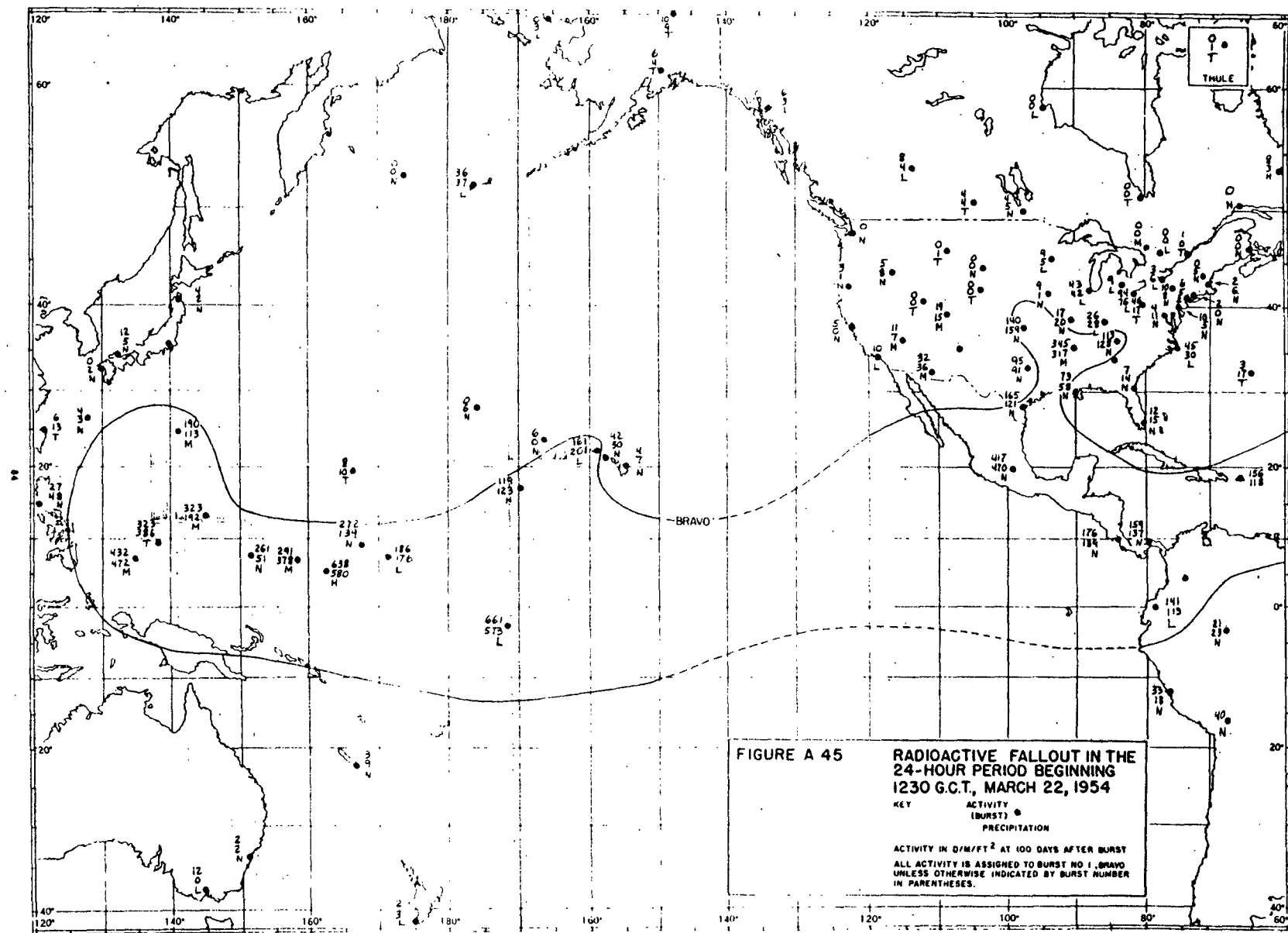


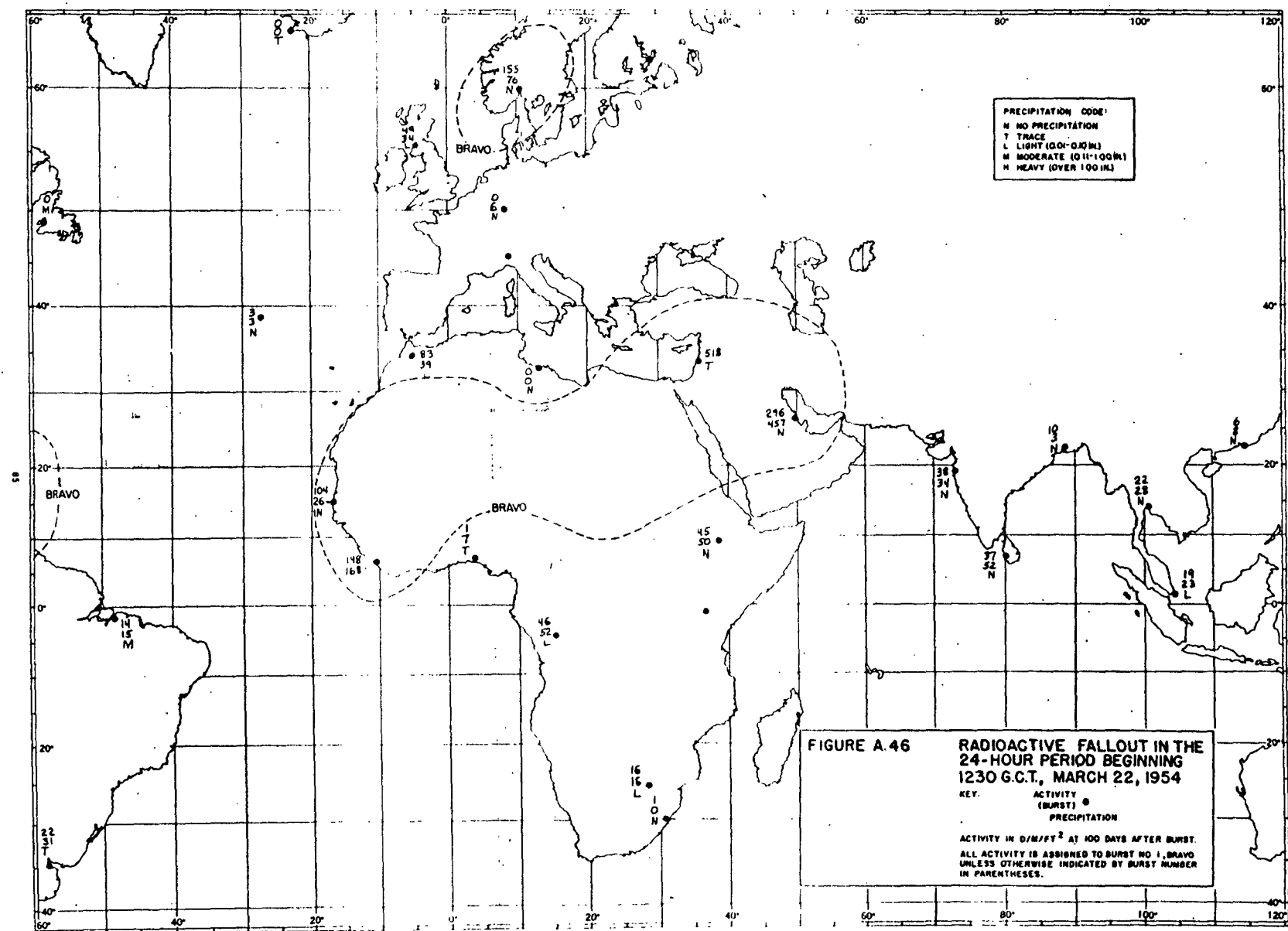


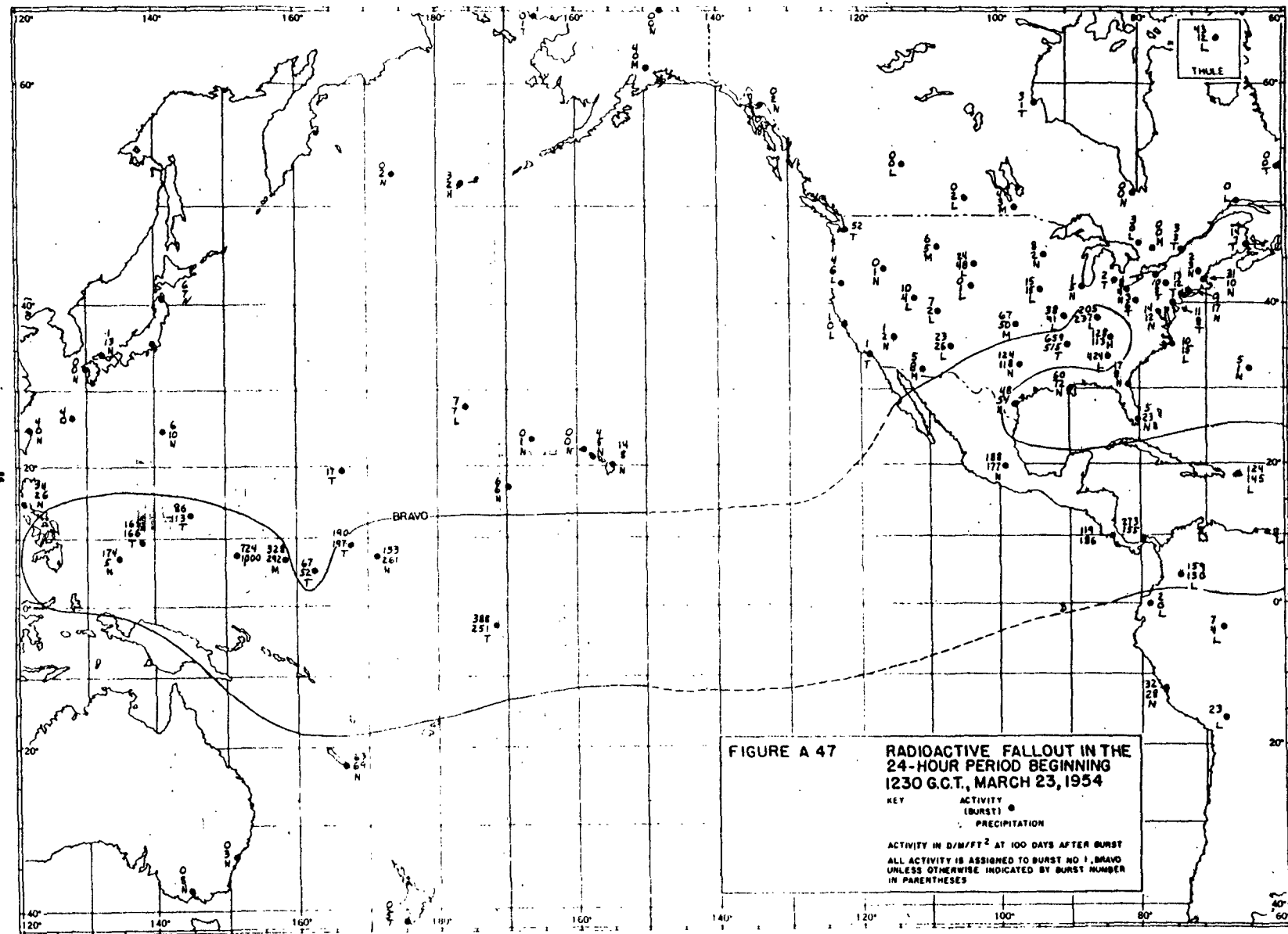


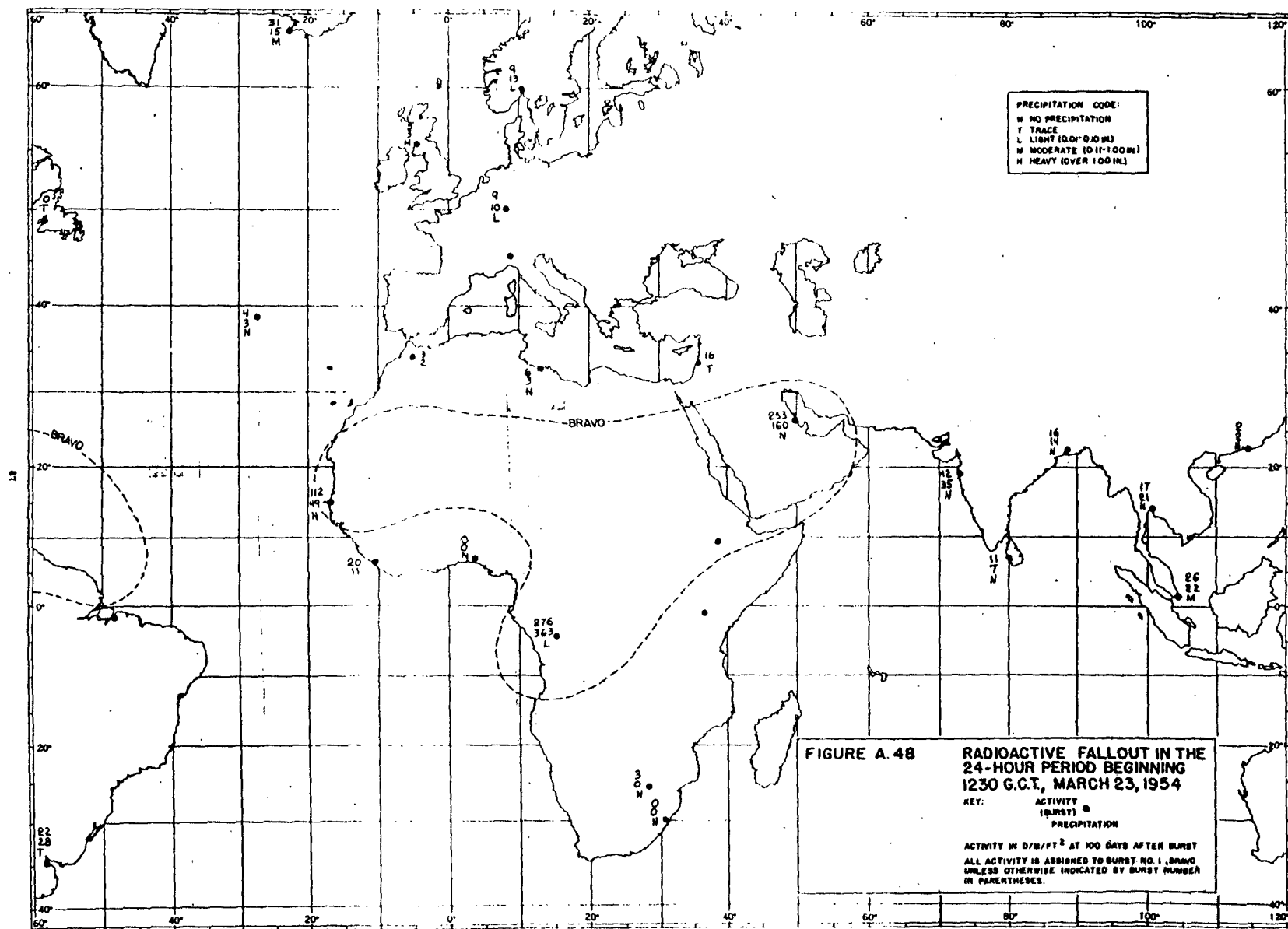


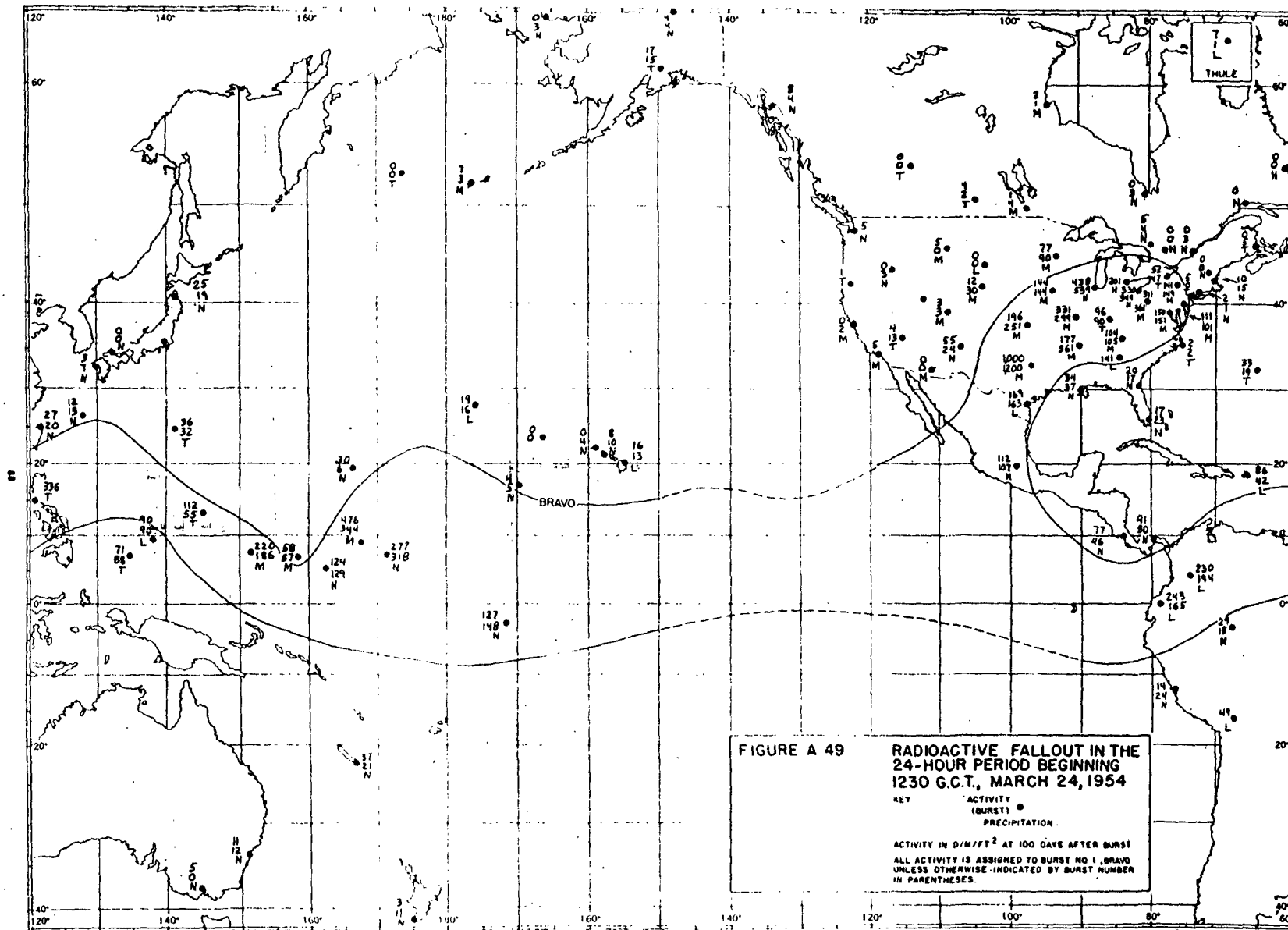


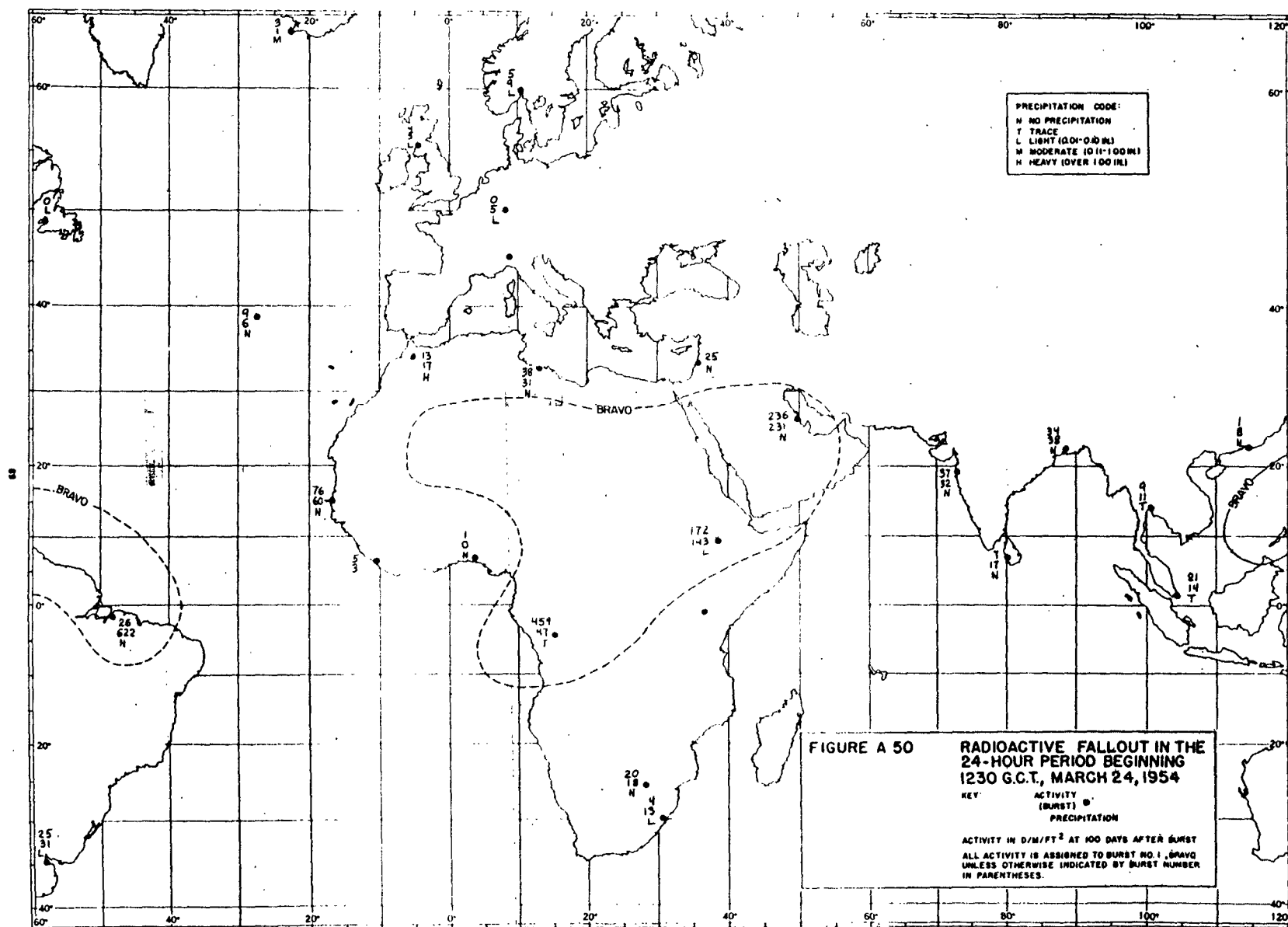












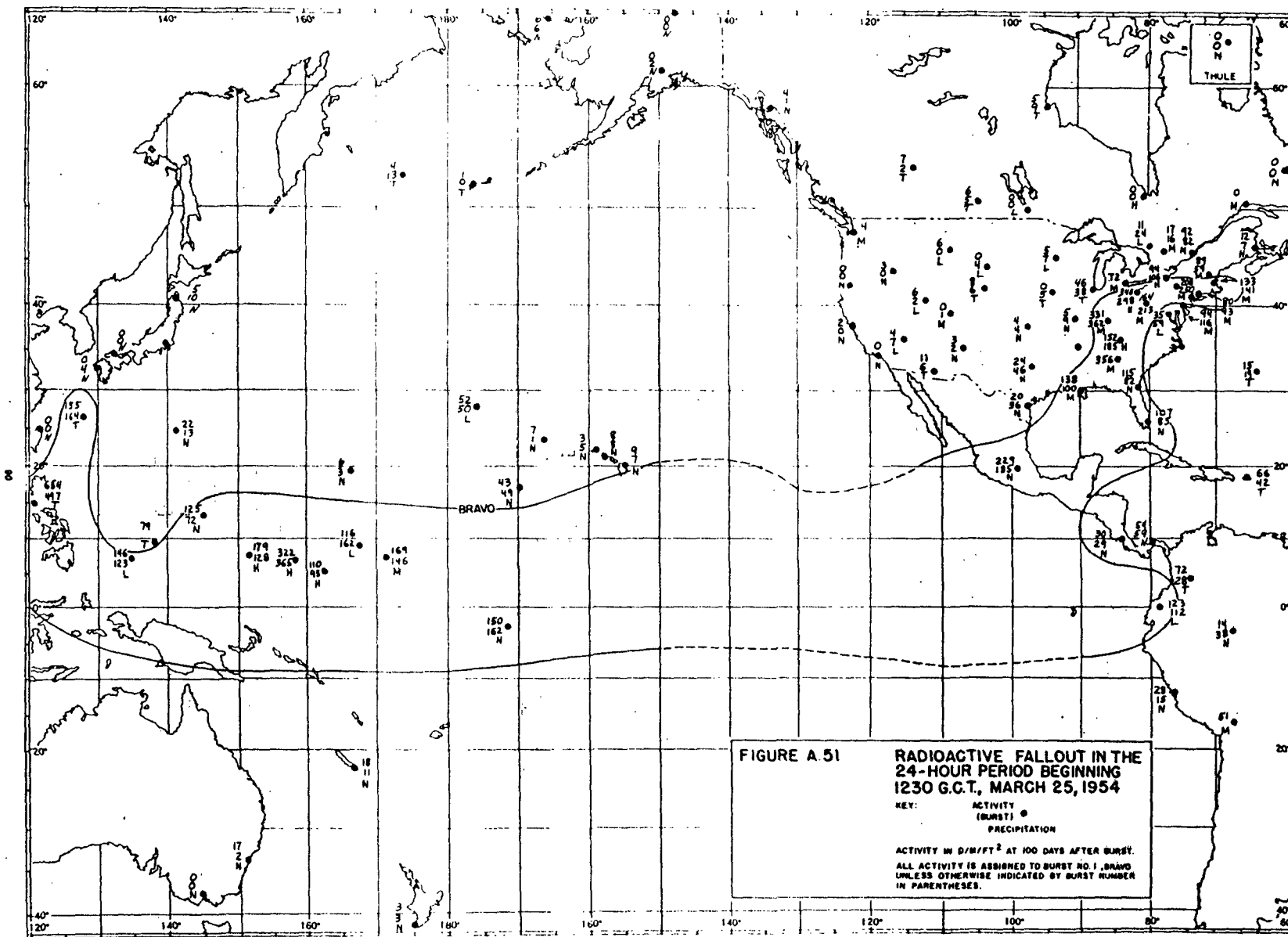
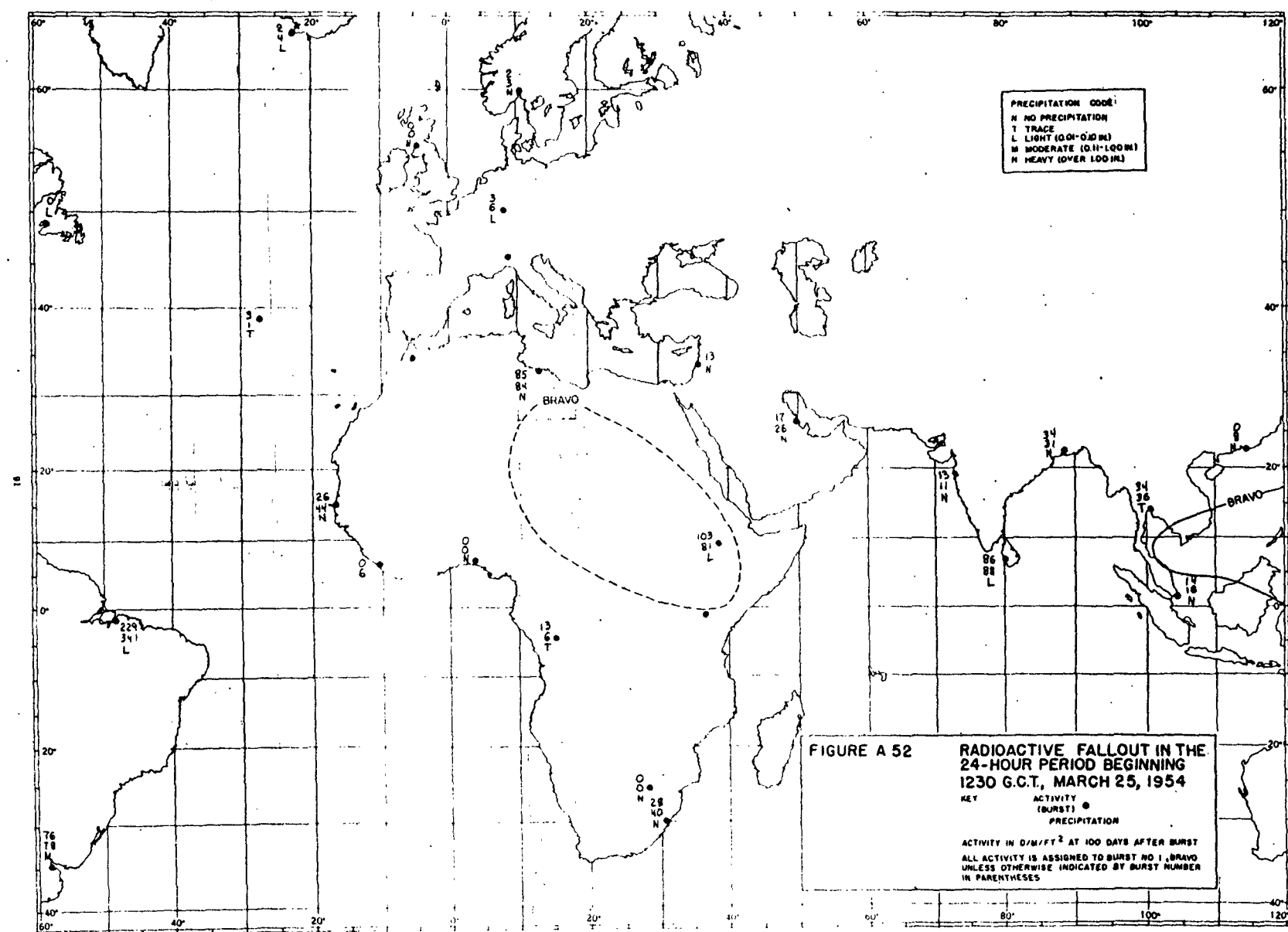


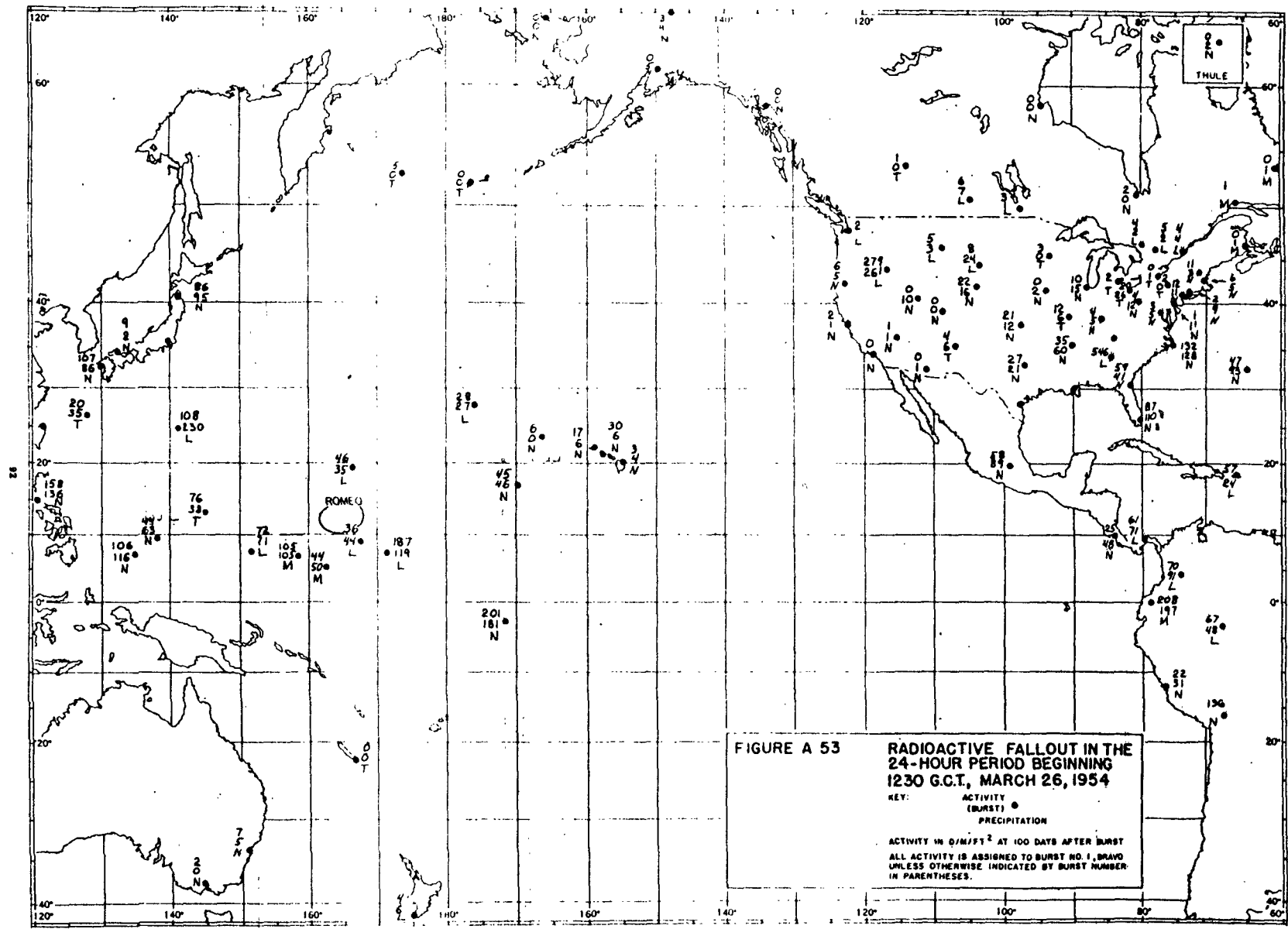
FIGURE A.51 RADIOACTIVE FALLOUT IN THE
24-HOUR PERIOD BEGINNING
1230 G.C.T., MARCH 25, 1954

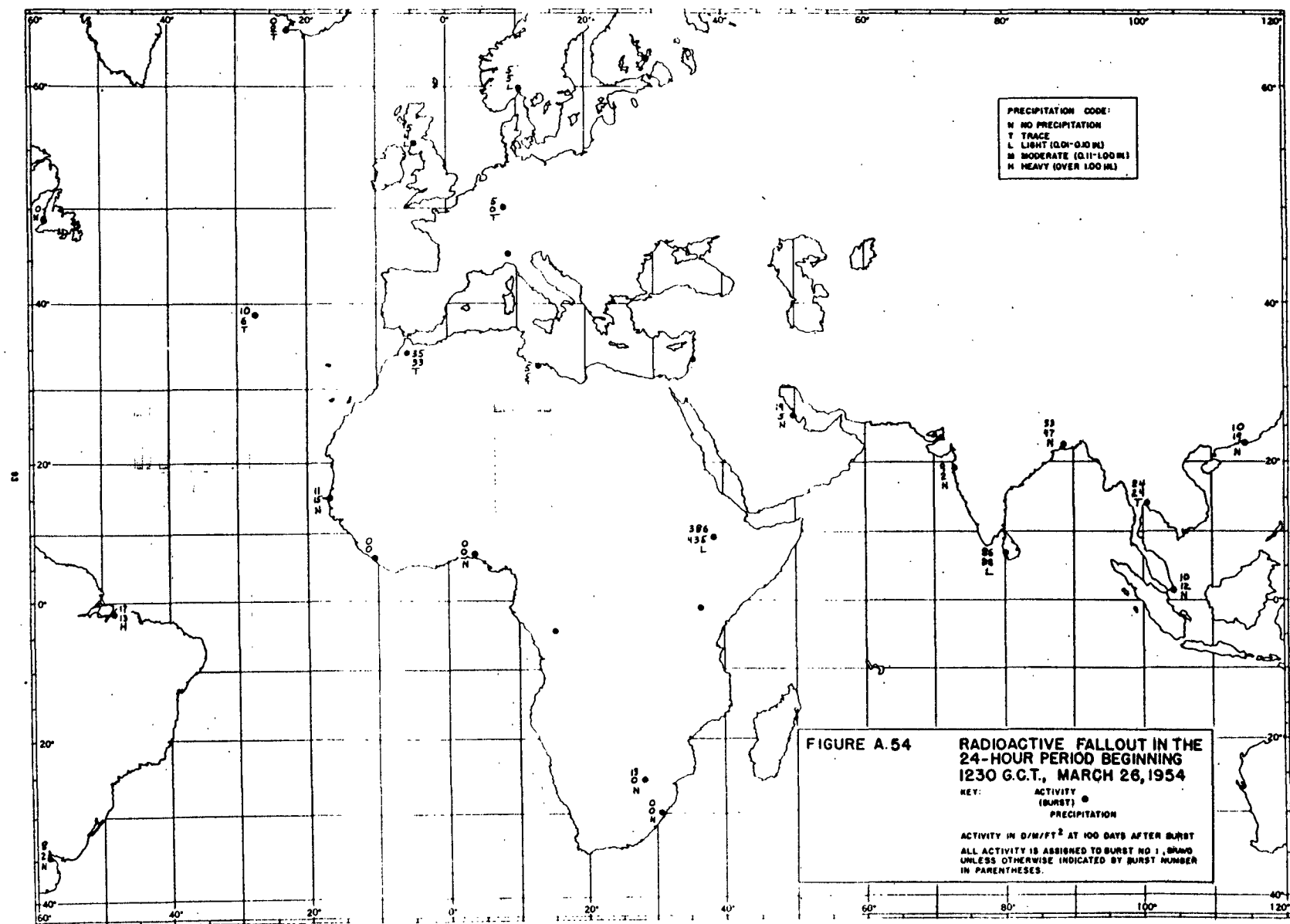
KEY:

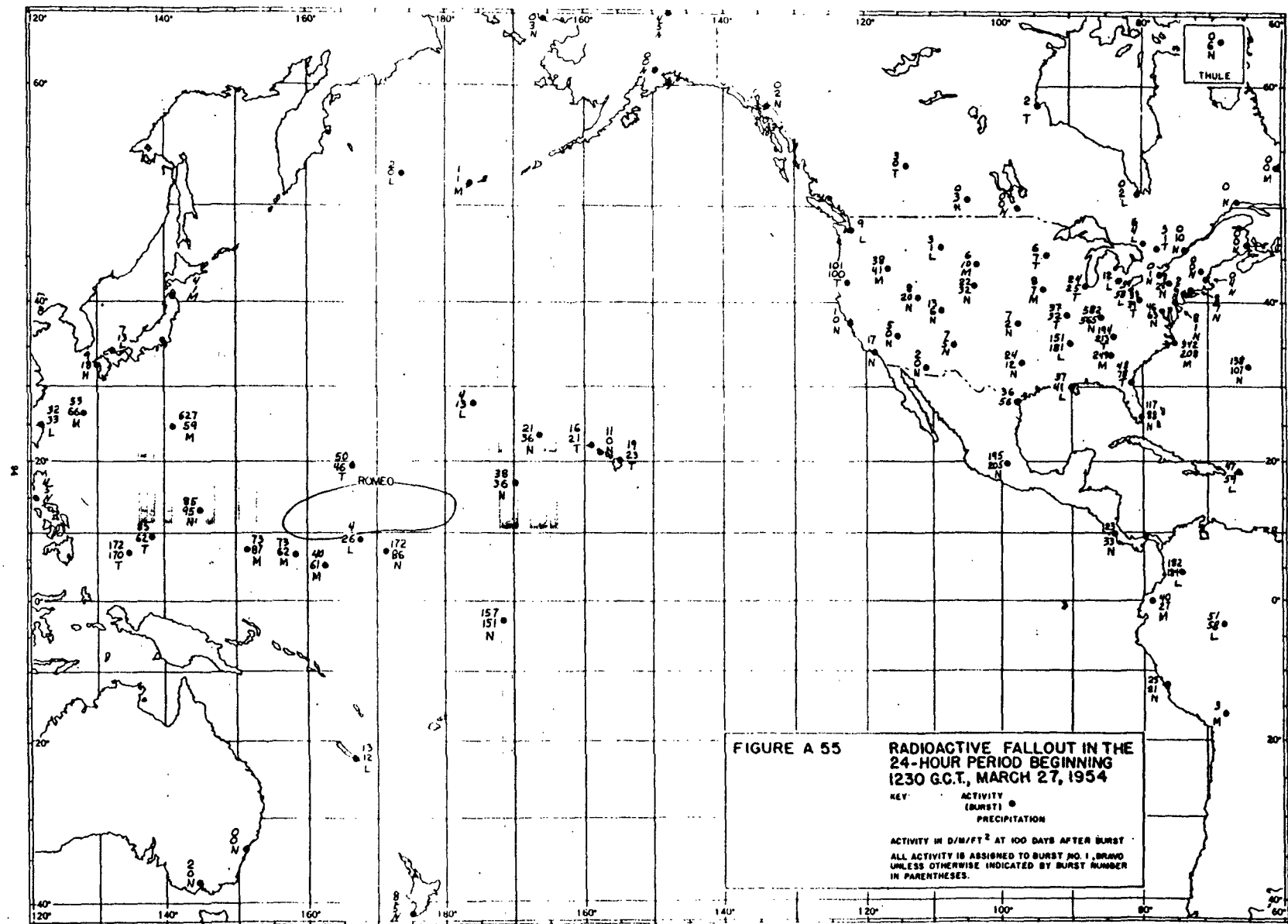
- ACTIVITY (SOLID ●)
- PRECIPITATION (OPEN ○)

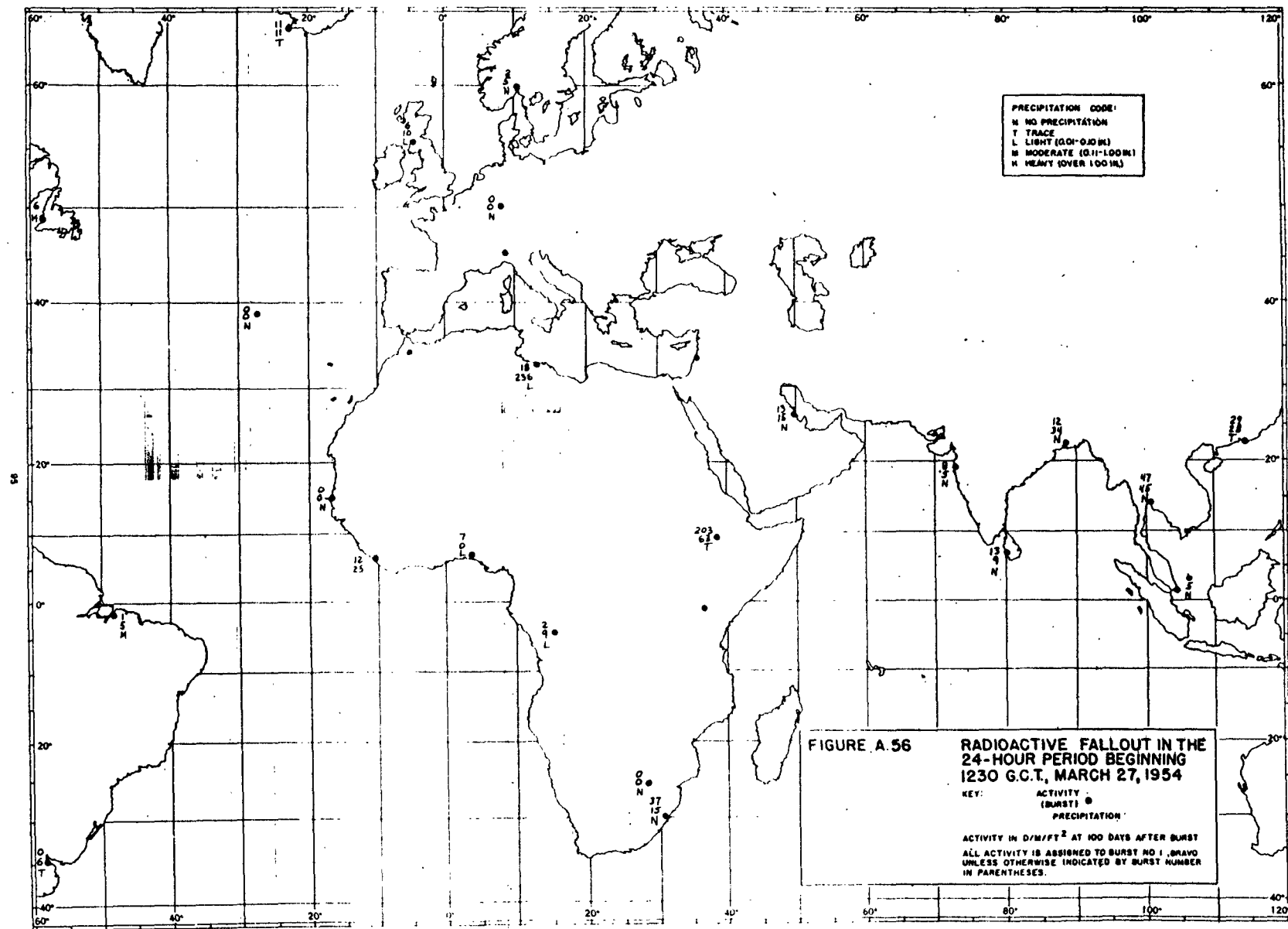
ACTIVITY IN $\mu\text{R}/\text{FT}^2$ AT 100 DAYS AFTER BURST.
ALL ACTIVITY IS ASSIGNED TO BURST NO. 1, BRAVO
UNLESS OTHERWISE INDICATED BY BURST NUMBER
IN PARENTHESES.

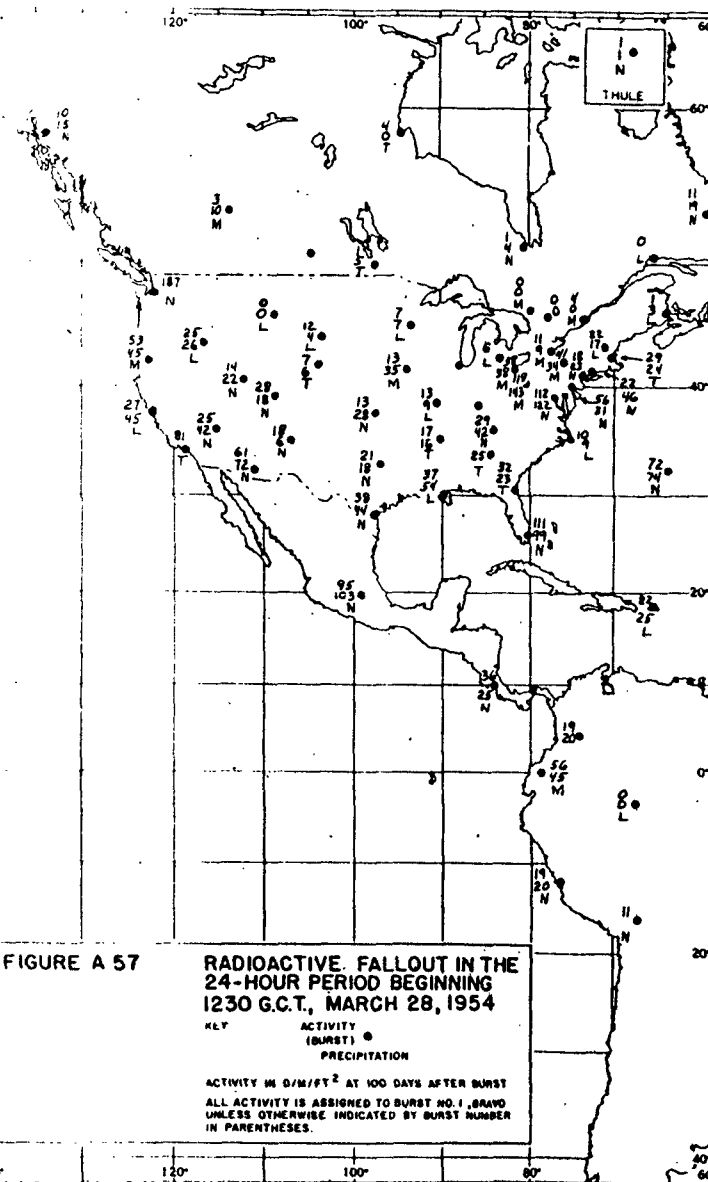
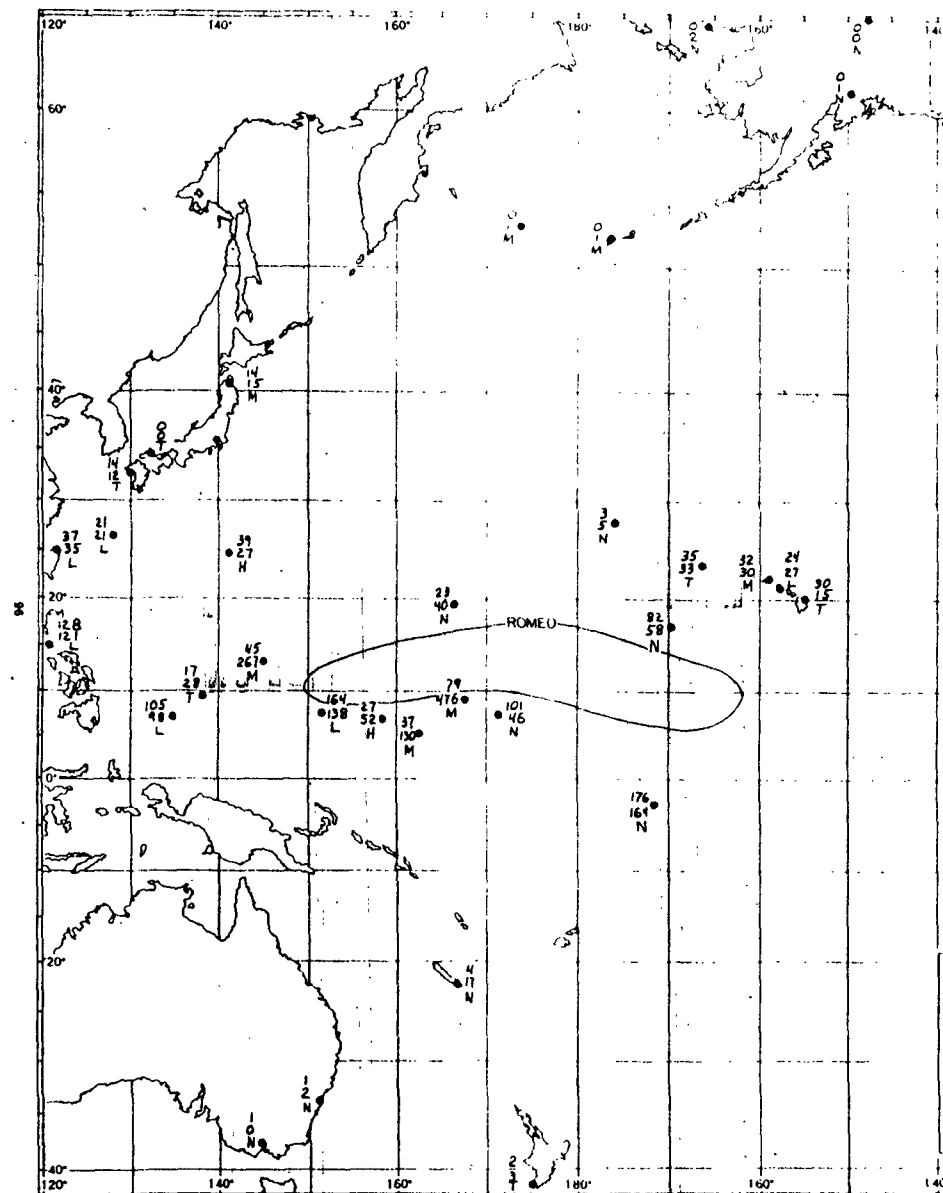


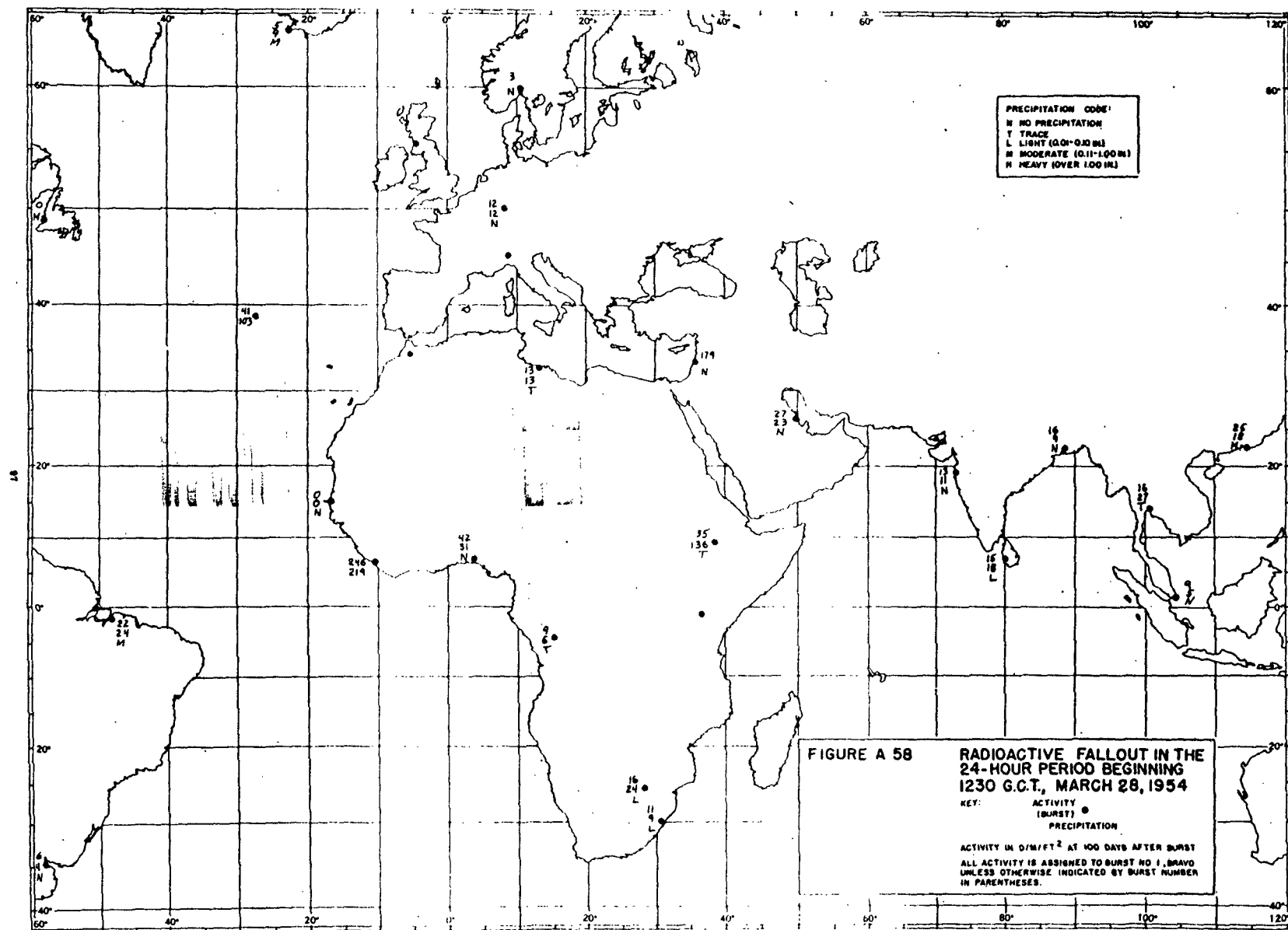


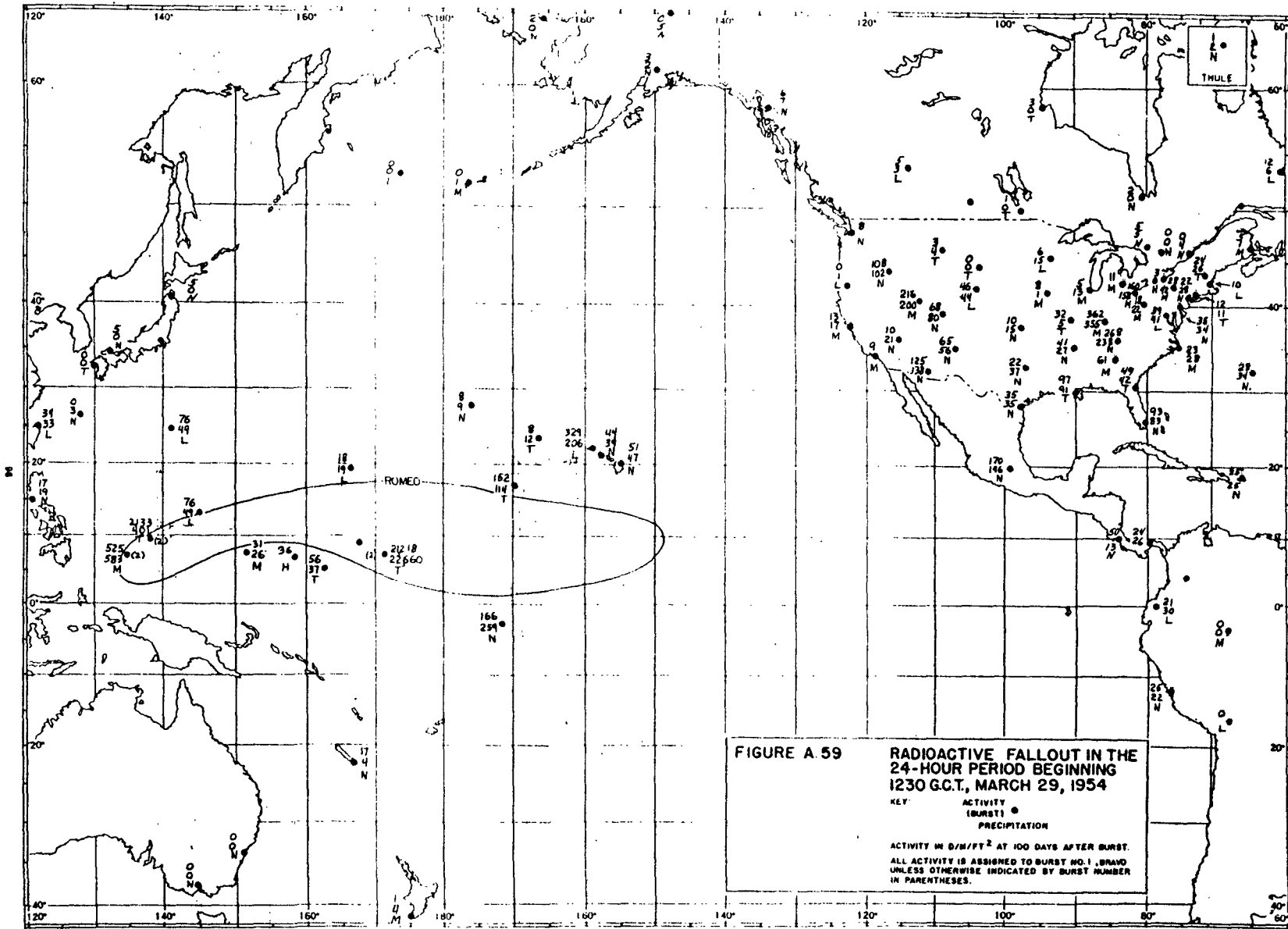


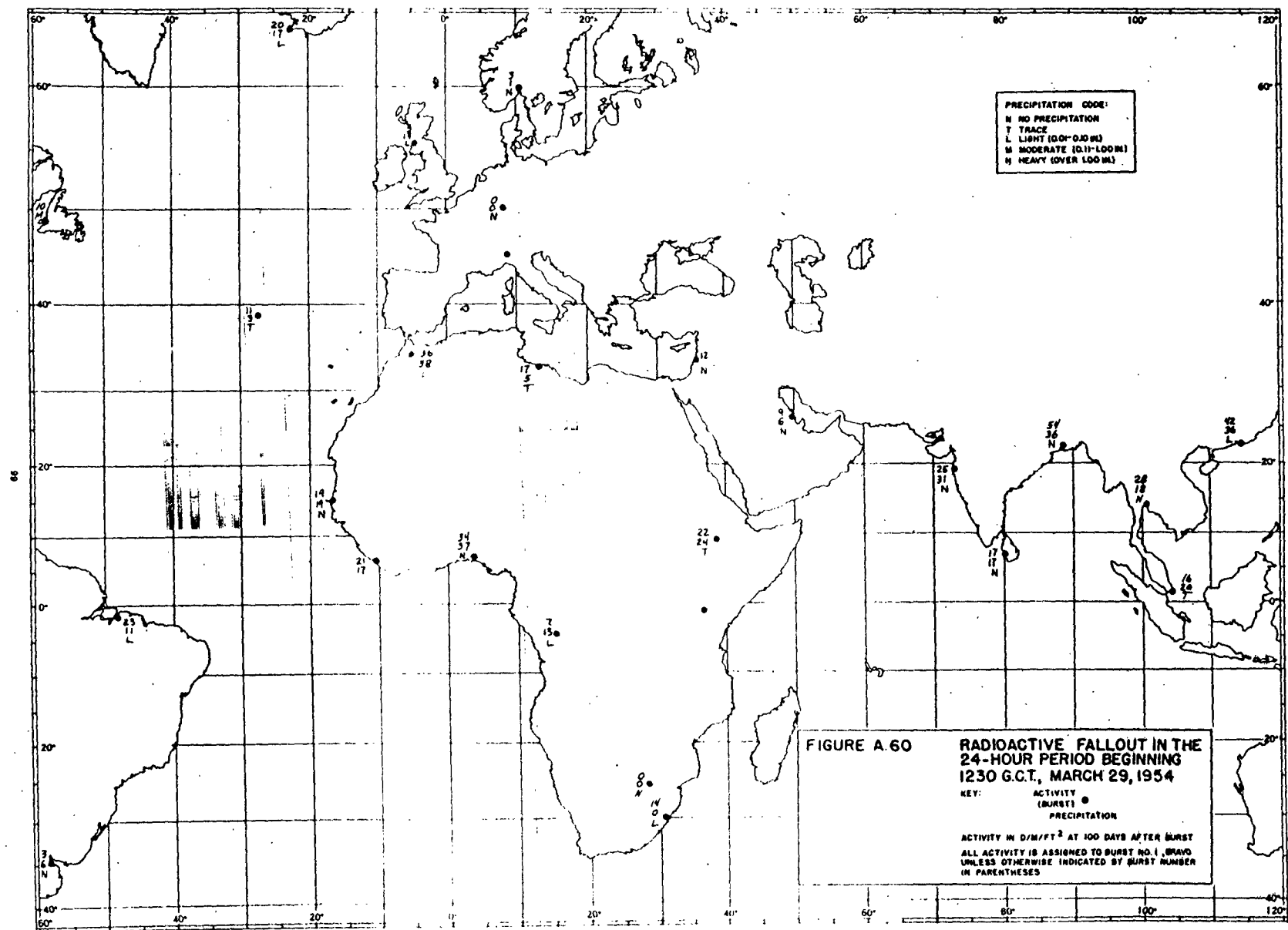


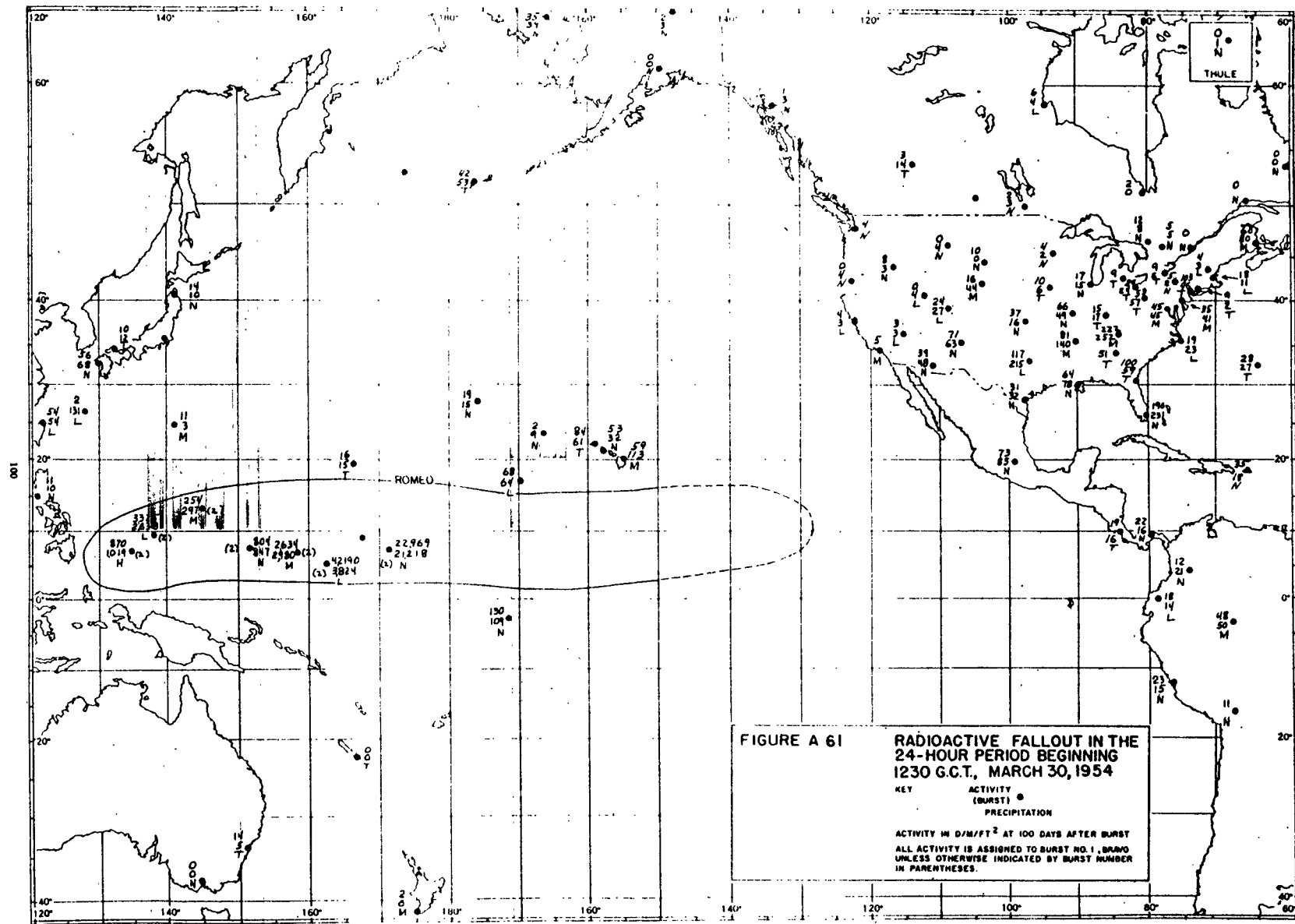


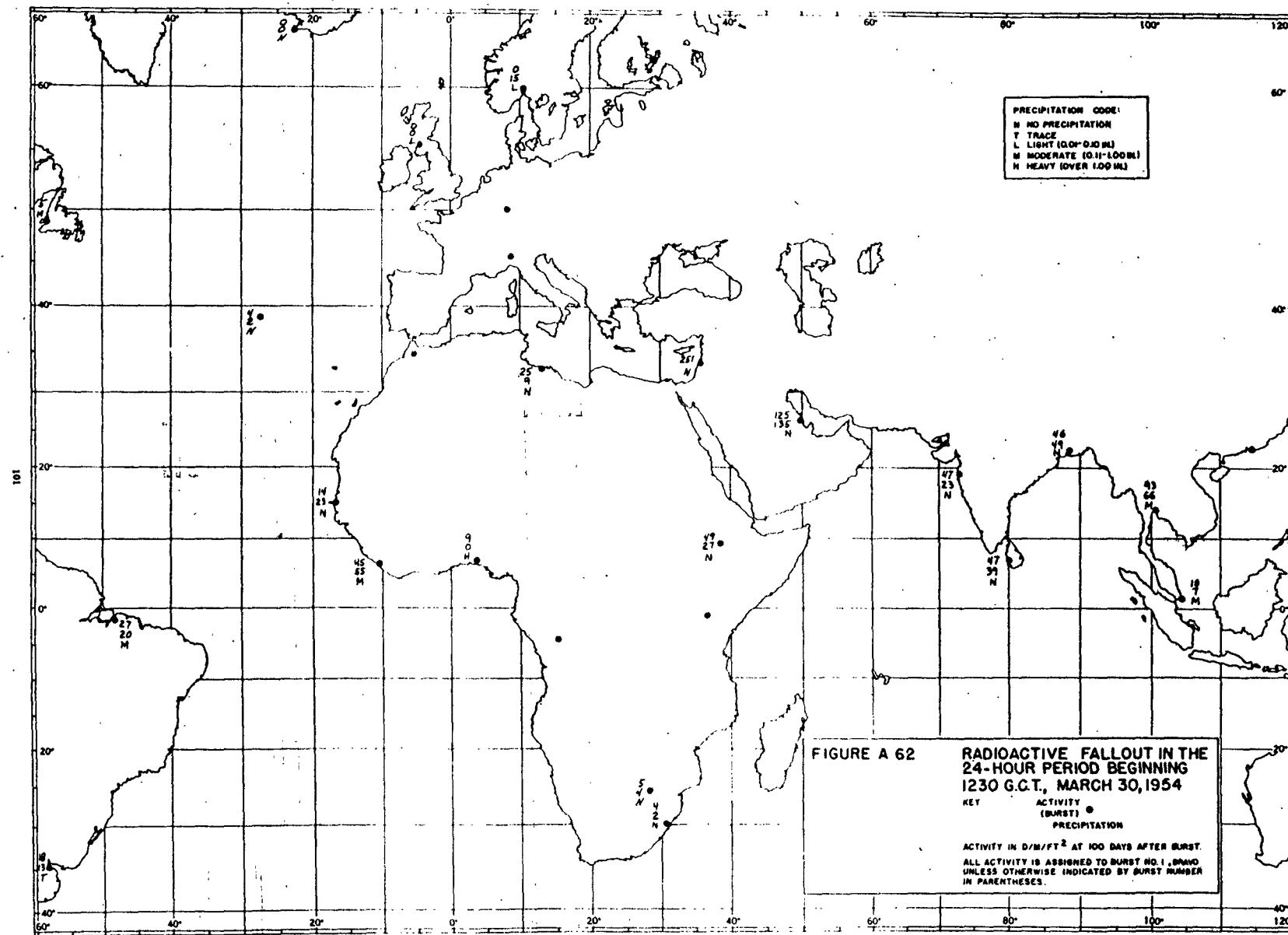












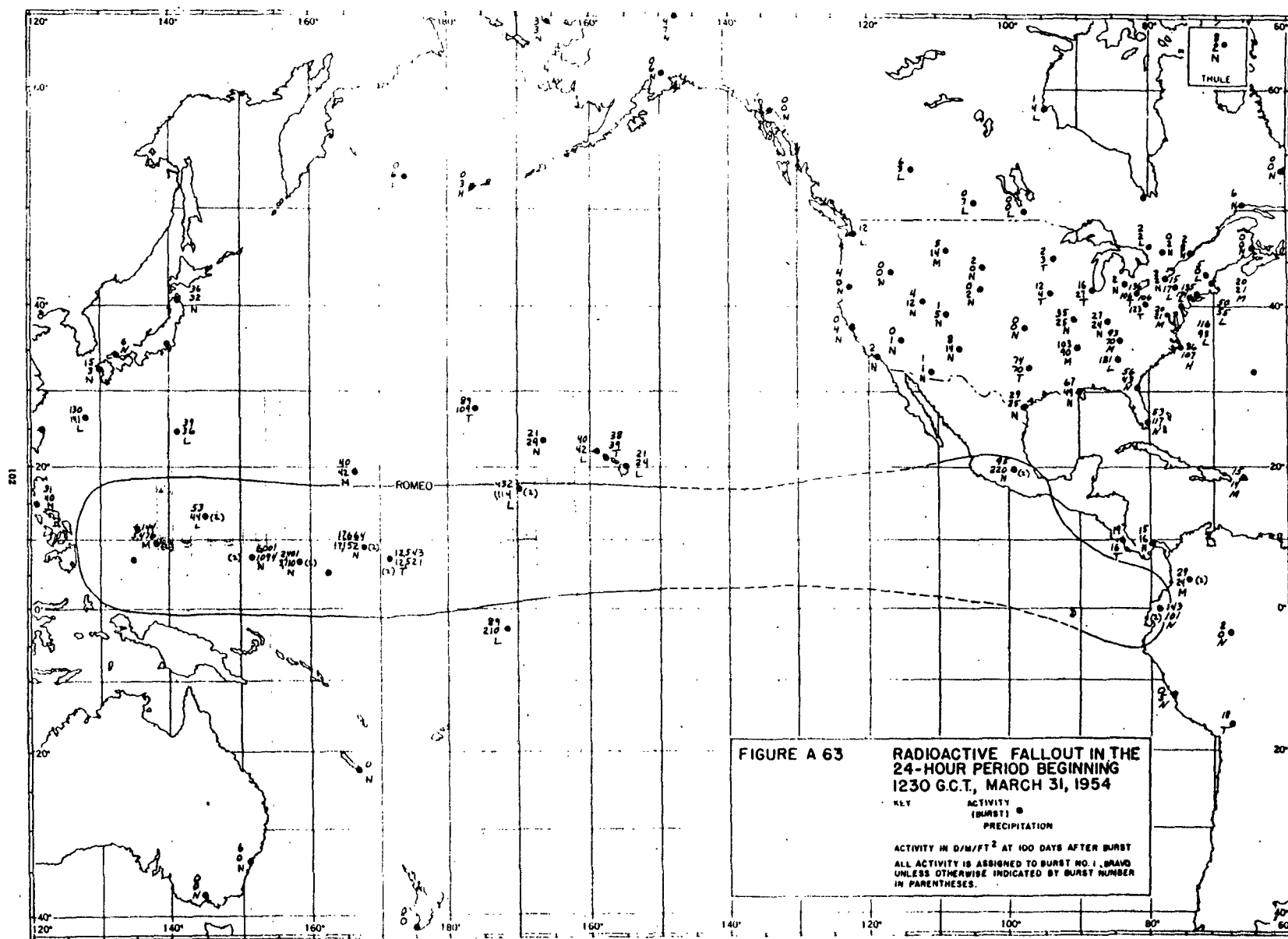
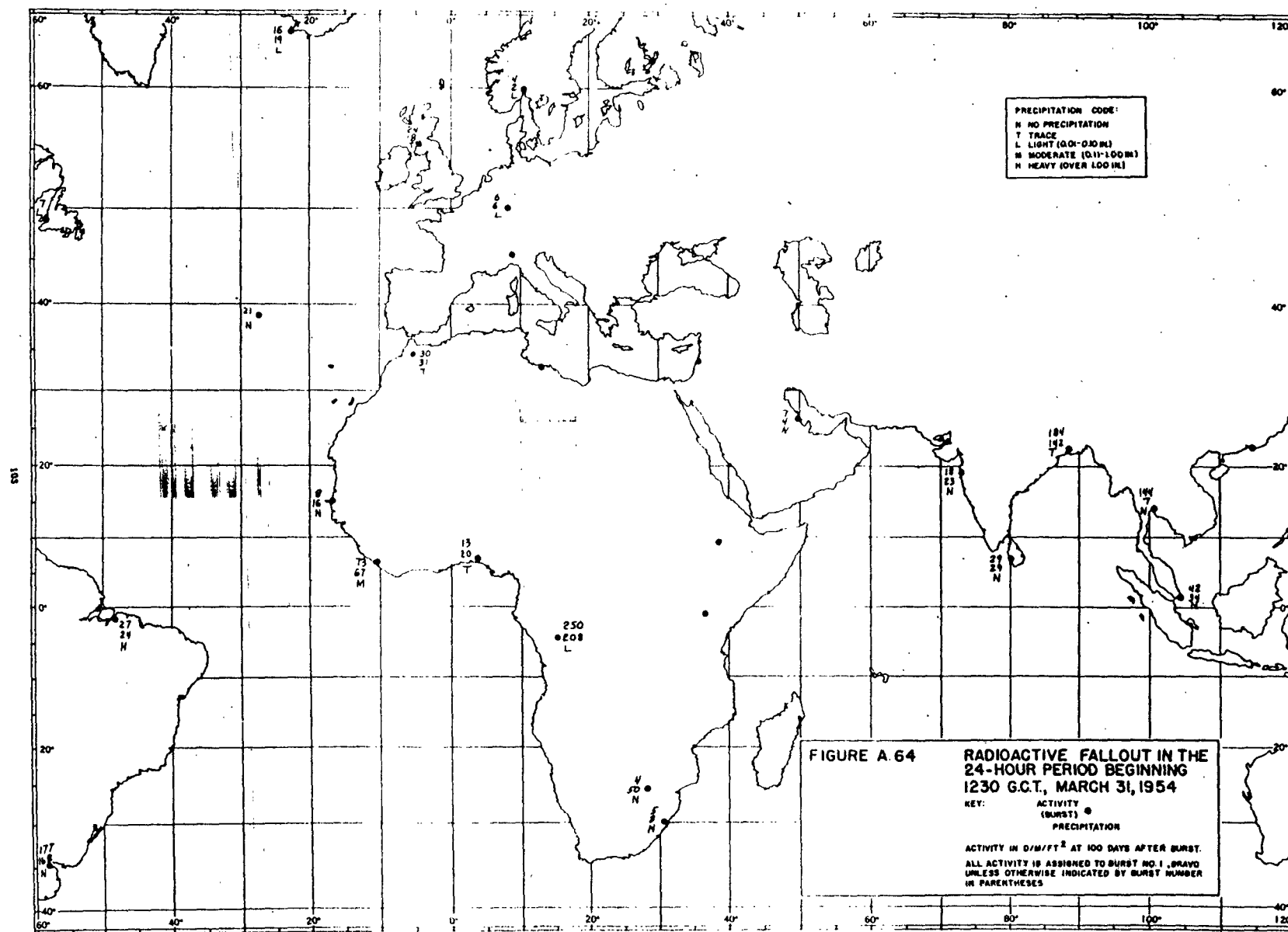
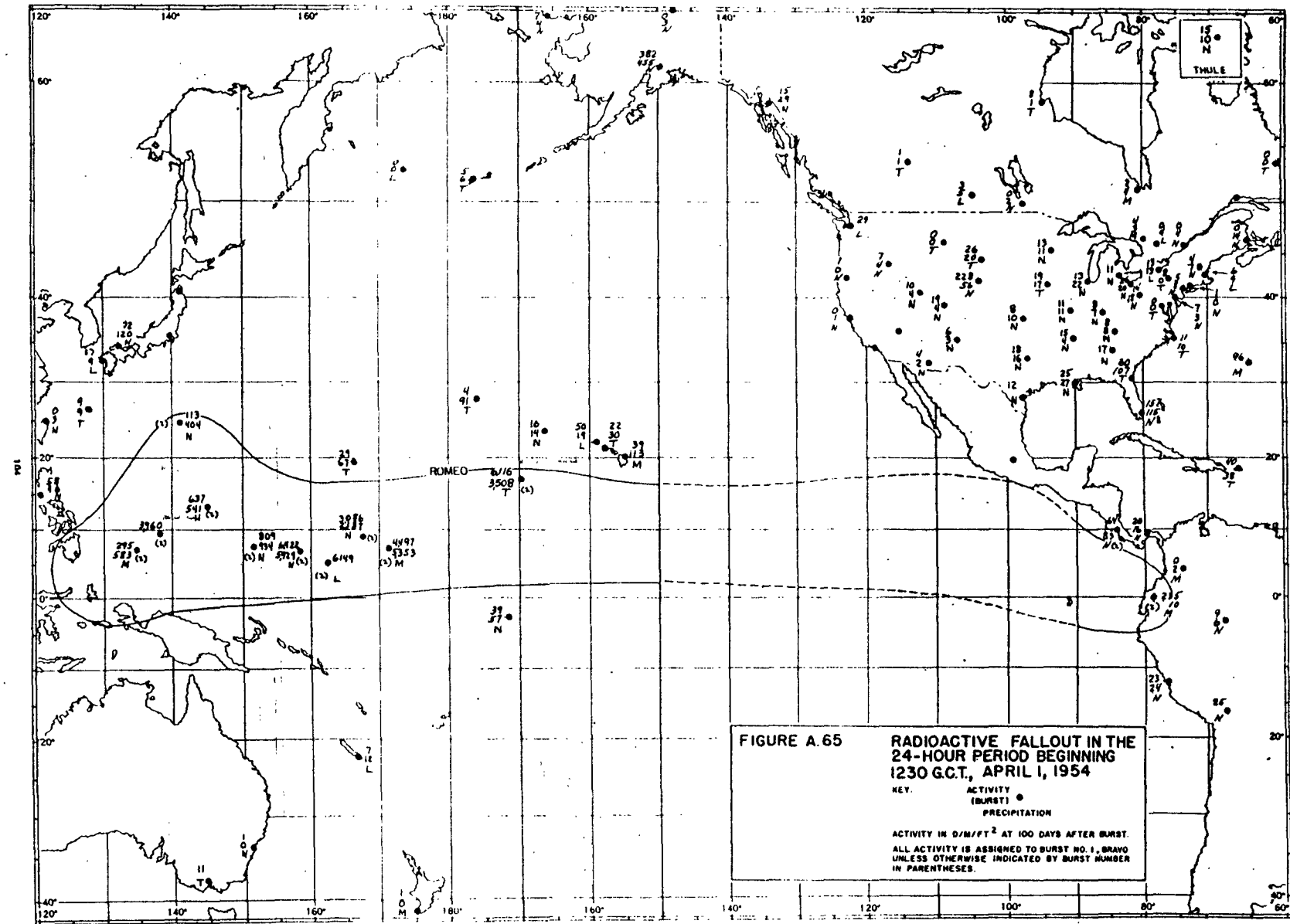


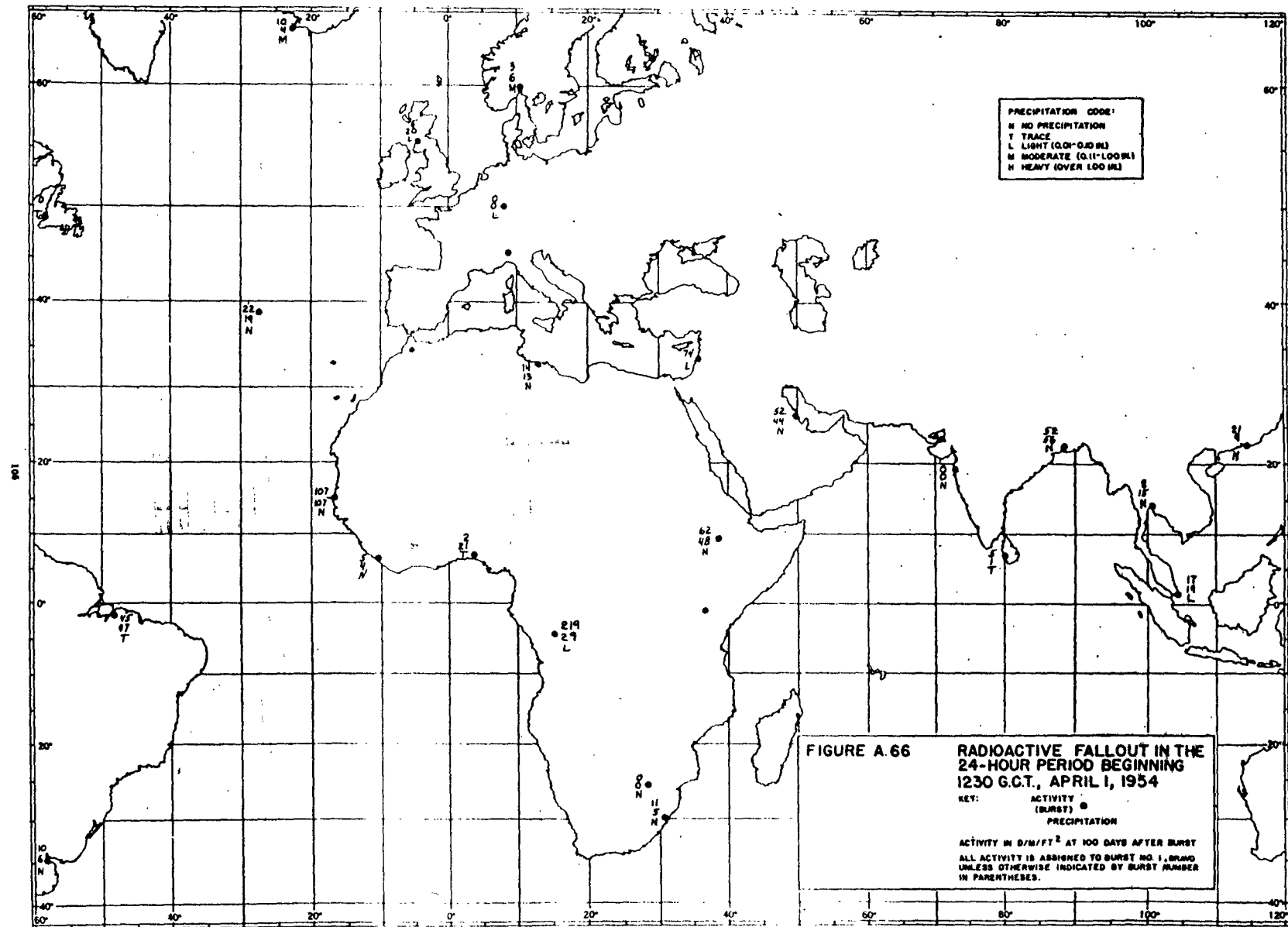
FIGURE A 63
RADIOACTIVE FALLOUT IN THE
24-HOUR PERIOD BEGINNING
1230 G.C.T., MARCH 31, 1954

KEY
ACTIVITY
(BURST) ●
PRECIPITATION

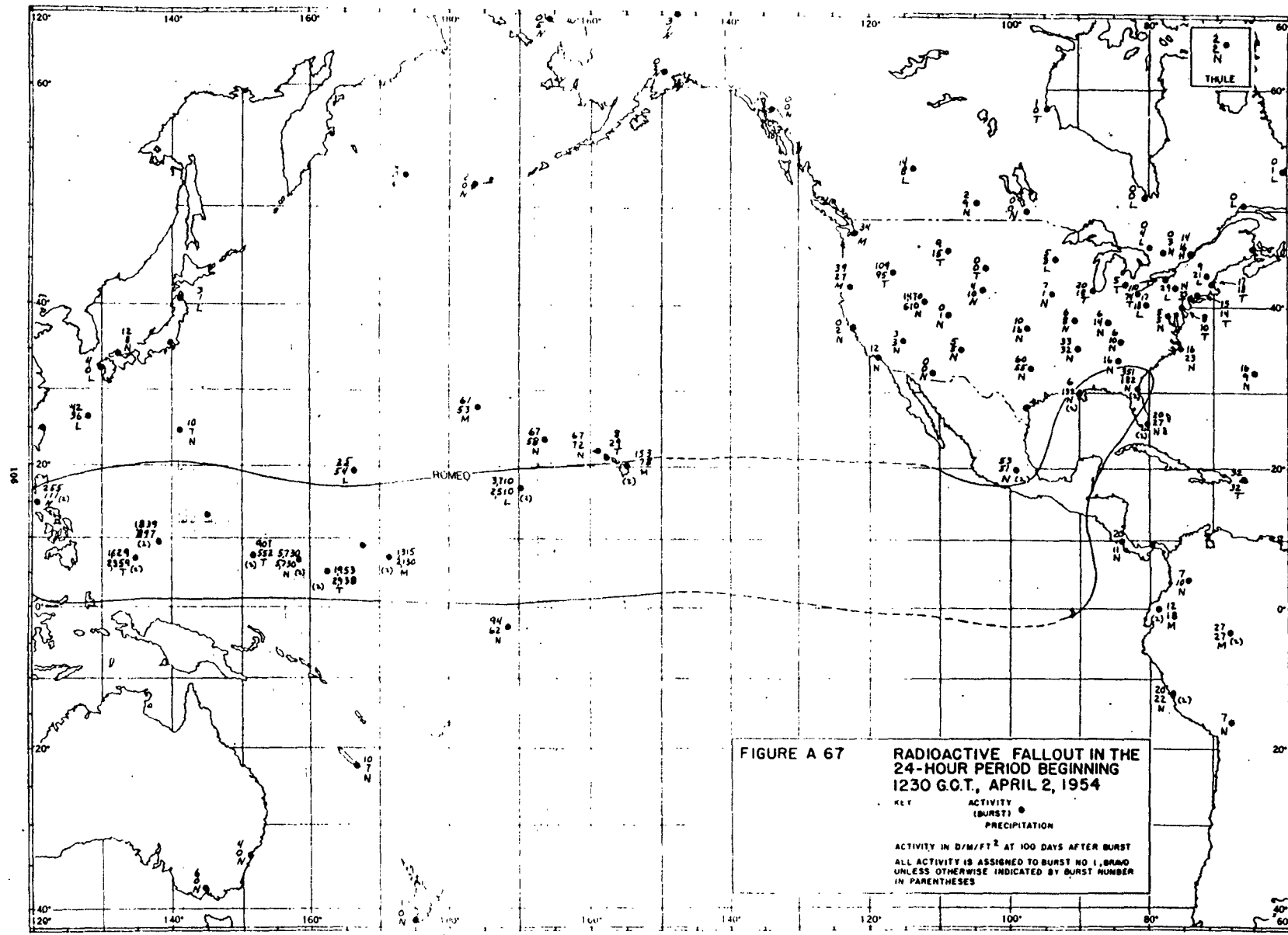
ACTIVITY IN $\mu\text{R}/\text{FT}^2$ AT 100 DAYS AFTER BURST
ALL ACTIVITY IS ASSIGNED TO BURST NO. 1, BRAVO
UNLESS OTHERWISE INDICATED BY BURST NUMBER
IN PARENTHESES.

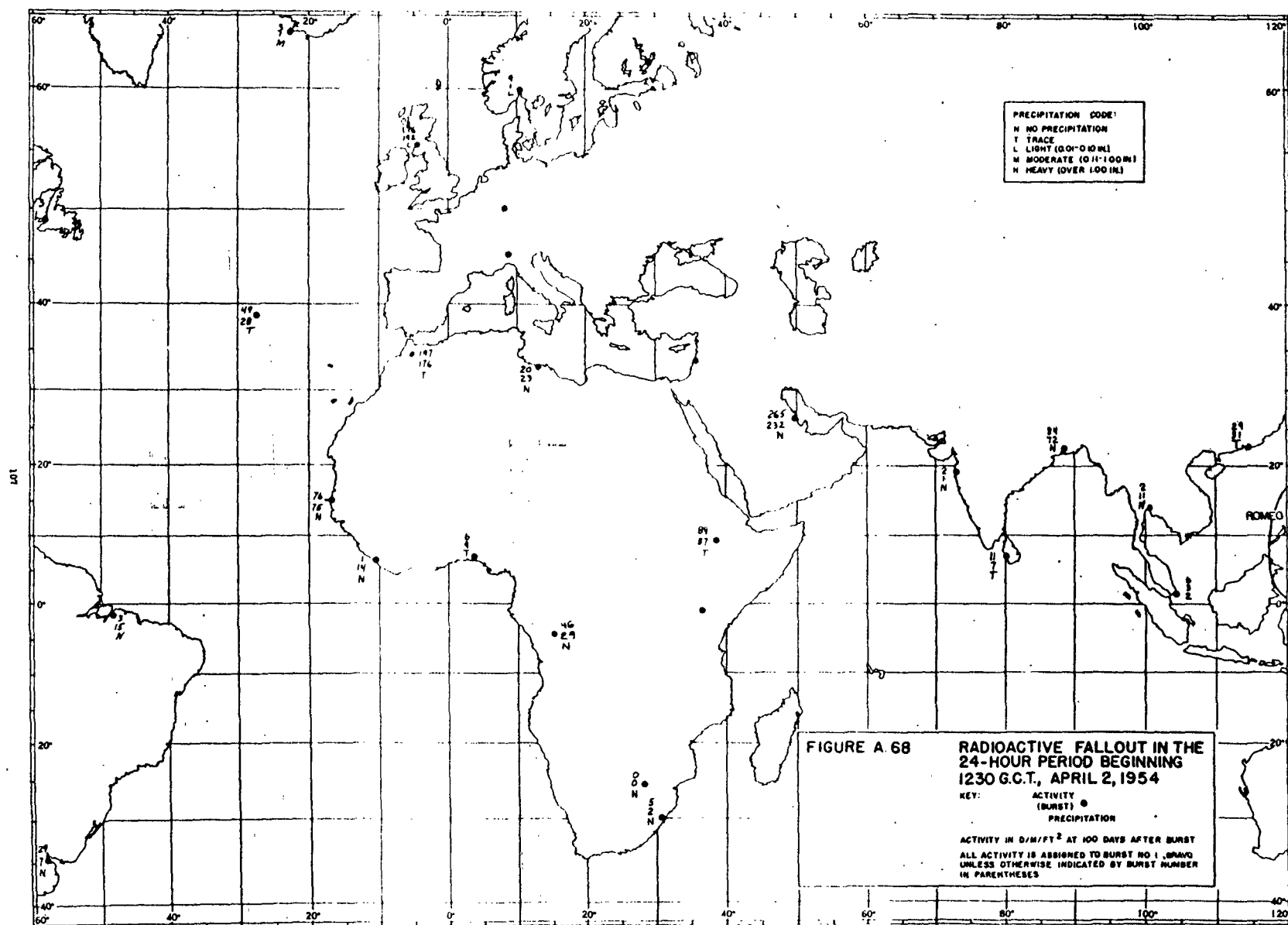






**FIGURE A.66 RADIOACTIVE FALLOUT IN THE
24-HOUR PERIOD BEGINNING
1230 G.C.T., APRIL 1, 1954**





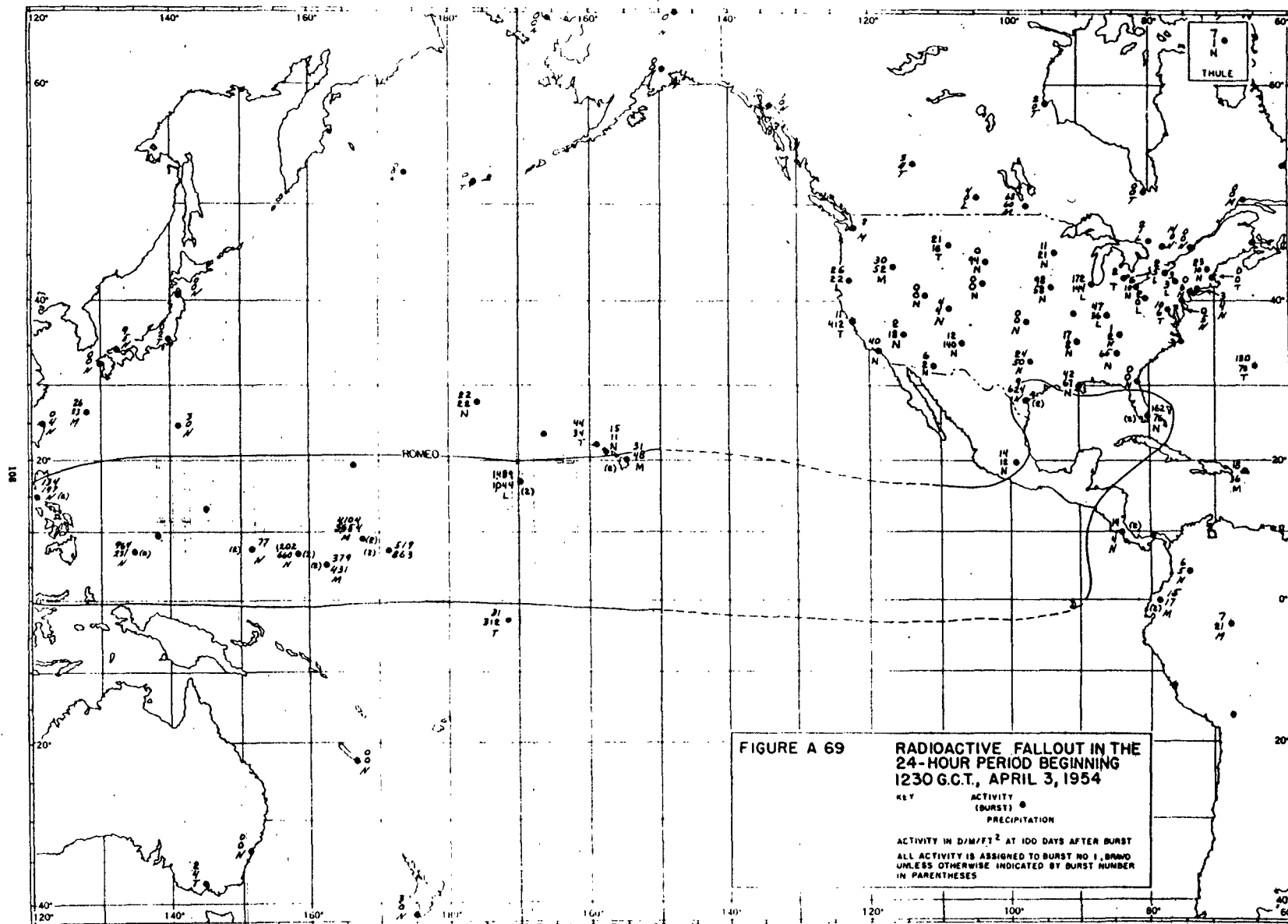
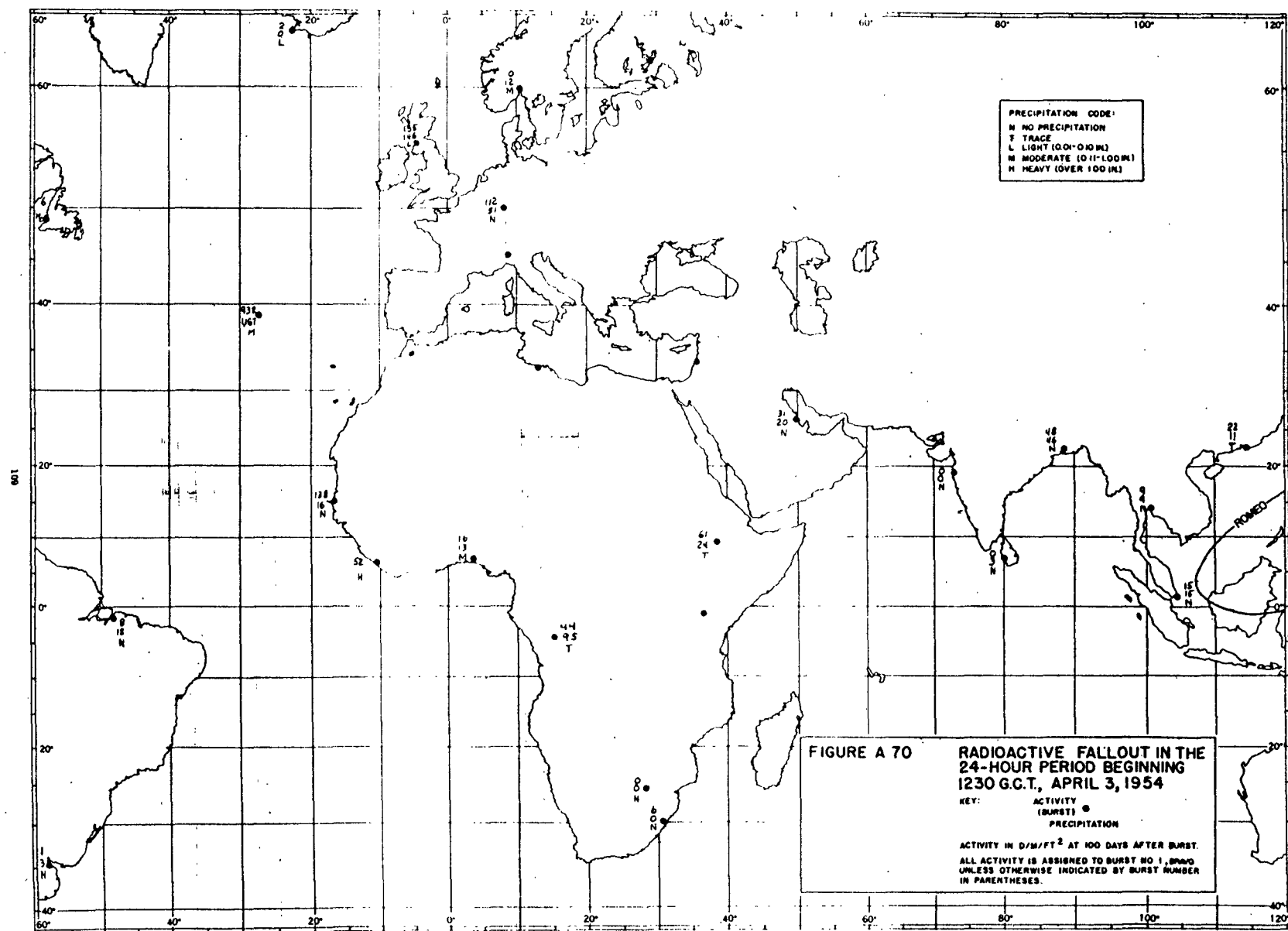
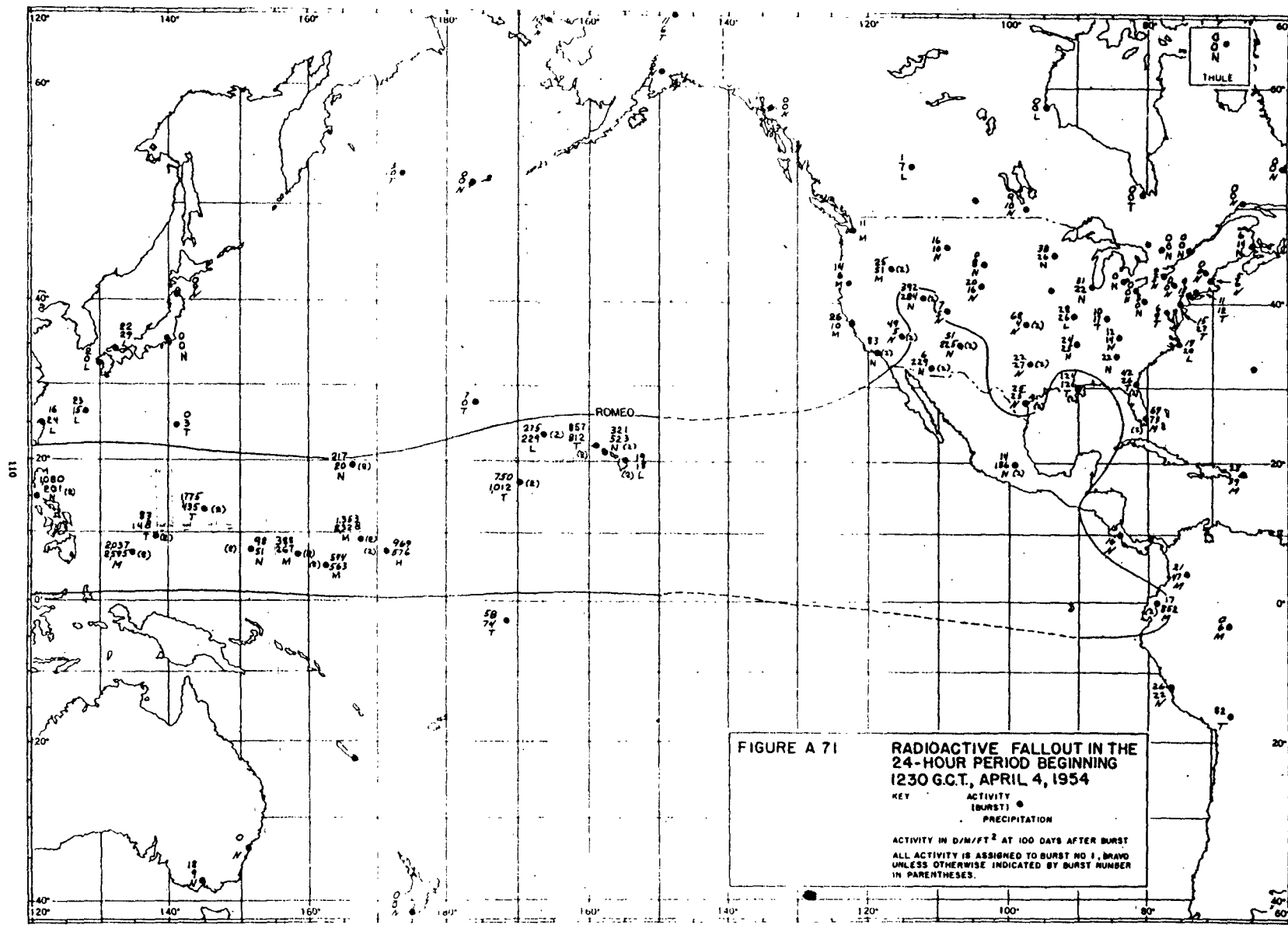
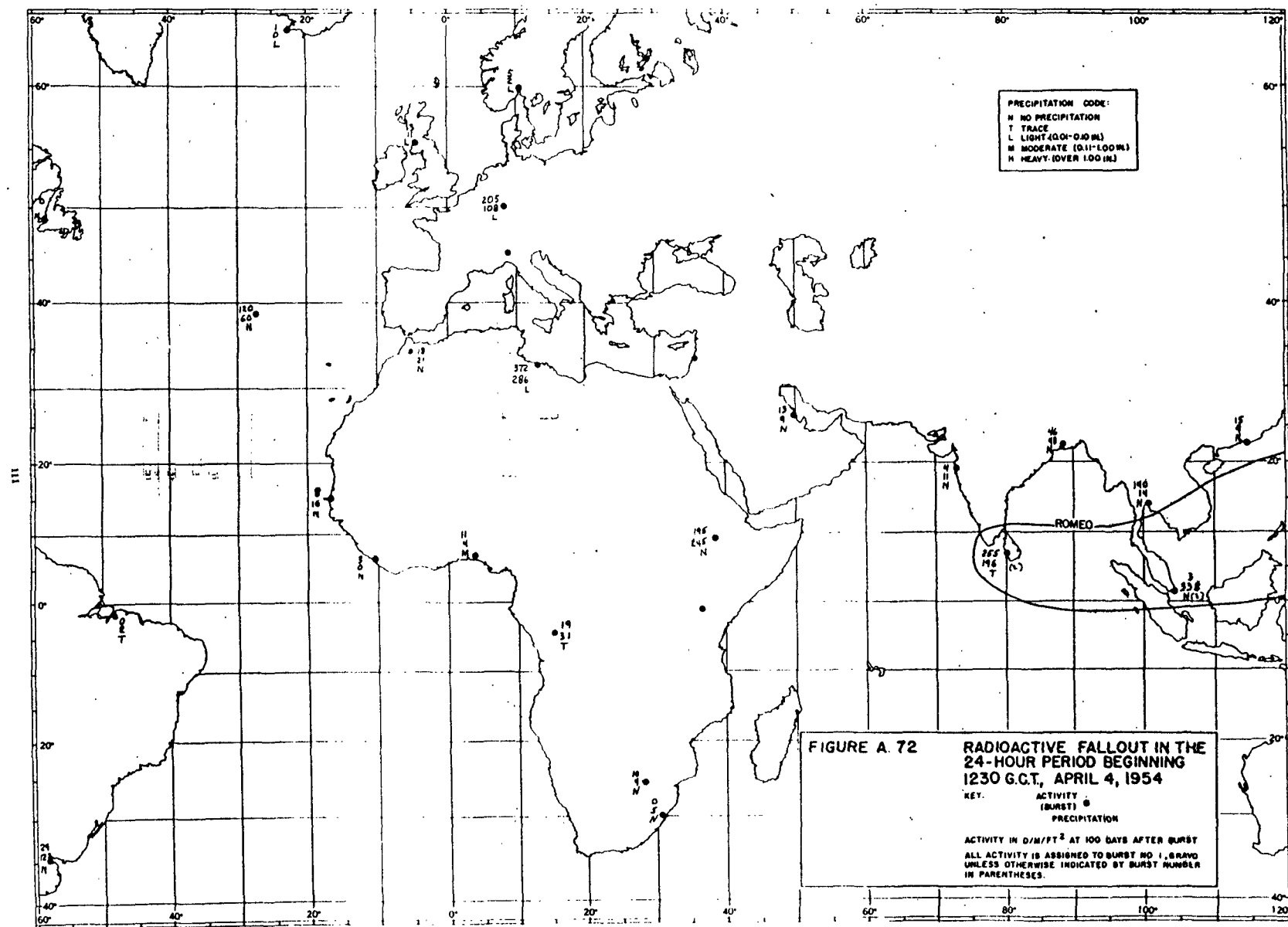
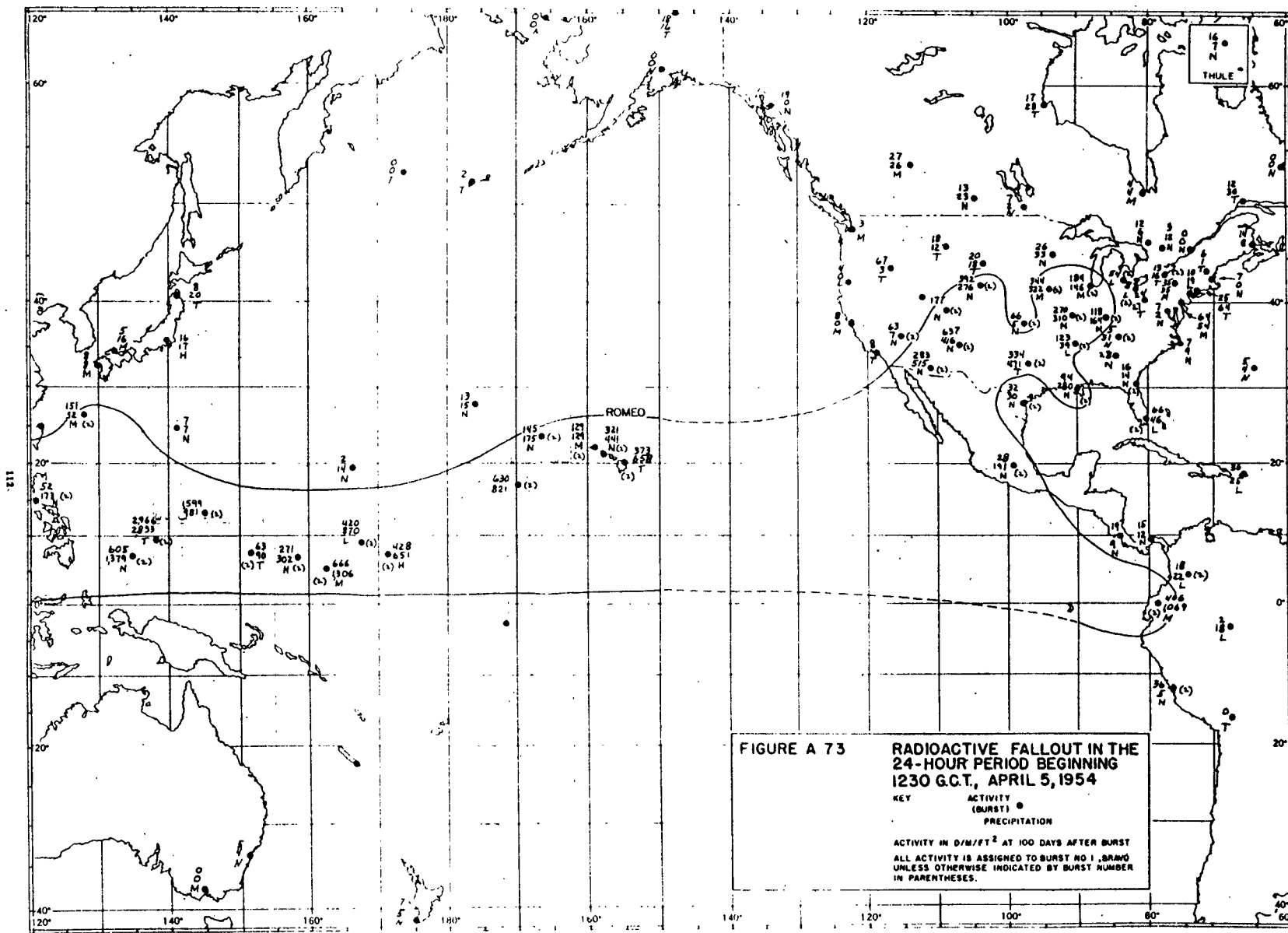


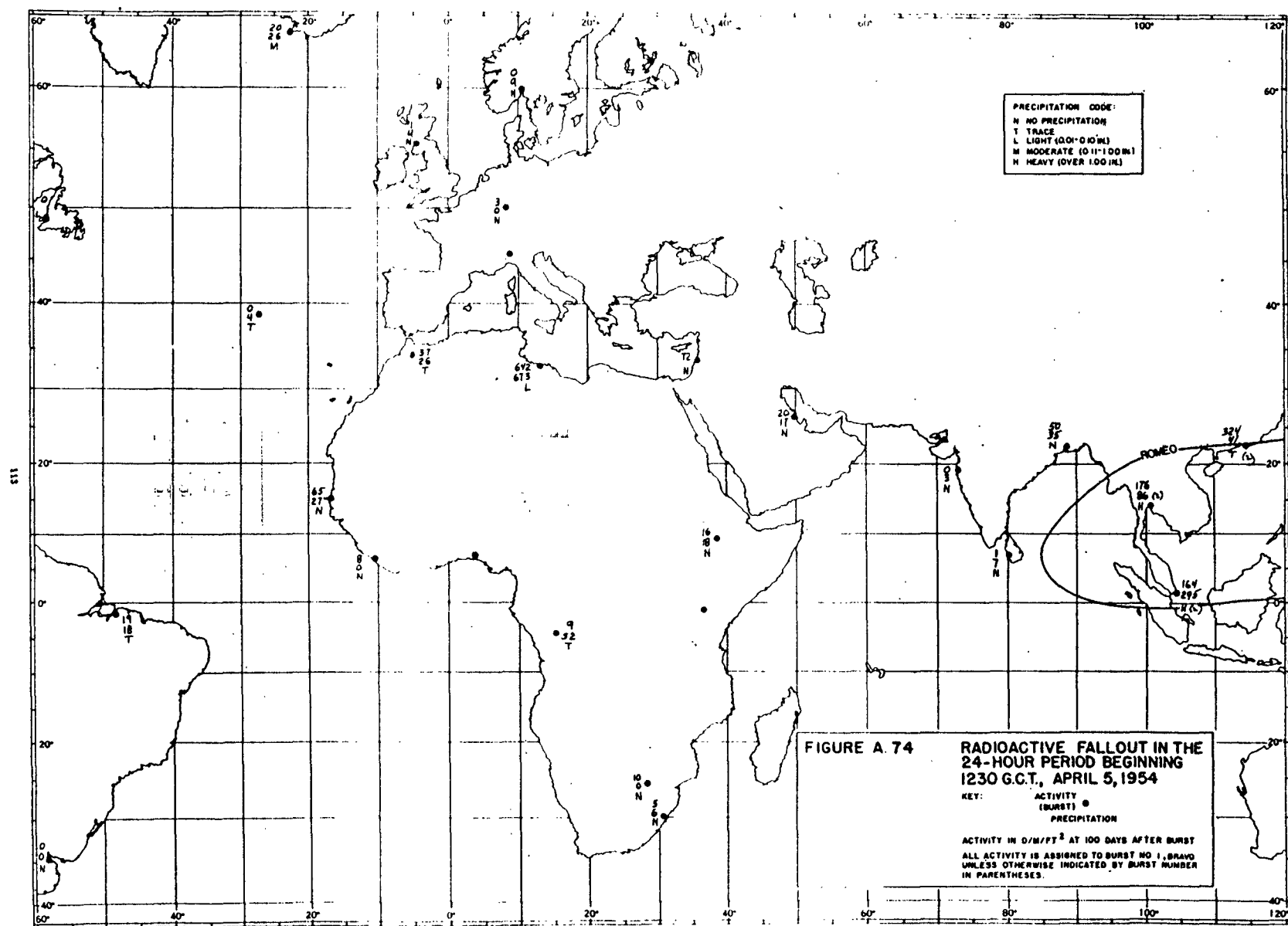
FIGURE A 69 **RADIOACTIVE FALLOUT IN THE
24-HOUR PERIOD BEGINNING
1230 G.C.T., APRIL 3, 1954**

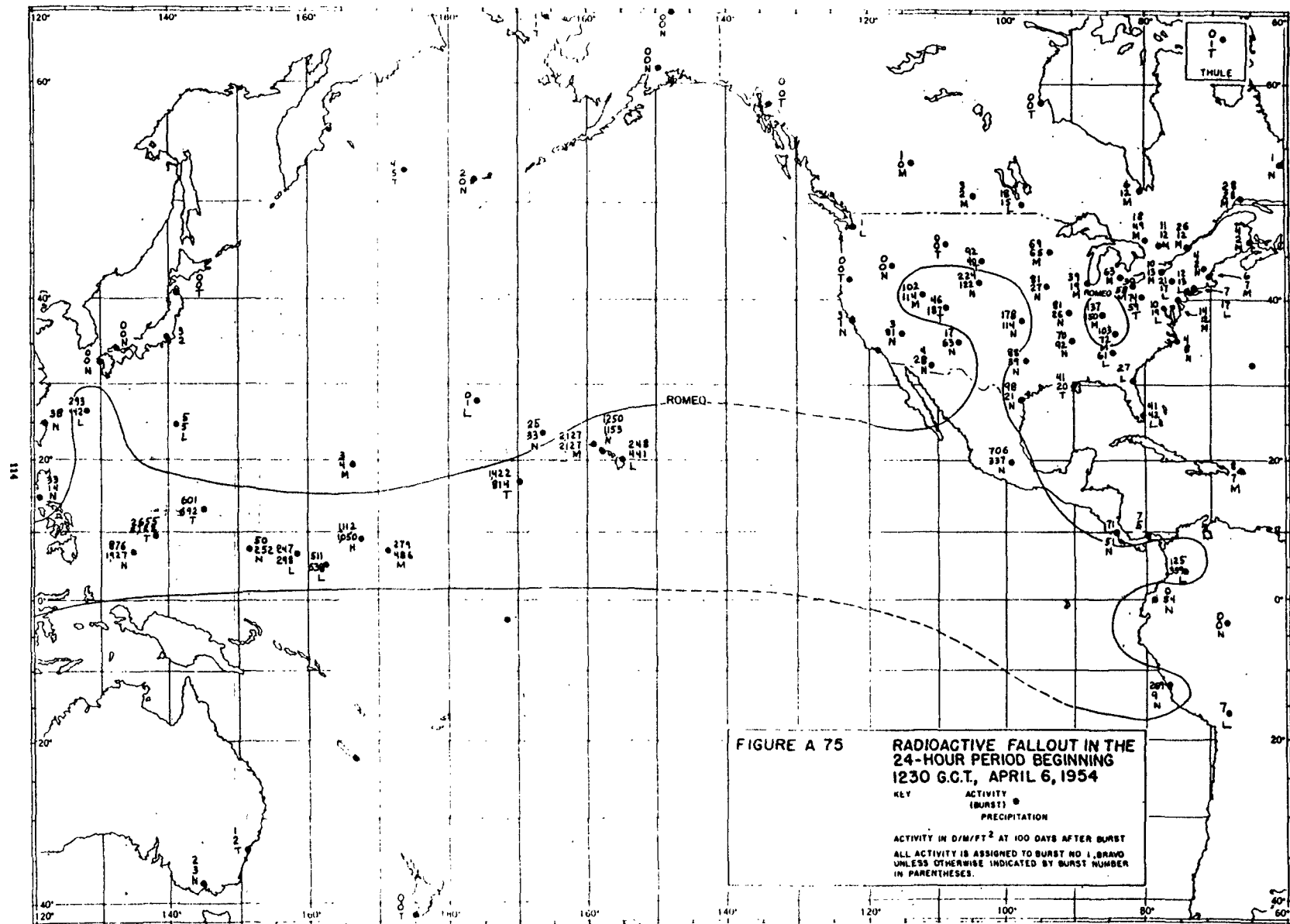


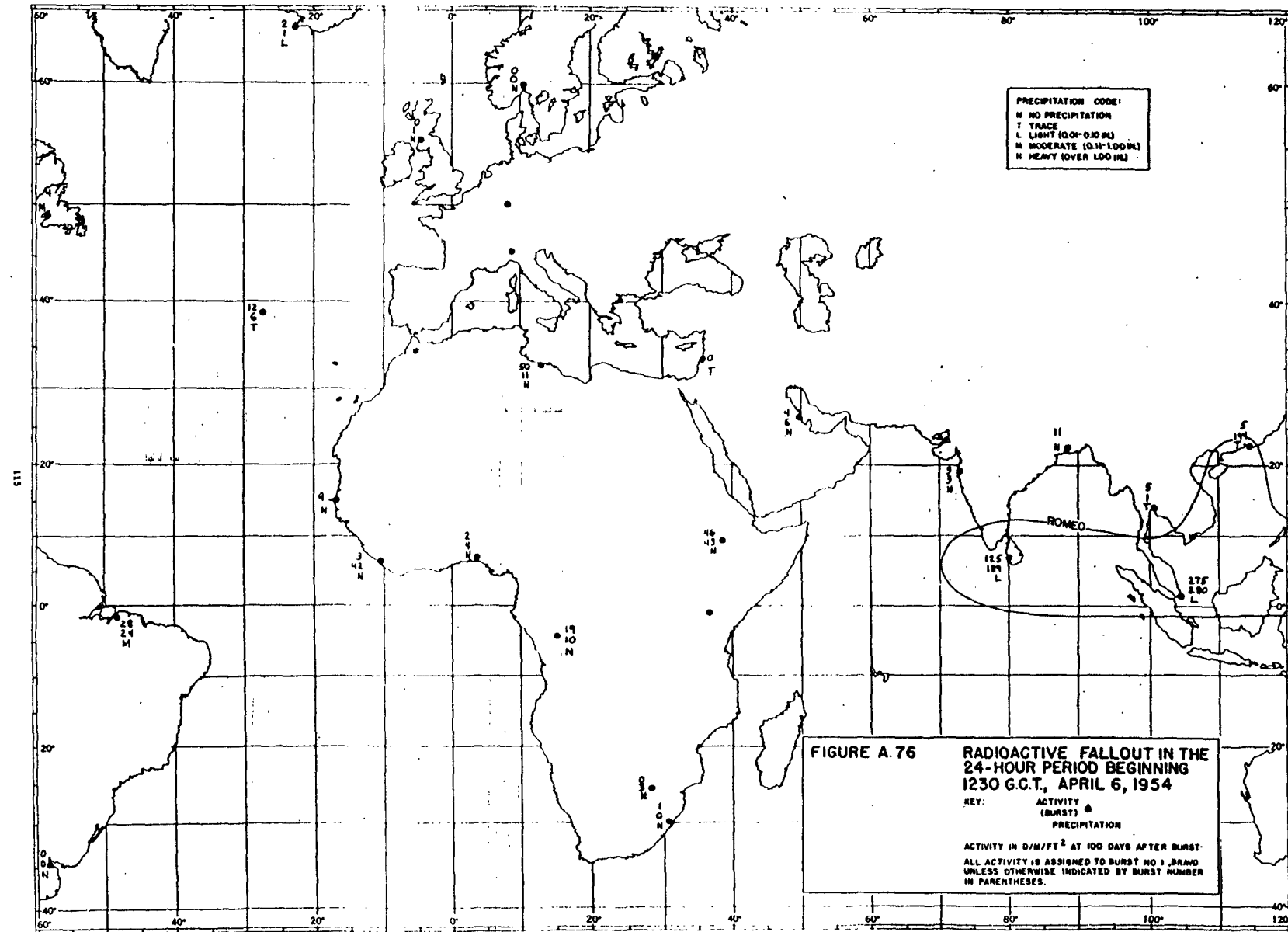


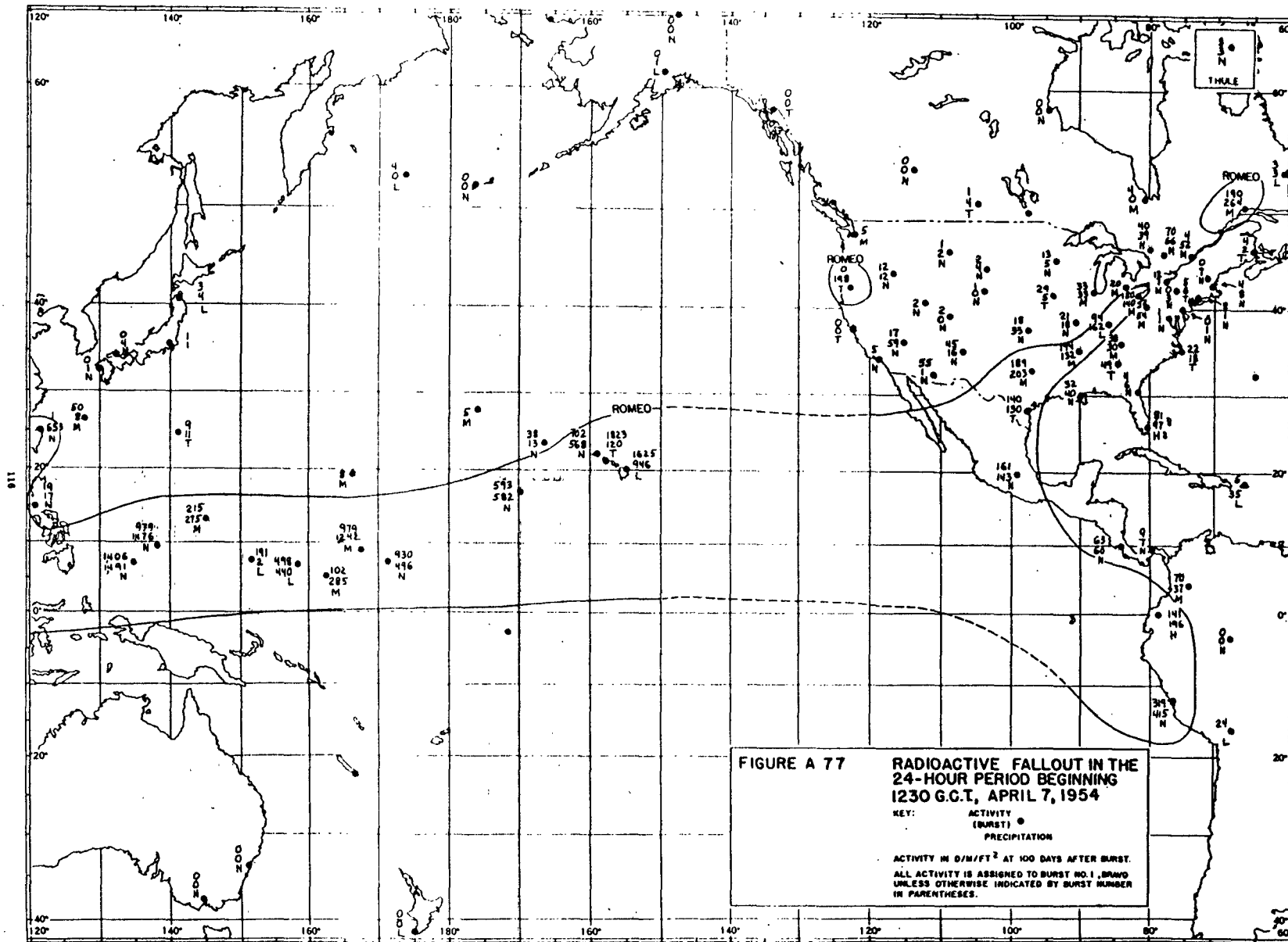


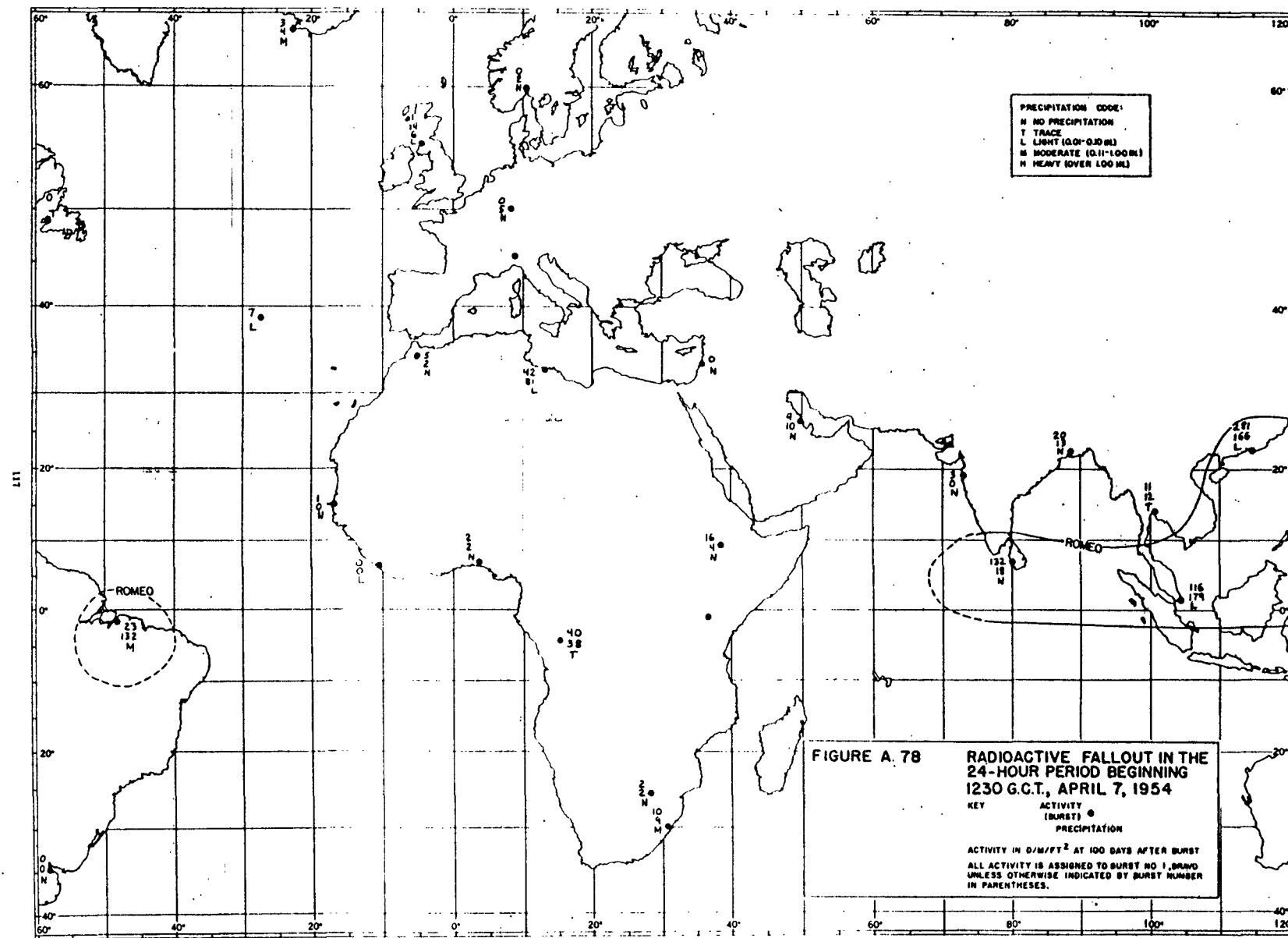












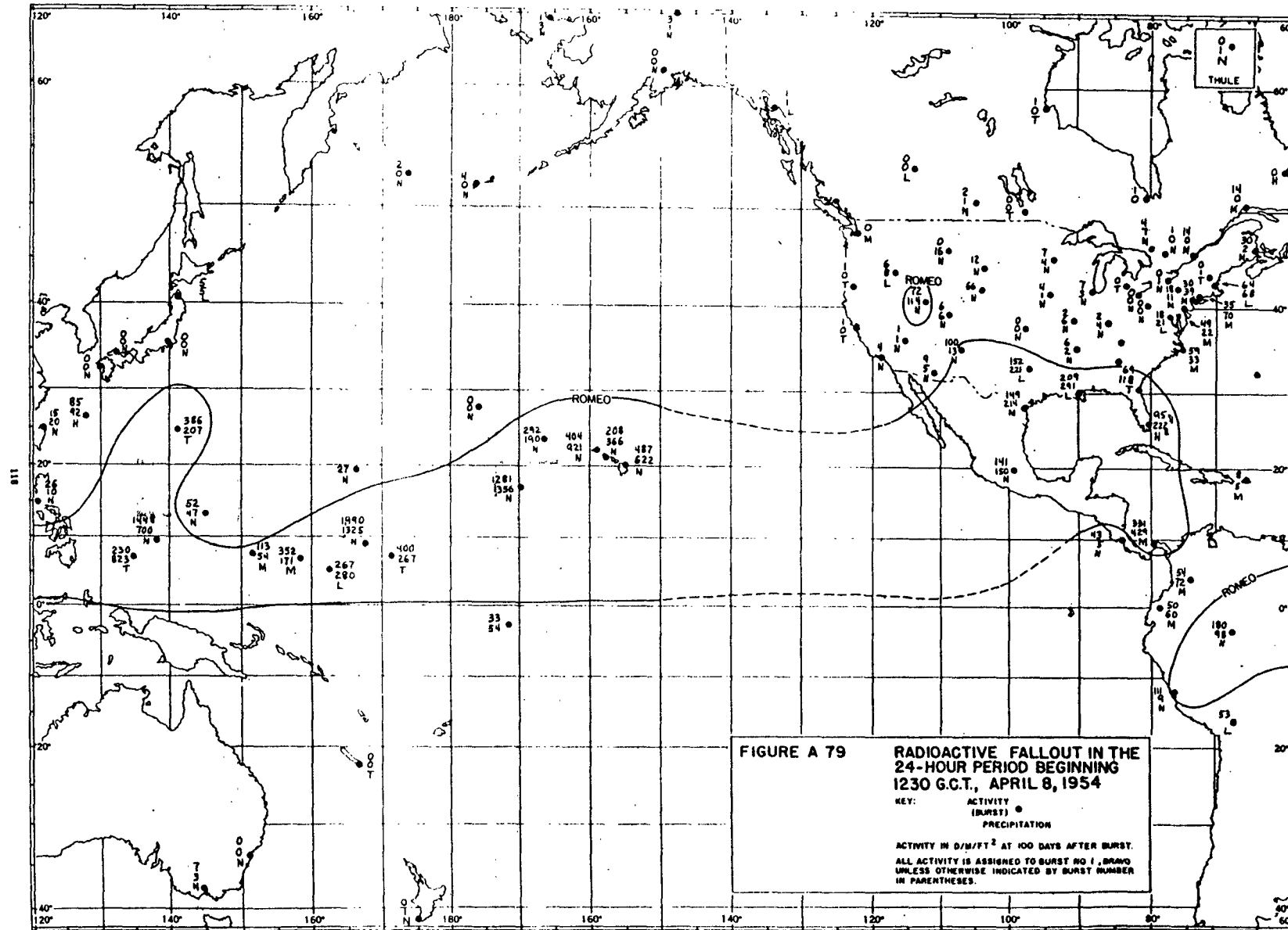
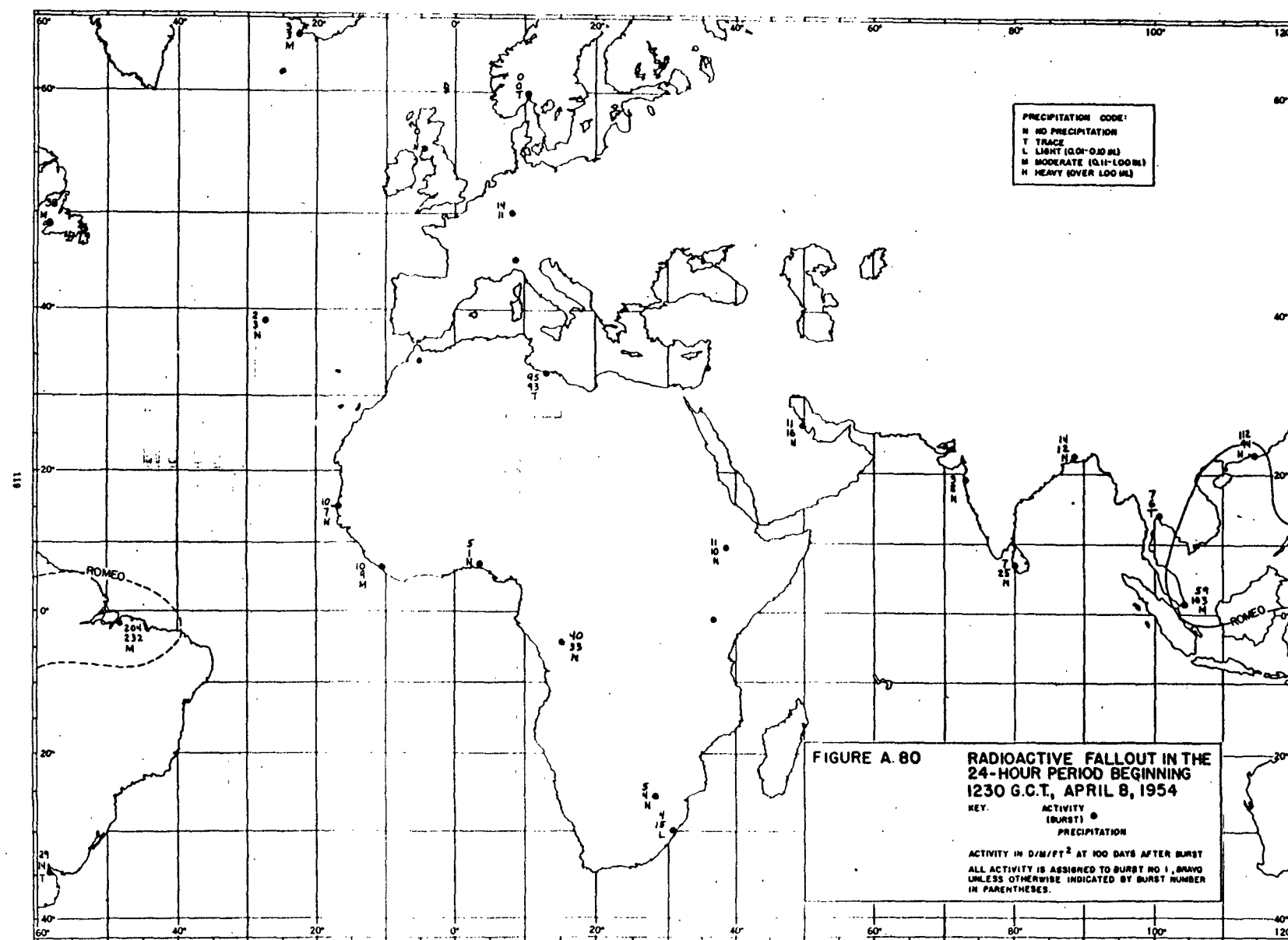
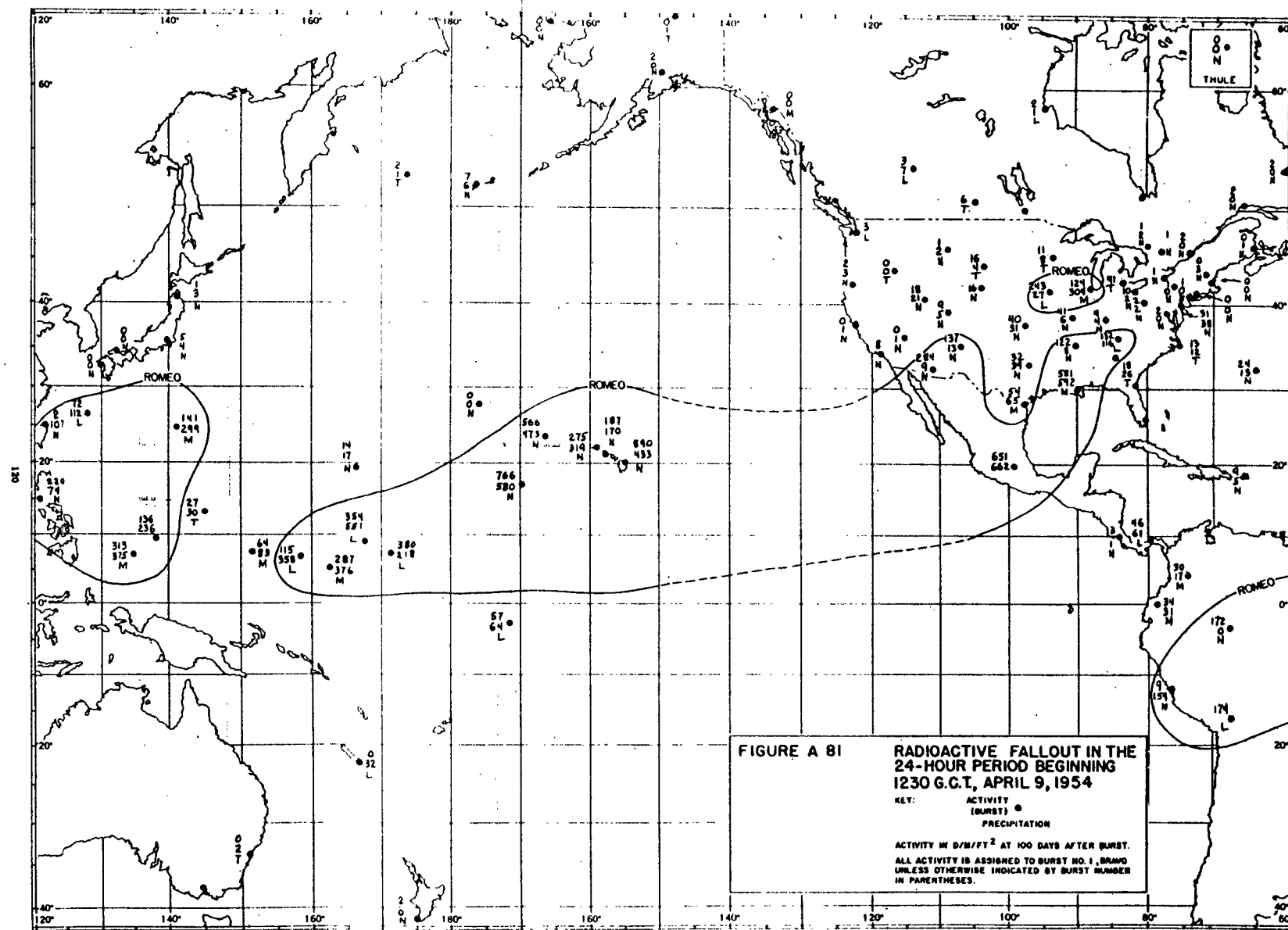


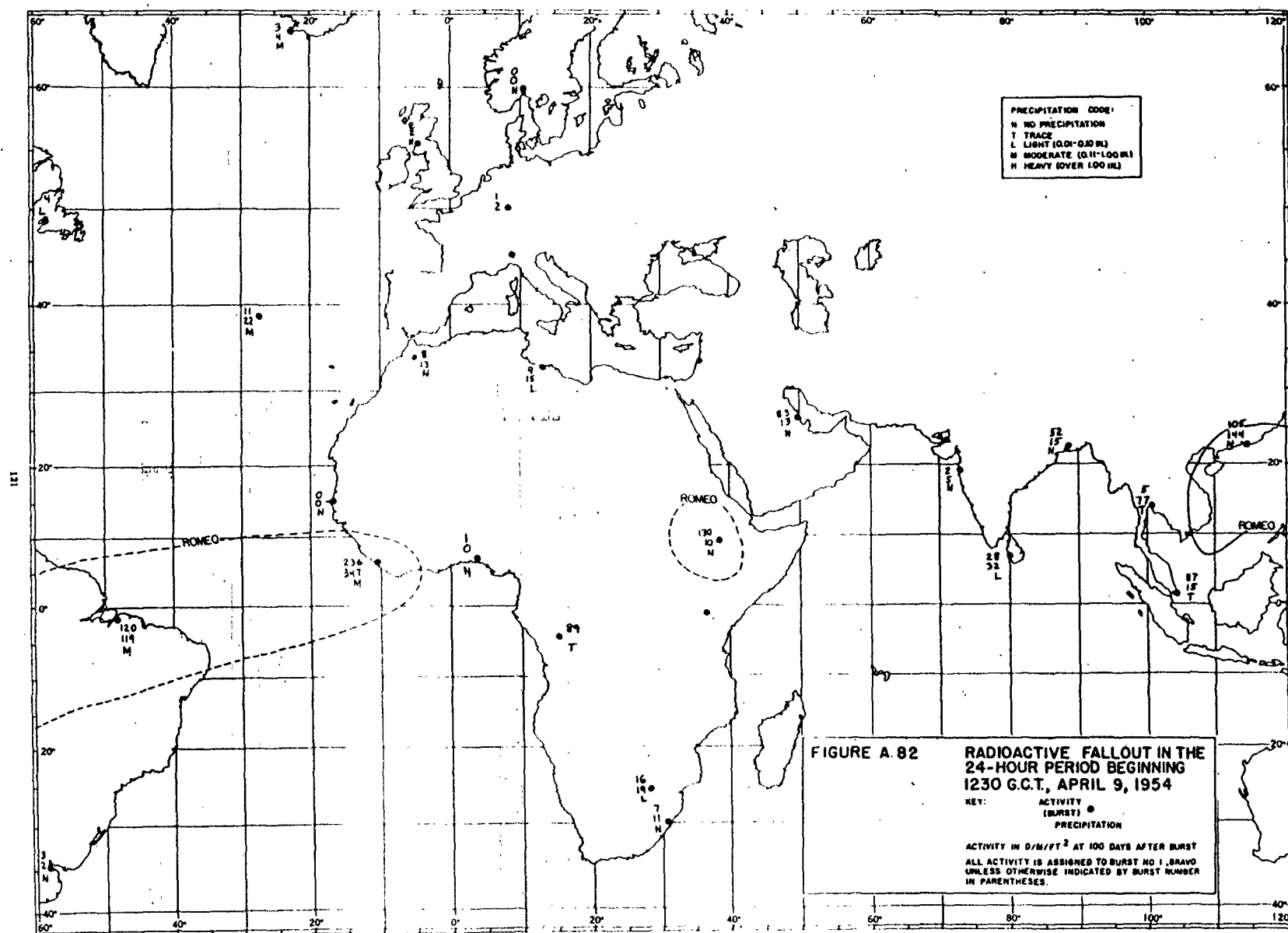
FIGURE A 79 **RADIOACTIVE FALLOUT IN THE
24-HOUR PERIOD BEGINNING
1230 G.C.T., APRIL 8, 1954**

KEY: ACTIVITY (BURST) • PRECIPITATION

ACTIVITY IN D/M² FT² AT 100 DAYS AFTER BURST
ALL ACTIVITY IS ASSIGNED TO BURST NO 1, BRAVO
UNLESS OTHERWISE INDICATED BY BURST NUMBER
IN PARENTHESES.







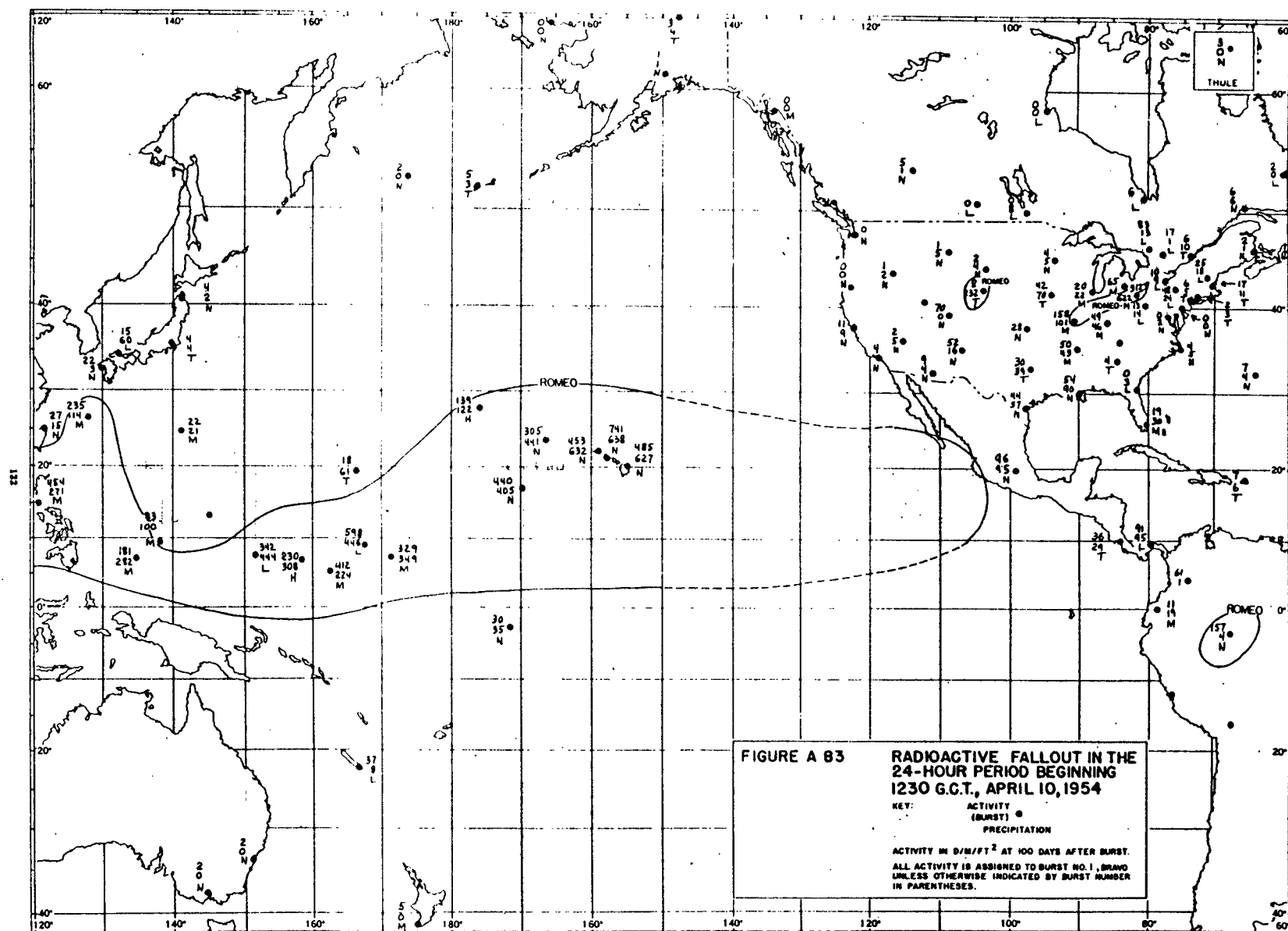
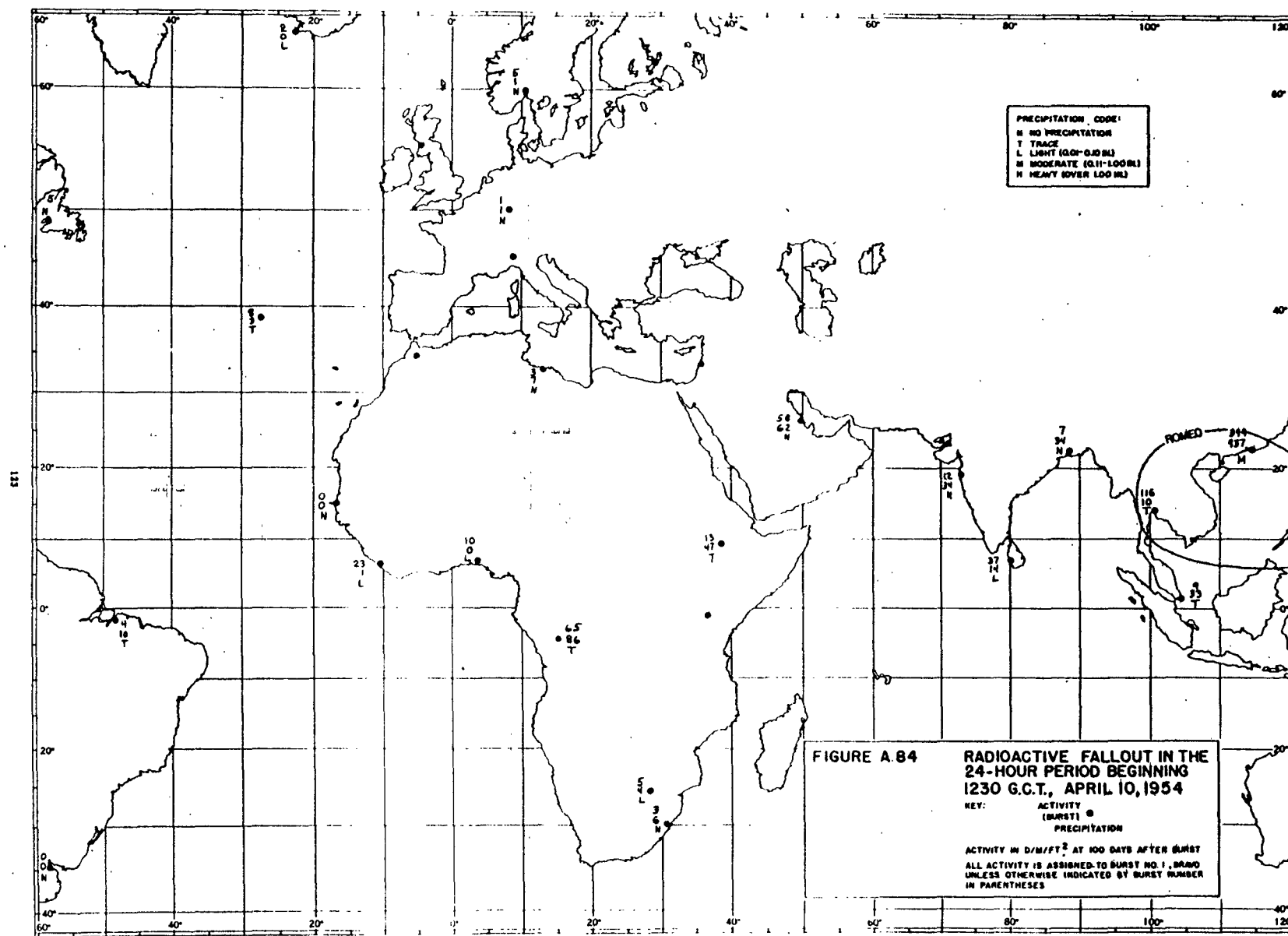
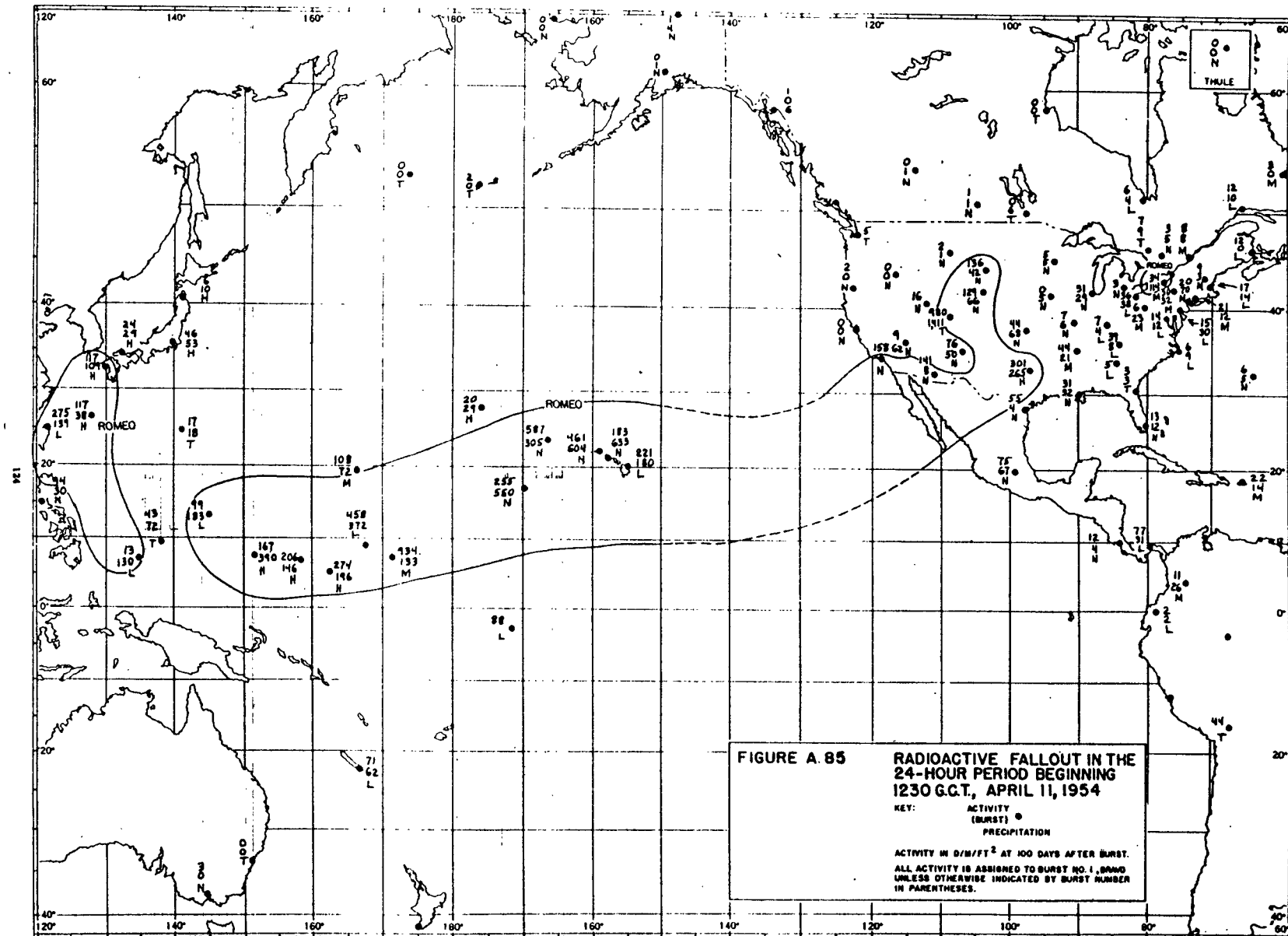


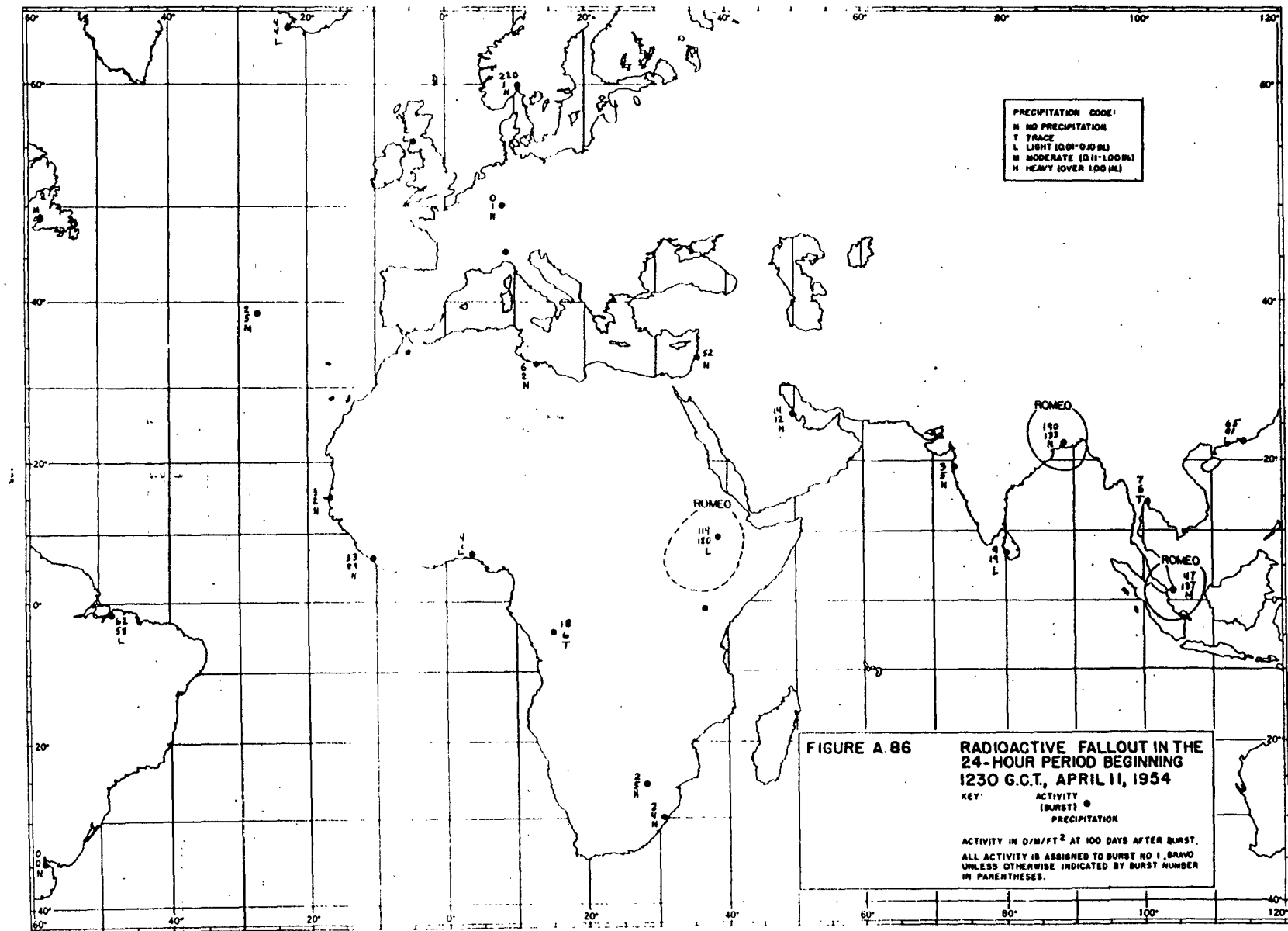
FIGURE A 83 **RADIOACTIVE FALLOUT IN THE
24-HOUR PERIOD BEGINNING
1230 G.C.T., APRIL 10, 1954**

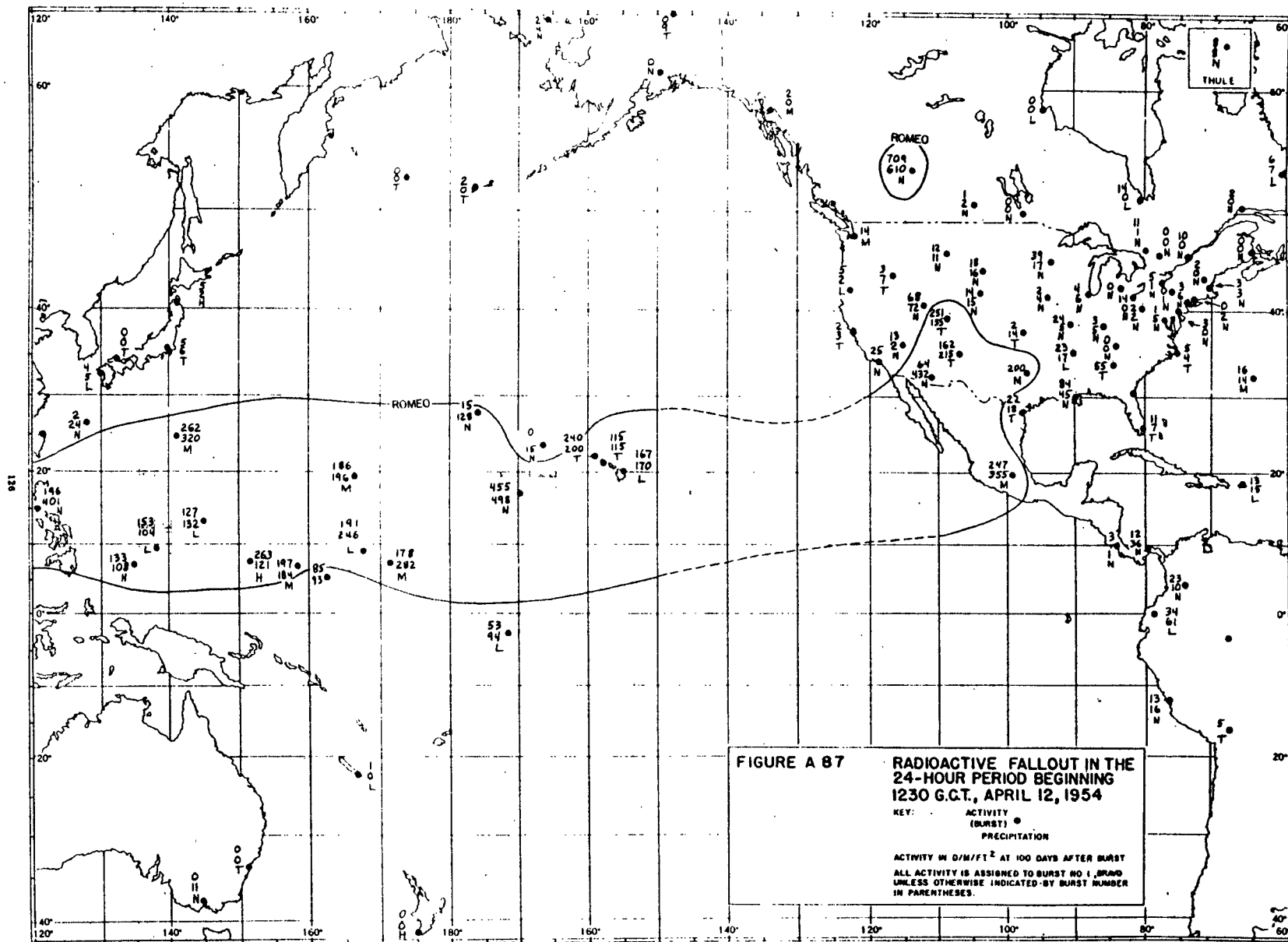
KEY:
 ACTIVITY
 (BURST) •
 PRECIPITATION

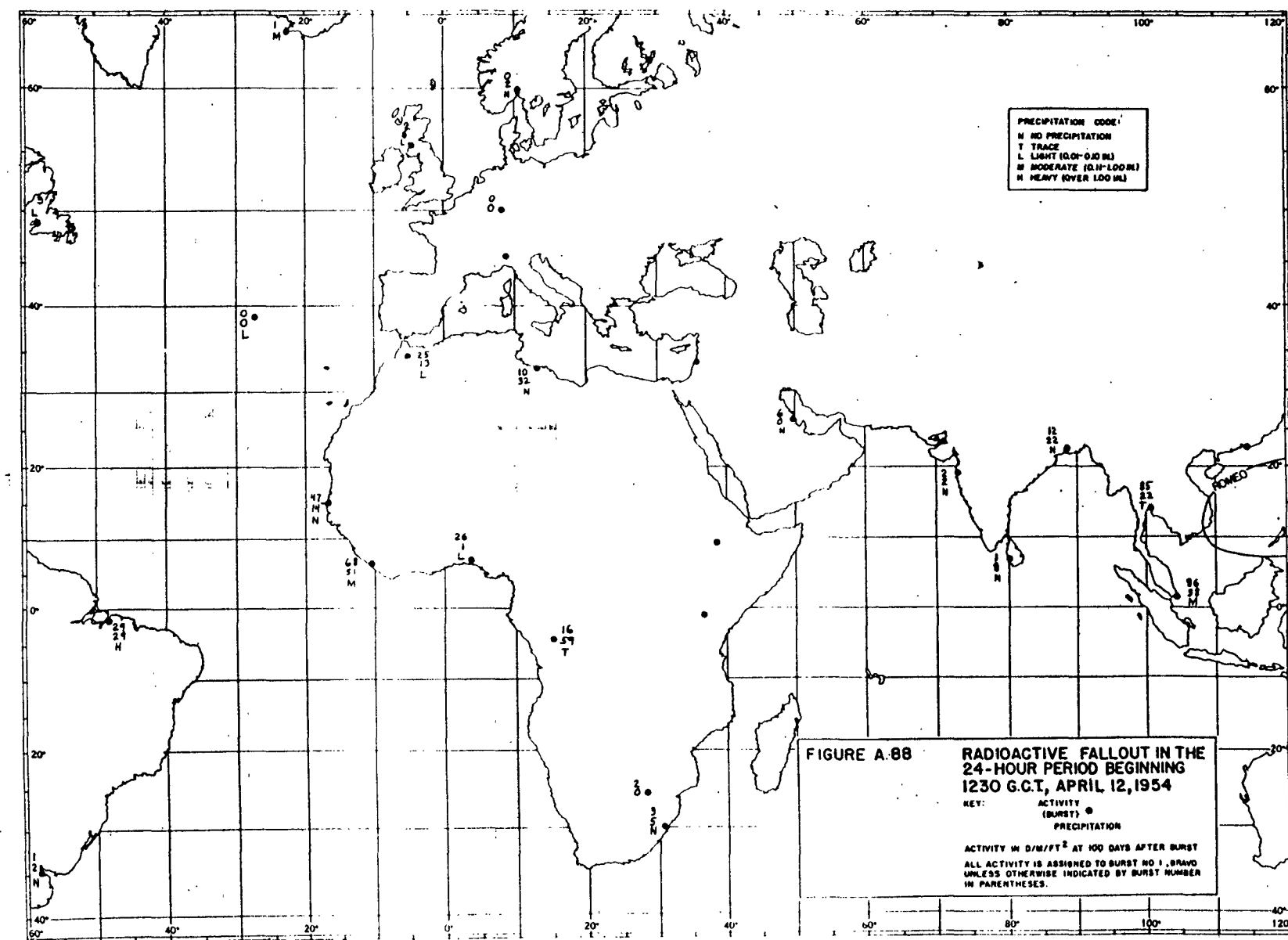
ACTIVITY IN dpm/ft^2 AT 100 DAYS AFTER BURST.
 ALL ACTIVITY IS ASSIGNED TO BURST NO. 1, BRAVO
 UNLESS OTHERWISE INDICATED BY BURST NUMBER
 IN PARENTHESES.

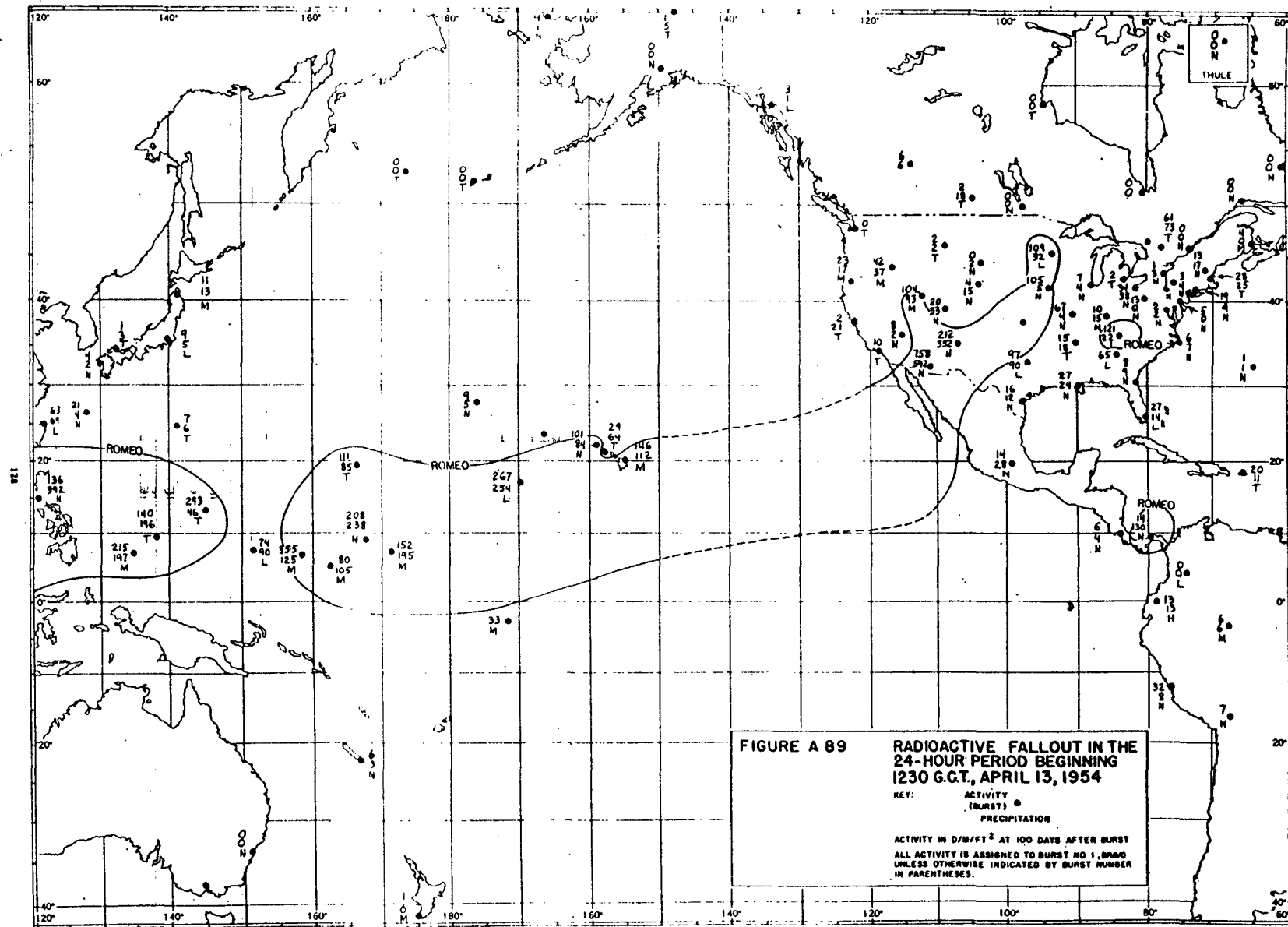












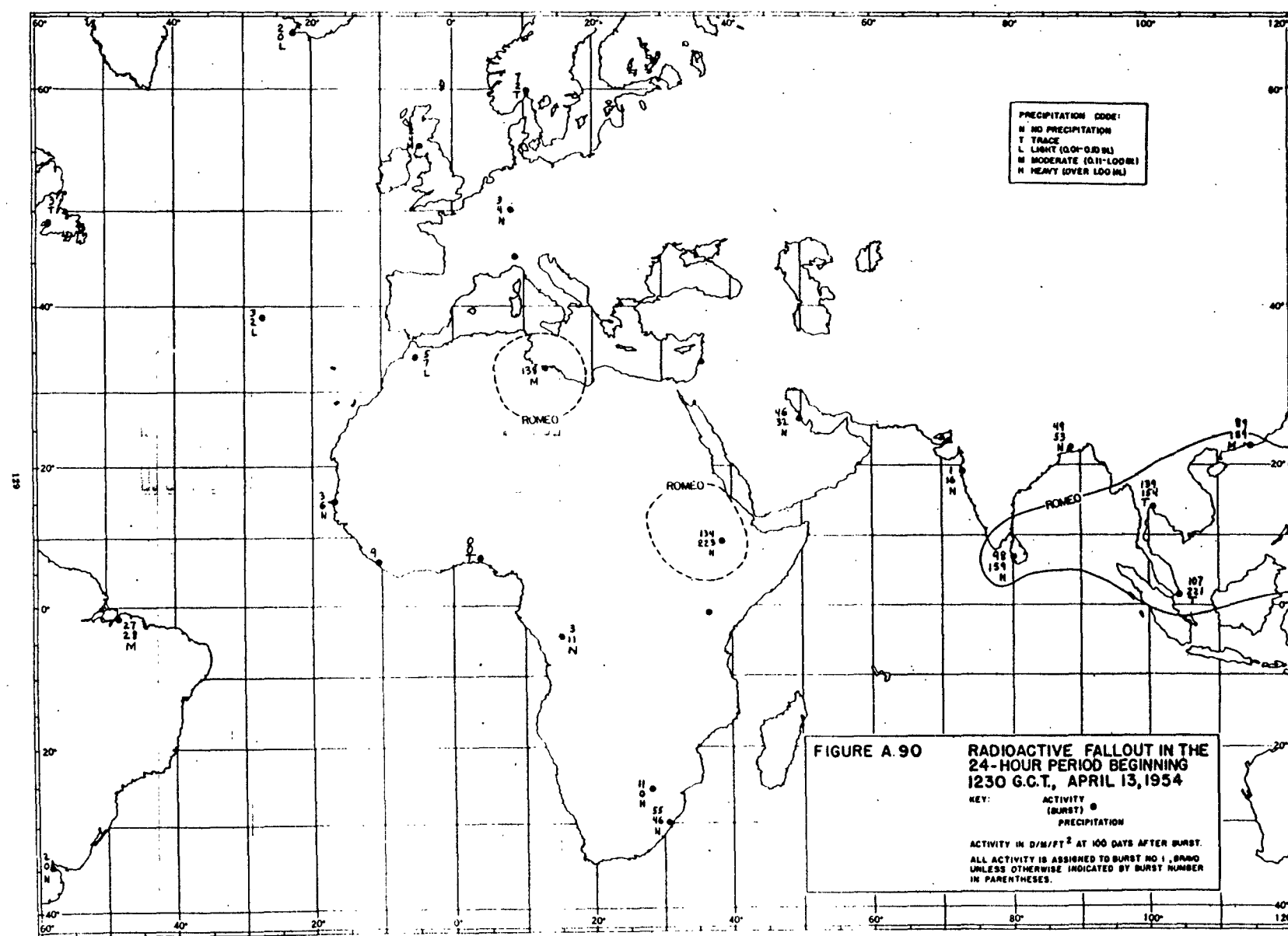


FIGURE A.90 **RADIOACTIVE FALLOUT IN THE
24-HOUR PERIOD BEGINNING
1230 G.C.T., APRIL 13, 1954**

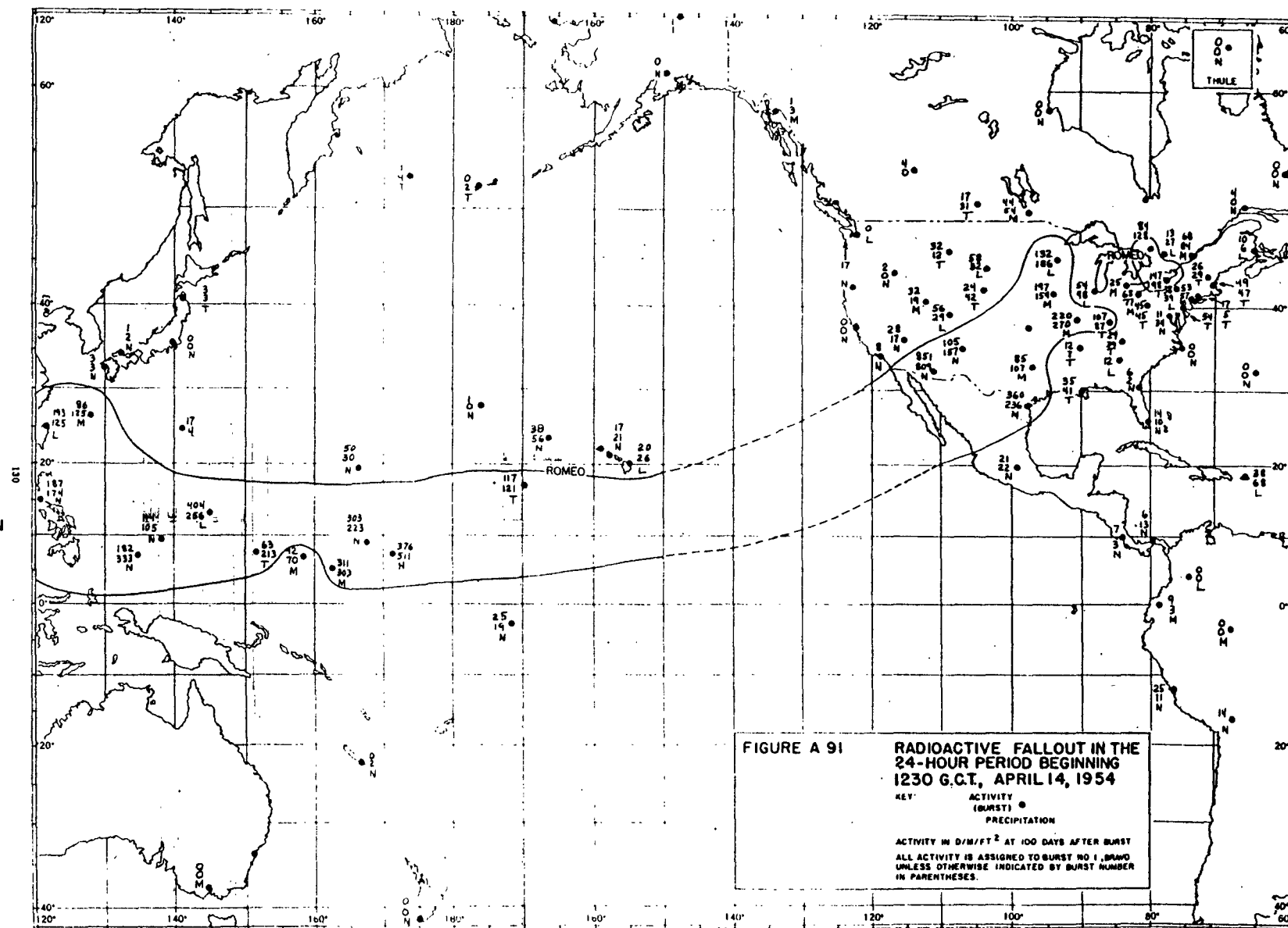


FIGURE A 91
RADIOACTIVE FALLOUT IN THE
24-HOUR PERIOD BEGINNING
1230 G.C.T., APRIL 14, 1954

KEY:
ACTIVITY
(BURST)
PRECIPITATION

ACTIVITY IN $\text{D}/\text{M}^2/\text{FT}^2$ AT 100 DAYS AFTER BURST
ALL ACTIVITY IS ASSIGNED TO BURST NO 1, BRAVO
UNLESS OTHERWISE INDICATED BY BURST NUMBER
IN PARENTHESES.

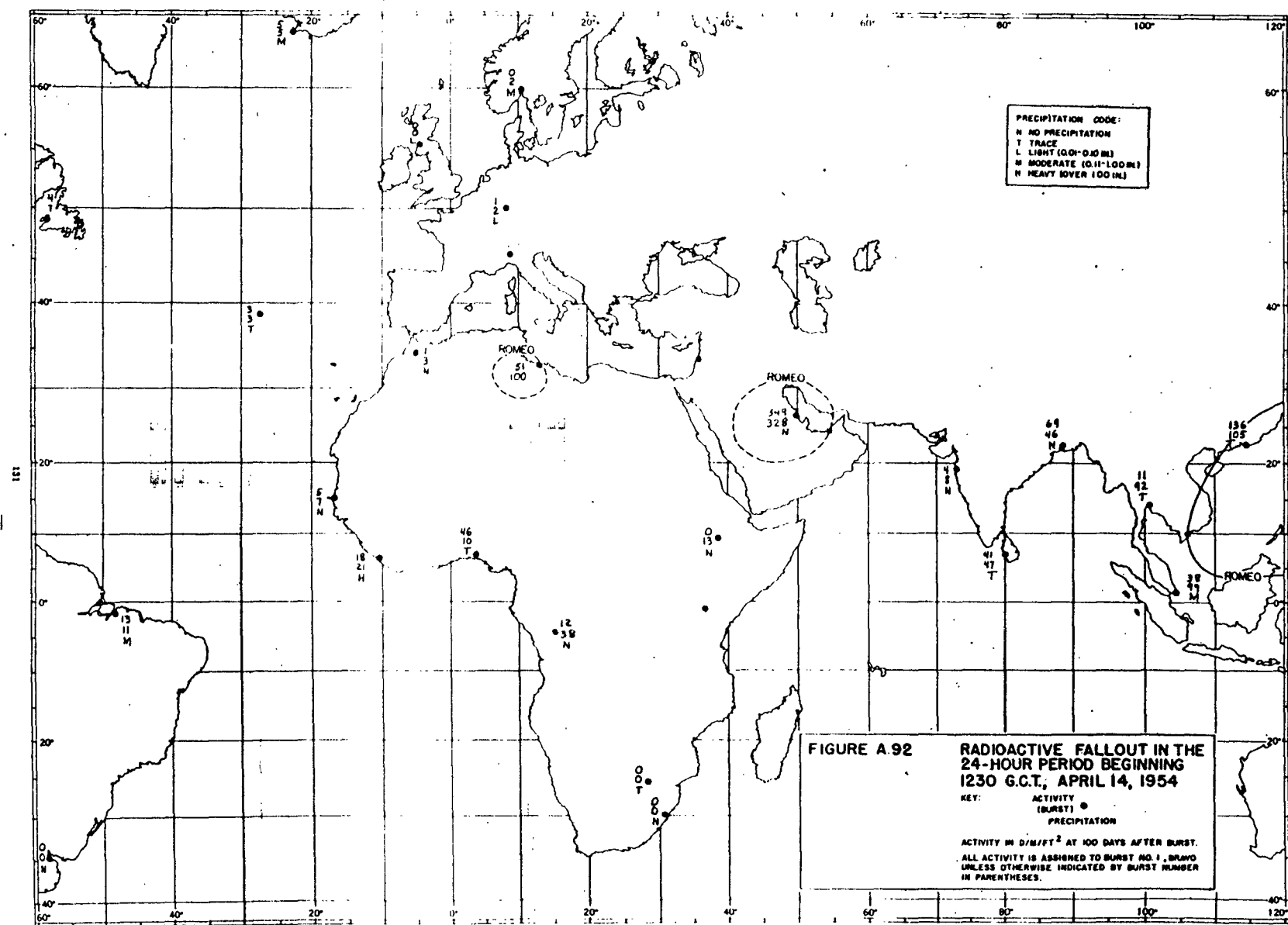


FIGURE A.92
RADIOACTIVE FALLOUT IN THE
24-HOUR PERIOD BEGINNING
1230 G.C.T., APRIL 14, 1954

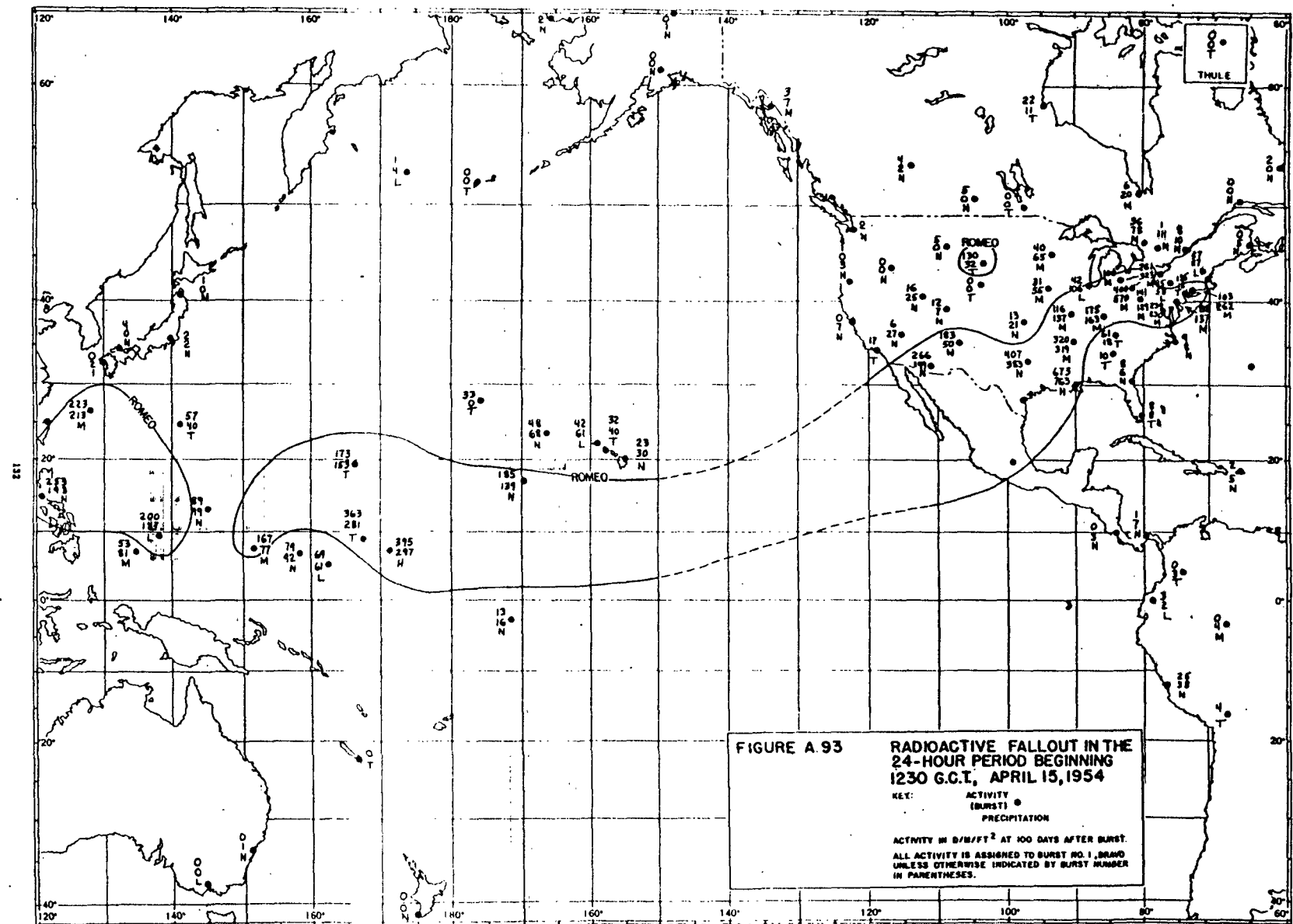
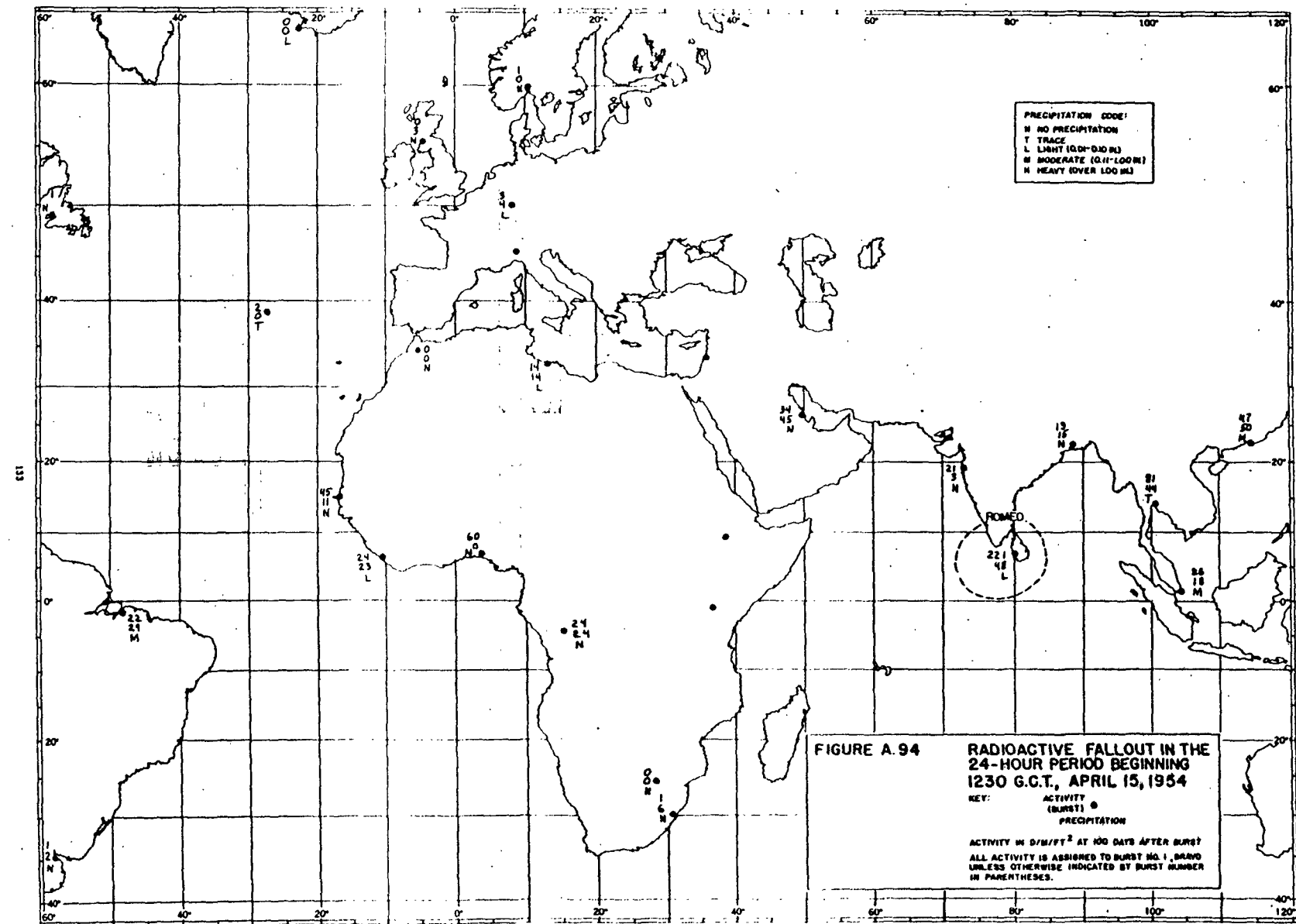
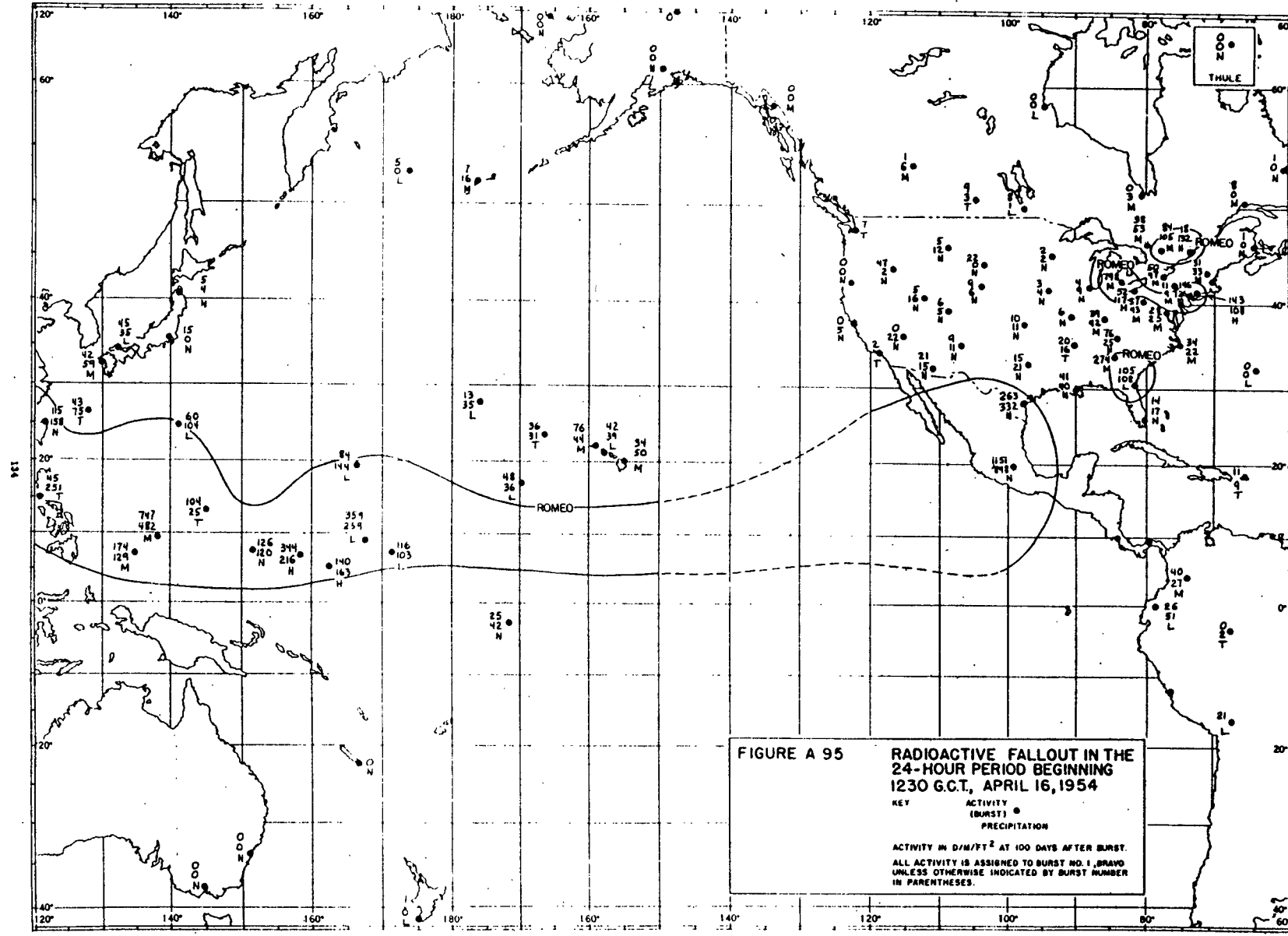
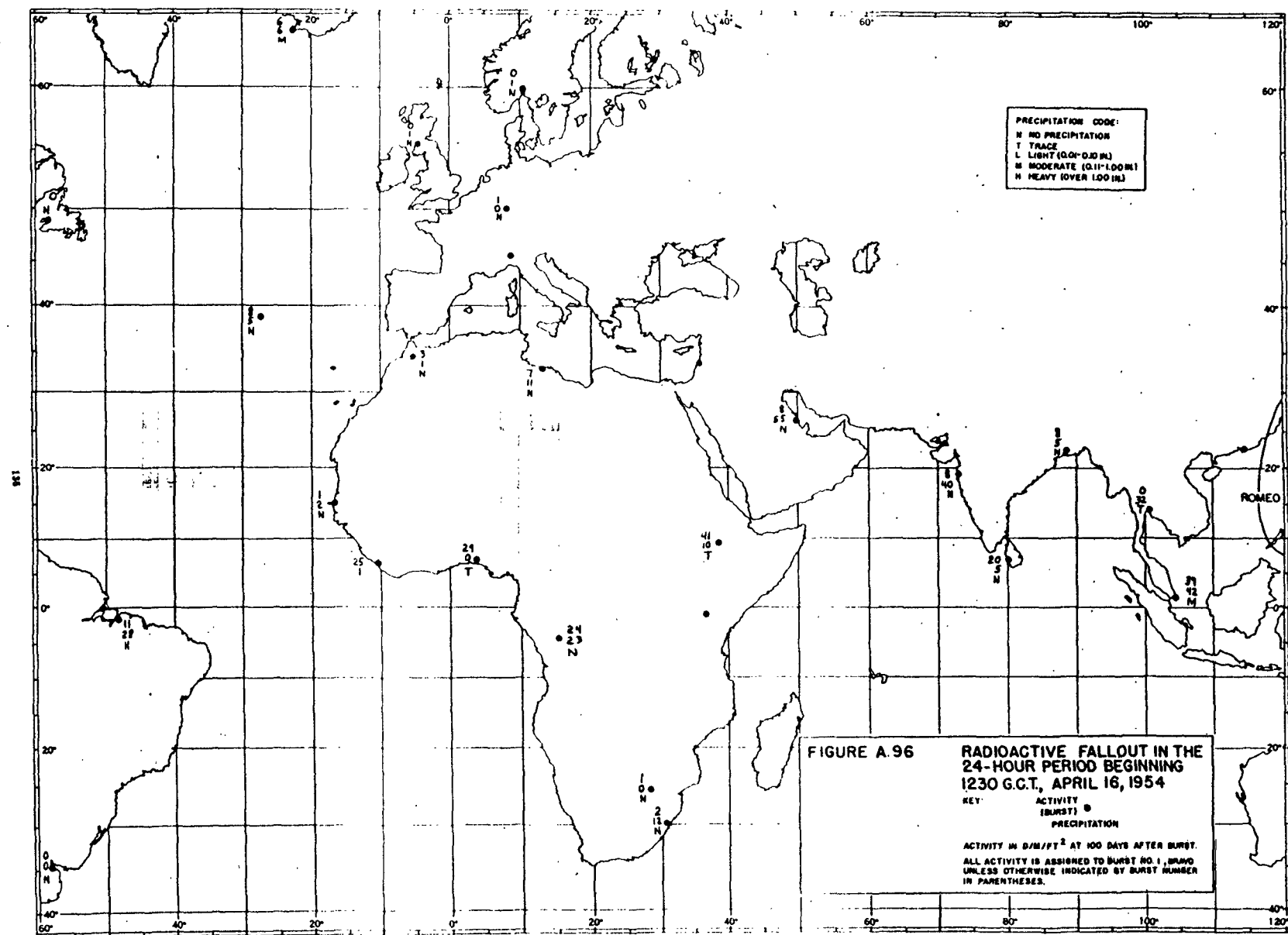
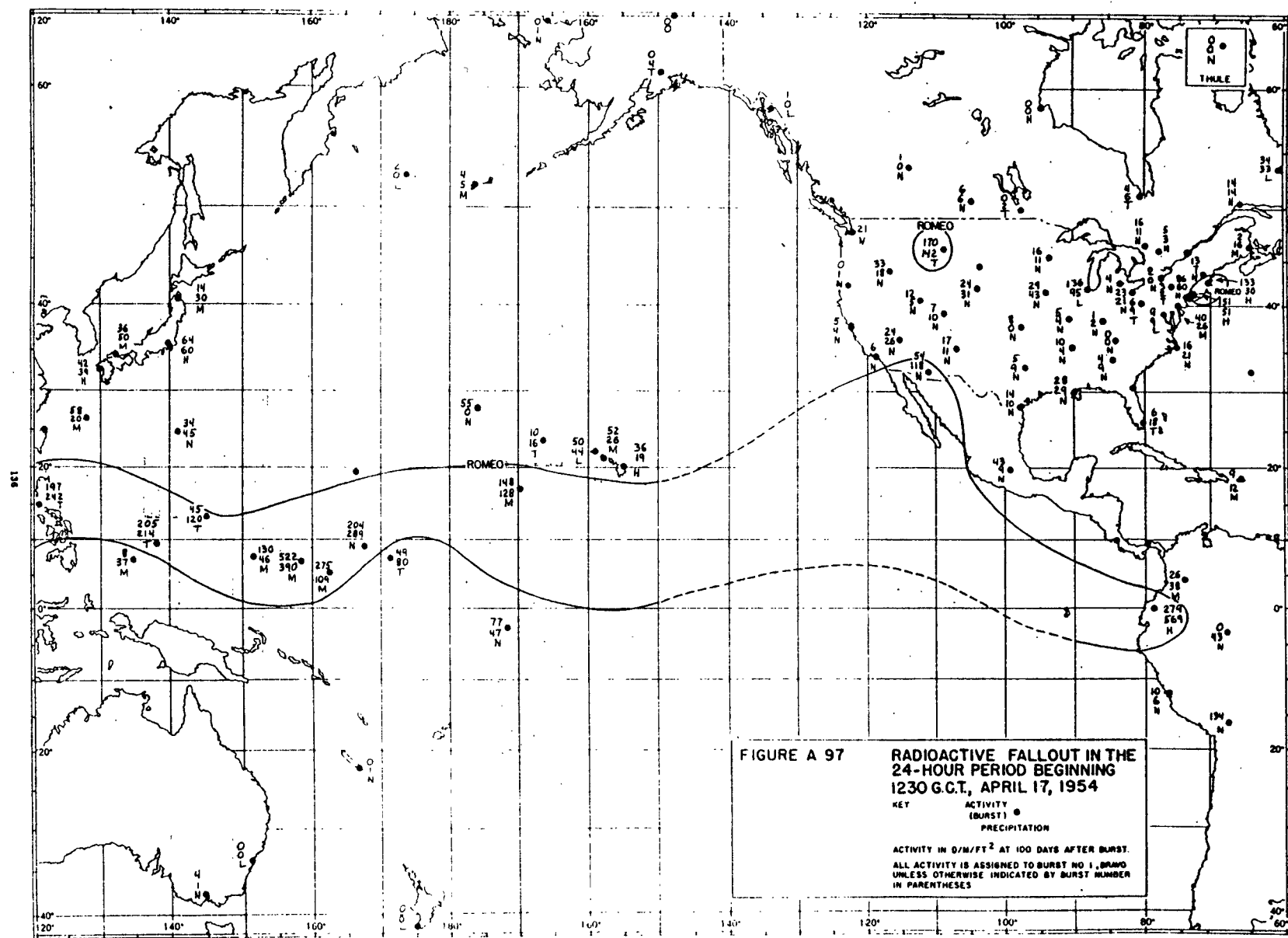


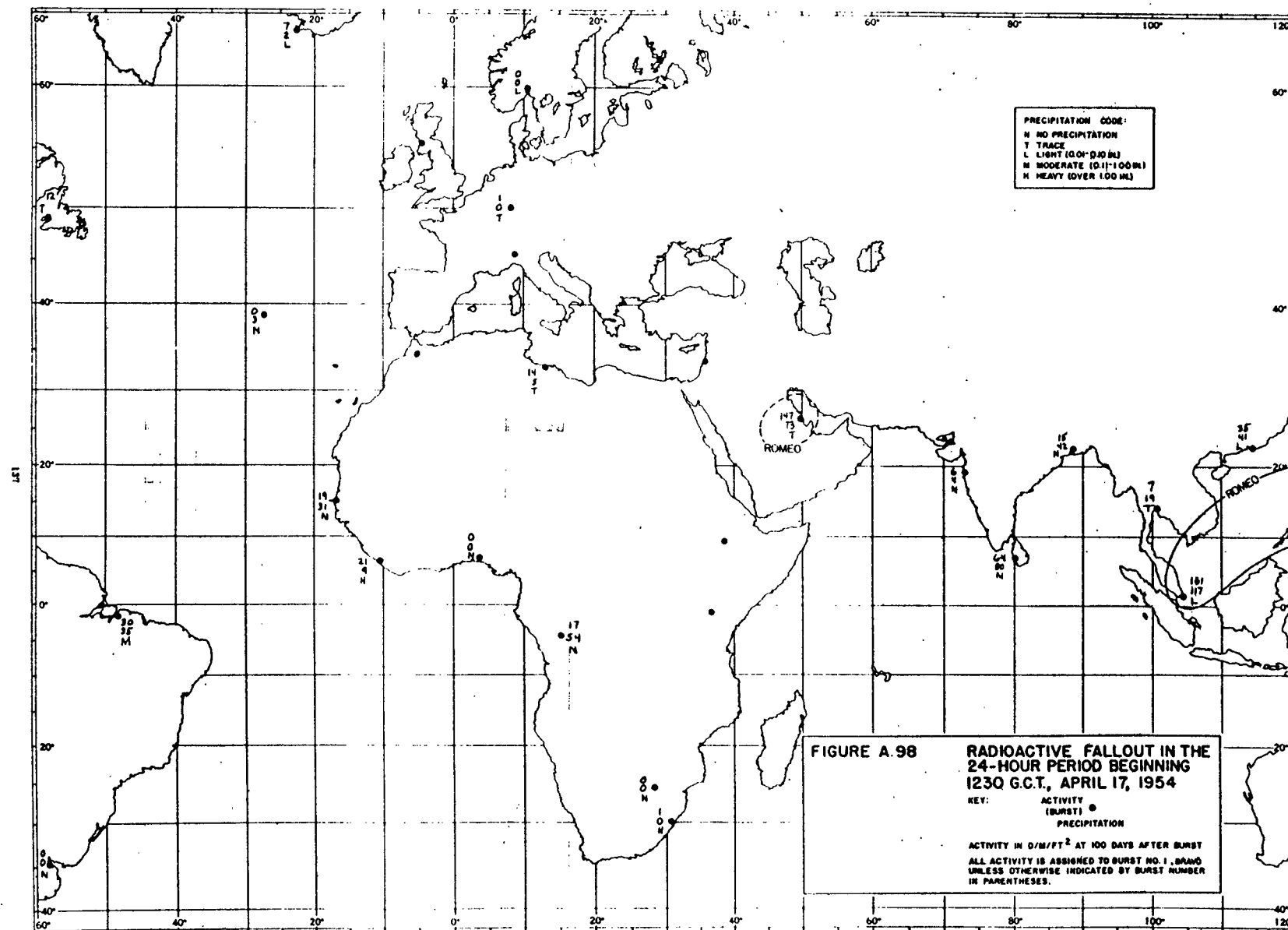
FIGURE A.93 **RADIOACTIVE FALLOUT IN THE
24-HOUR PERIOD BEGINNING
1230 G.C.T., APRIL 15, 1954**

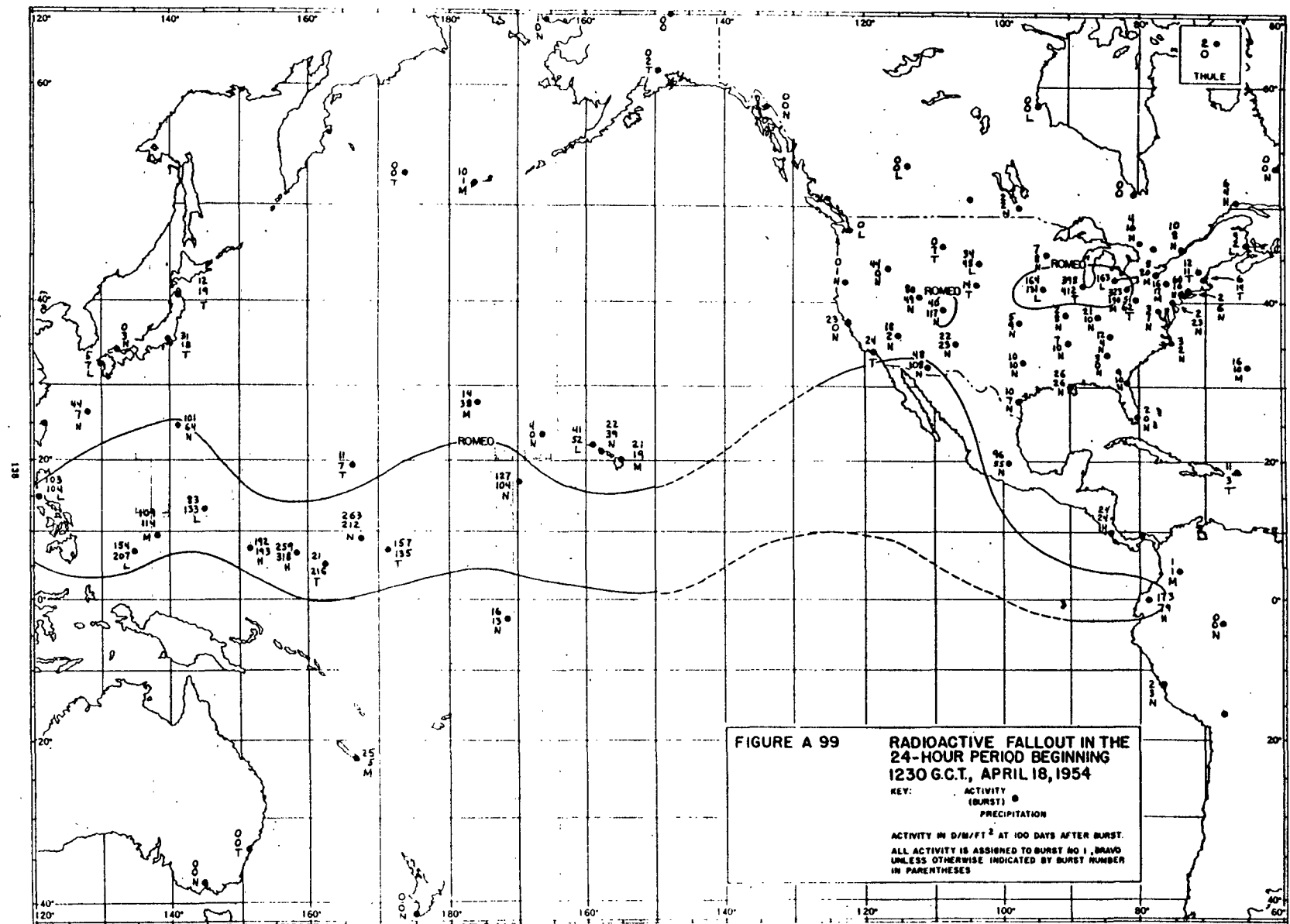


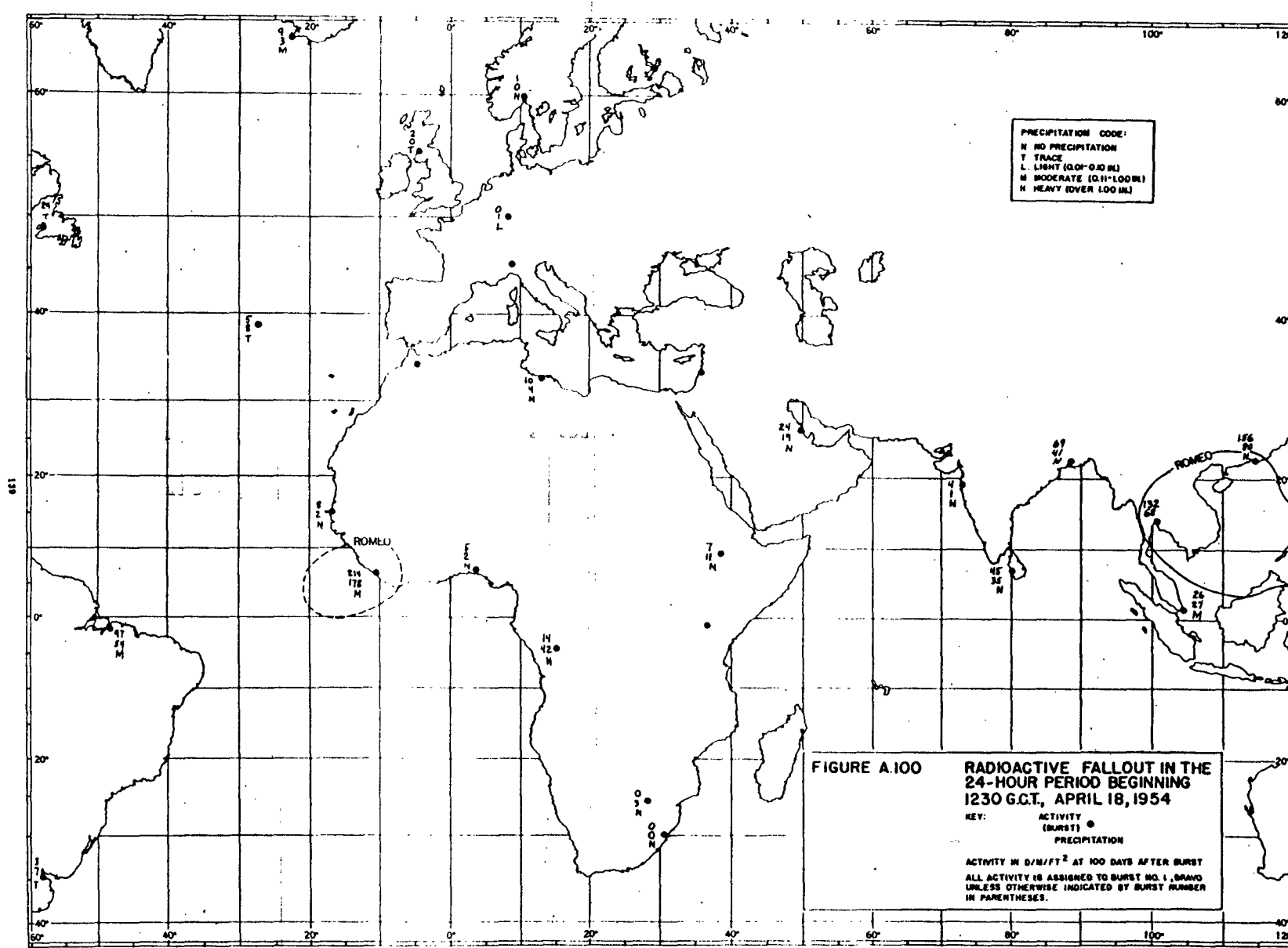


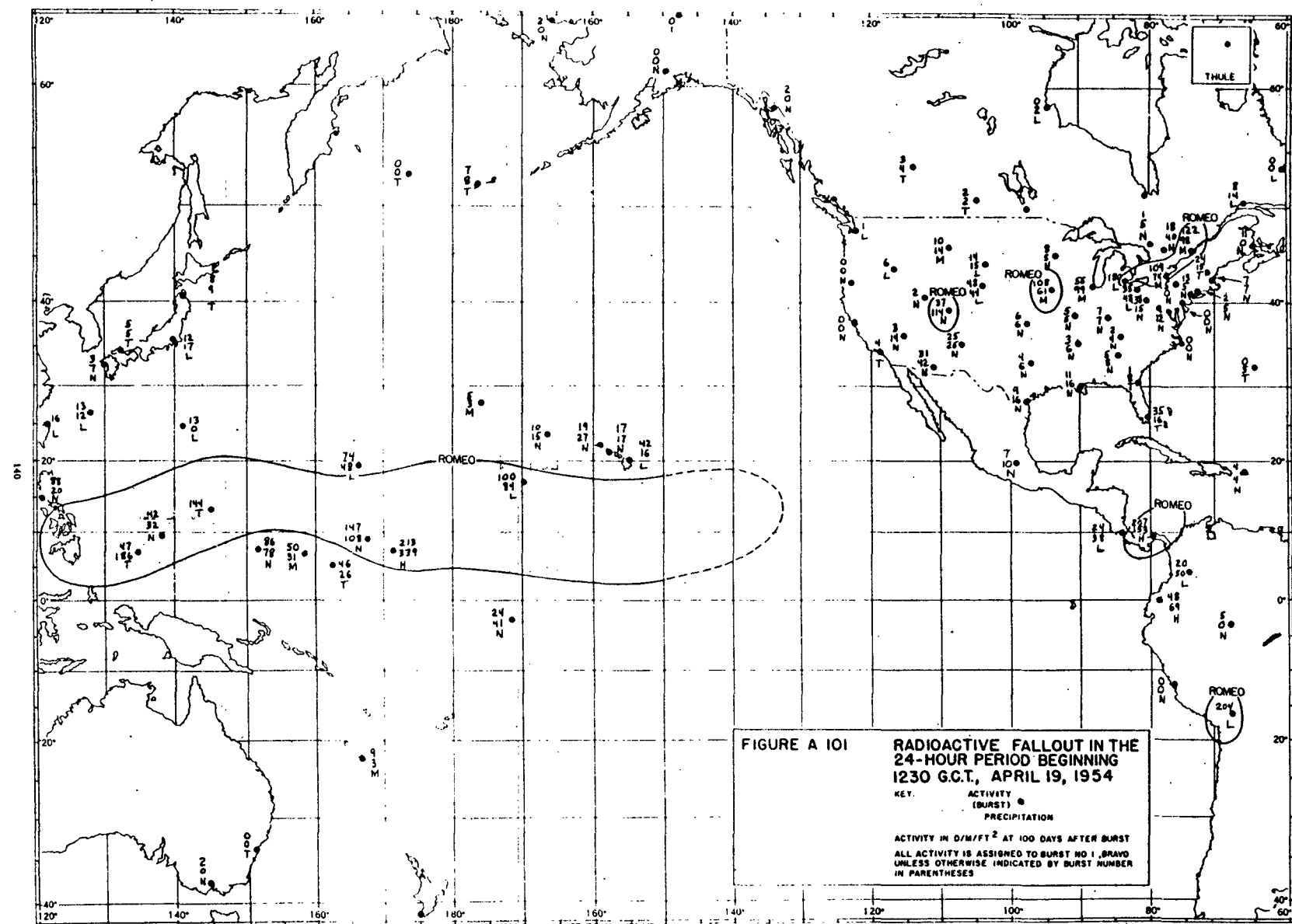


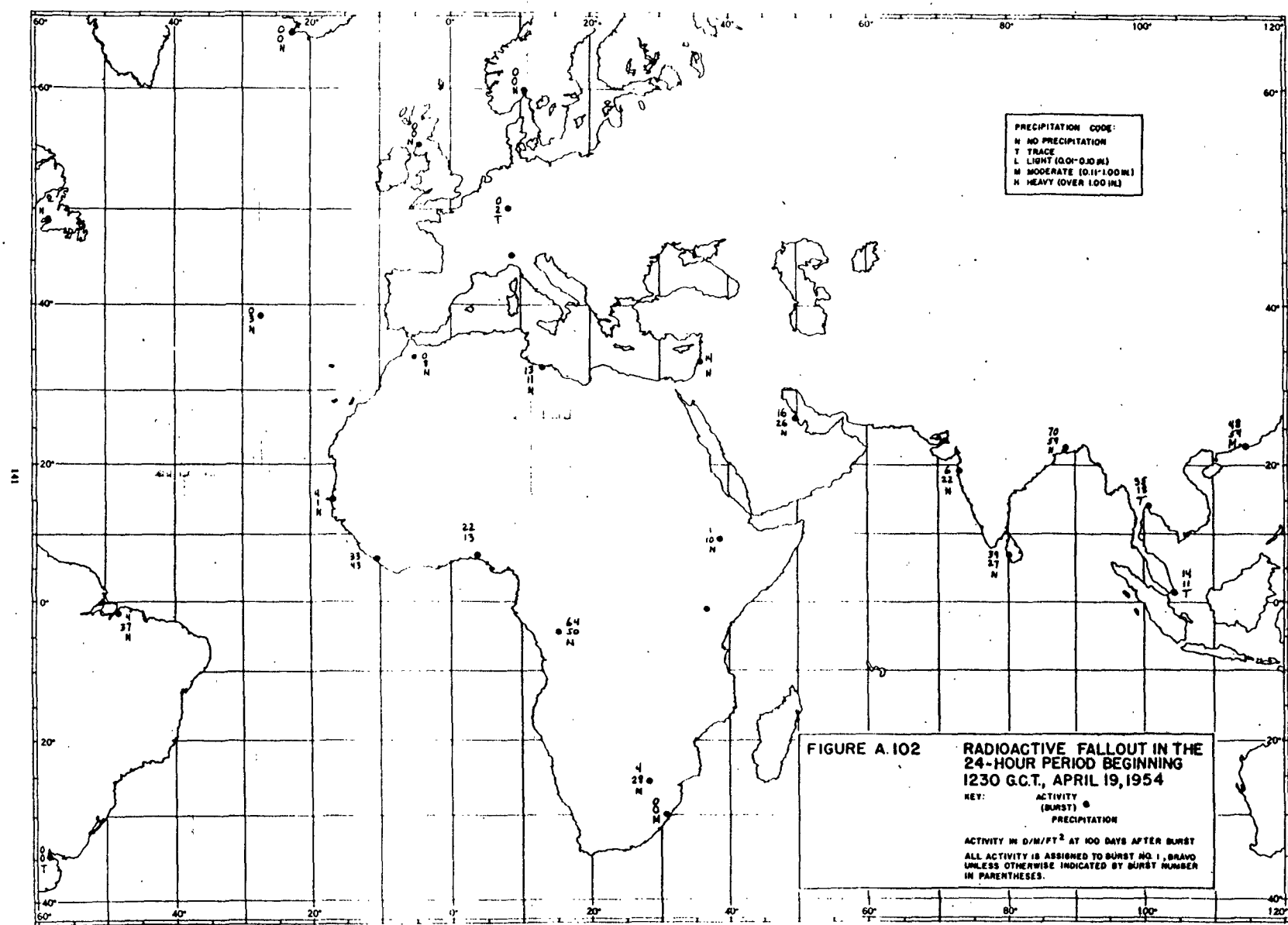


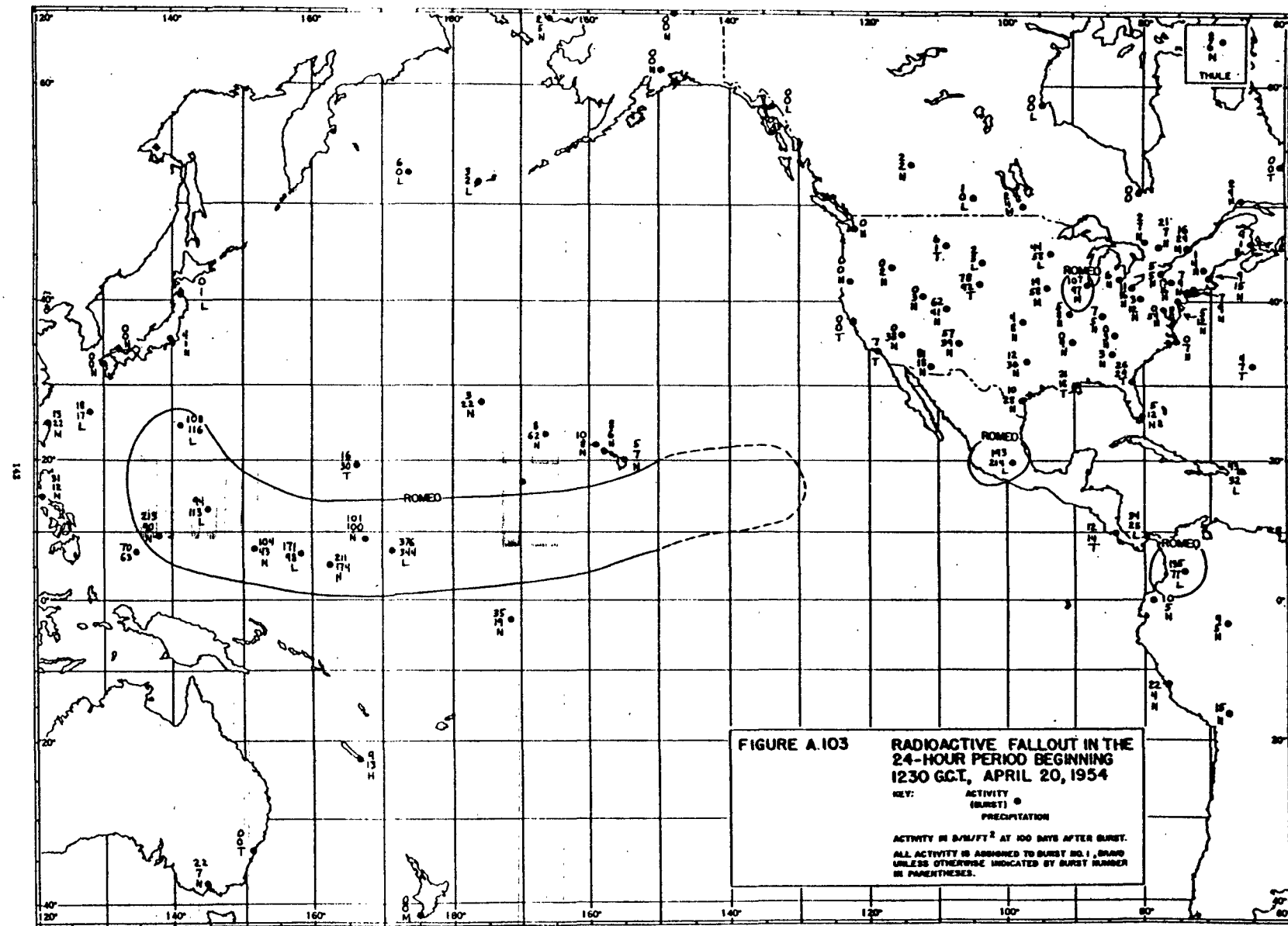


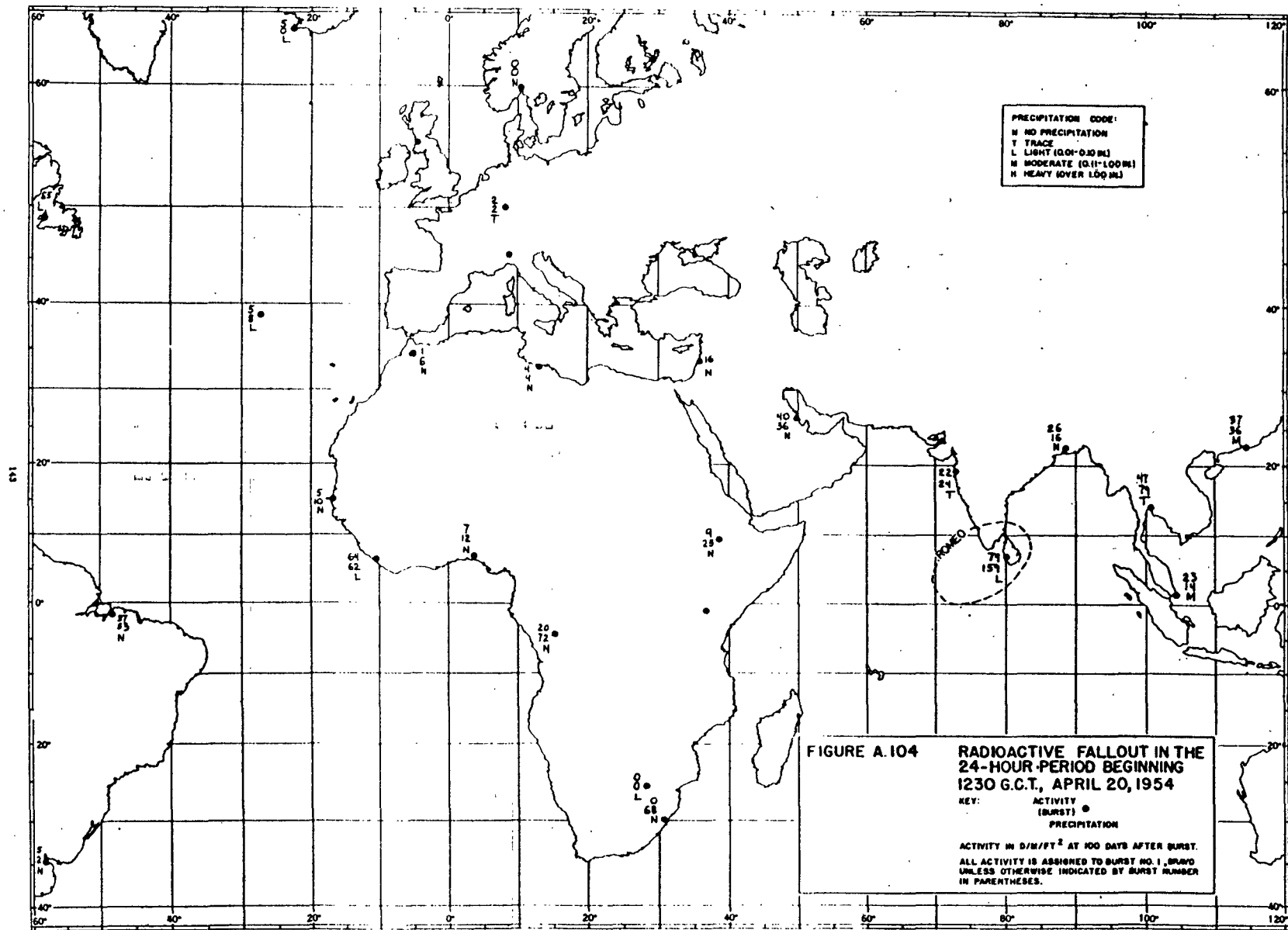


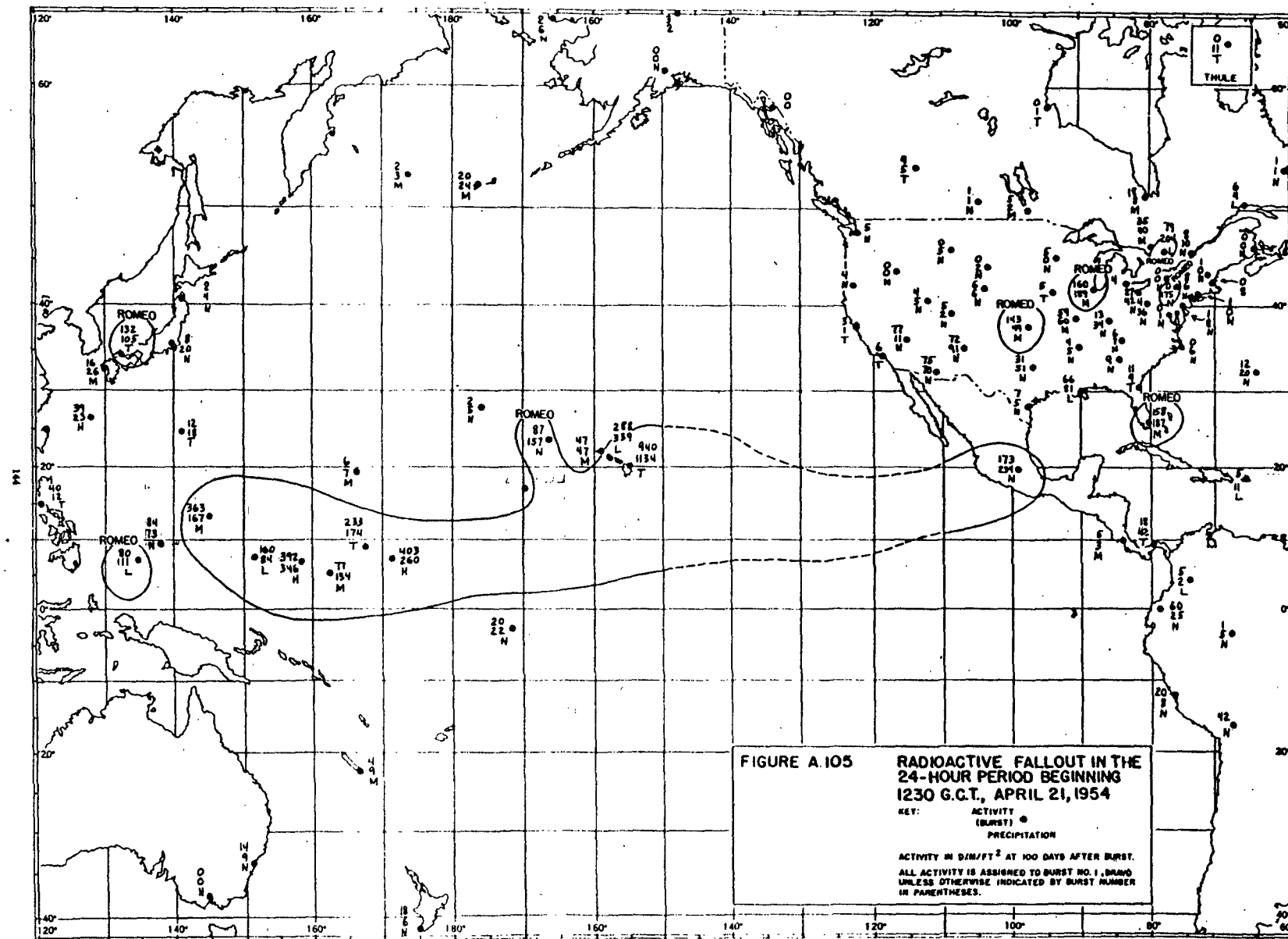


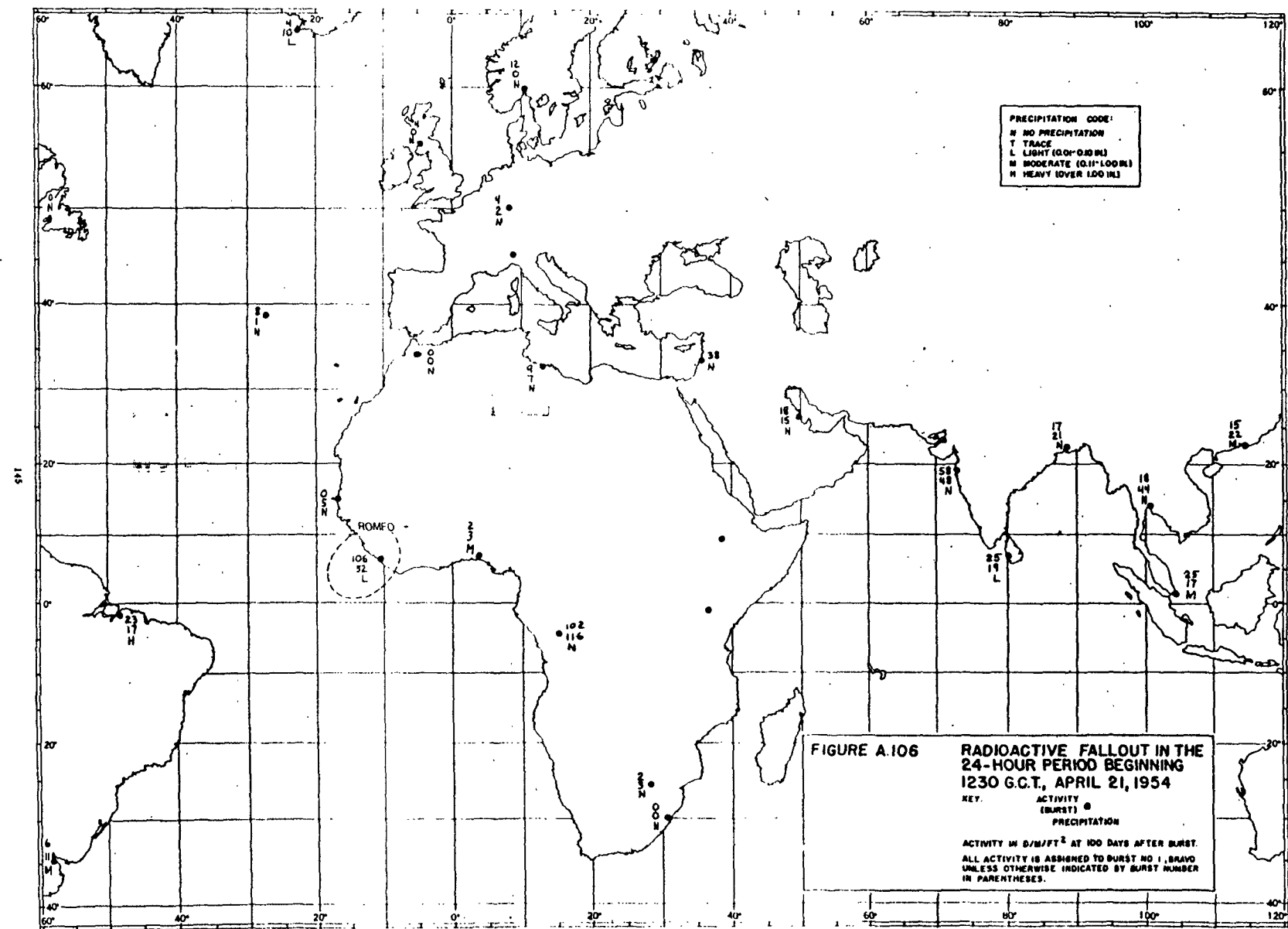


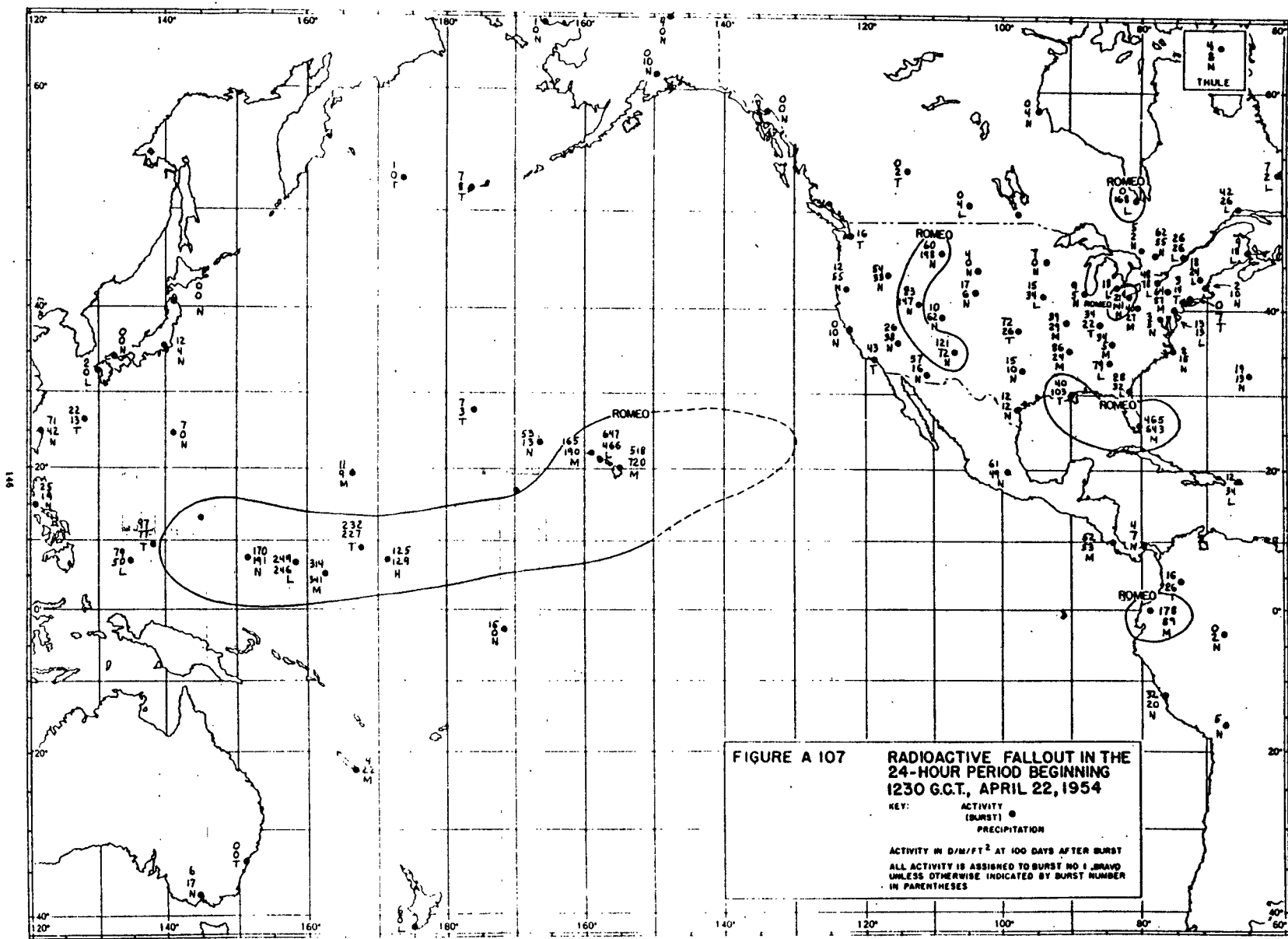


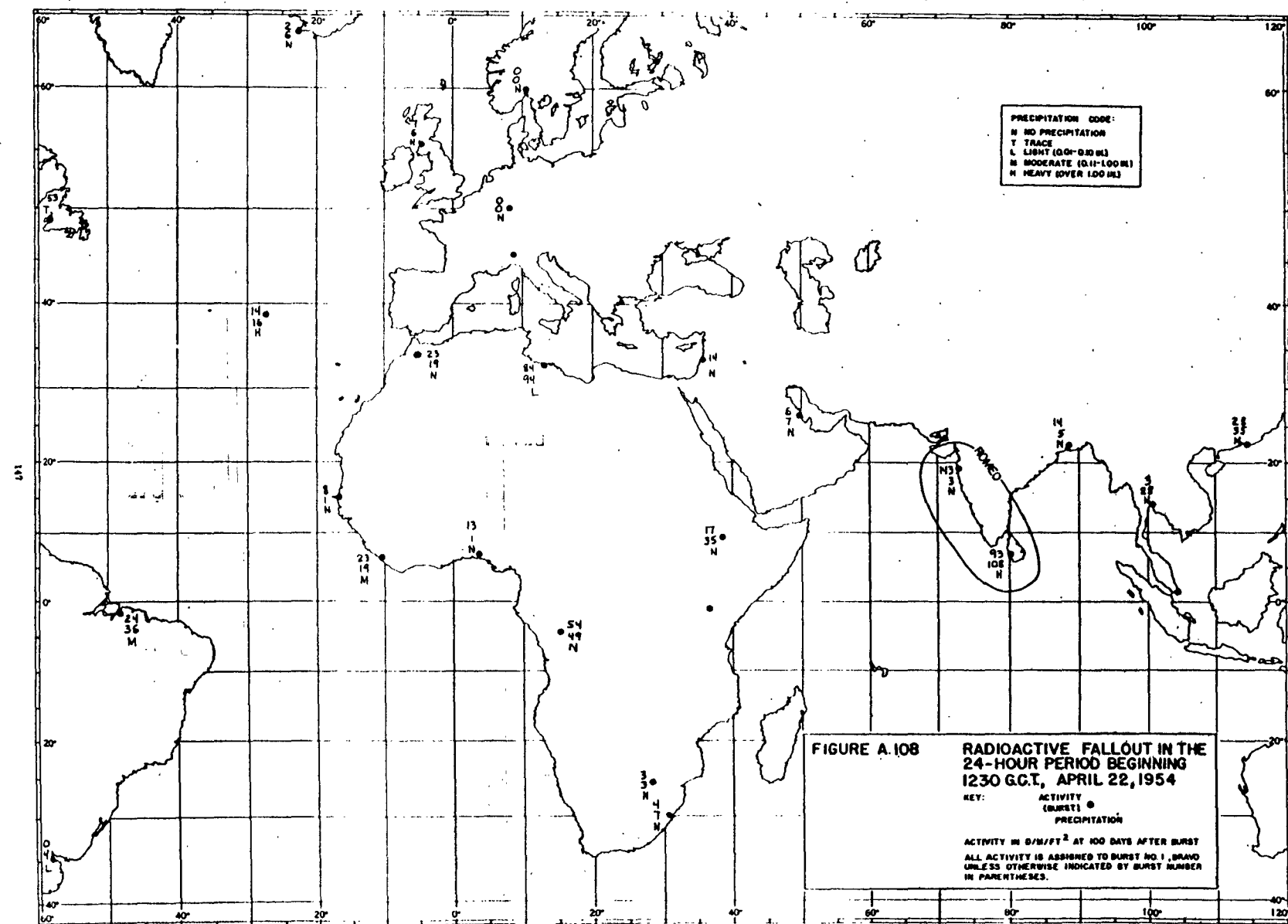


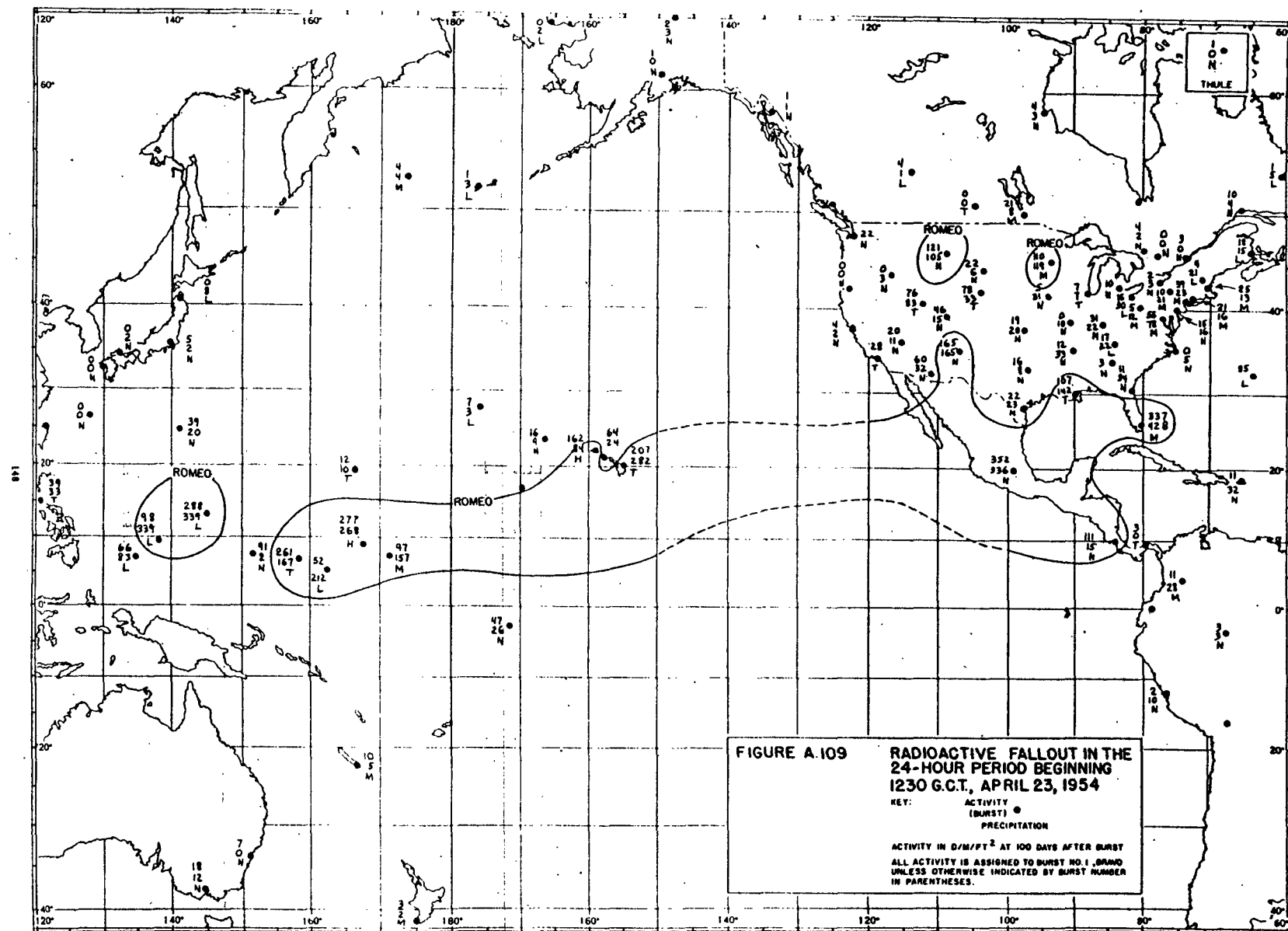


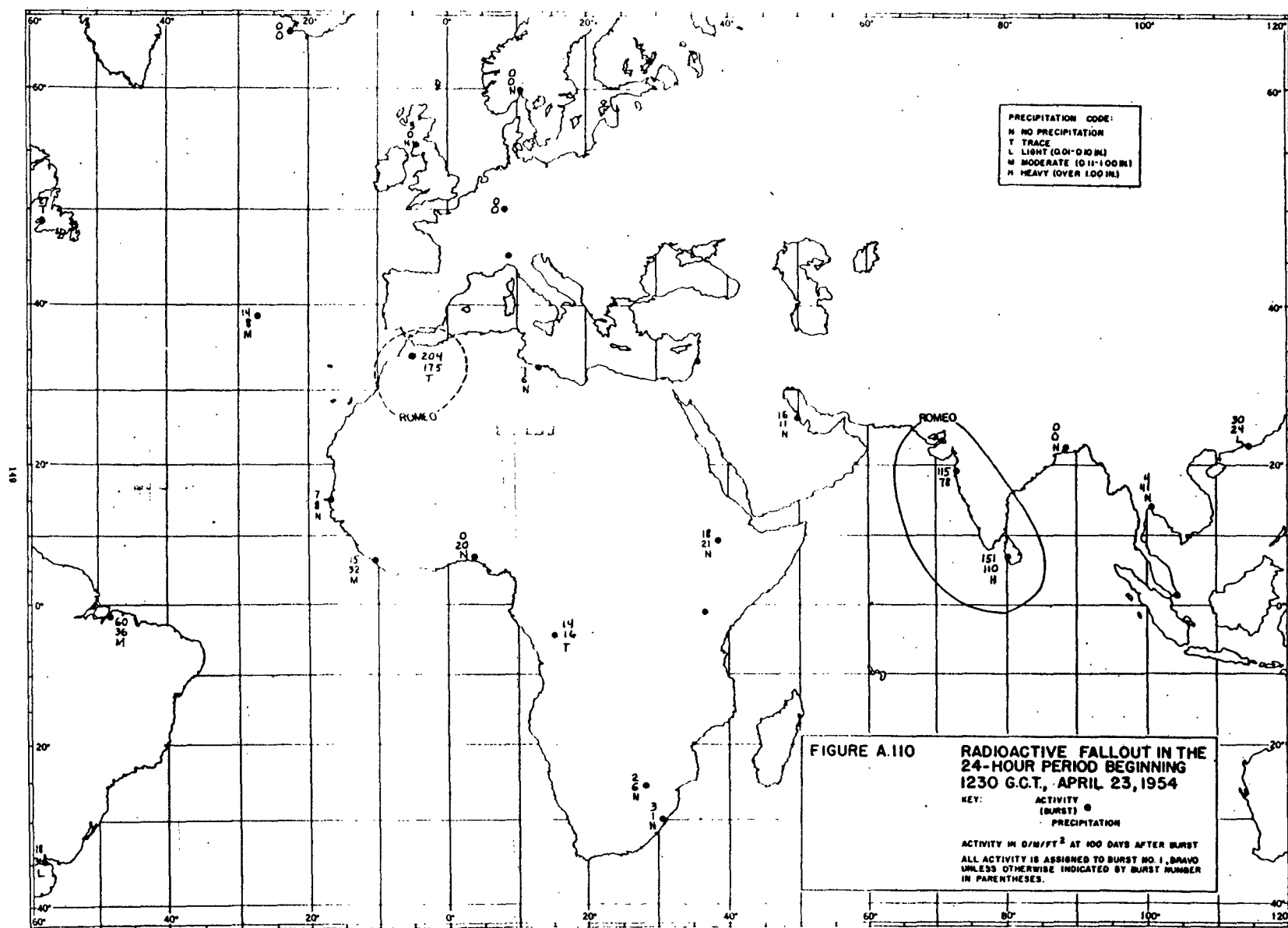


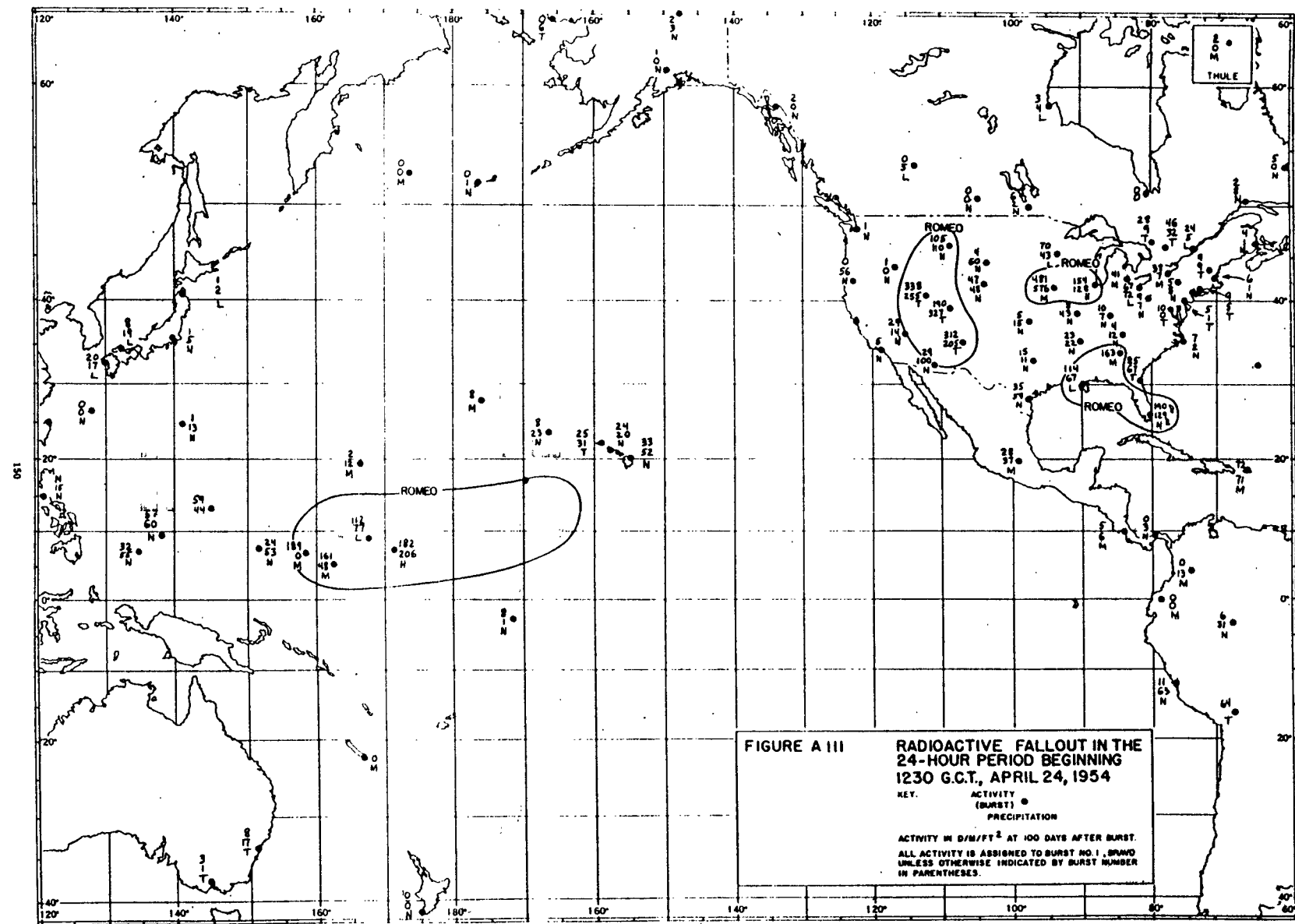


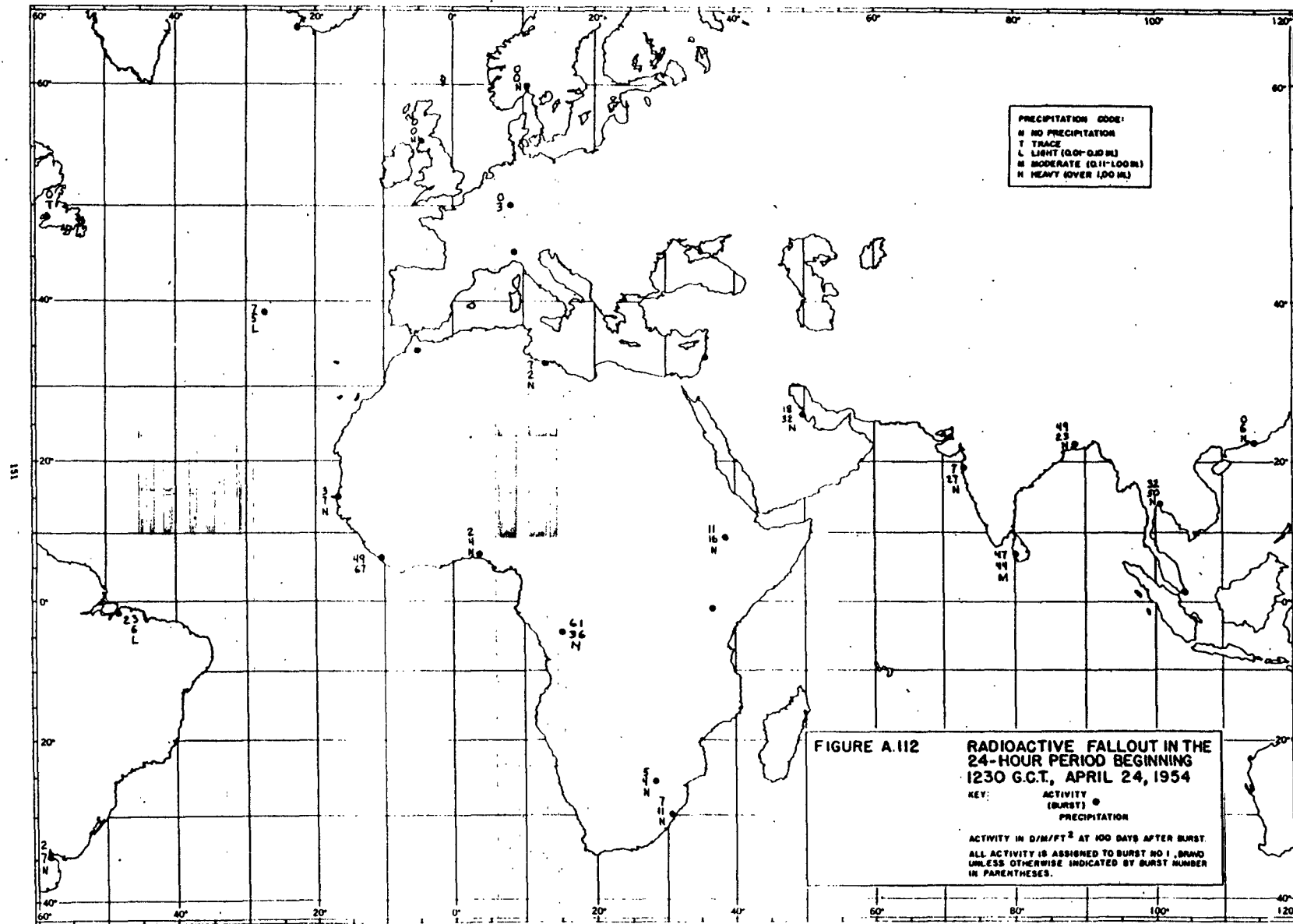


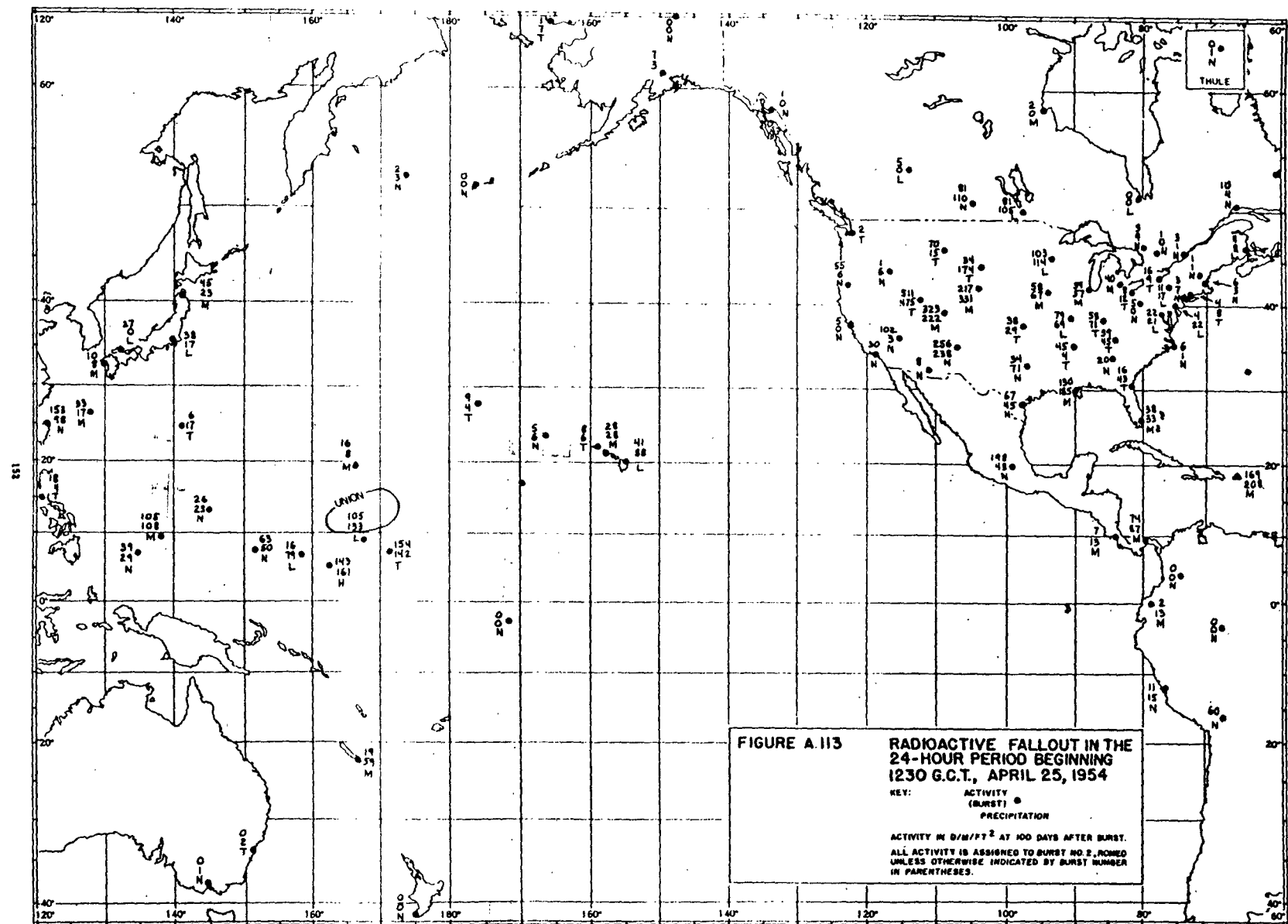


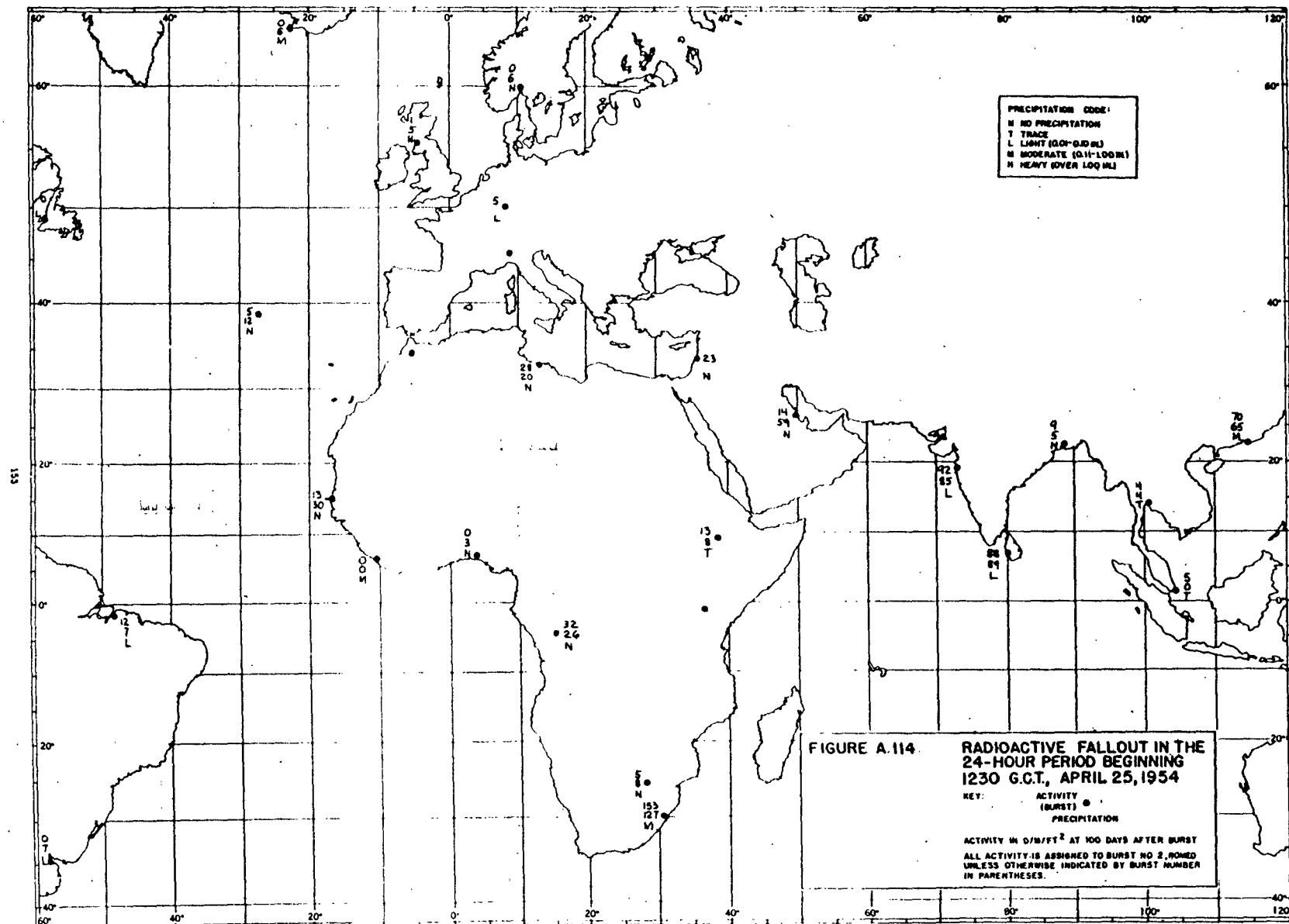




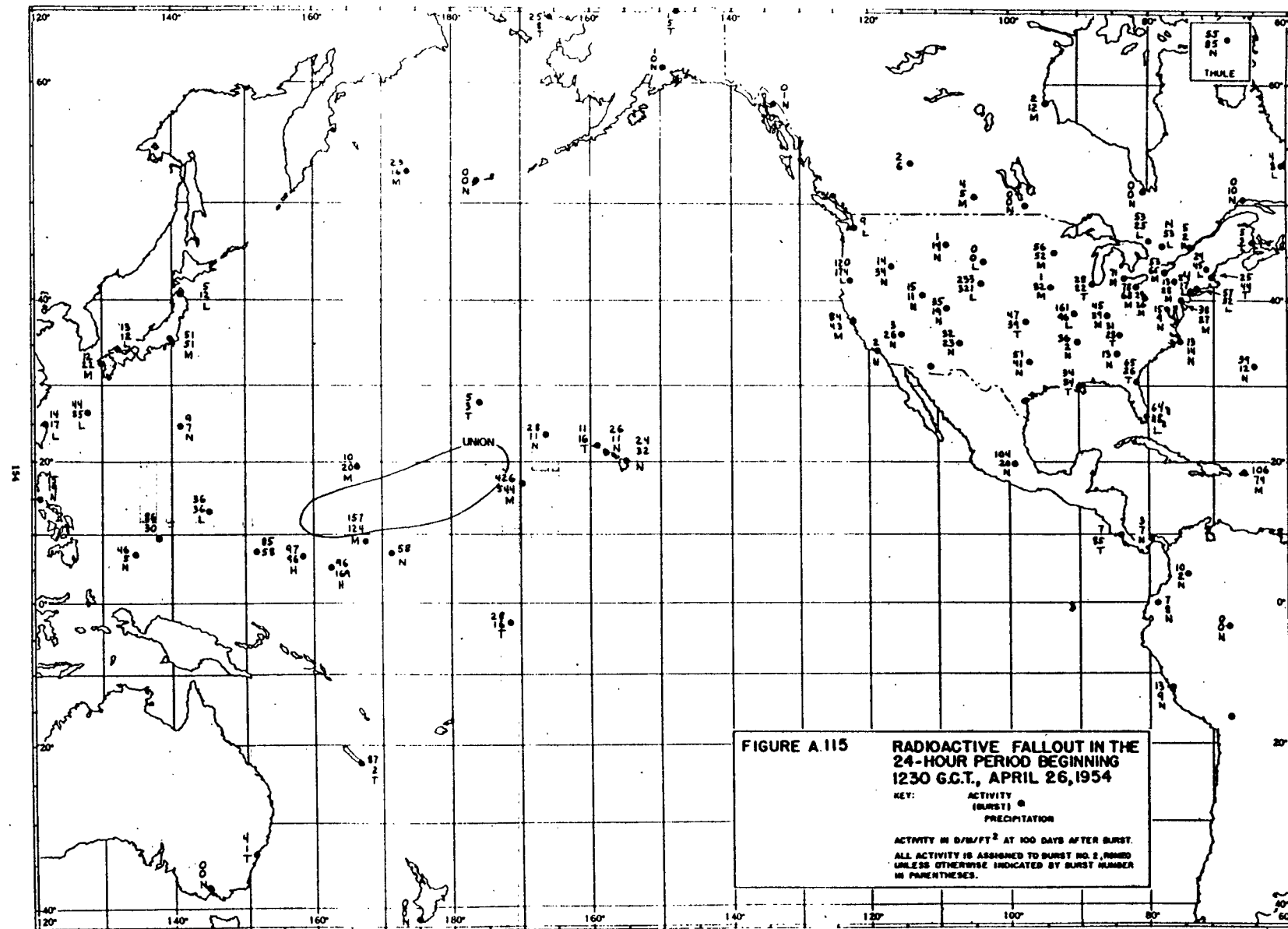


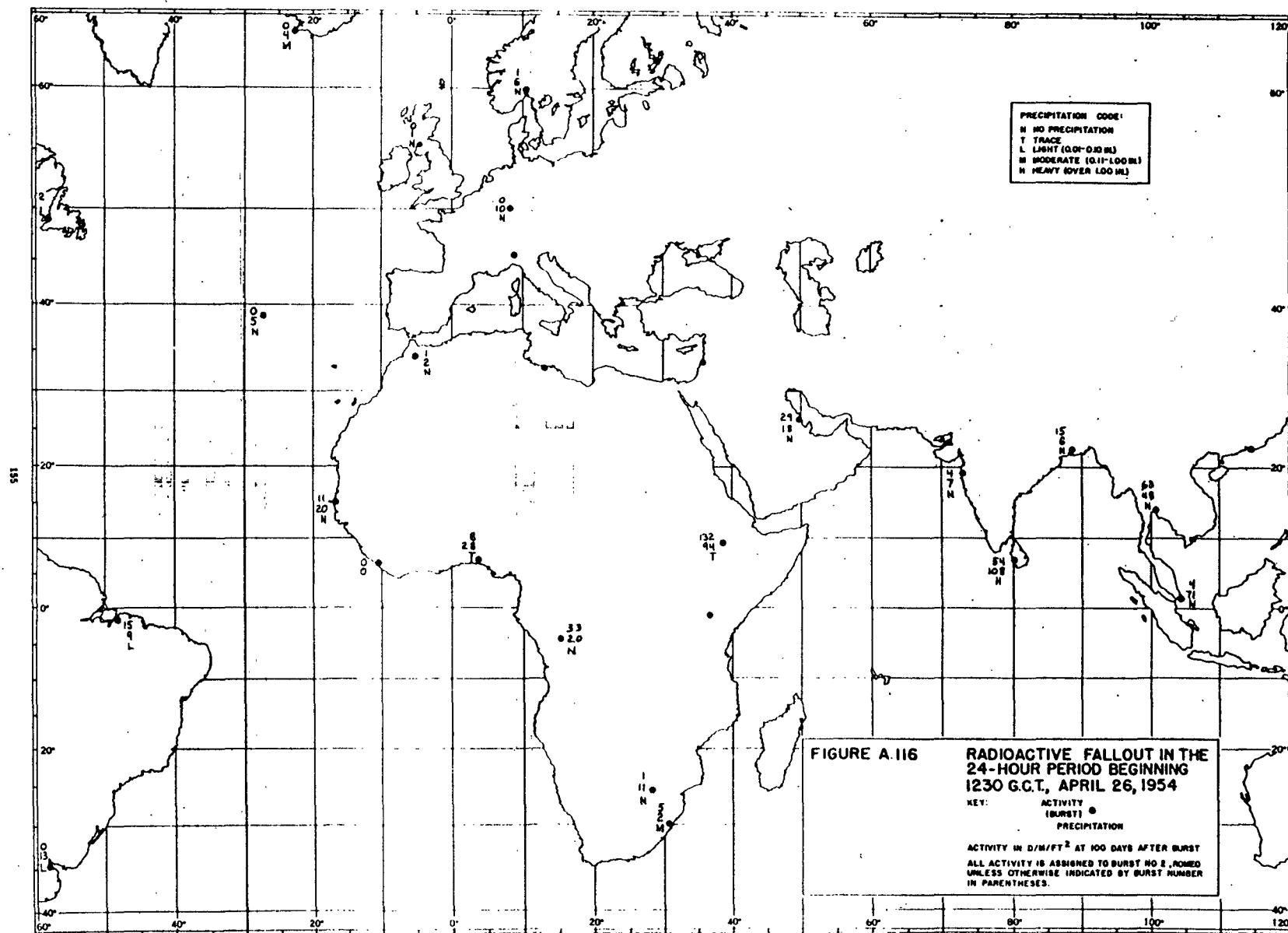


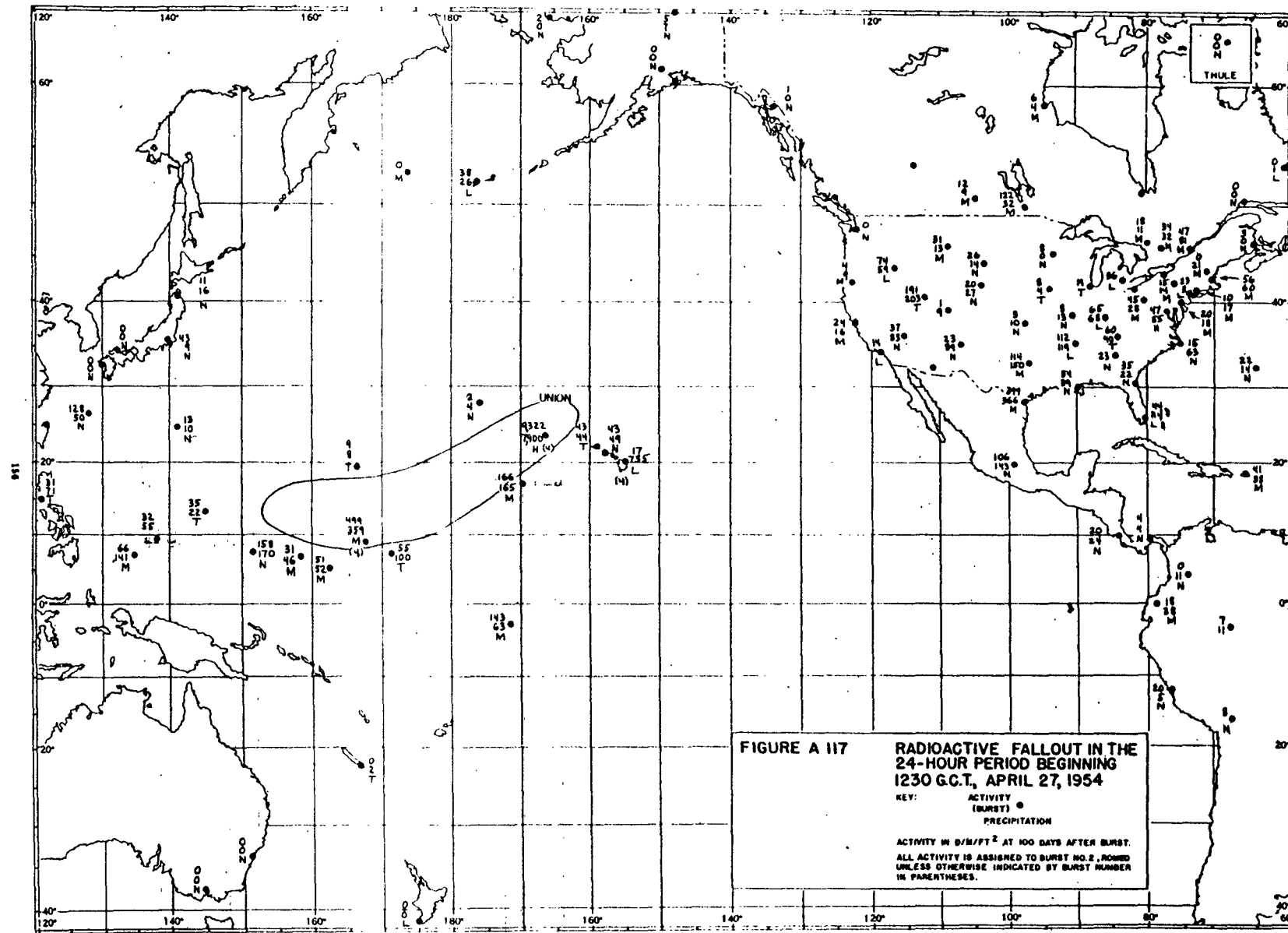




**FIGURE A.114. RADIOACTIVE FALLOUT IN THE
24-HOUR PERIOD BEGINNING
1230 G.C.T., APRIL 25, 1954**







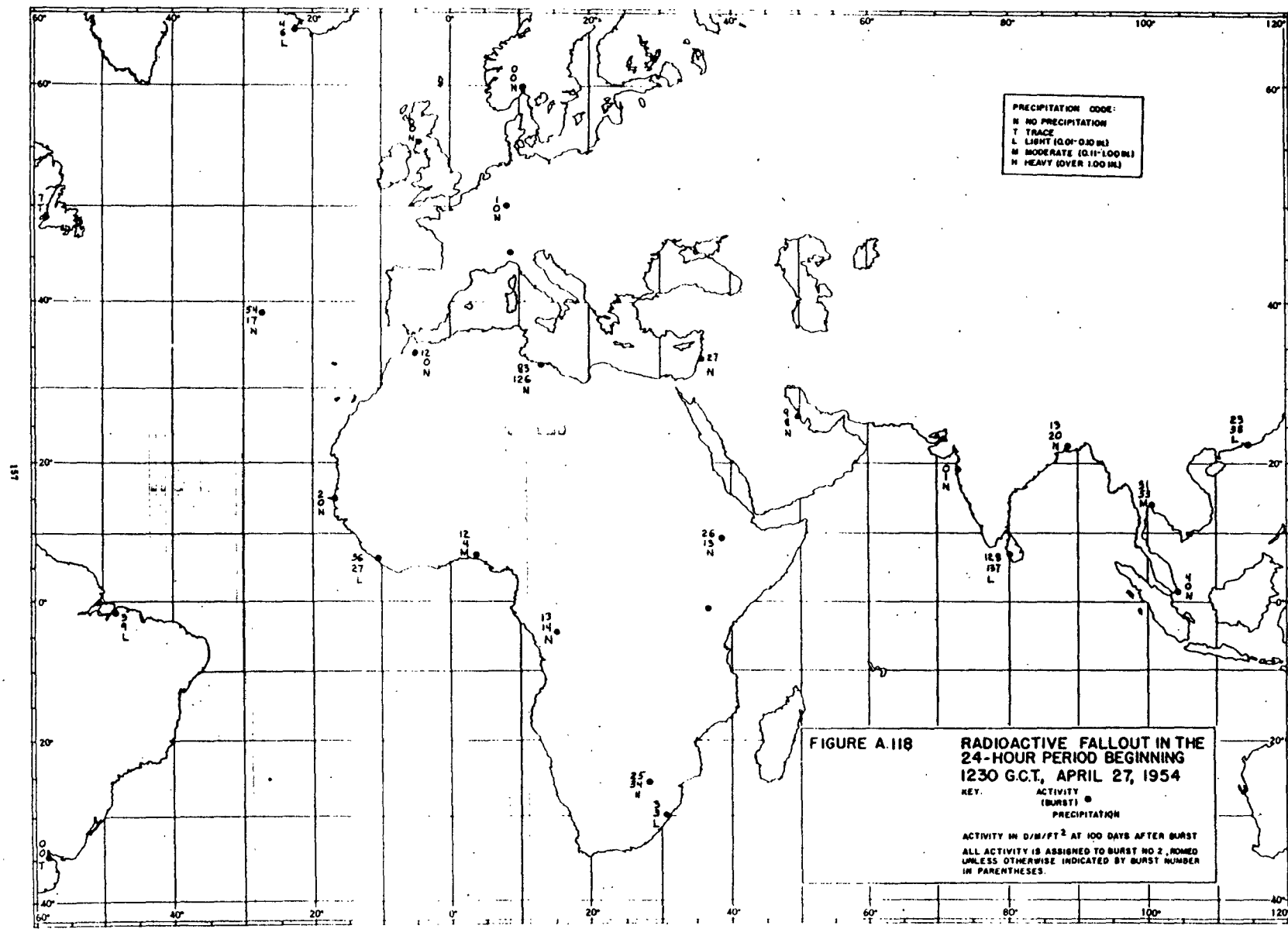
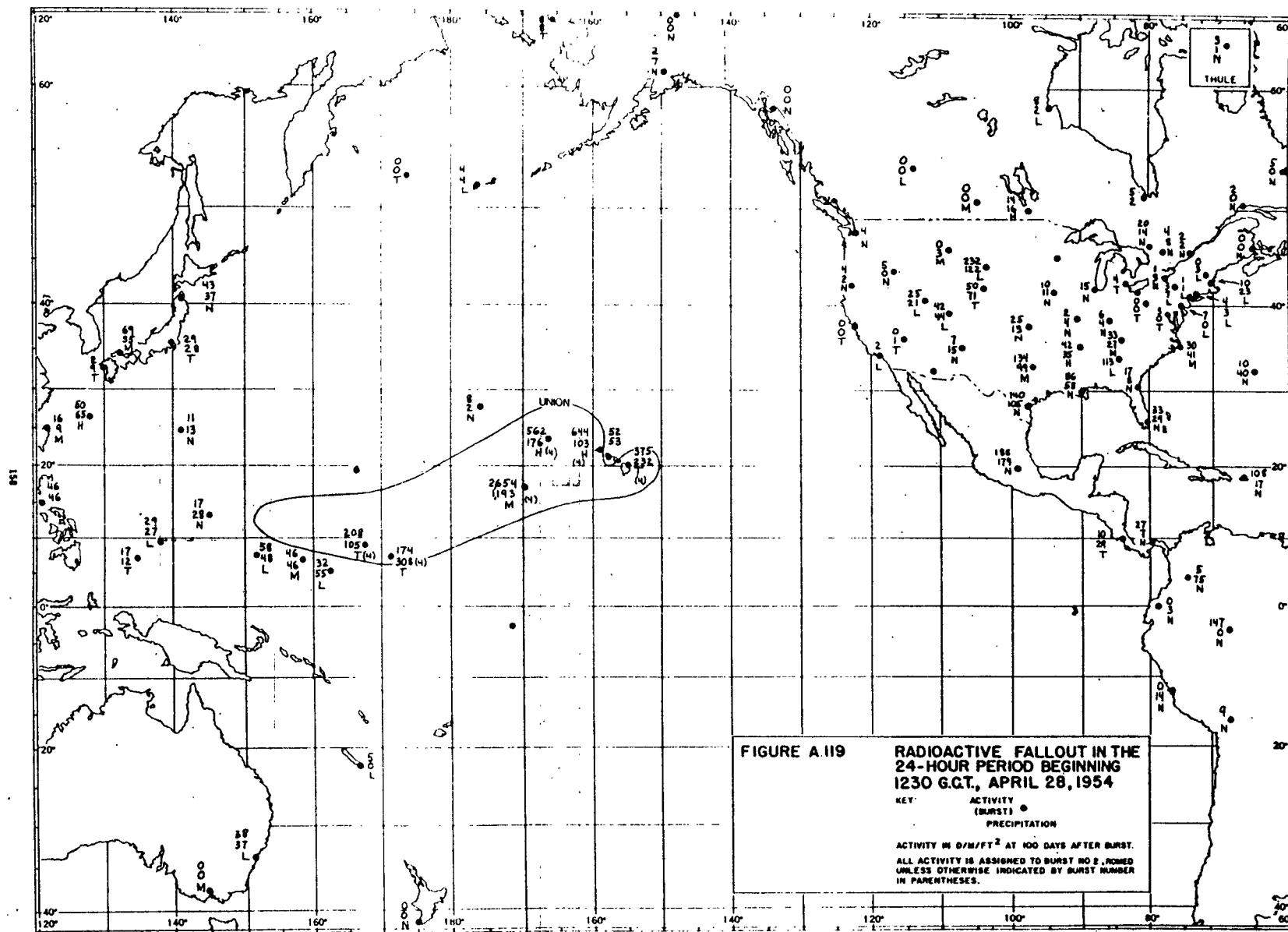


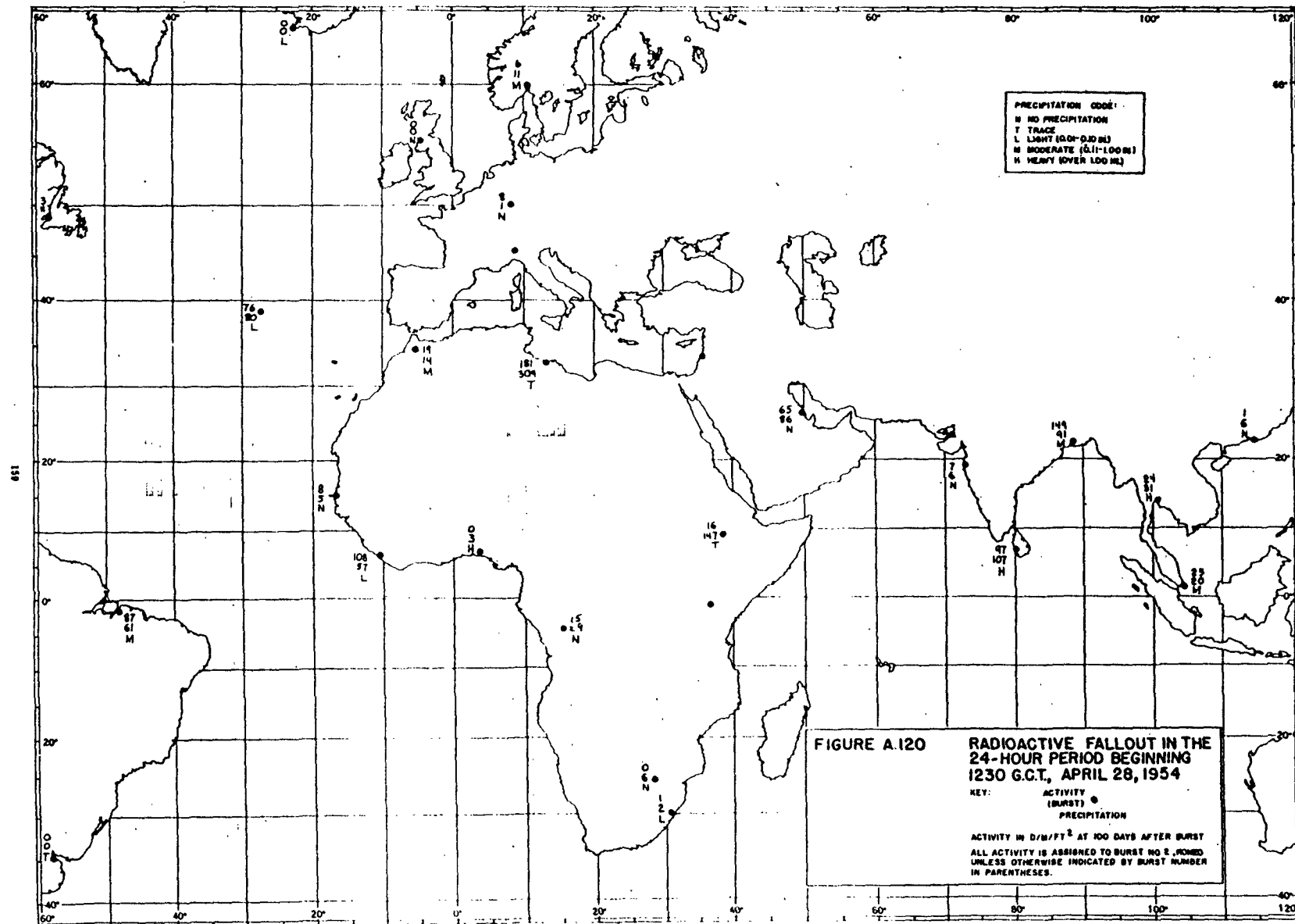
FIGURE A.118 **RADIOACTIVE FALLOUT IN THE
24-HOUR PERIOD BEGINNING
1230 G.C.T., APRIL 27, 1954**

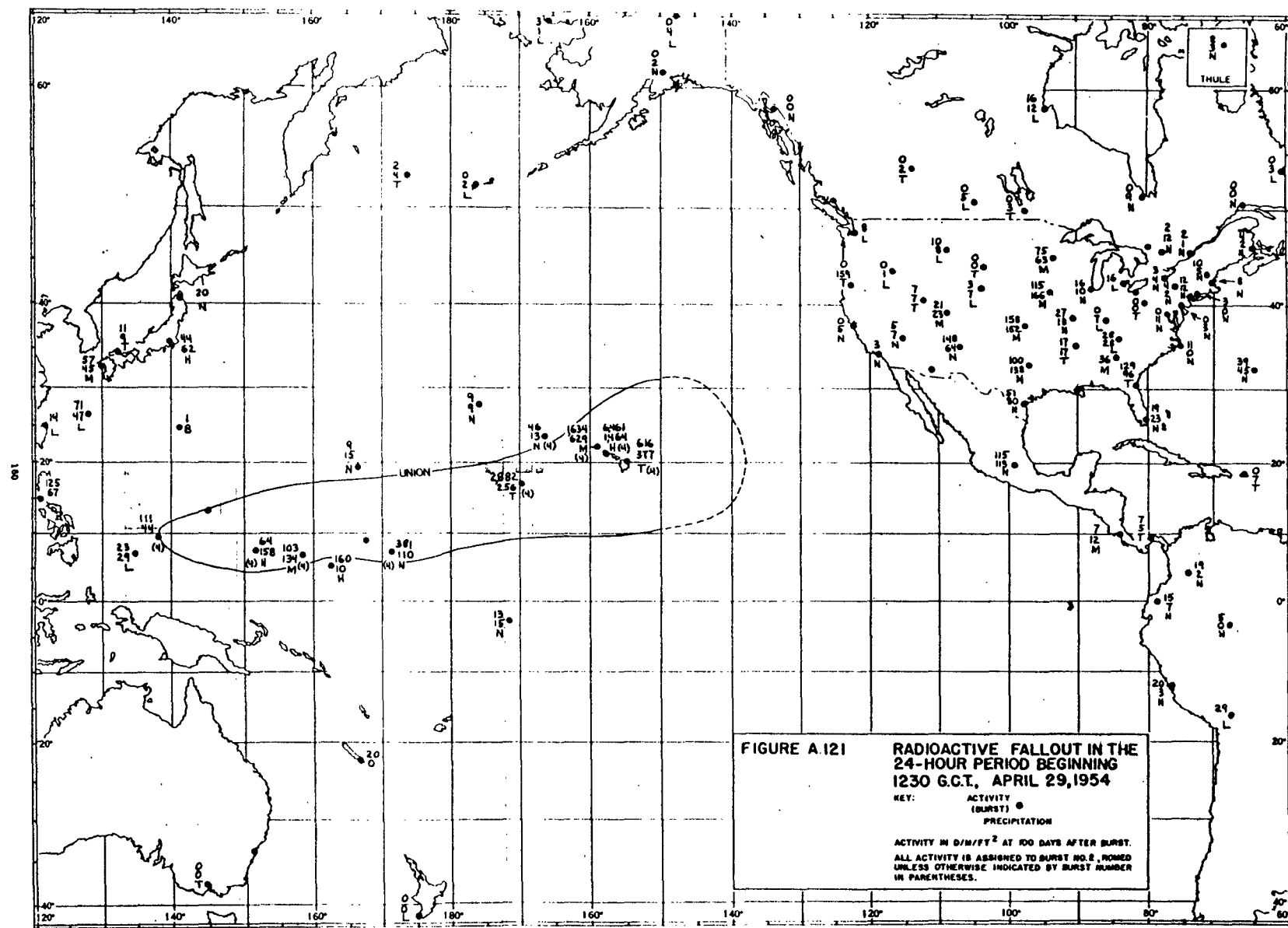
KEY. **ACTIVITY**
 (**BURSTS**)

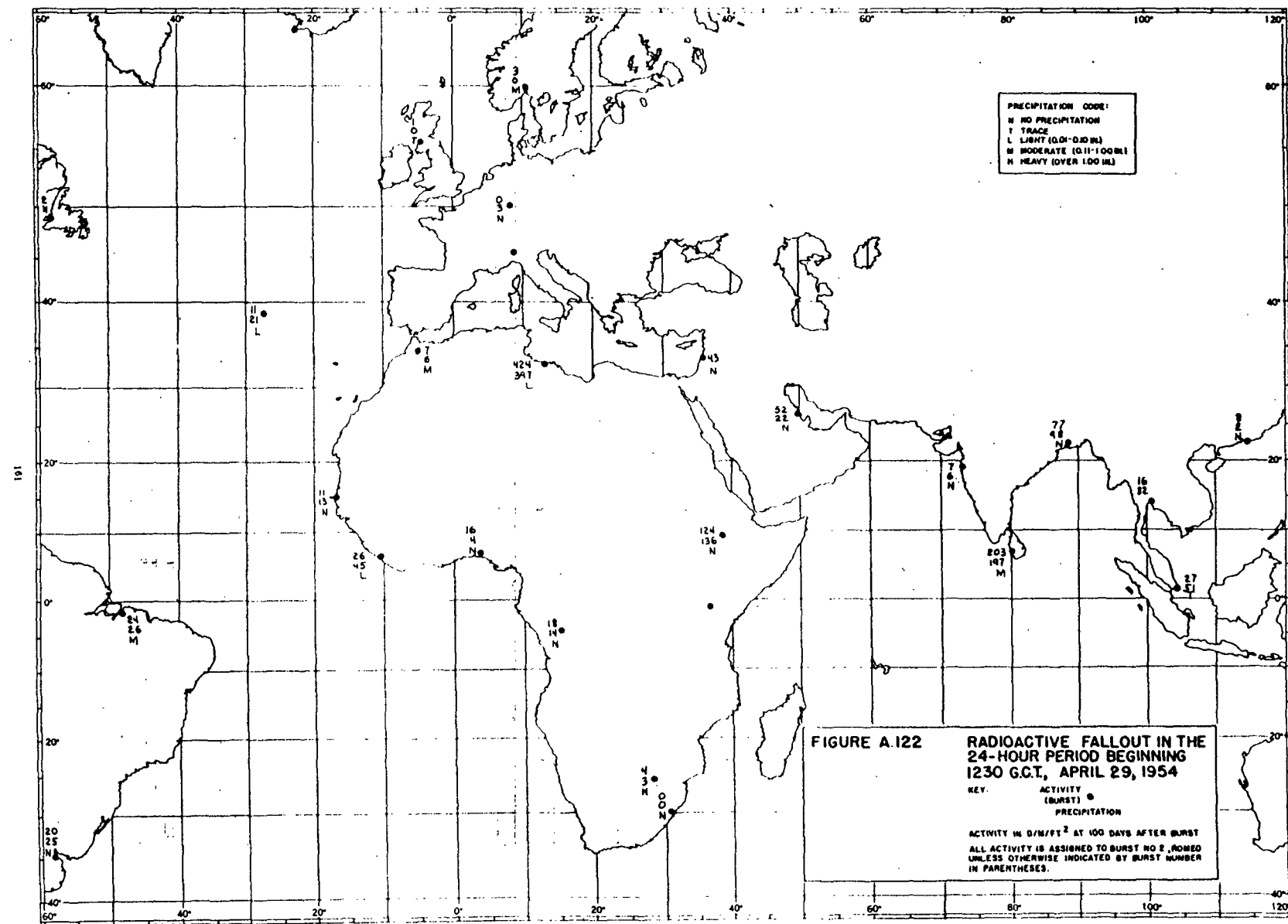
PRECIPITATION

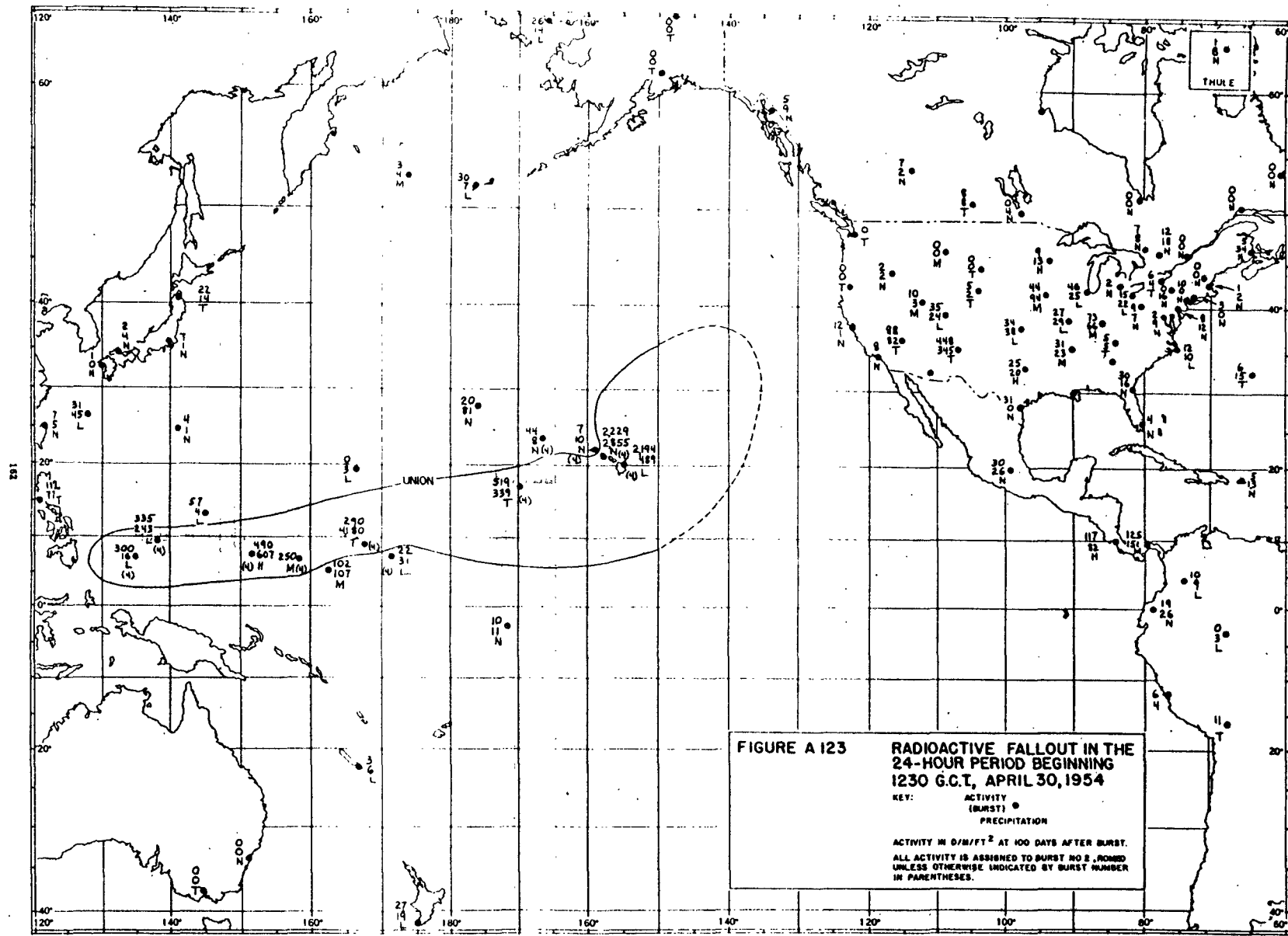
ACTIVITY IN D/M²/FT² AT 100 DAYS AFTER BURST
ALL ACTIVITY IS ASSIGNED TO BURST NO 2, UNLESS
UNLESS OTHERWISE INDICATED BY BURST NUMBER
IN PARENTHESES.

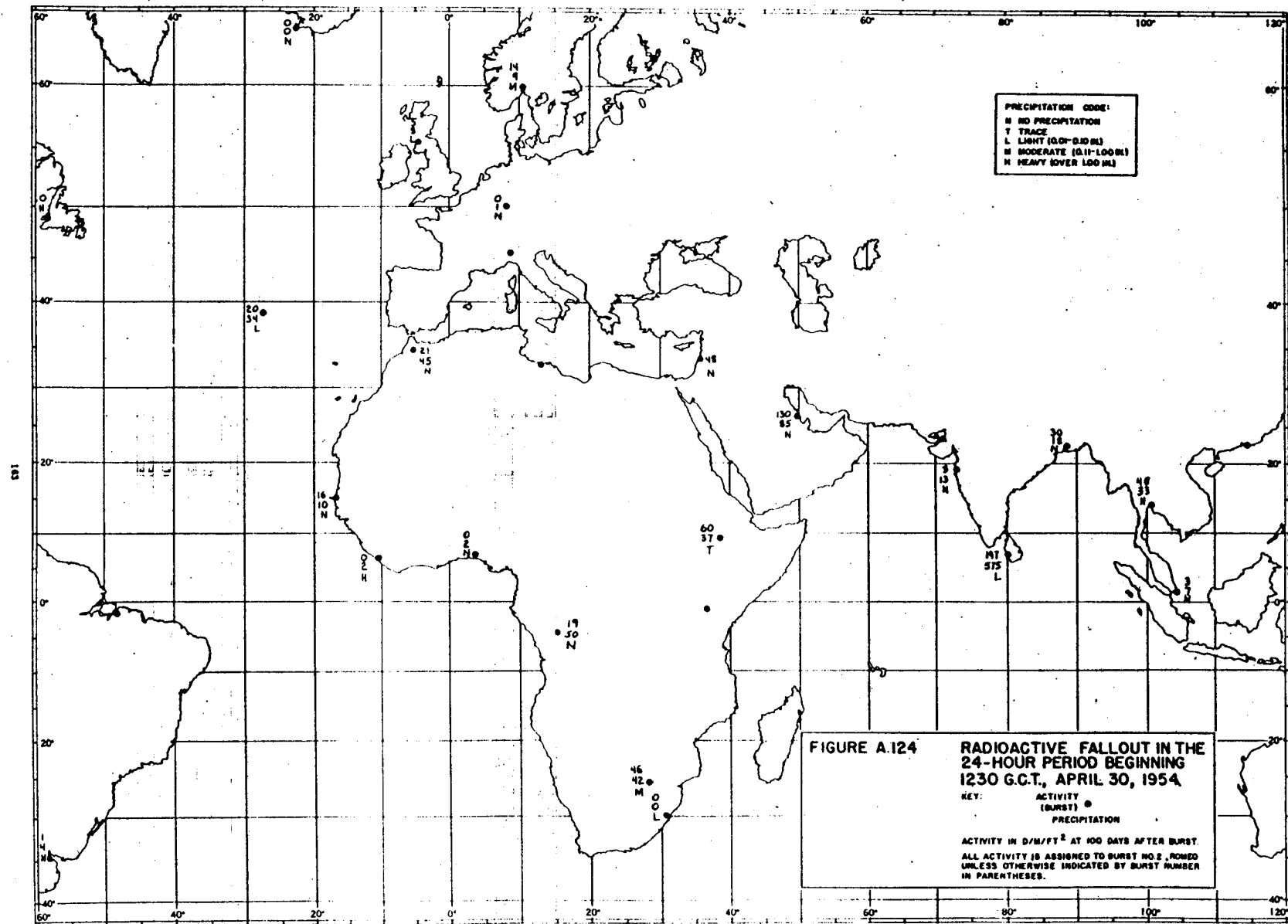


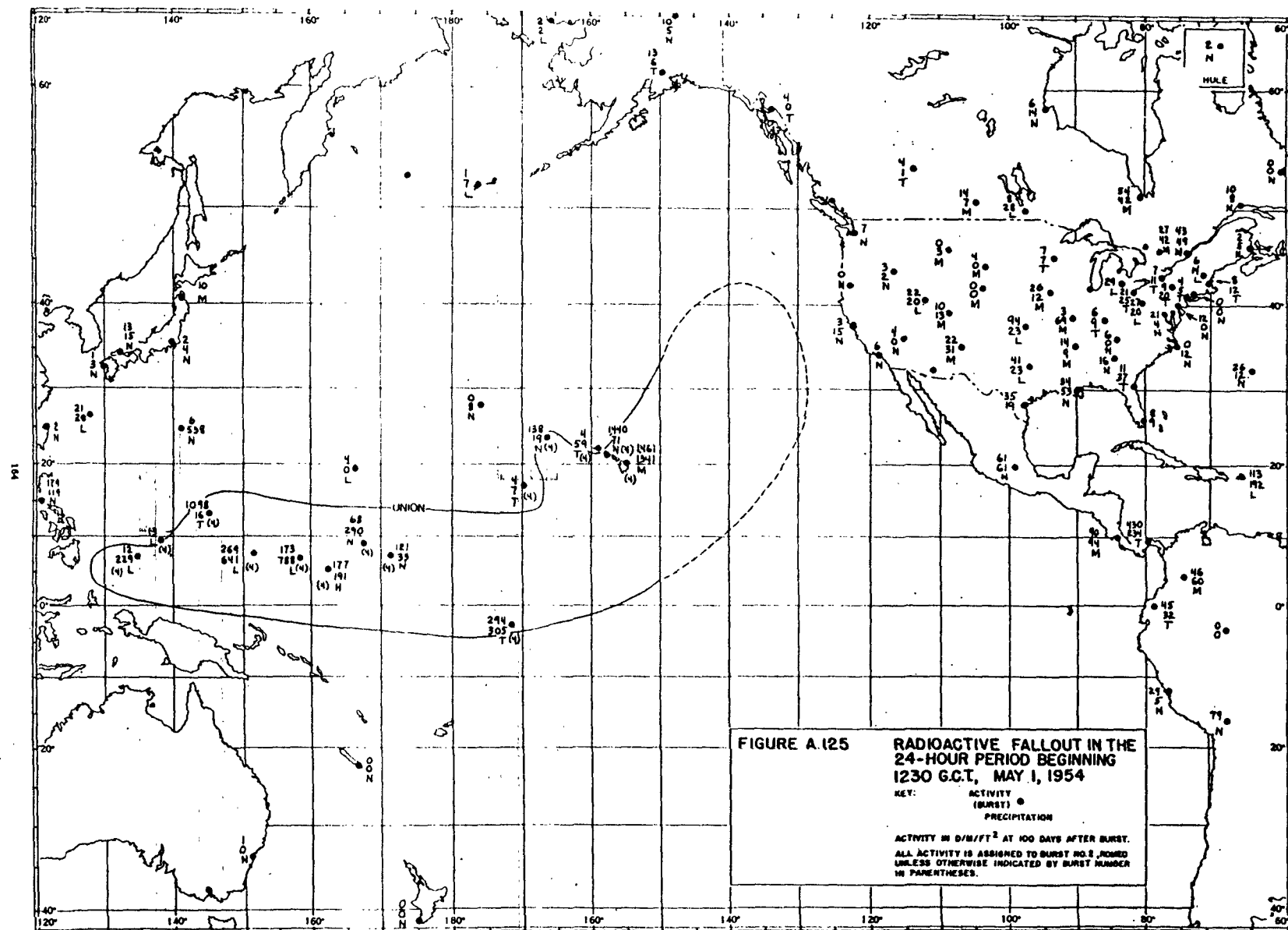


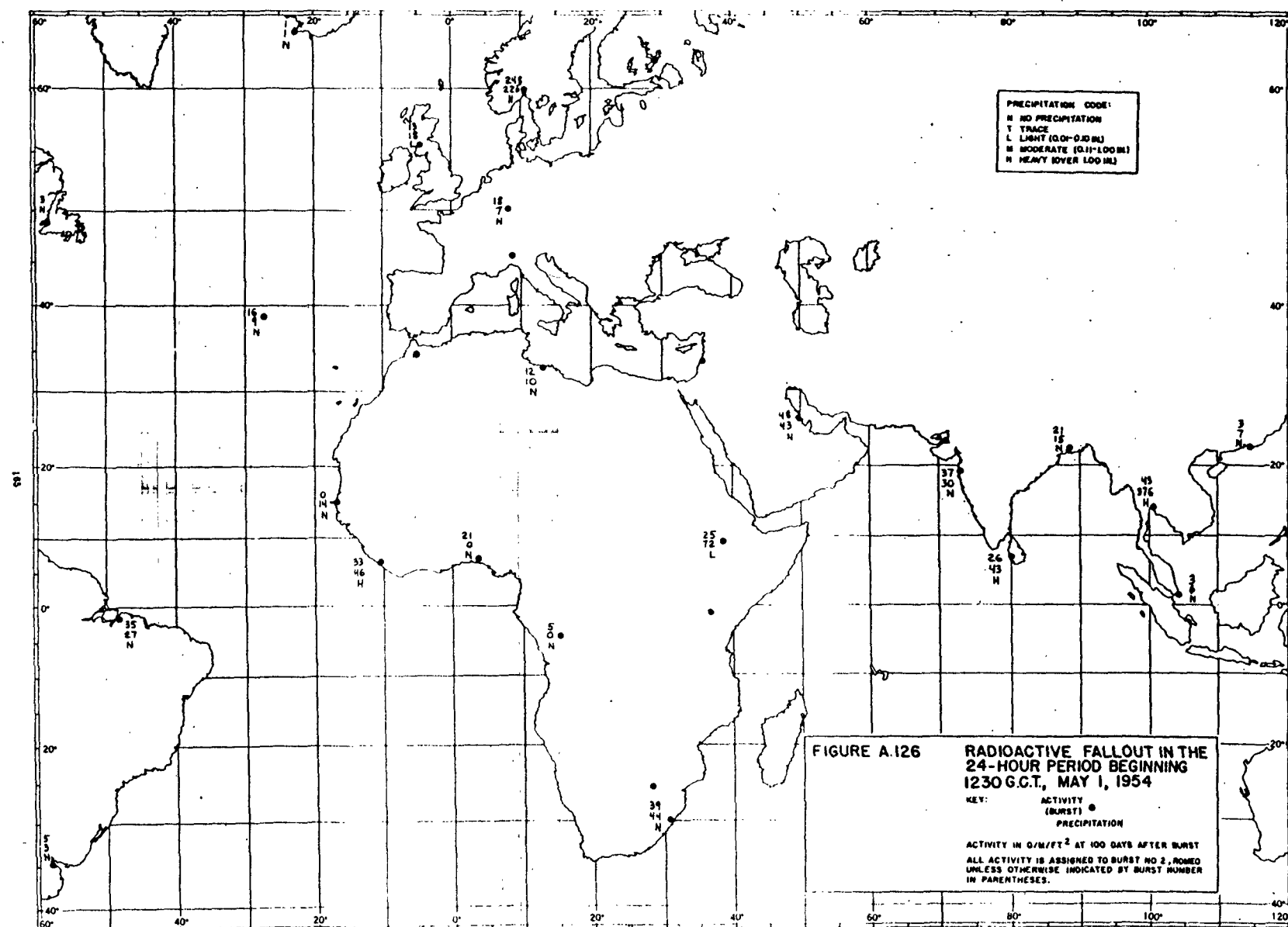


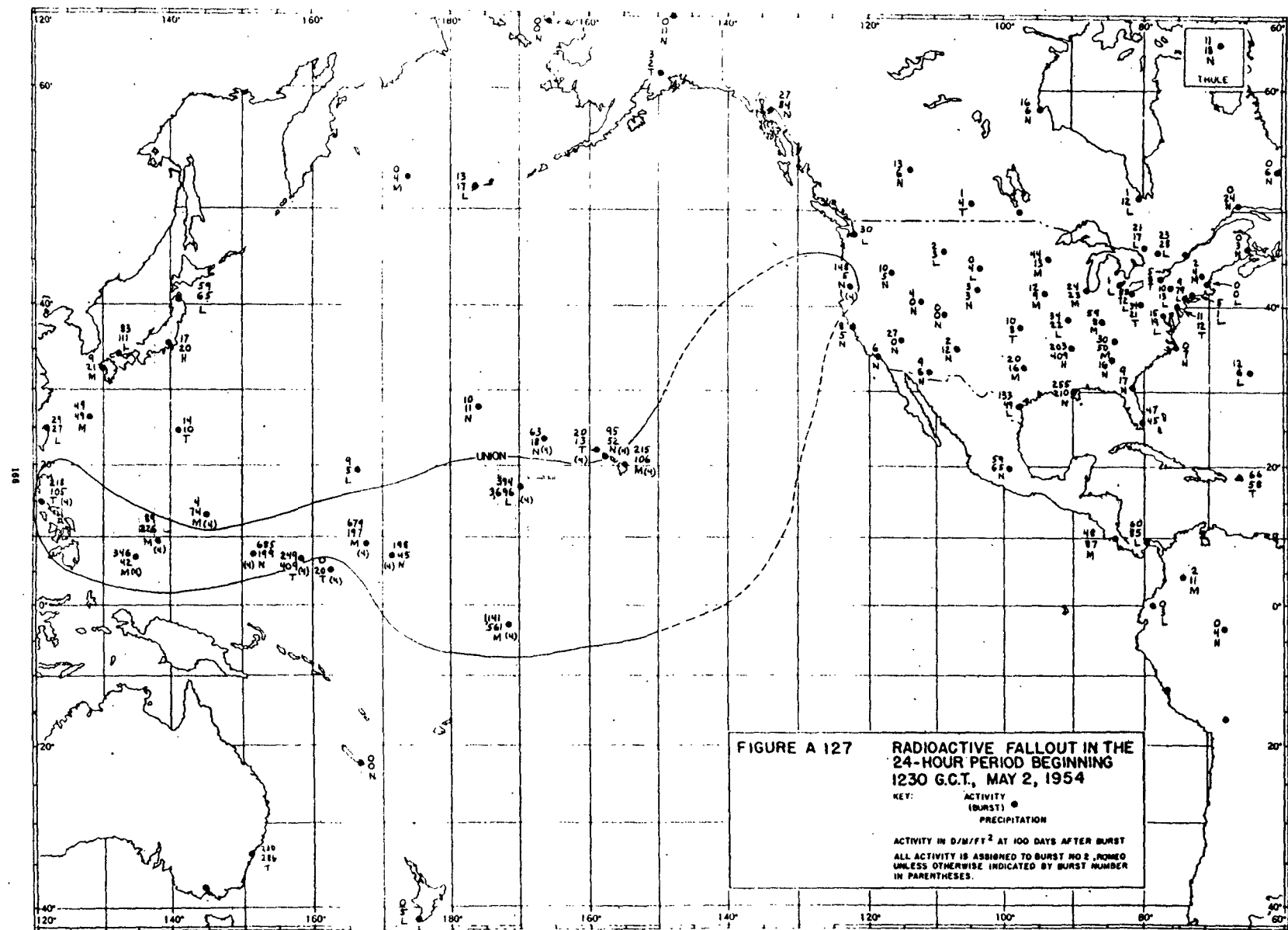


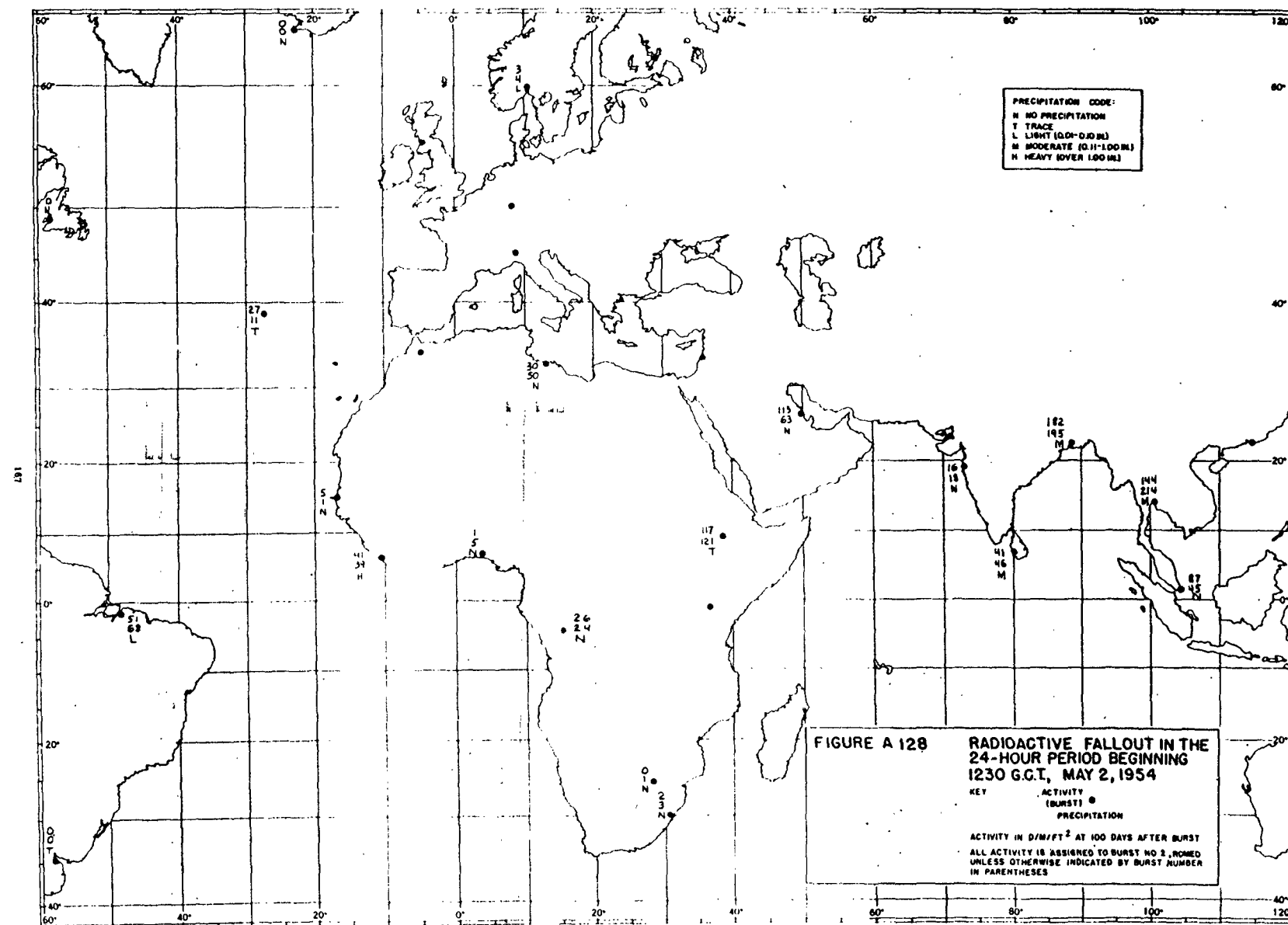


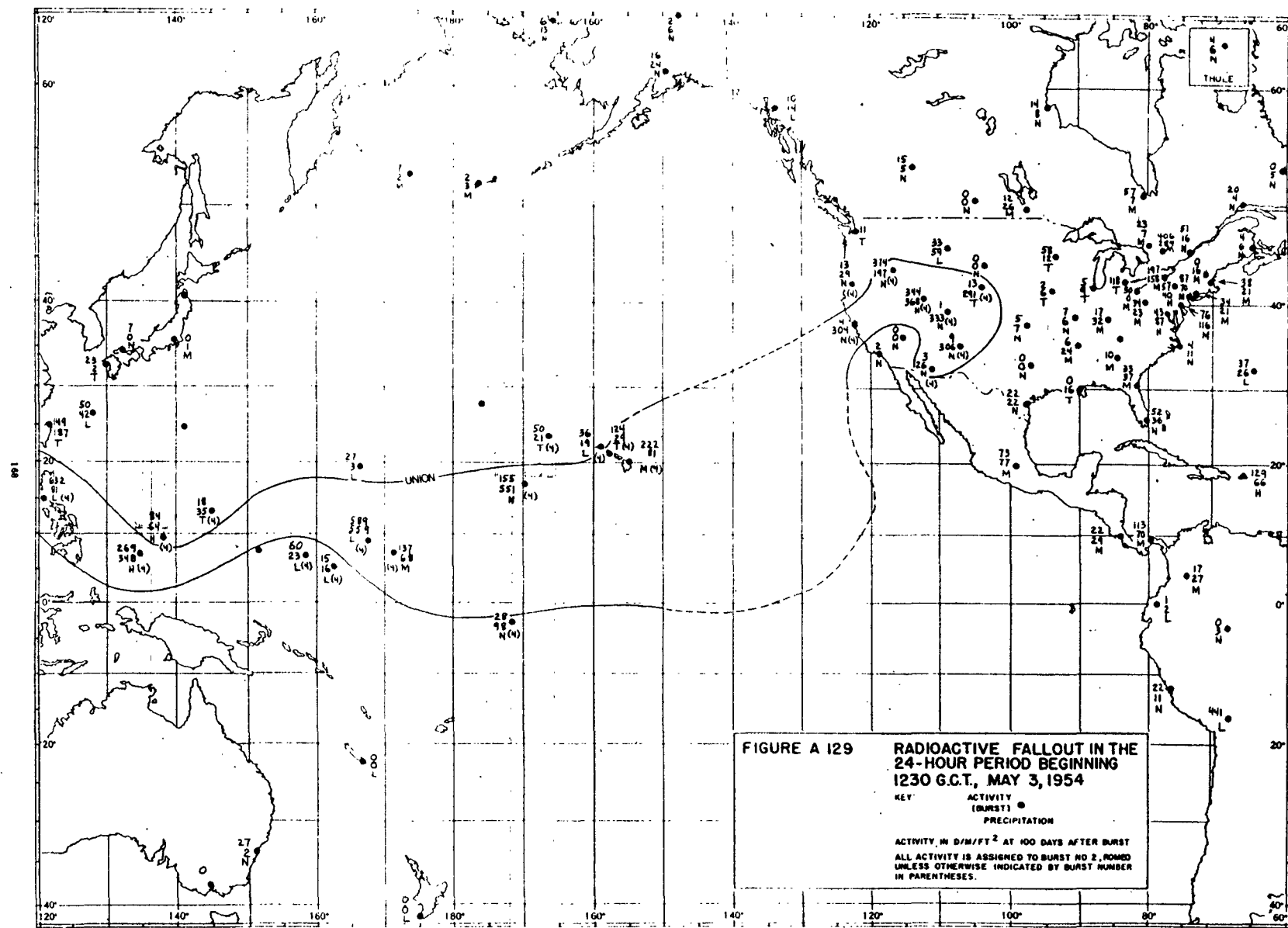


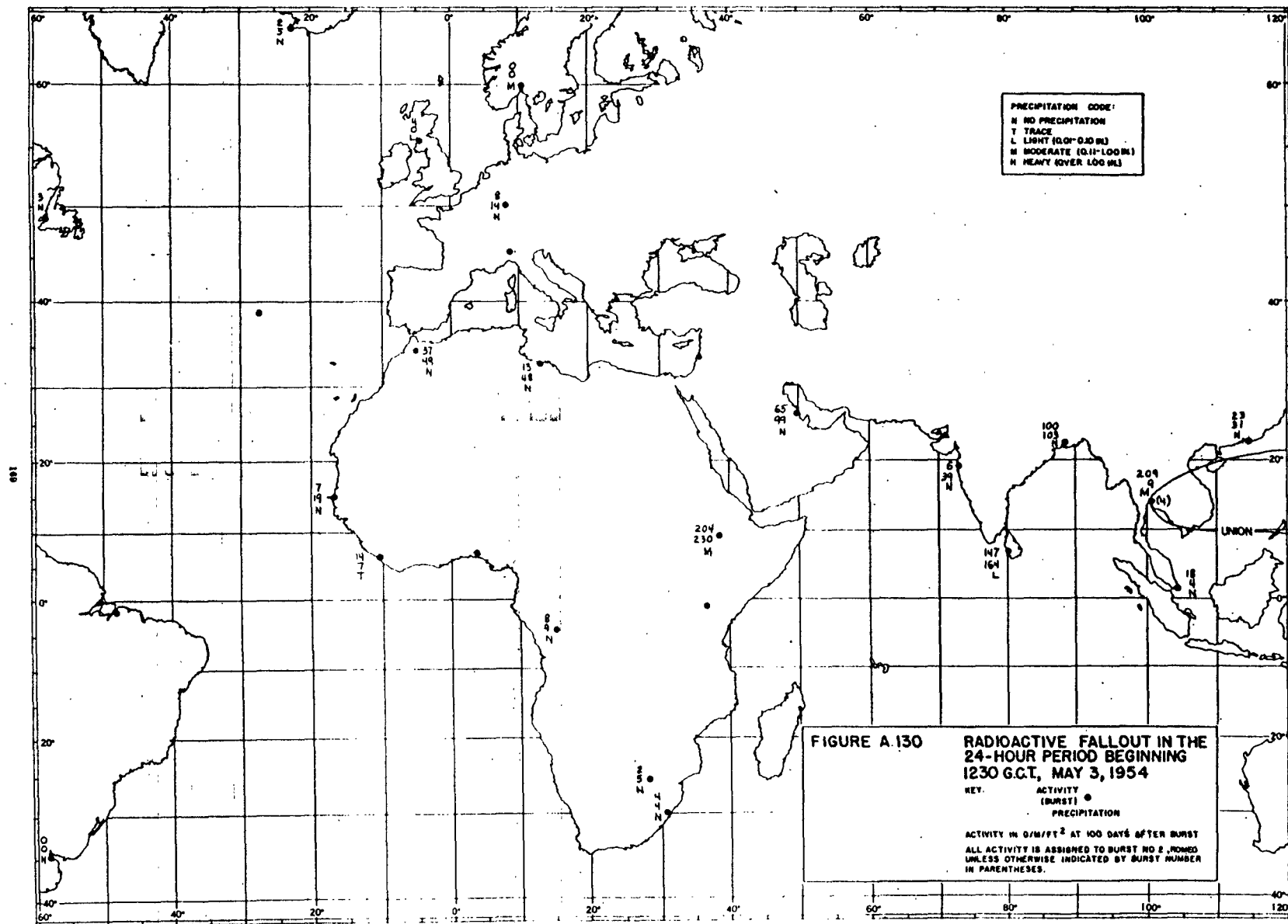












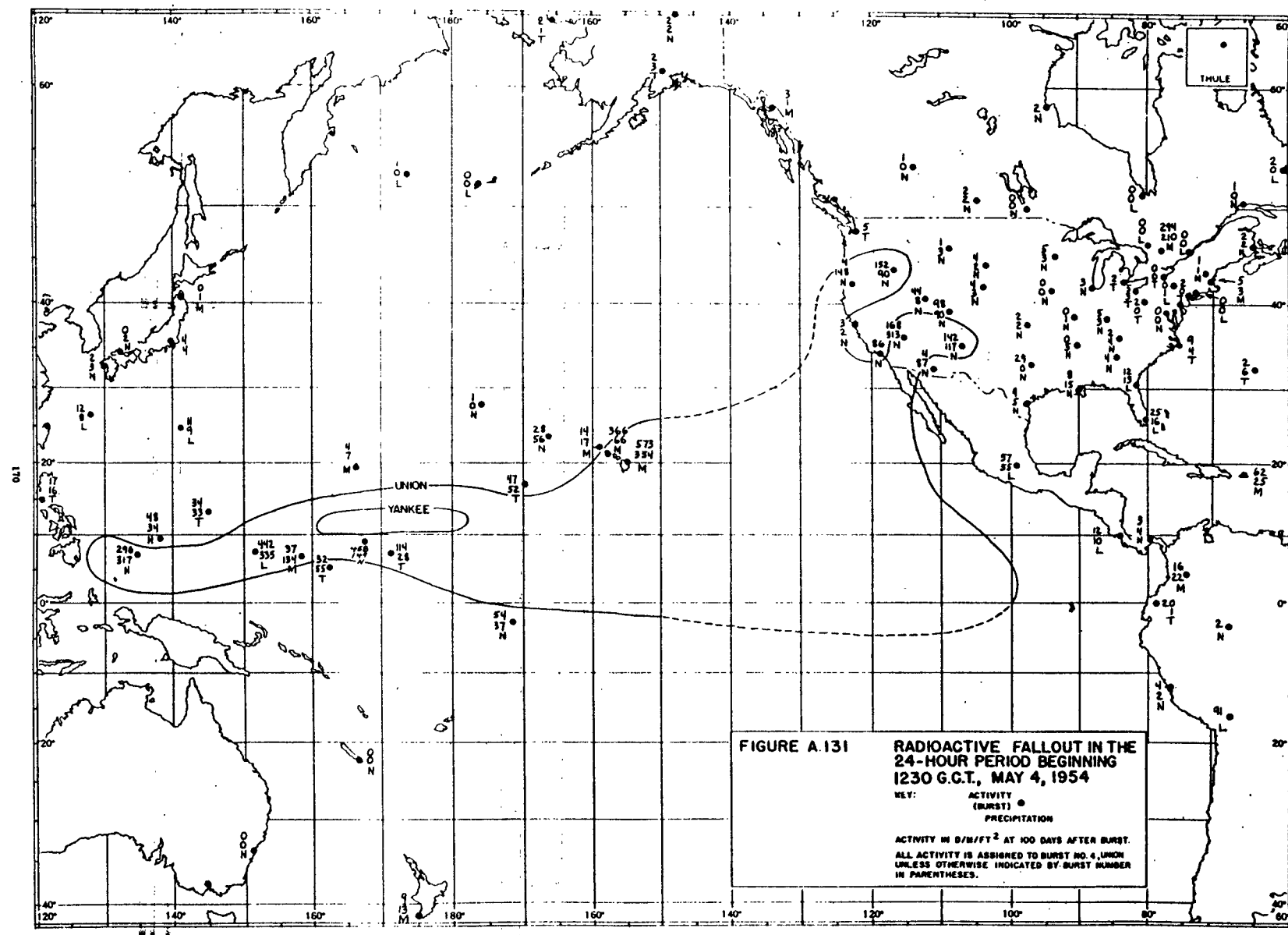
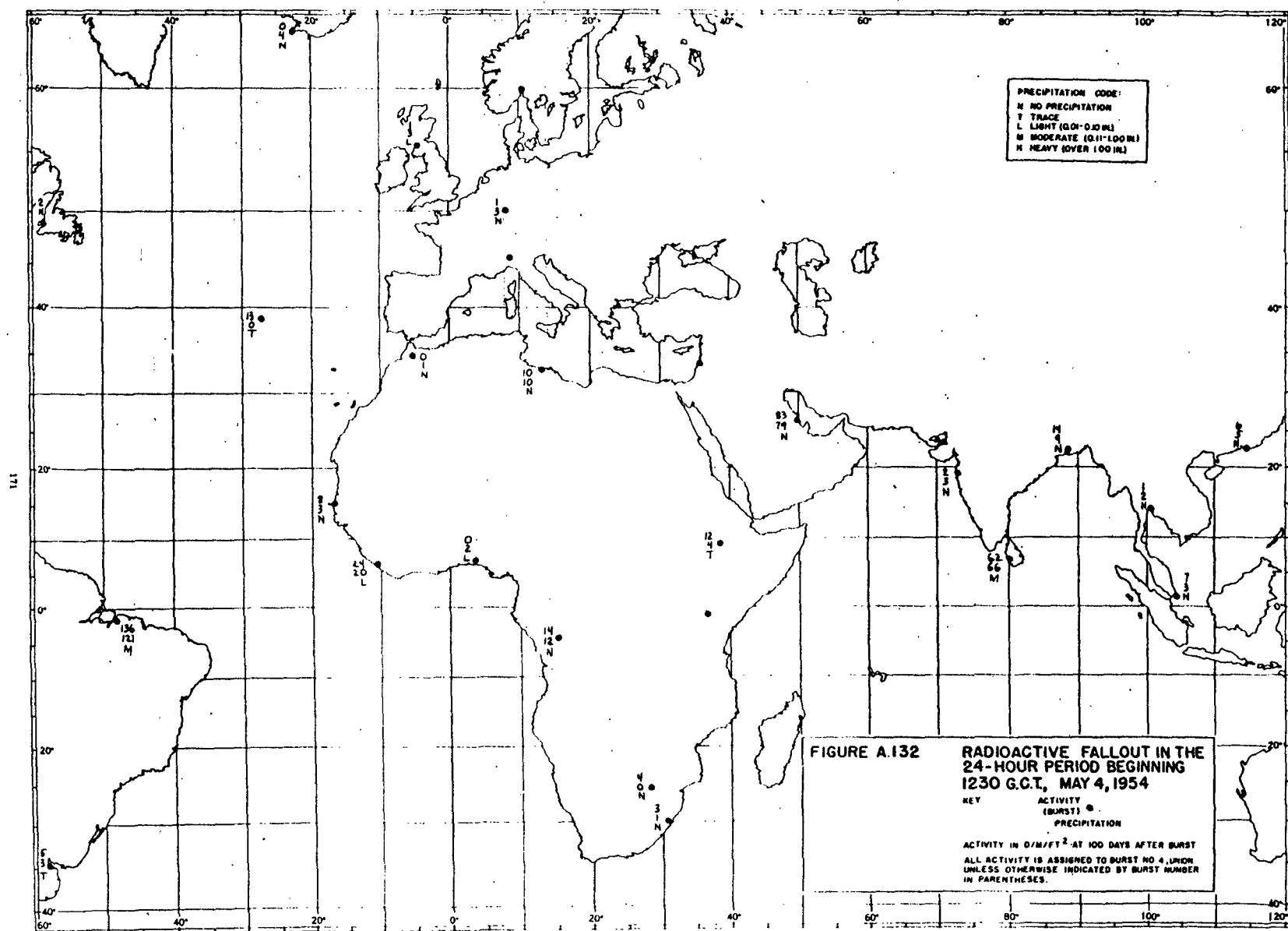
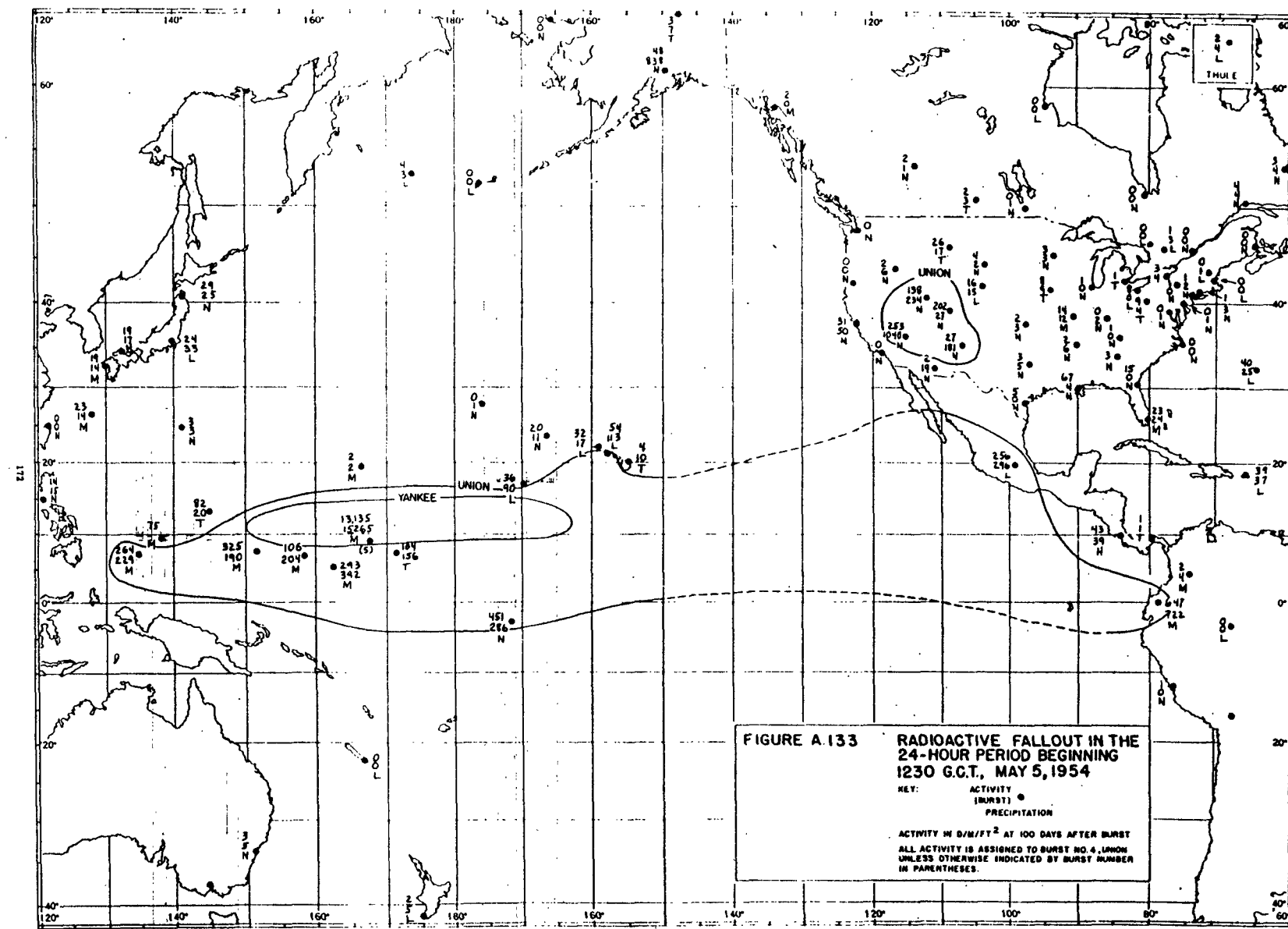


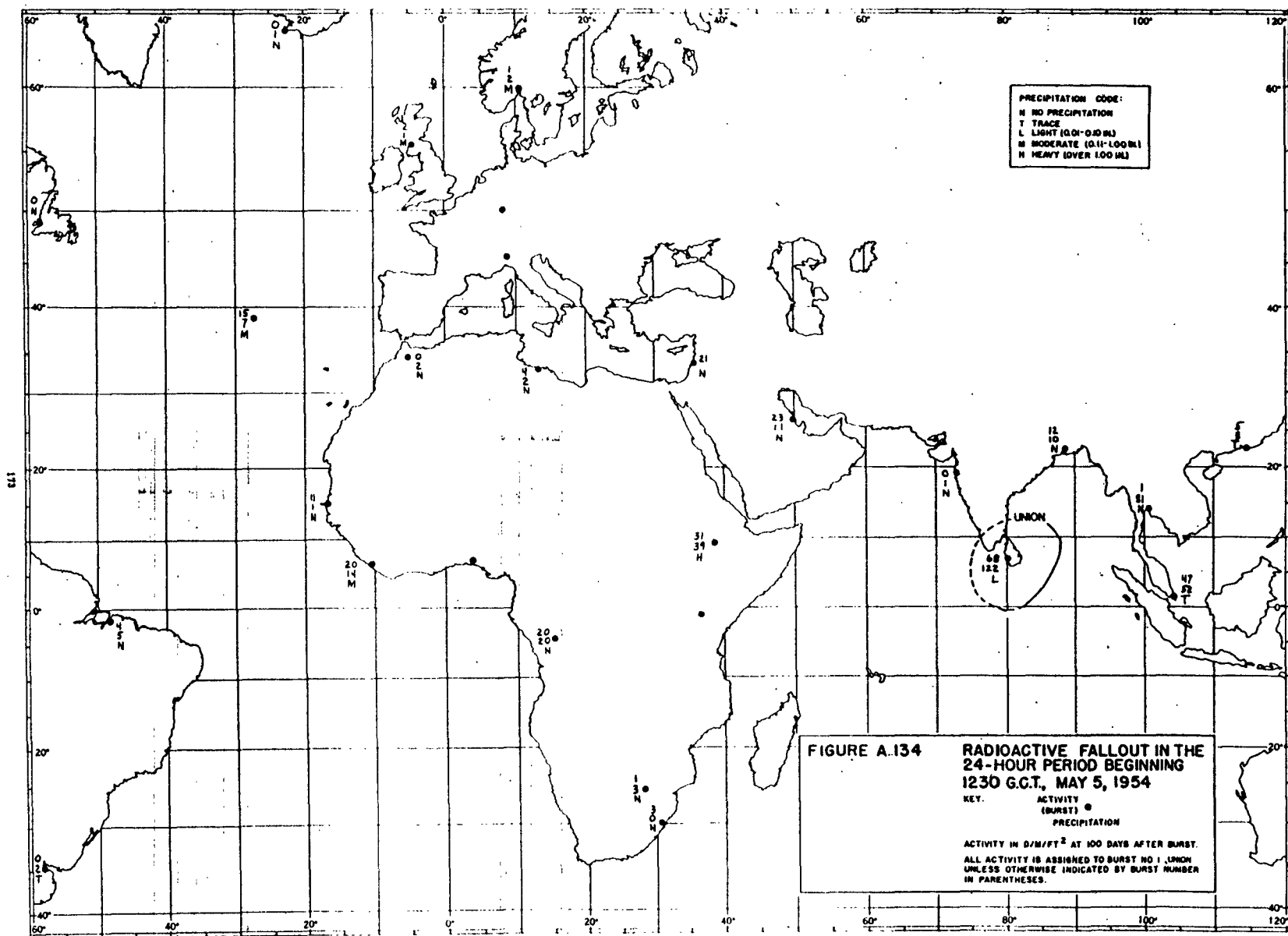
FIGURE A.131
RADIOACTIVE FALLOUT IN THE
24-HOUR PERIOD BEGINNING
1230 G.C.T., MAY 4, 1954

KEY:
 ACTIVITY
 (BURST) •
 PRECIPITATION

ACTIVITY IN $\mu\text{R}/\text{HR}/\text{FT}^2$ AT 100 DAYS AFTER BURST.
 ALL ACTIVITY IS ASSIGNED TO BURST NO. 4, UNION
 UNLESS OTHERWISE INDICATED BY BURST NUMBER
 IN PARENTHESES.







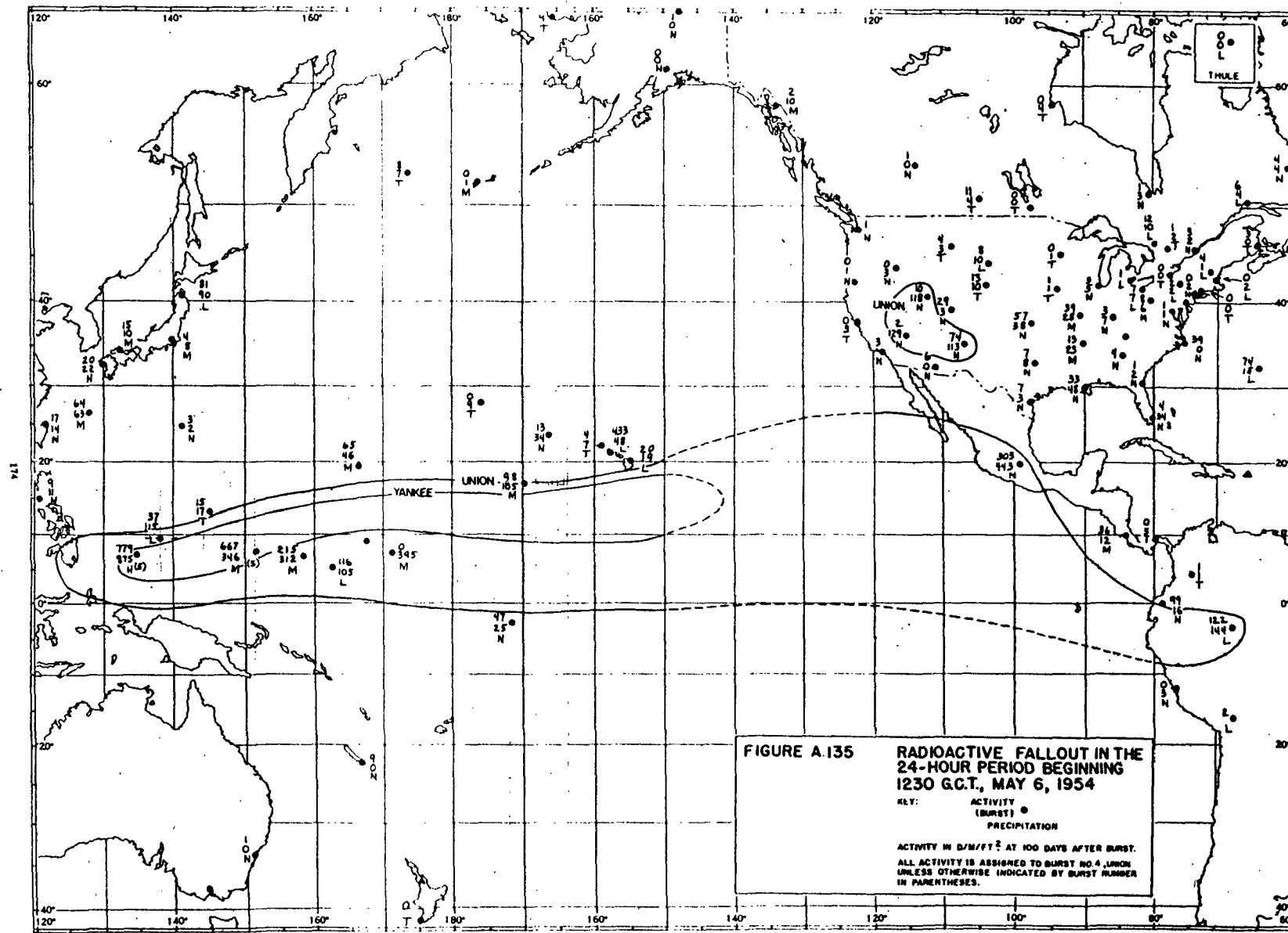
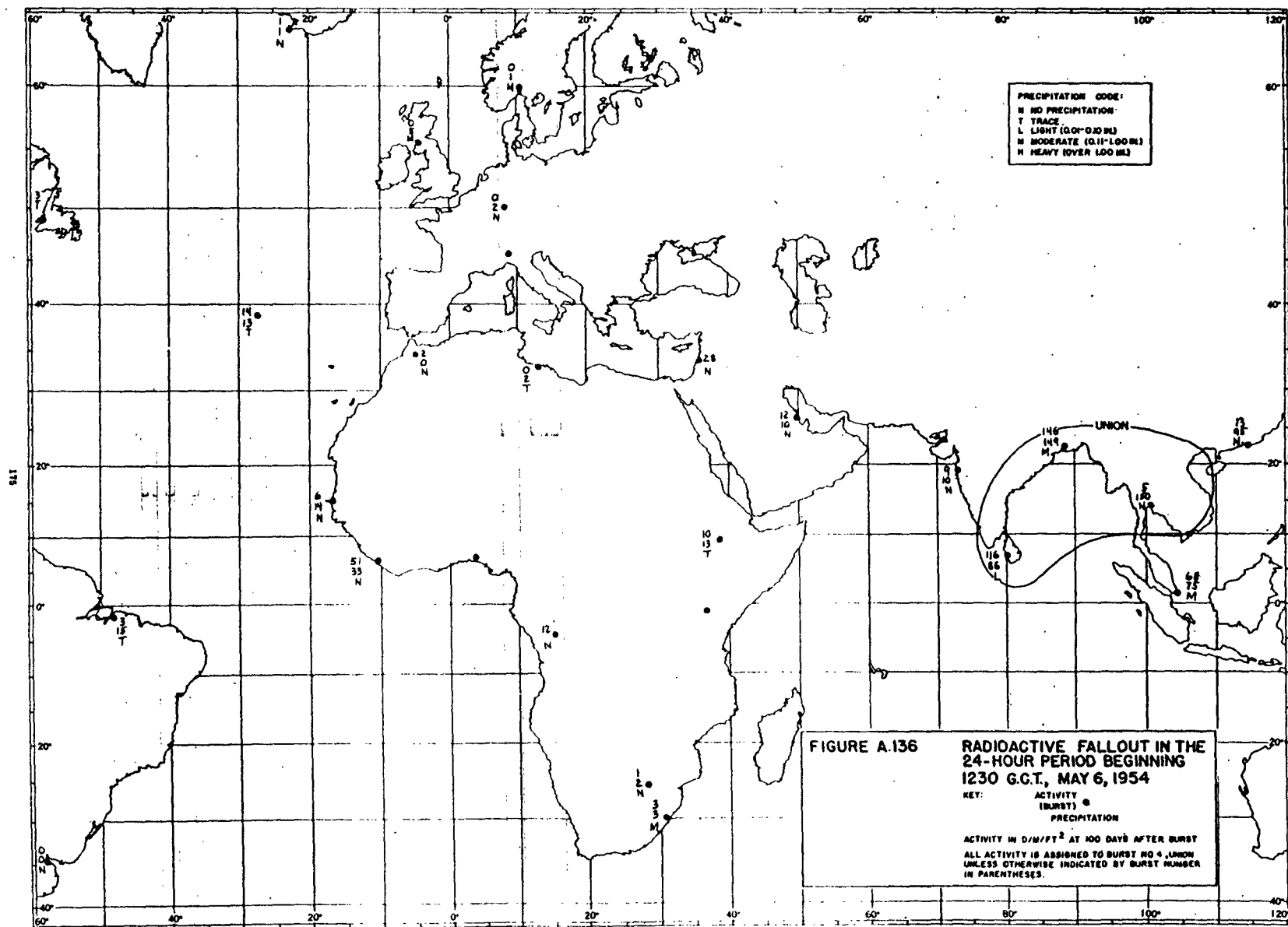


FIGURE A.135 **RADIOACTIVE FALLOUT IN THE
24-HOUR PERIOD BEGINNING
1230 G.C.T., MAY 6, 1954**

KEY: ACTIVITY (BURST) • PRECIPITATION

ACTIVITY IN B/M/FT² AT 100 DAYS AFTER BURST.
ALL ACTIVITY IS ASSIGNED TO BURST NO. 4, UNLESS OTHERWISE INDICATED BY BURST NUMBER
IN PARENTHESES.



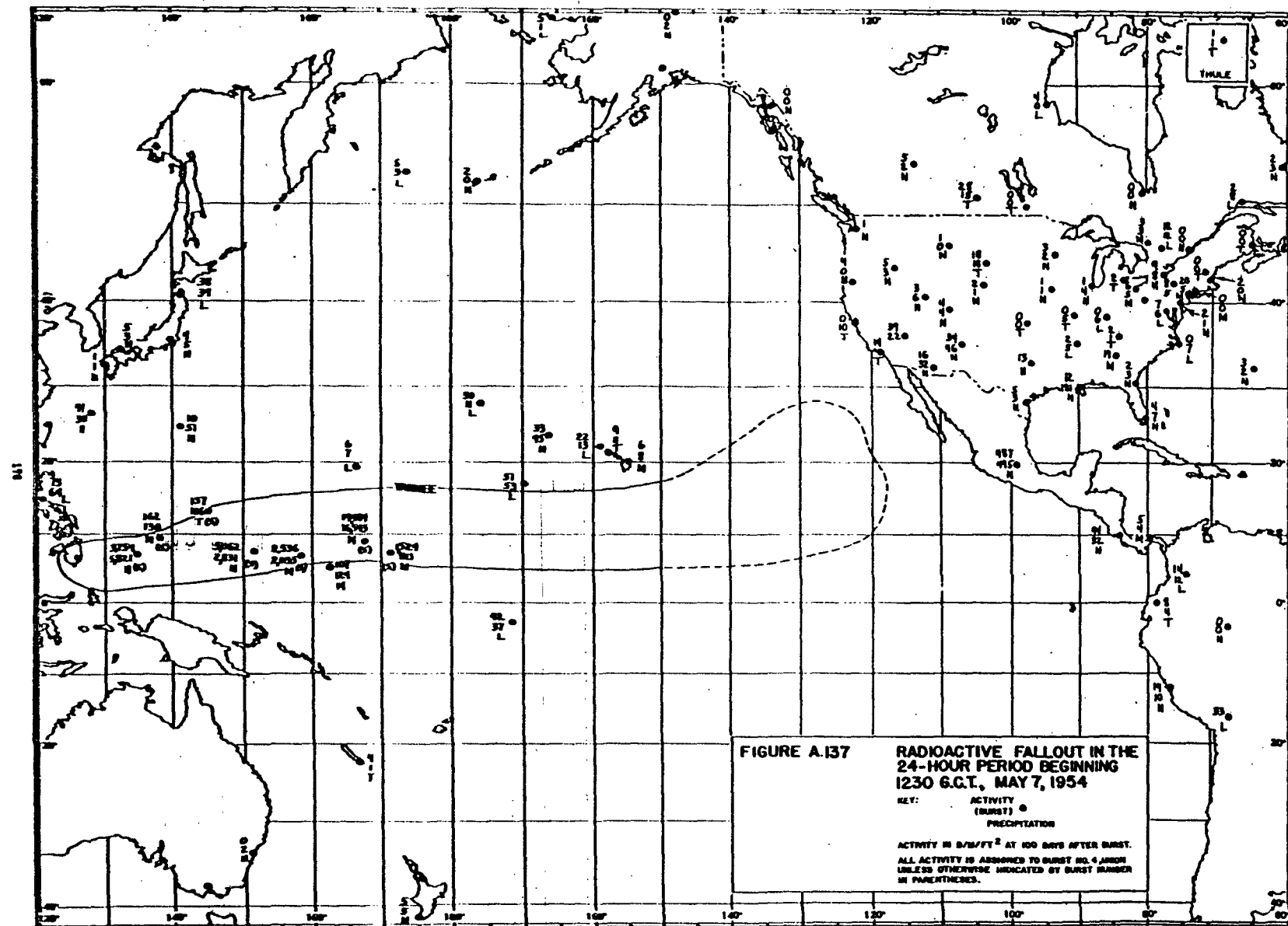


FIGURE A.137 RADIOACTIVE FALLOUT IN THE
24-HOUR PERIOD BEGINNING
1230 G.C.T., MAY 7, 1954

KEY: ACTIVITY
 (BURST) •
 PRECIPITATION

ACTIVITY IN $\mu\text{R}/\text{FT}^2$ AT 100 DAYS AFTER BURST.
ALL ACTIVITY IS ASSIGNED TO BURST NO. 4 UNLESS
LESS OTHERWISE INDICATED BY BURST NUMBER
IN PARENTHESES.

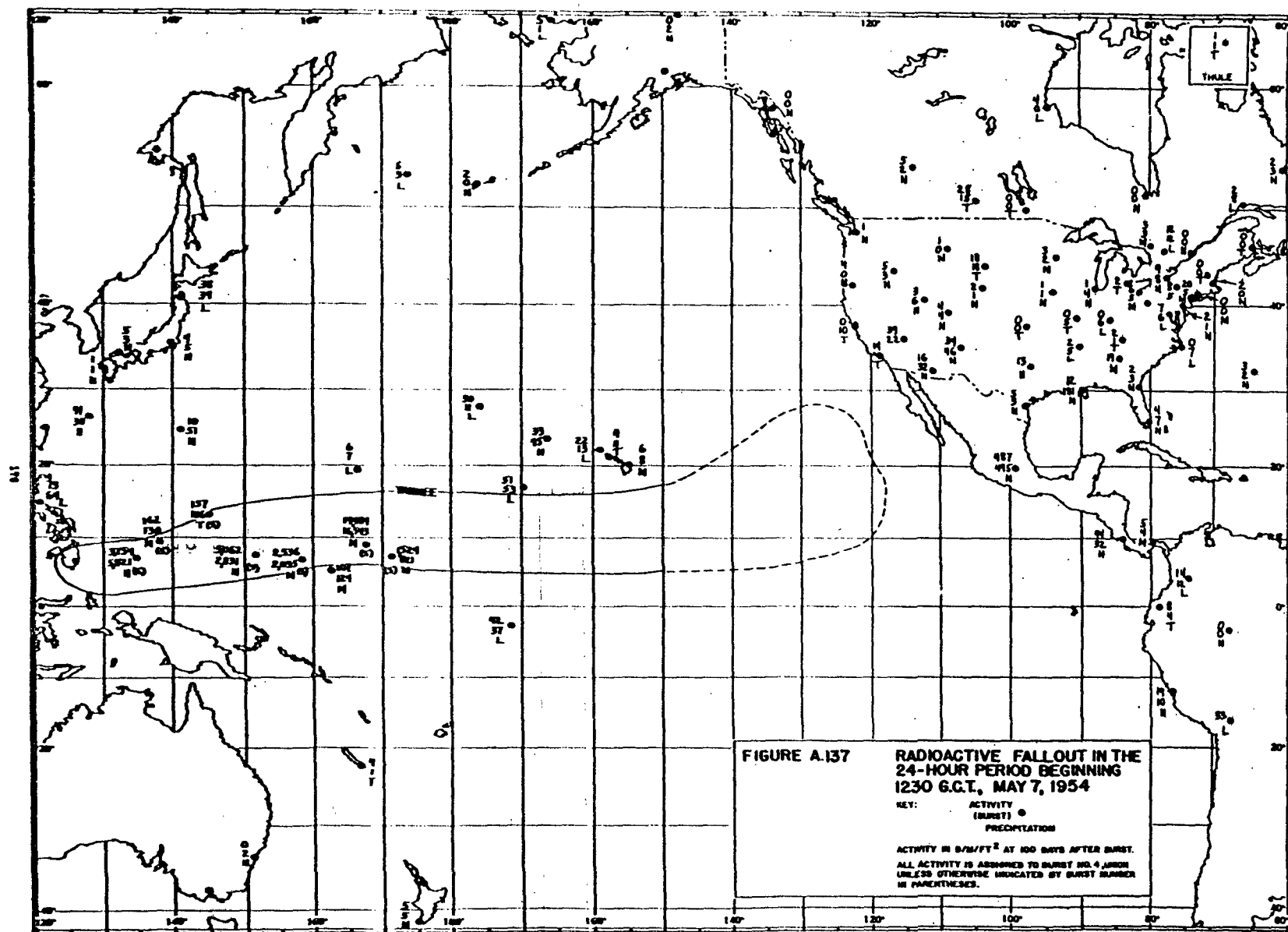


FIGURE A.137
RADIOACTIVE FALLOUT IN THE
24-HOUR PERIOD BEGINNING
1230 G.C.T., MAY 7, 1954

KEY:
ACTIVITY
(BURST) ●
PRECIPITATION

ACTIVITY IN $\mu\text{R}/\text{ft}^2$ AT 100 DAYS AFTER BURST.
ALL ACTIVITY IS ATTRIBUTED TO BURST NO. 4 UNLESS
UNLESS OTHERWISE INDICATED BY BURST NUMBER
IN PARENTHESES.

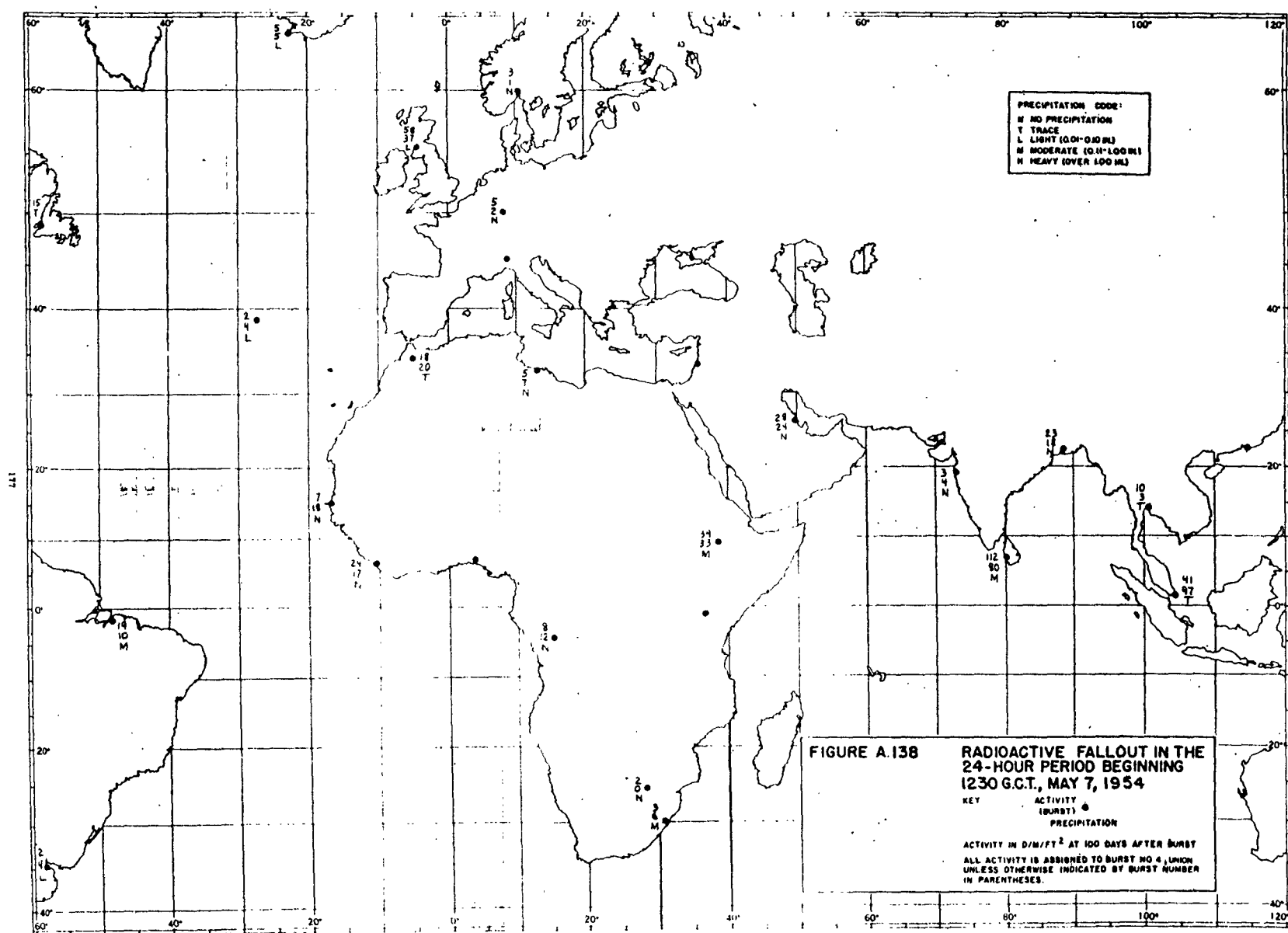
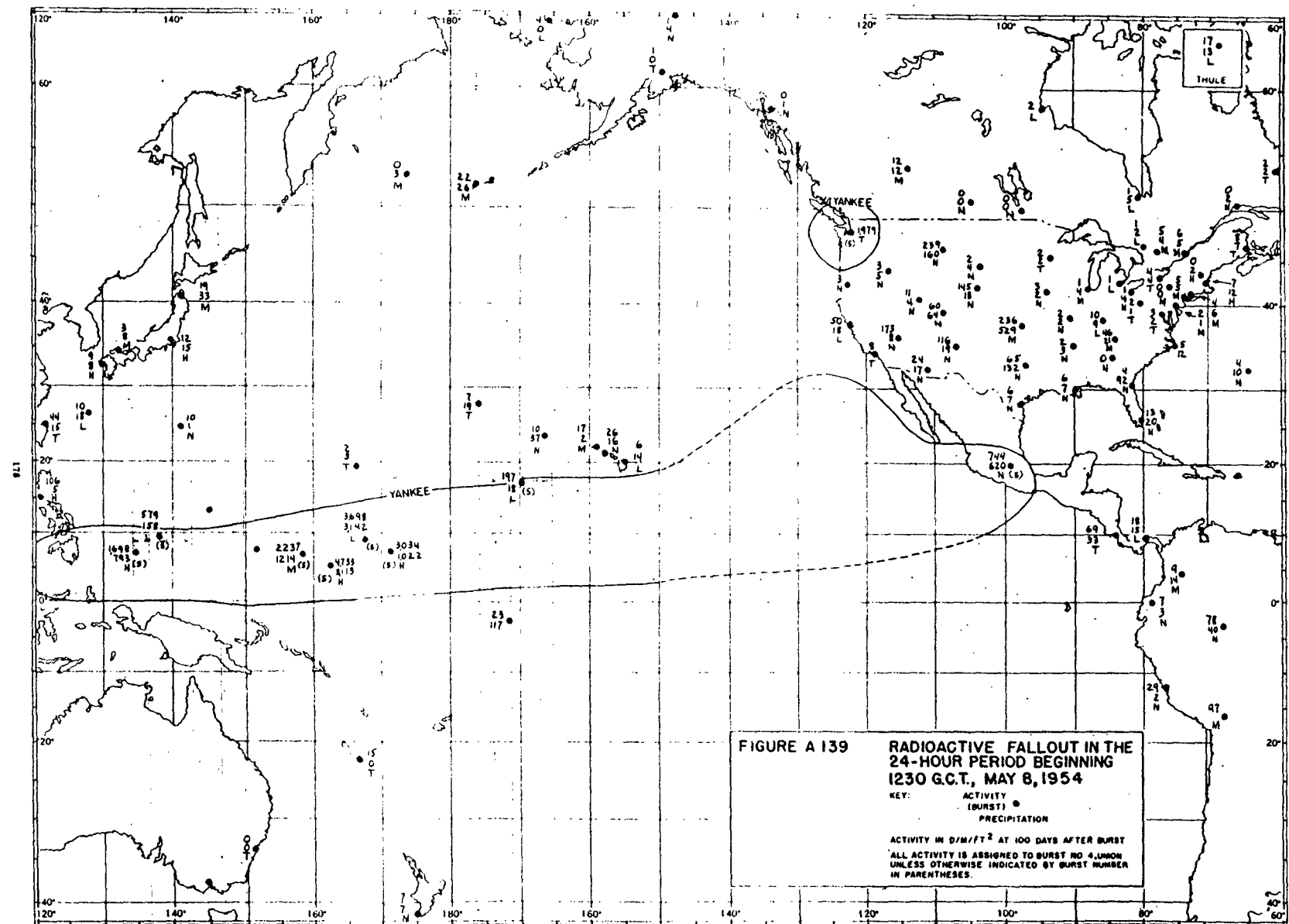
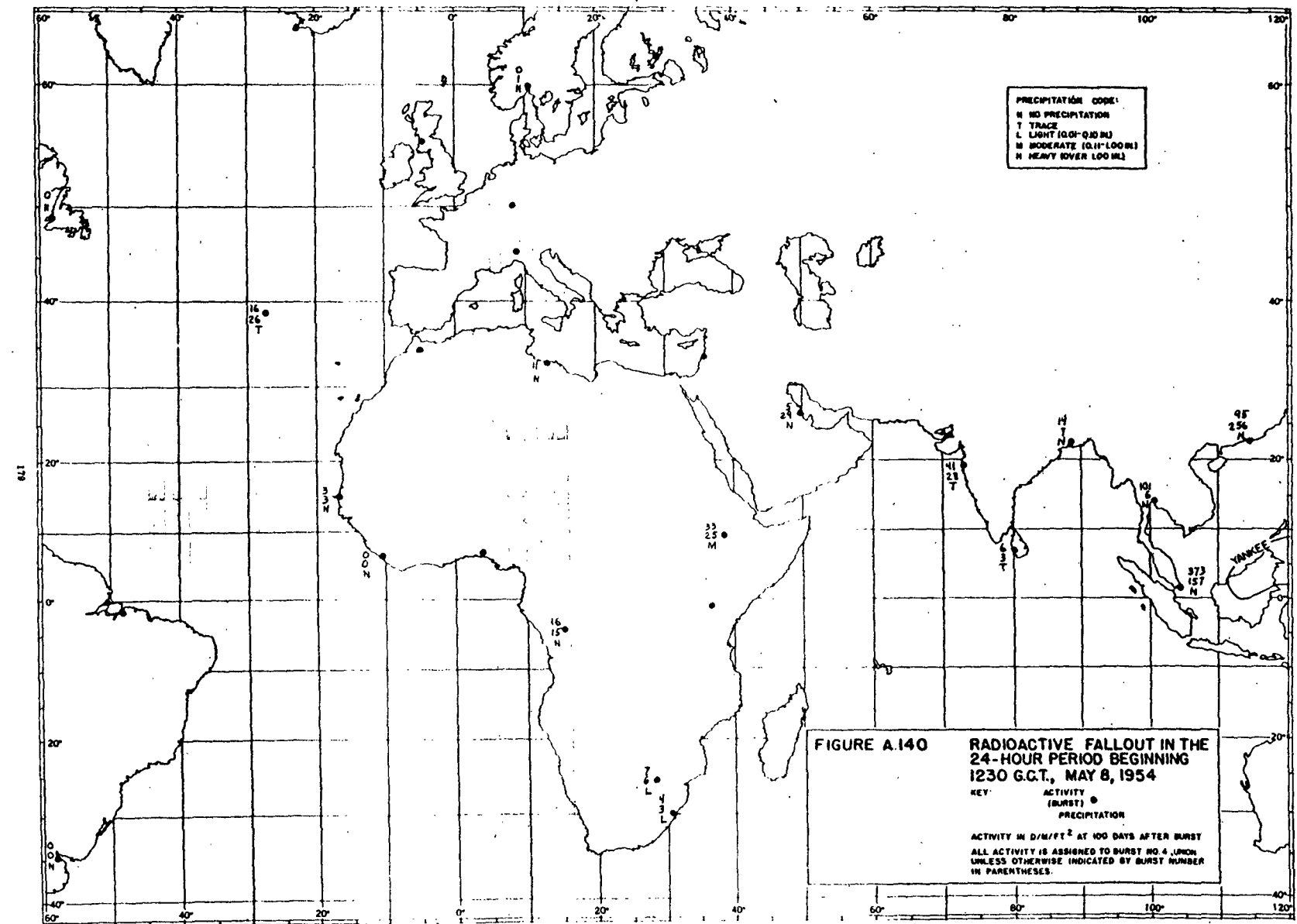
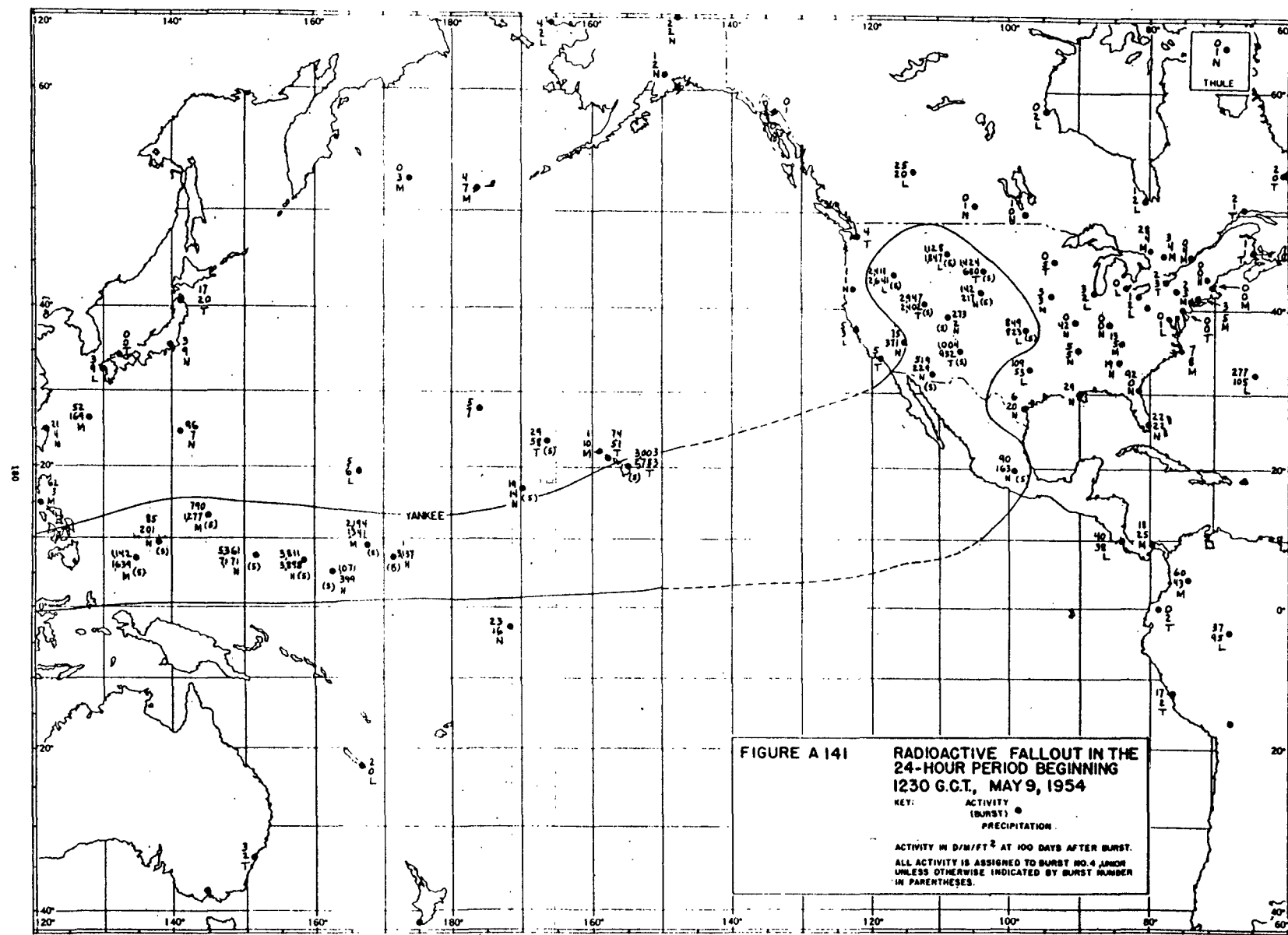
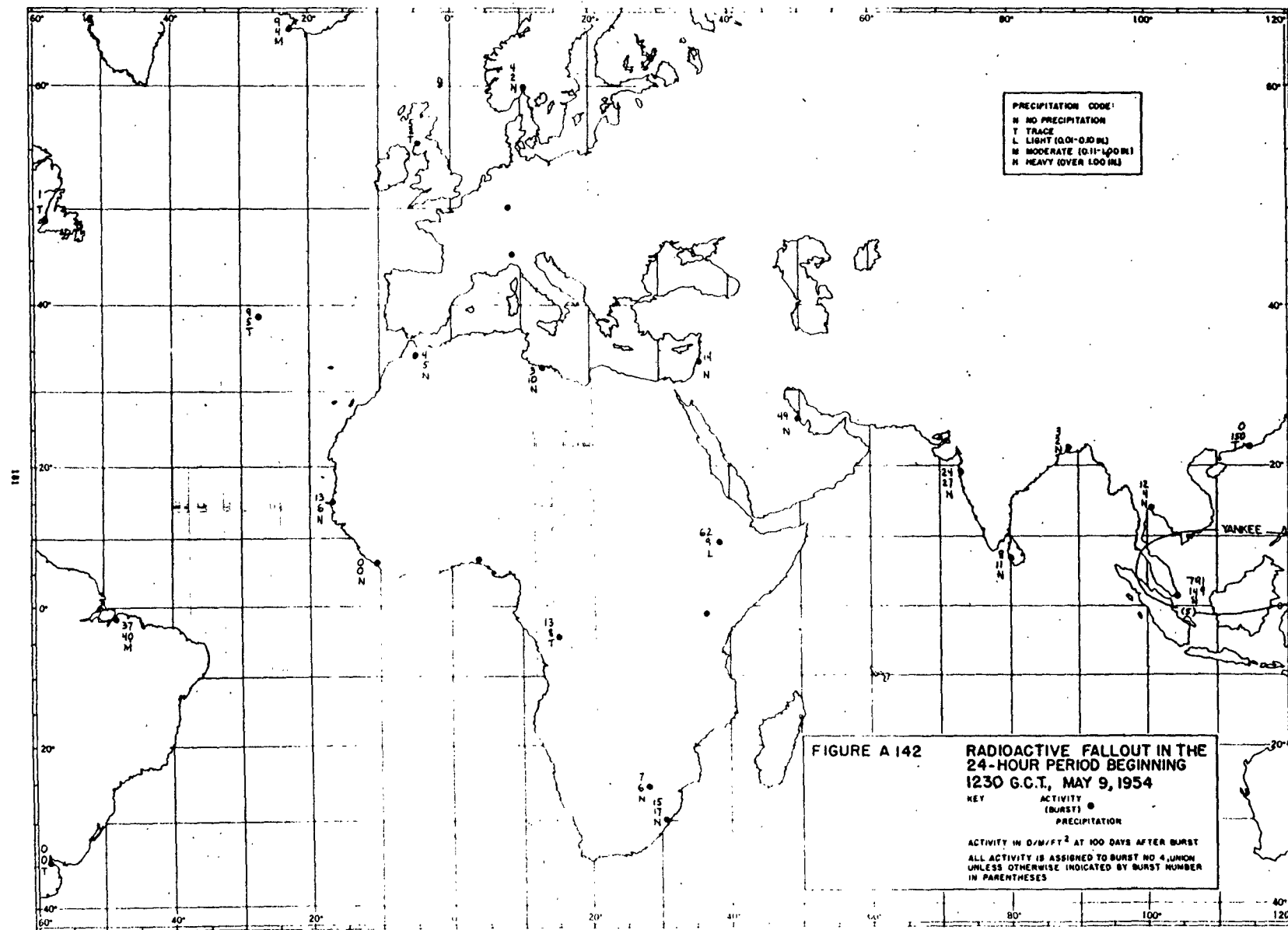


FIGURE A.138 **RADIOACTIVE FALLOUT IN THE
24-HOUR PERIOD BEGINNING
1230 G.C.T., MAY 7, 1954**









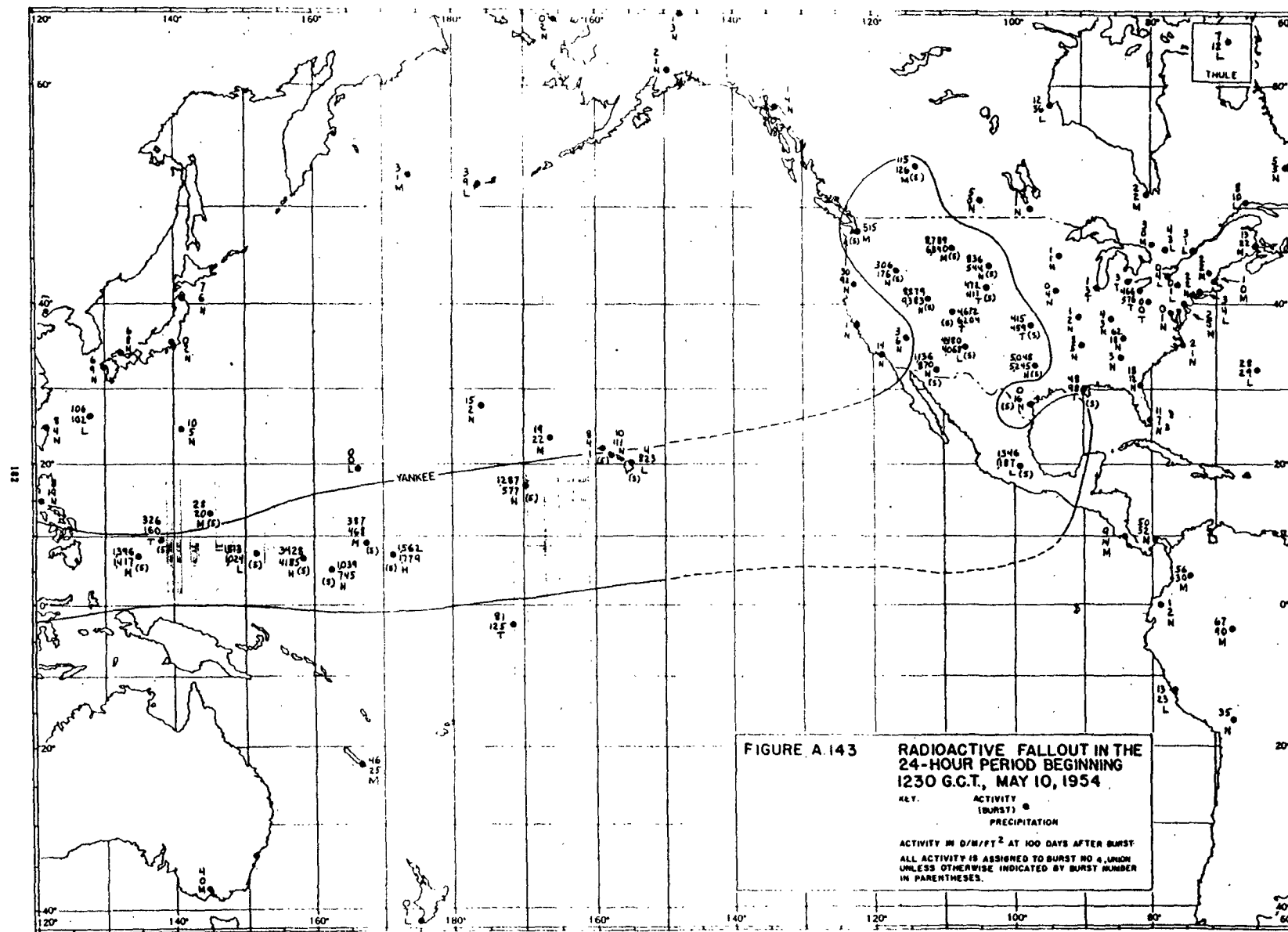


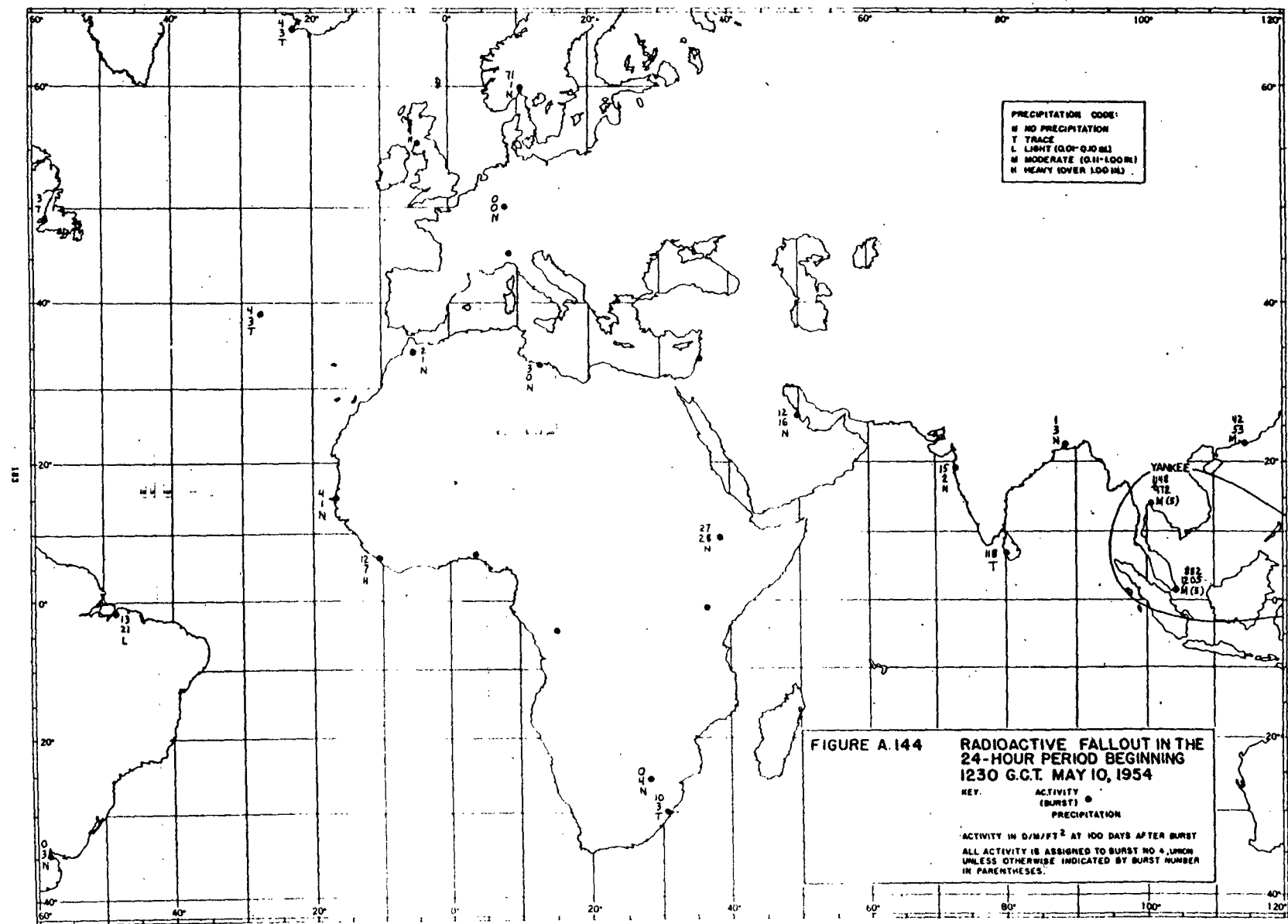
FIGURE A.143 **RADIOACTIVE FALLOUT IN THE
24-HOUR PERIOD BEGINNING
1230 G.C.T., MAY 10, 1954**

ACTIVITY
(BURST) @
PRECIPITATION

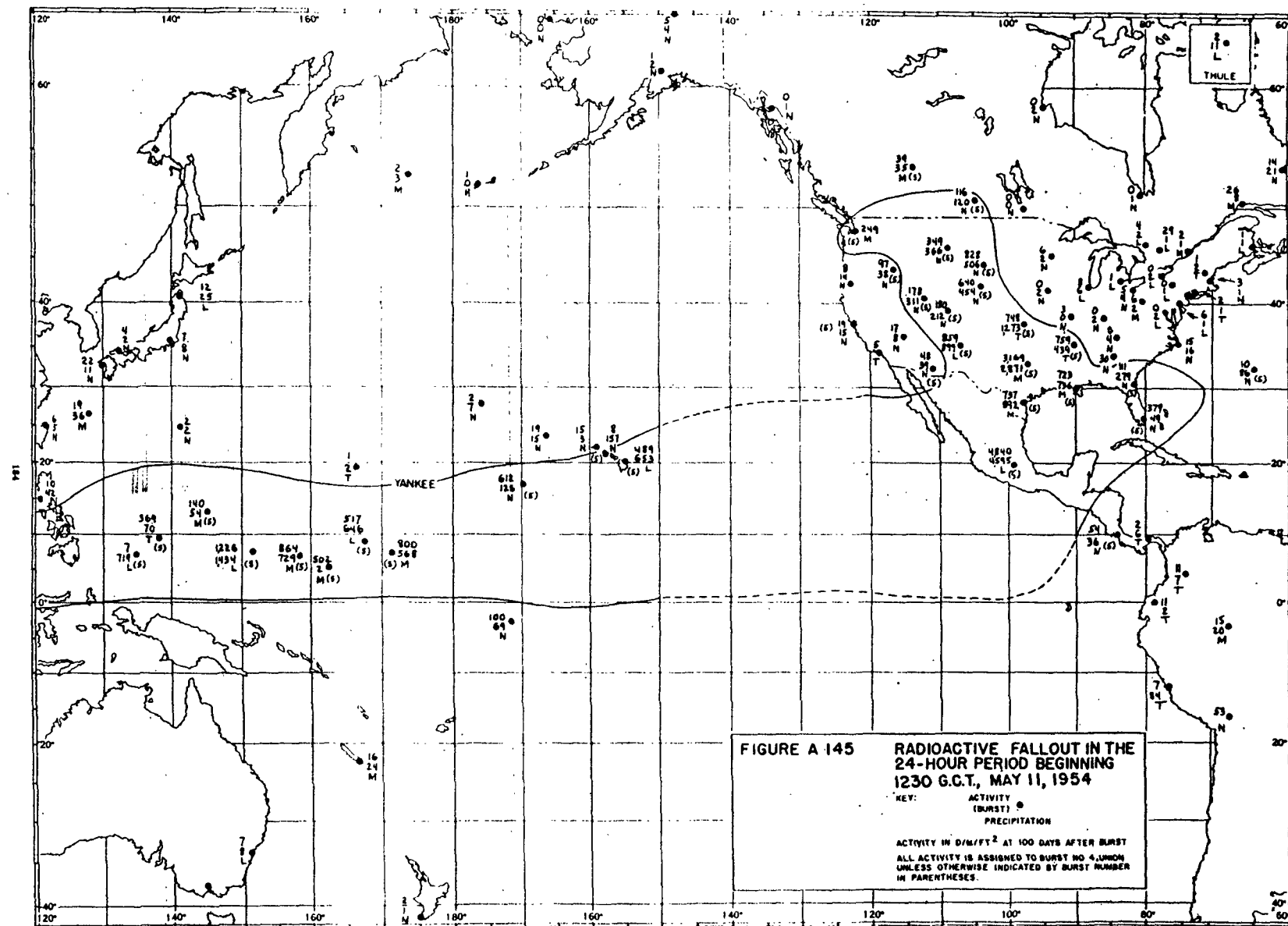
Precipitation

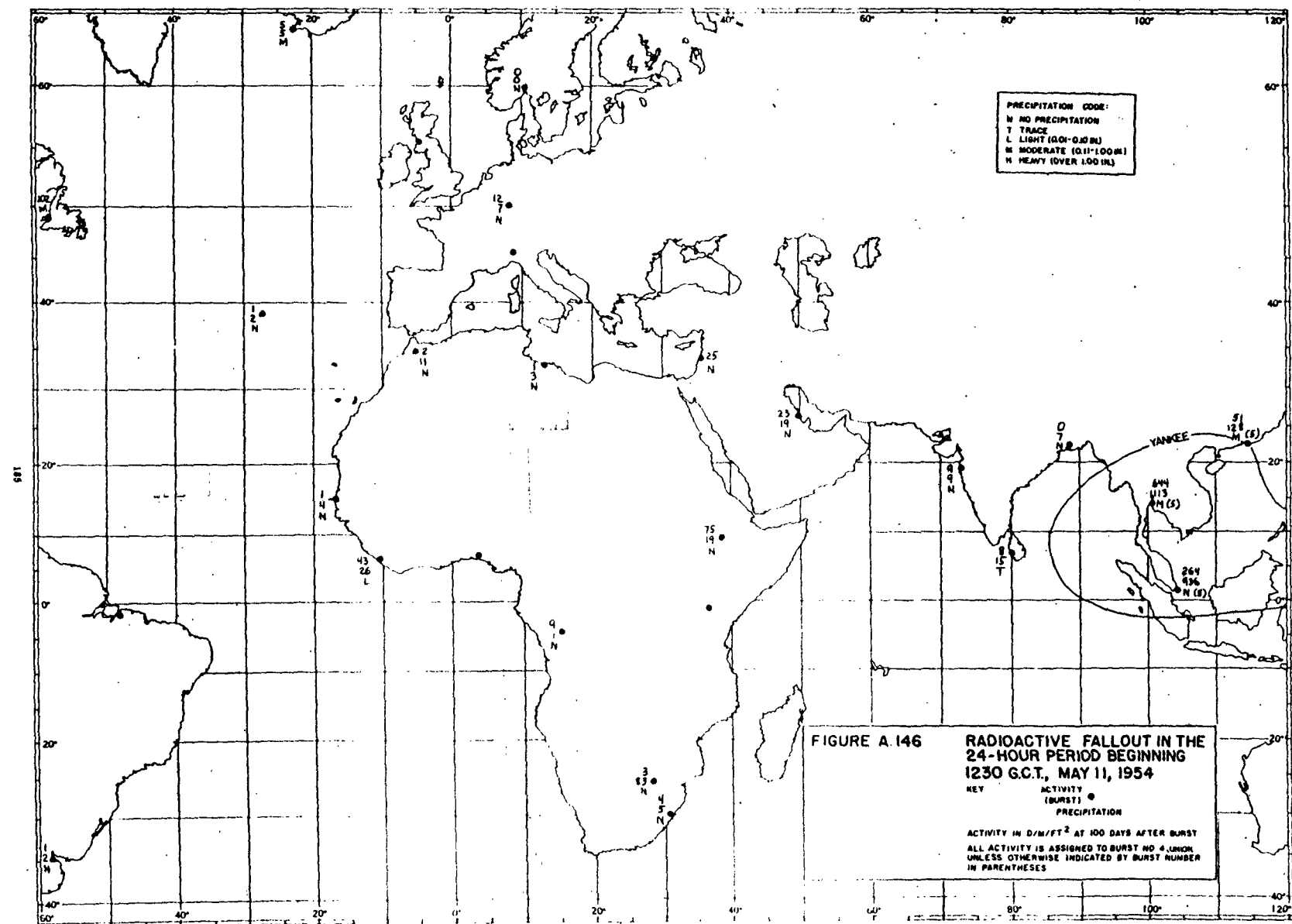
ACTIVITY IN $\mu\text{Ci}/\text{ft}^2$ AT 100 DAYS AFTER BURST

ALL ACTIVITY IS ASSIGNED TO BURST NO 4, UNION
UNLESS OTHERWISE INDICATED BY BURST NUMBER
IN PARENTHESES.



**FIGURE A.144 RADIOACTIVE FALLOUT IN THE
24-HOUR PERIOD BEGINNING
1230 G.C.T. MAY 10, 1954**





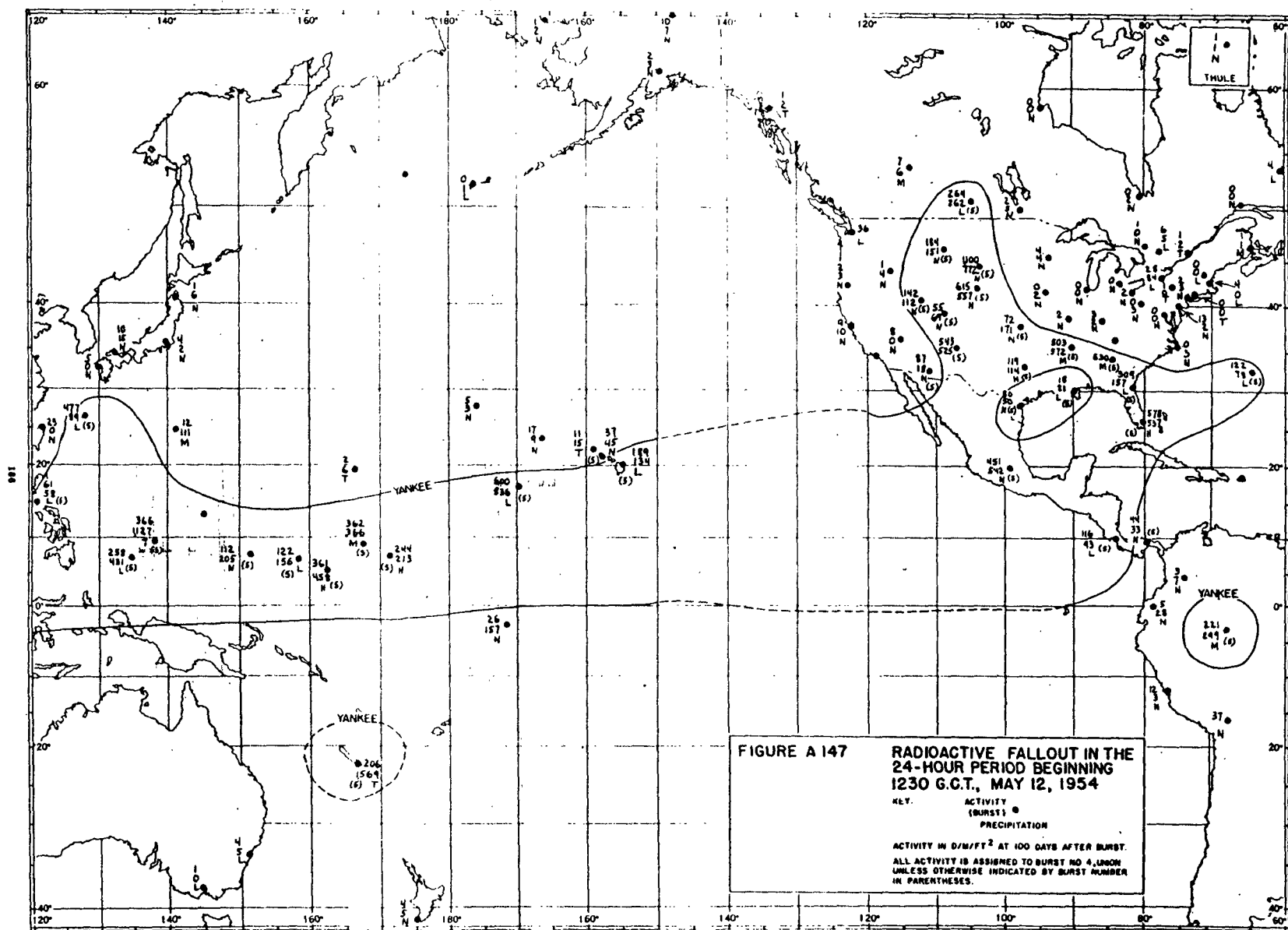
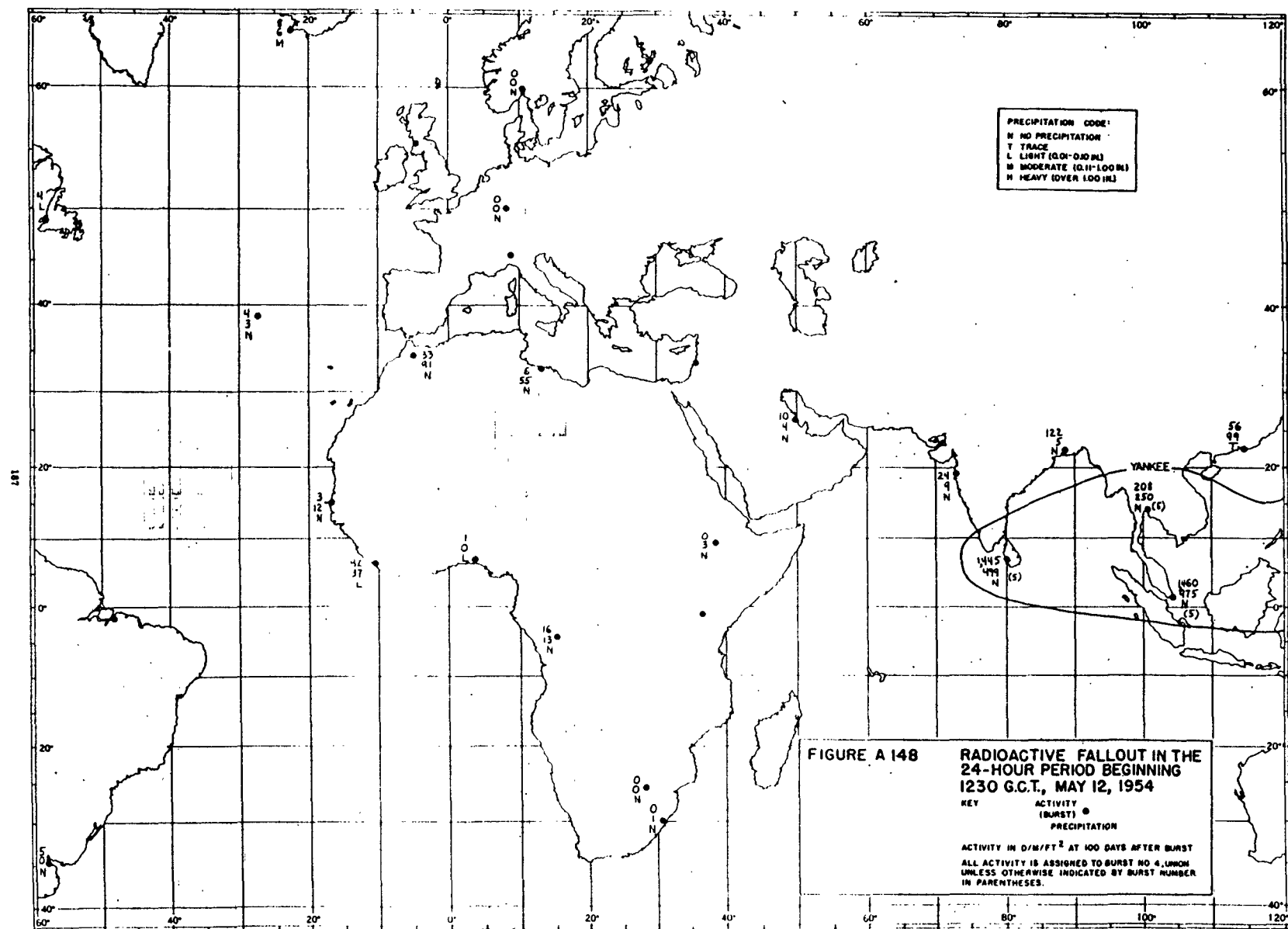


FIGURE A 147

RADIOACTIVE FALLOUT IN THE
24-HOUR PERIOD BEGINNING
1230 G.C.T., MAY 12, 1954

KEY: ACTIVITY
 (BURST) PRECIPITATION

ACTIVITY IN $\mu\text{R}/\text{hr}$ AT 100 DAYS AFTER BURST.
ALL ACTIVITY IS ASSIGNED TO BURST NO. 4, UNION
UNLESS OTHERWISE INDICATED BY BURST NUMBER
IN PARENTHESES.



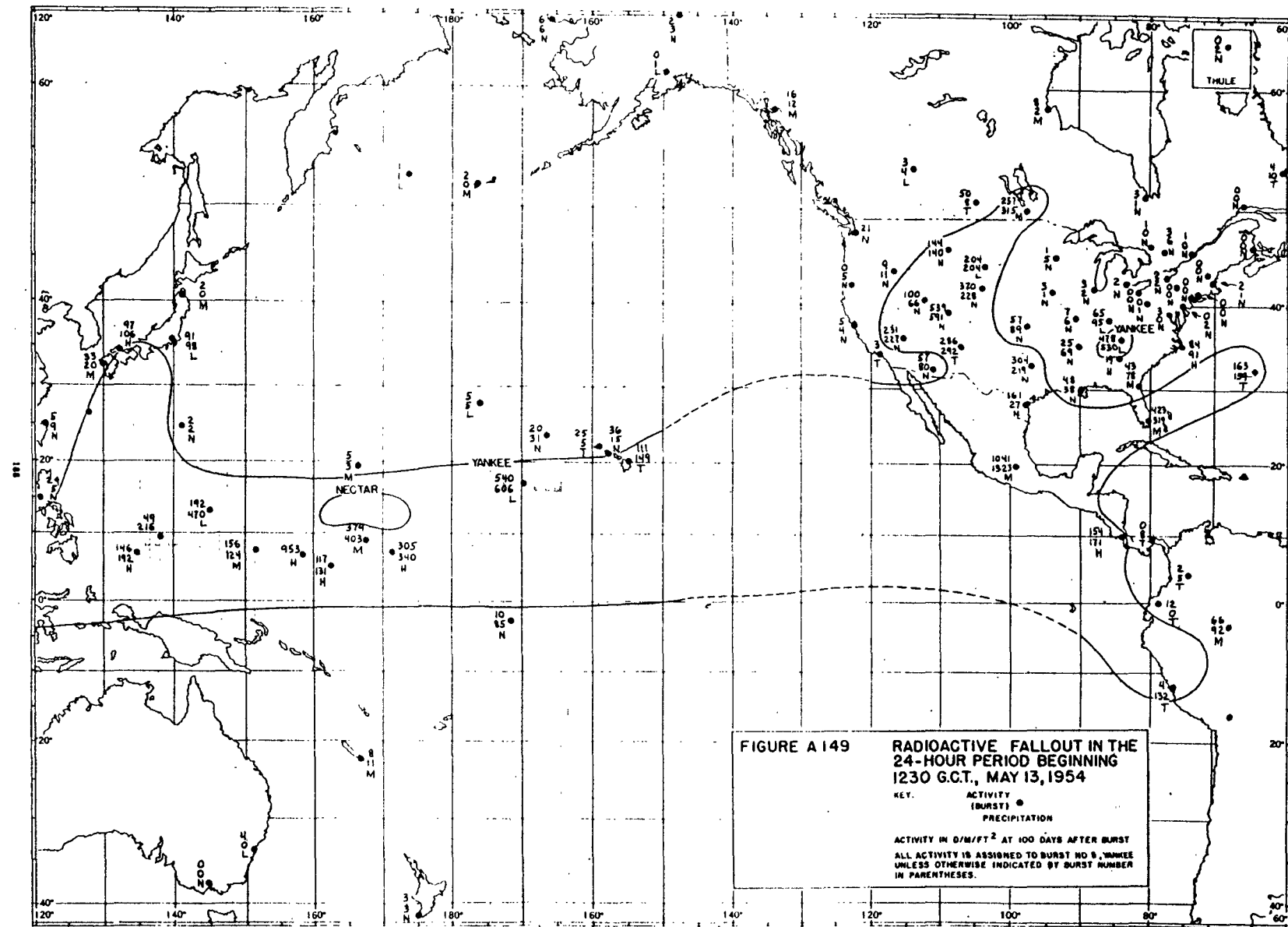
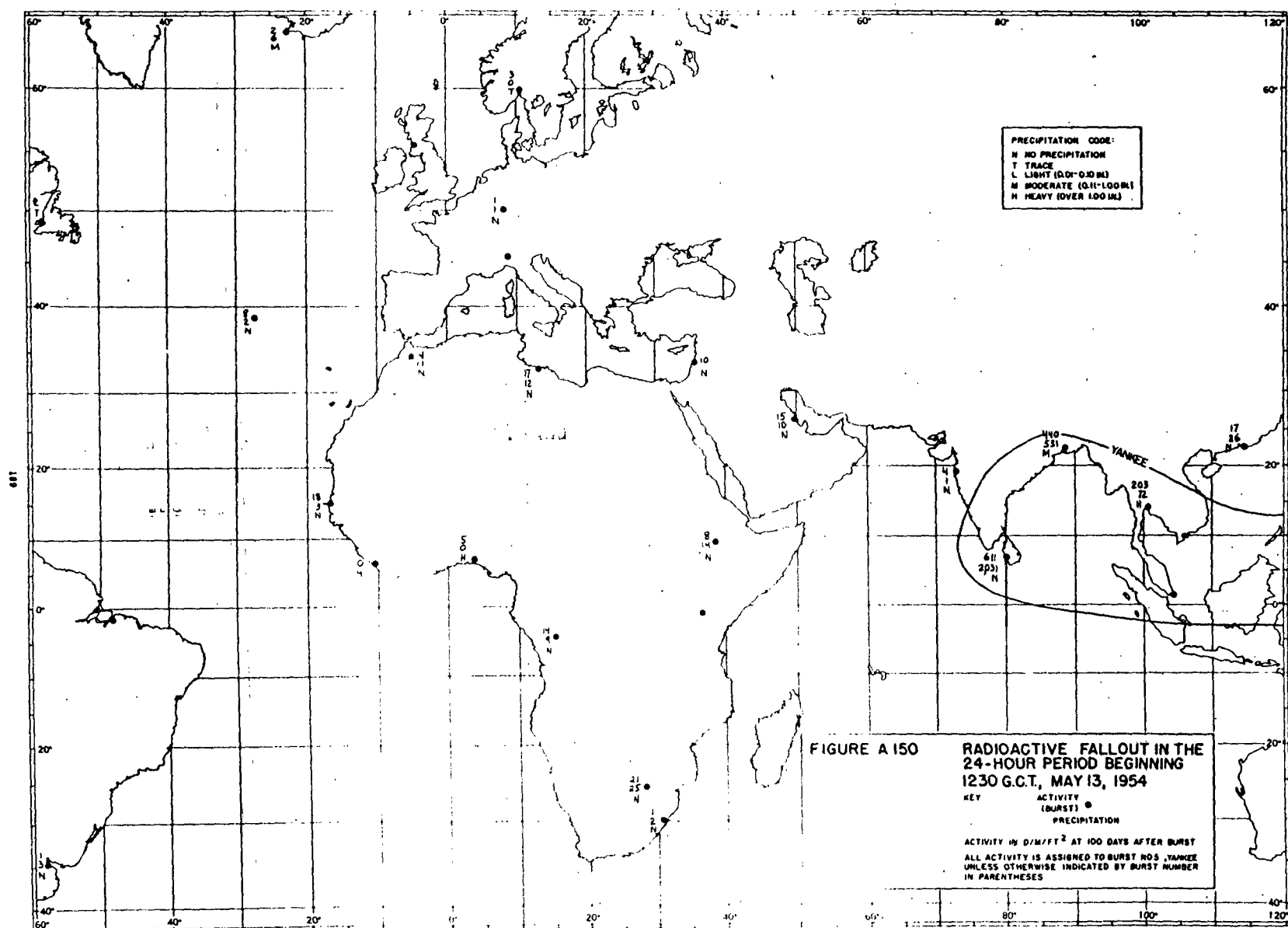


FIGURE A149 **RADIOACTIVE FALLOUT IN THE
24-HOUR PERIOD BEGINNING
1230 G.C.T., MAY 13, 1954**



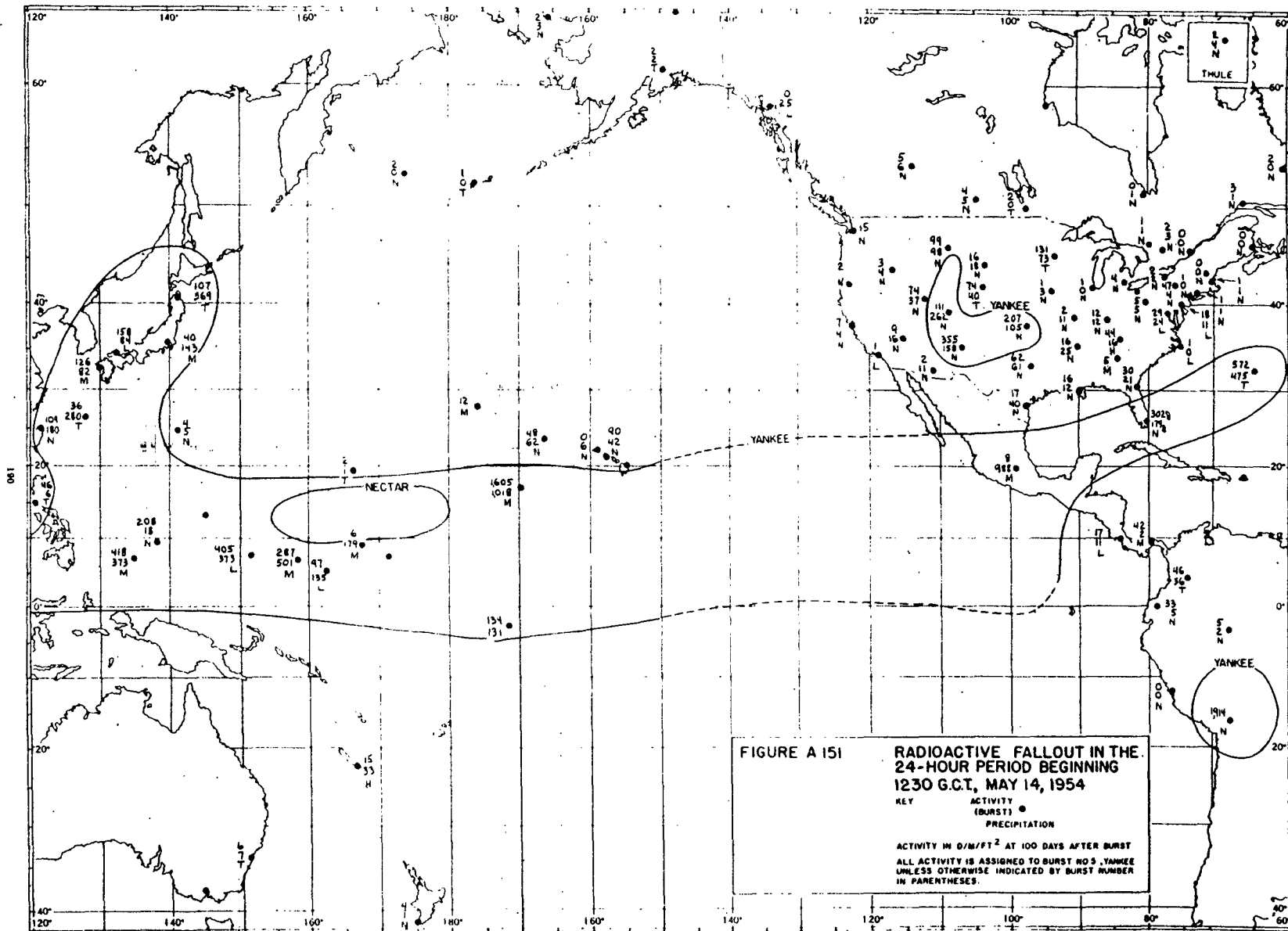
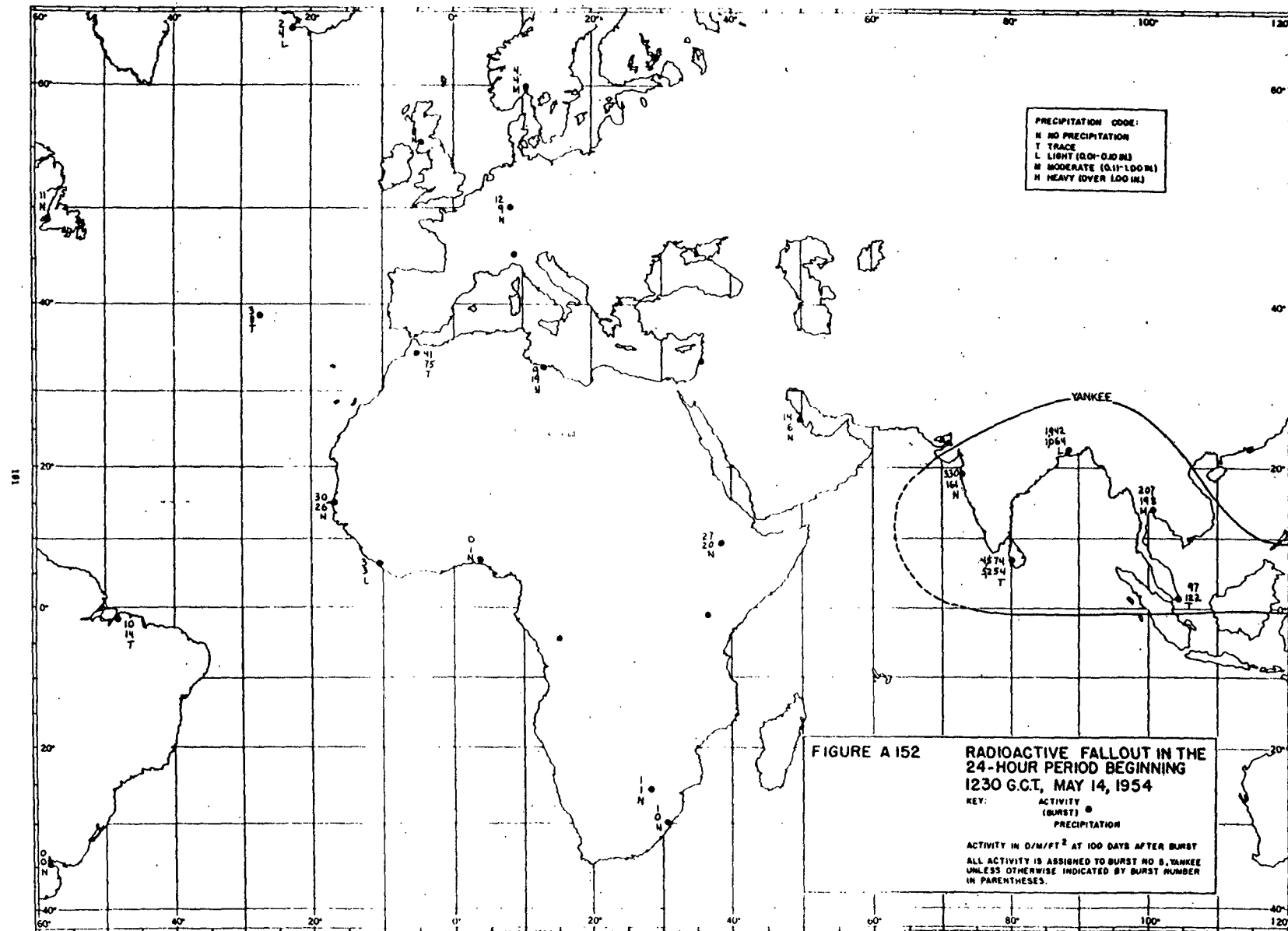
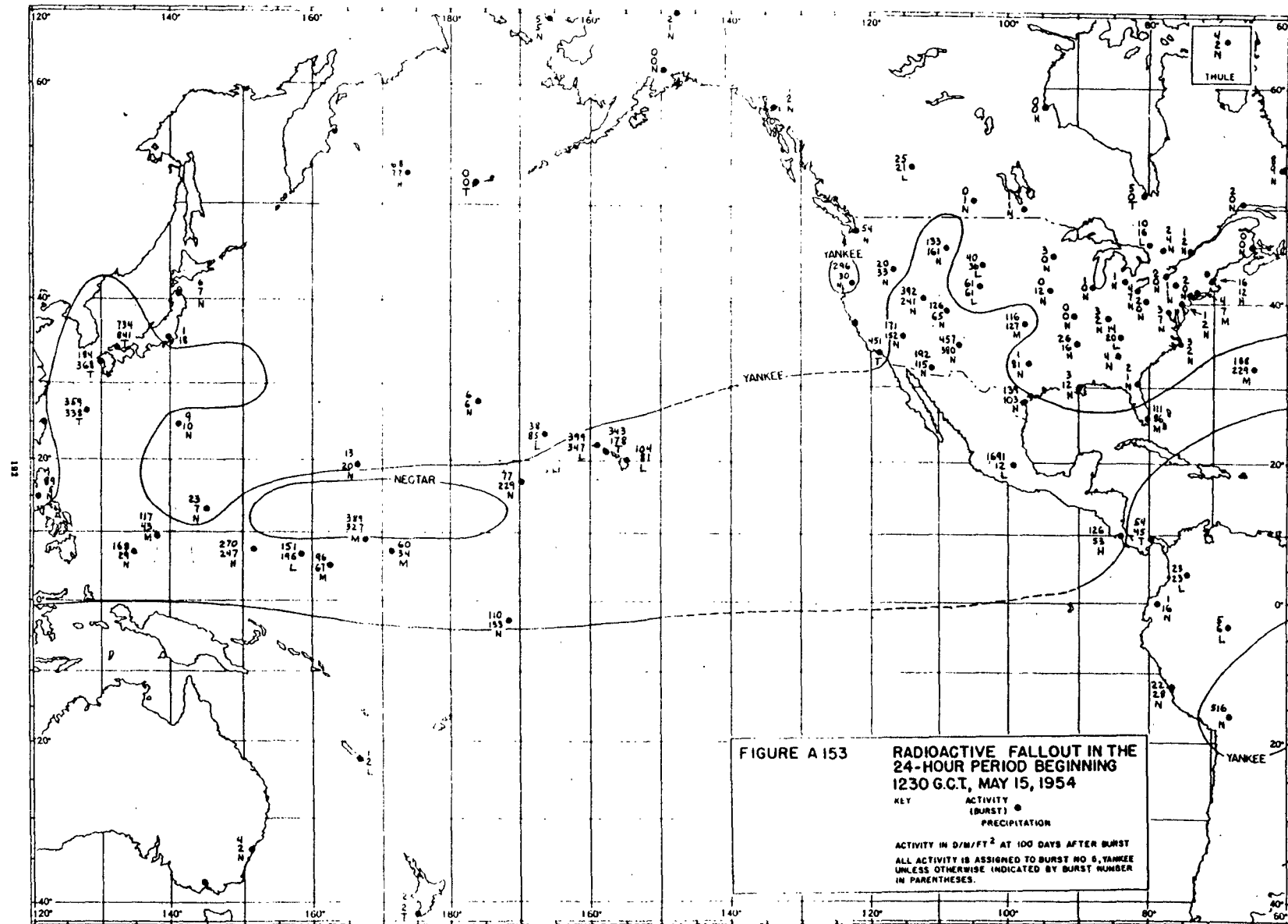


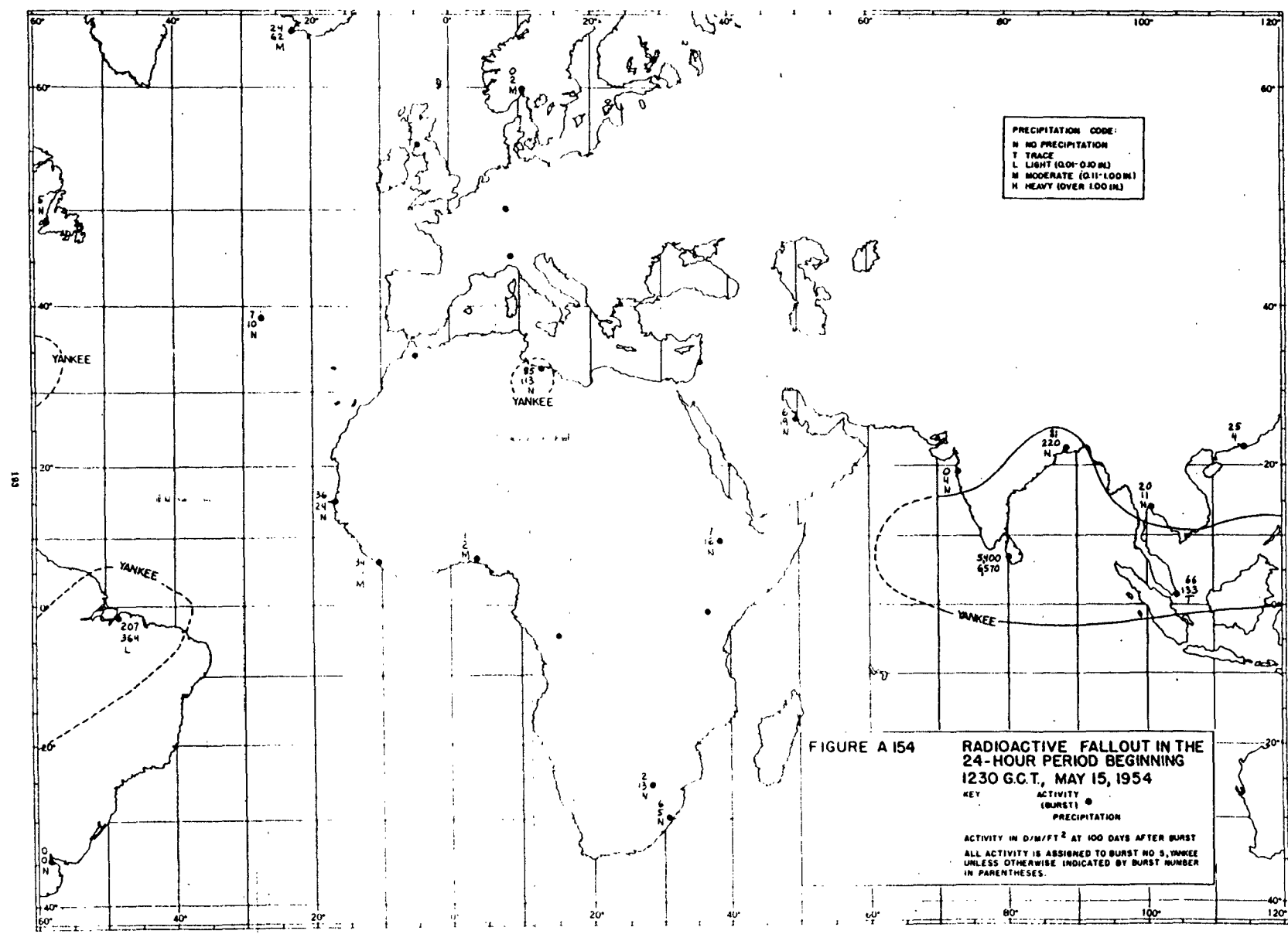
FIGURE A 151 RADIOACTIVE FALLOUT IN THE
24-HOUR PERIOD BEGINNING
1230 G.C.T., MAY 14, 1954

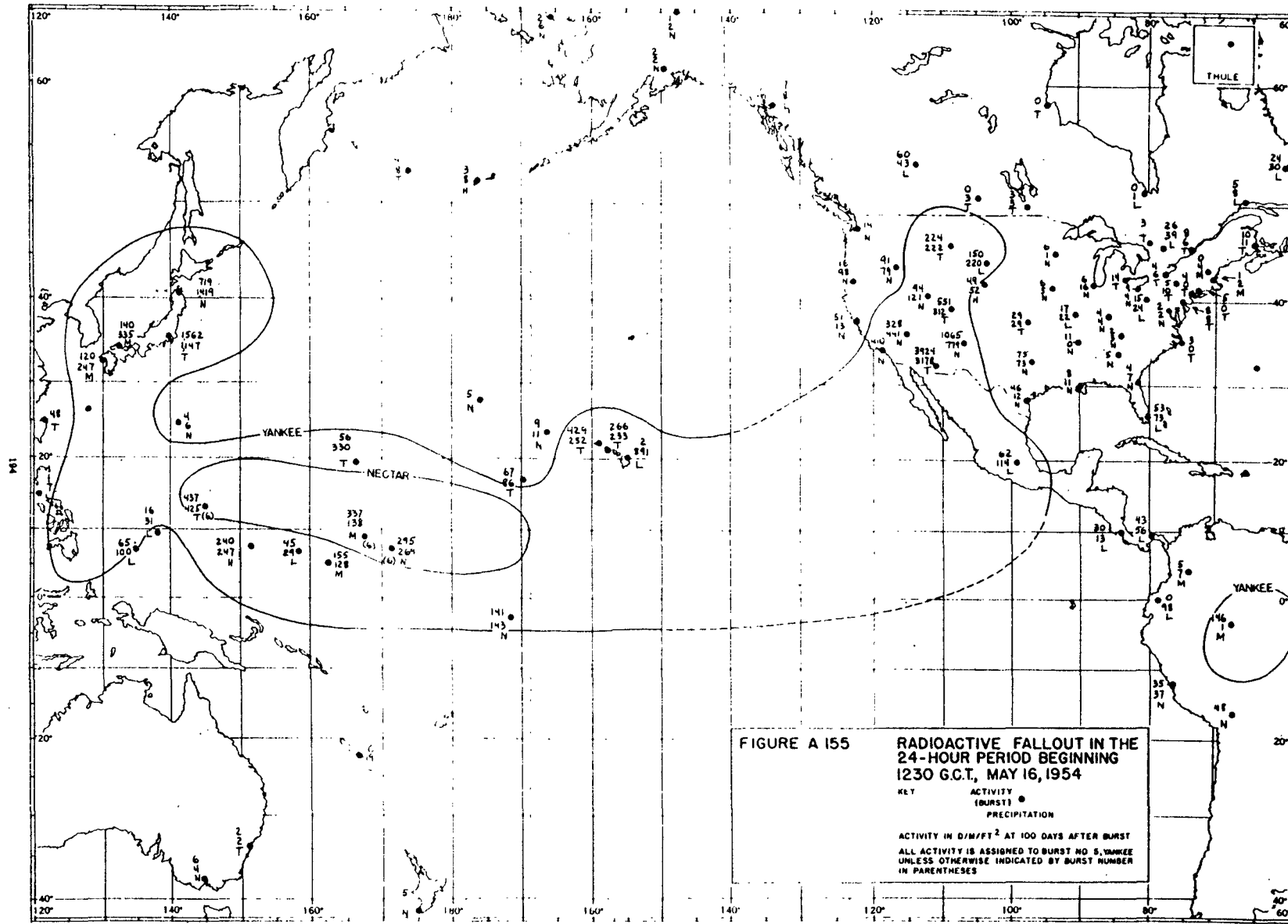
KEY ACTIVITY
(BURST) ●
PRECIPITATION

ACTIVITY IN $\mu\text{R}/\text{FT}^2$ AT 100 DAYS AFTER BURST
ALL ACTIVITY IS ASSIGNED TO BURST NO. YANKEE
UNLESS OTHERWISE INDICATED BY BURST NUMBER
IN PARENTHESES.









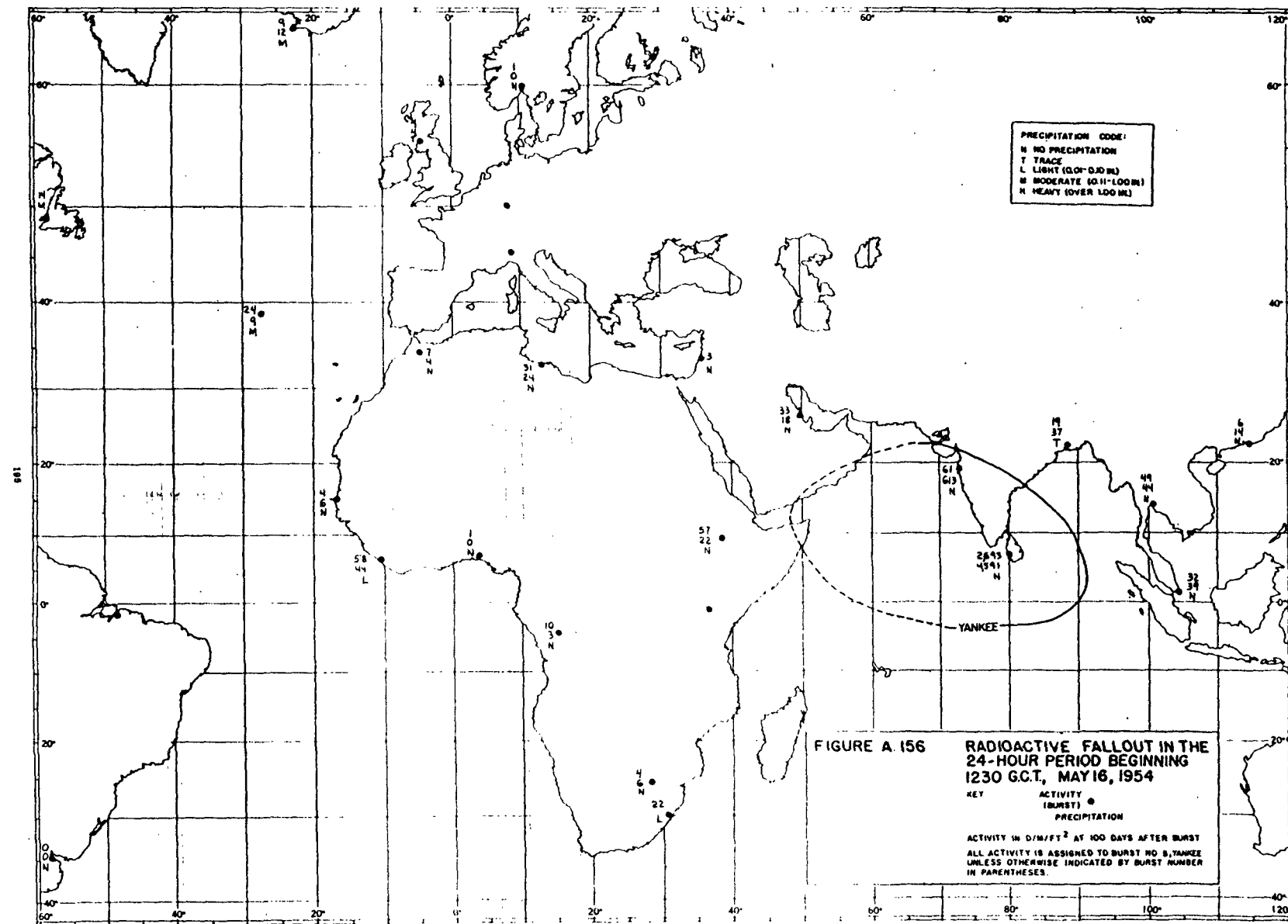
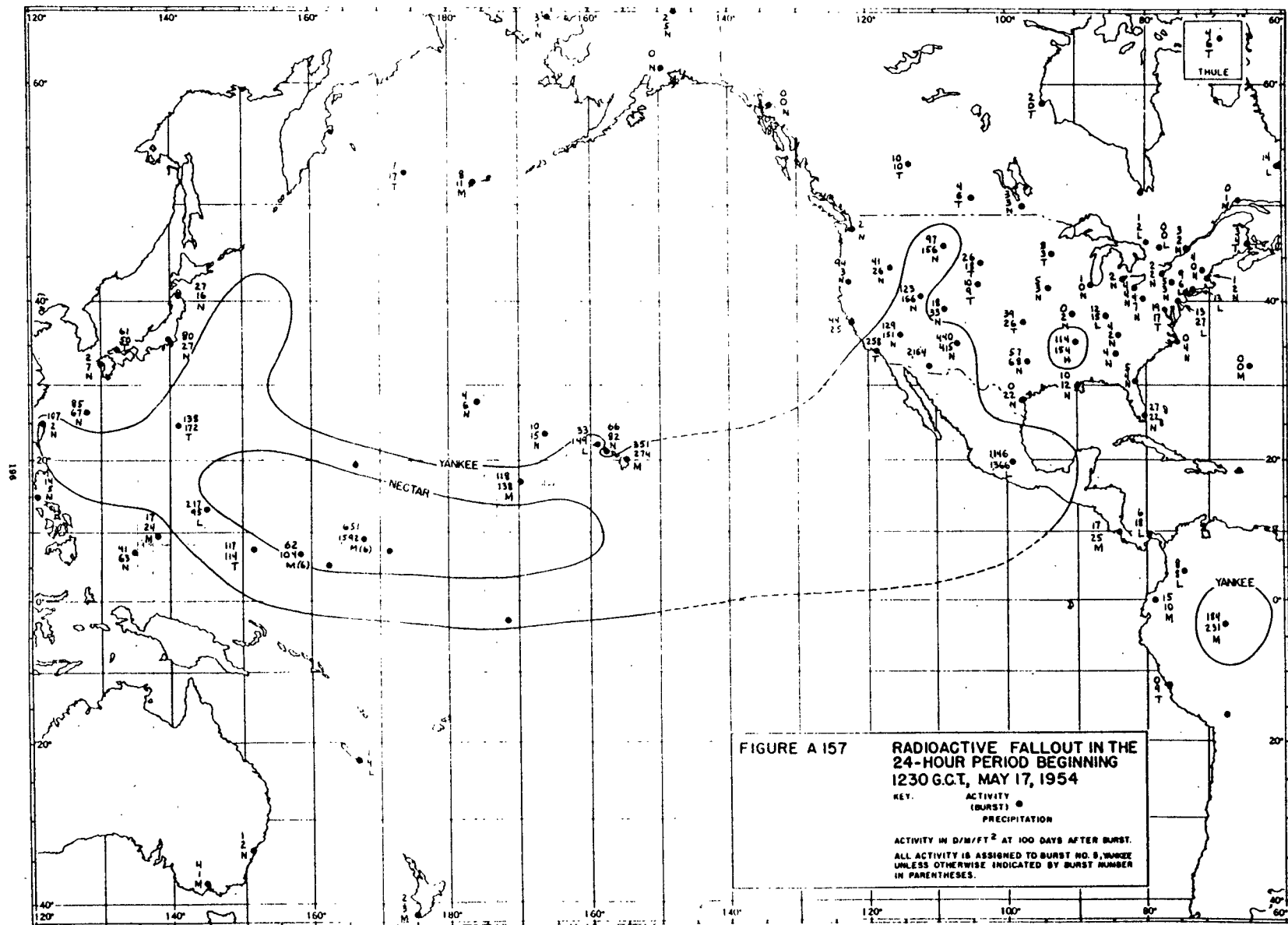


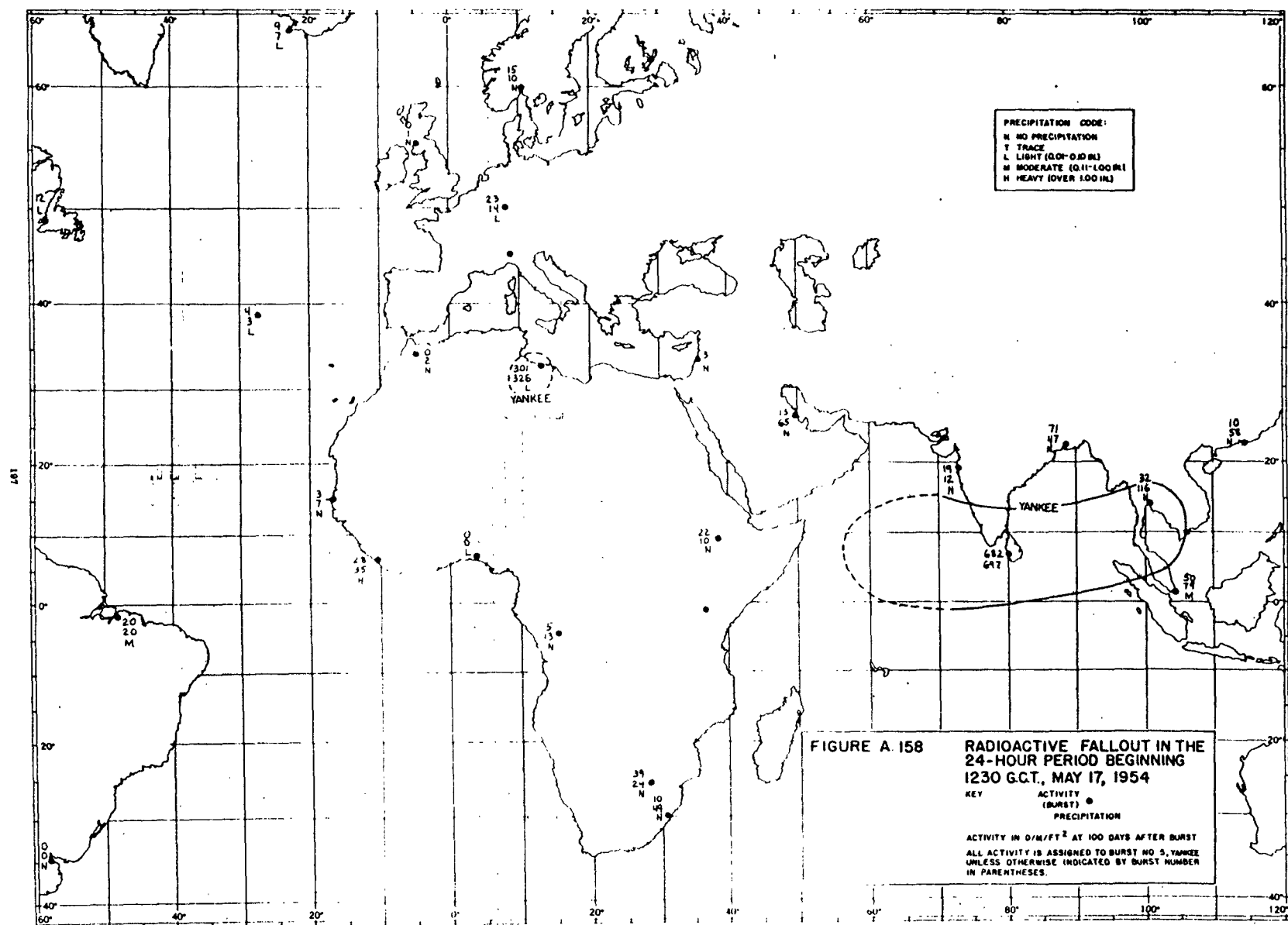
FIGURE A.156

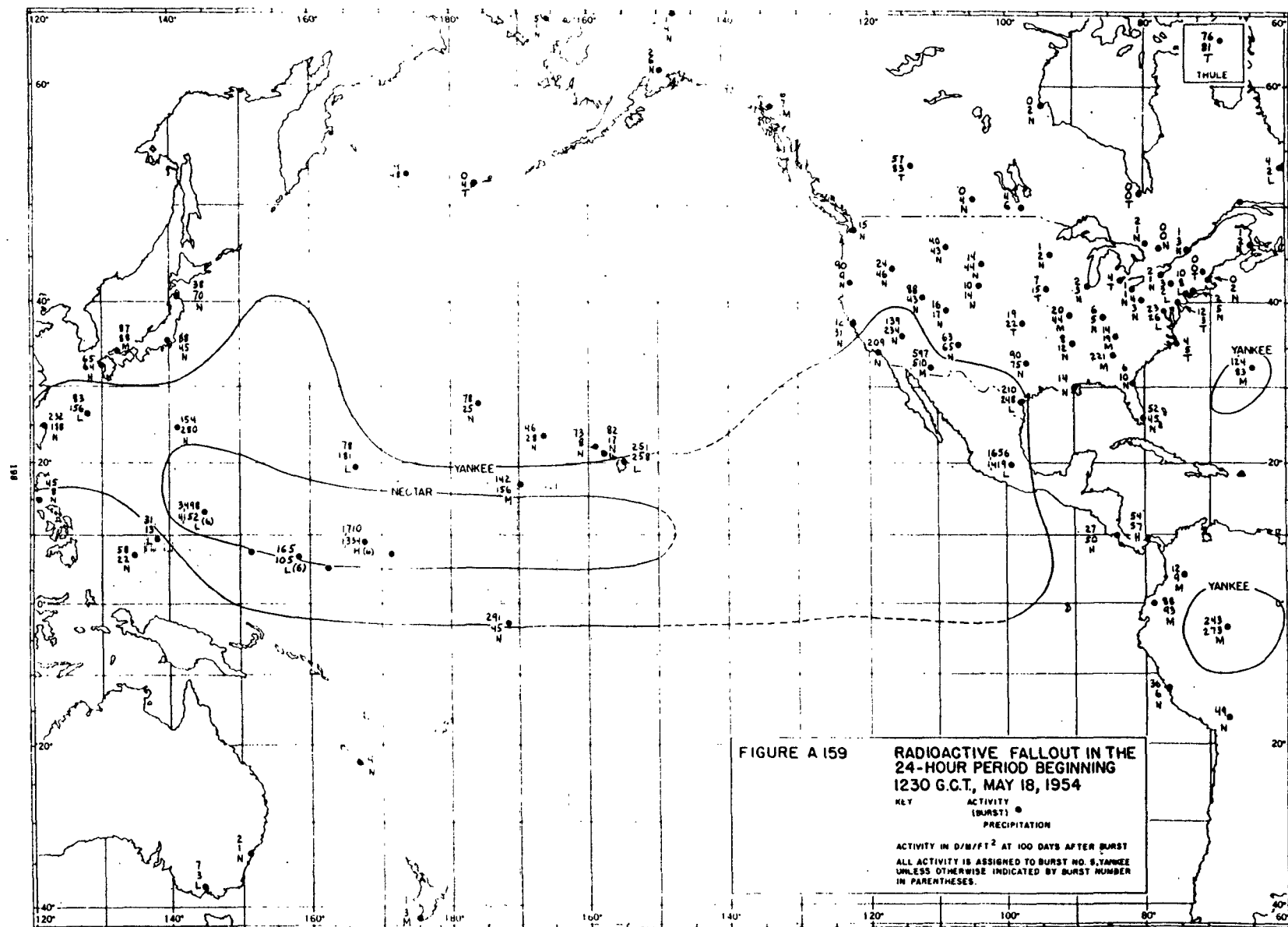
RADIOACTIVE FALLOUT IN THE
24-HOUR PERIOD BEGINNING
1230 G.C.T., MAY 16, 1954

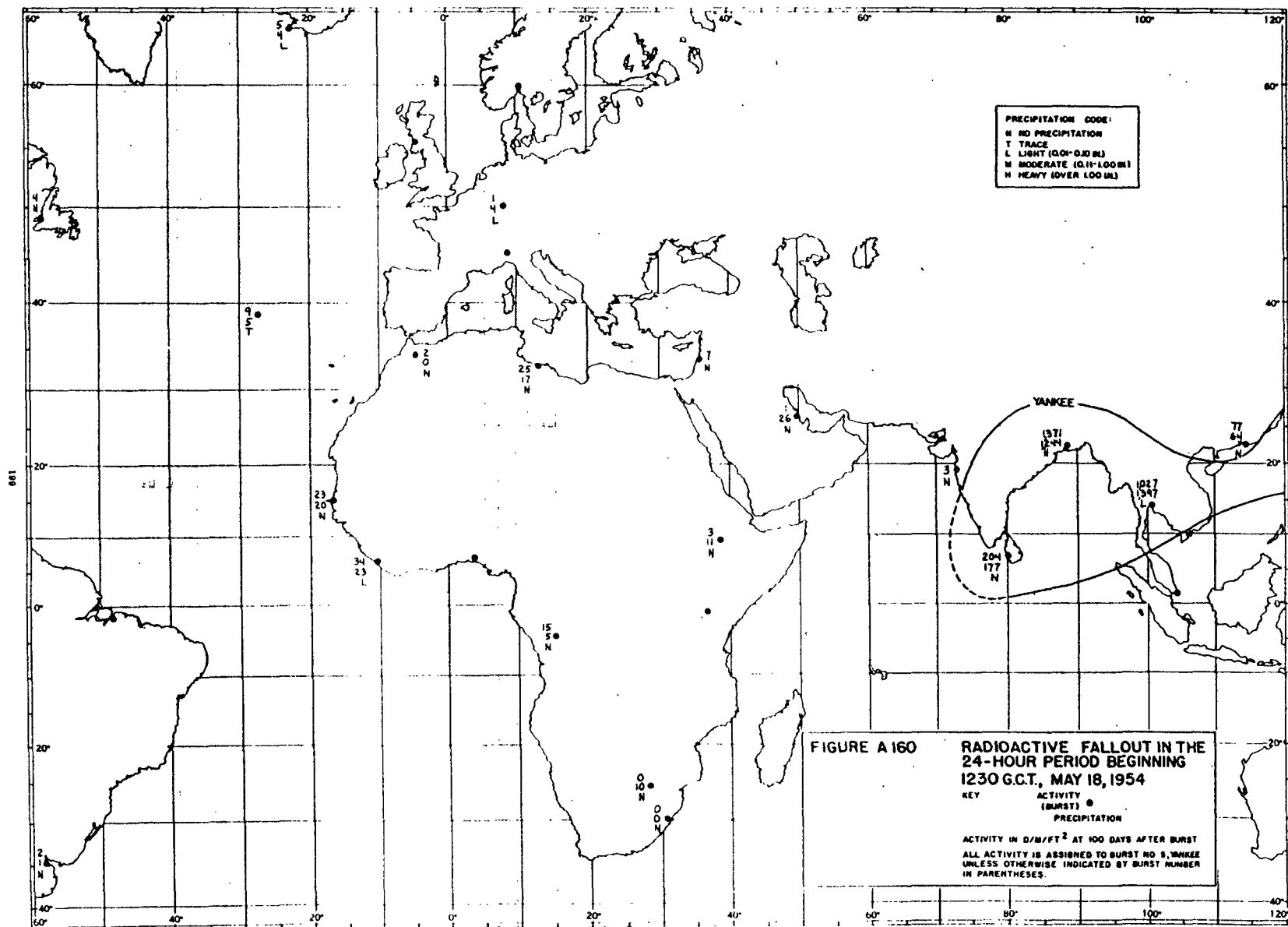
KEY ACTIVITY (BURST) ●
PRECIPITATION

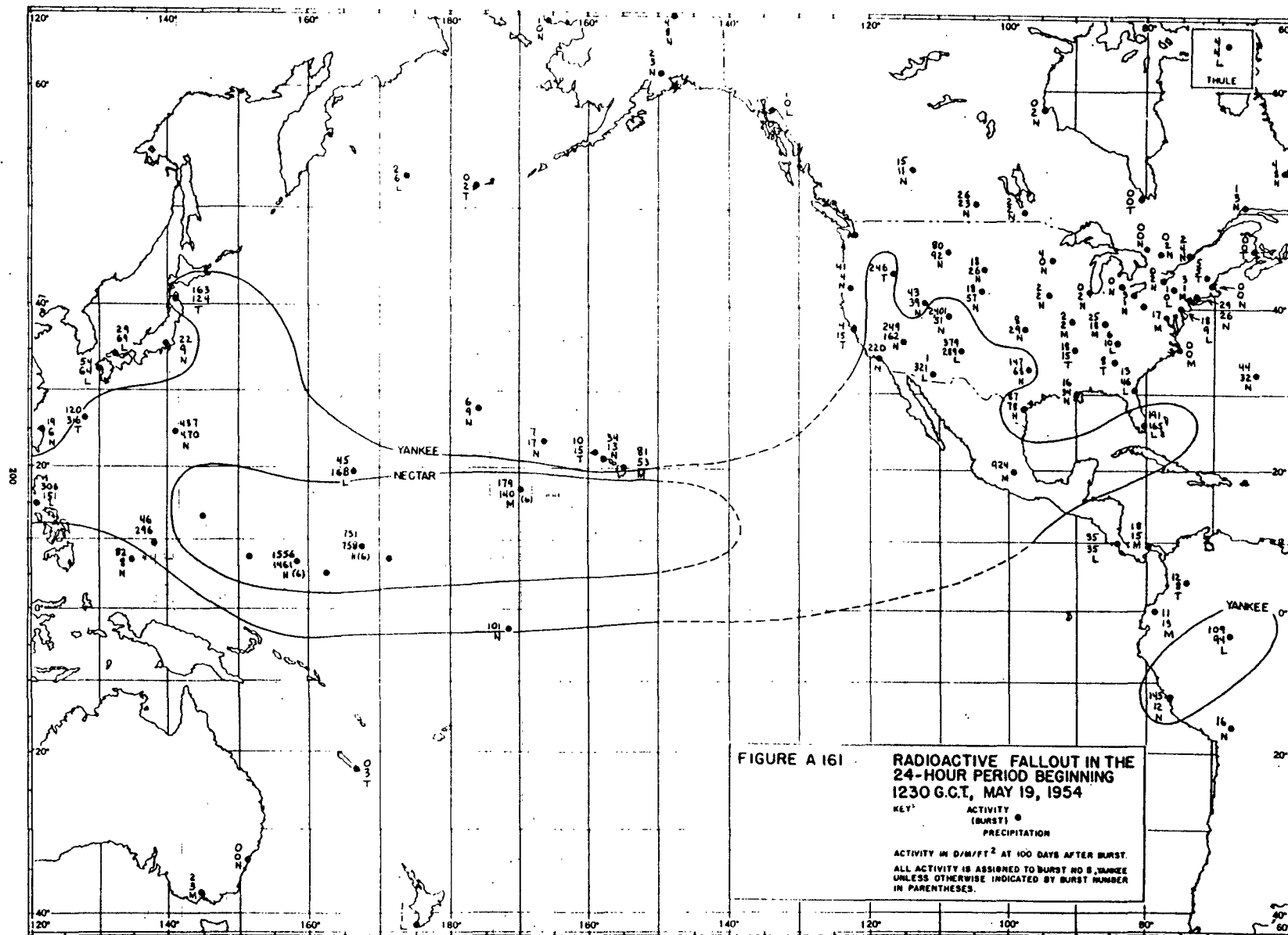
ACTIVITY IN D/M² AT 100 DAYS AFTER BURST
ALL ACTIVITY IS ASSIGNED TO BURST NO. 8, YANKEE
UNLESS OTHERWISE INDICATED BY BURST NUMBER
IN PARENTHESES.

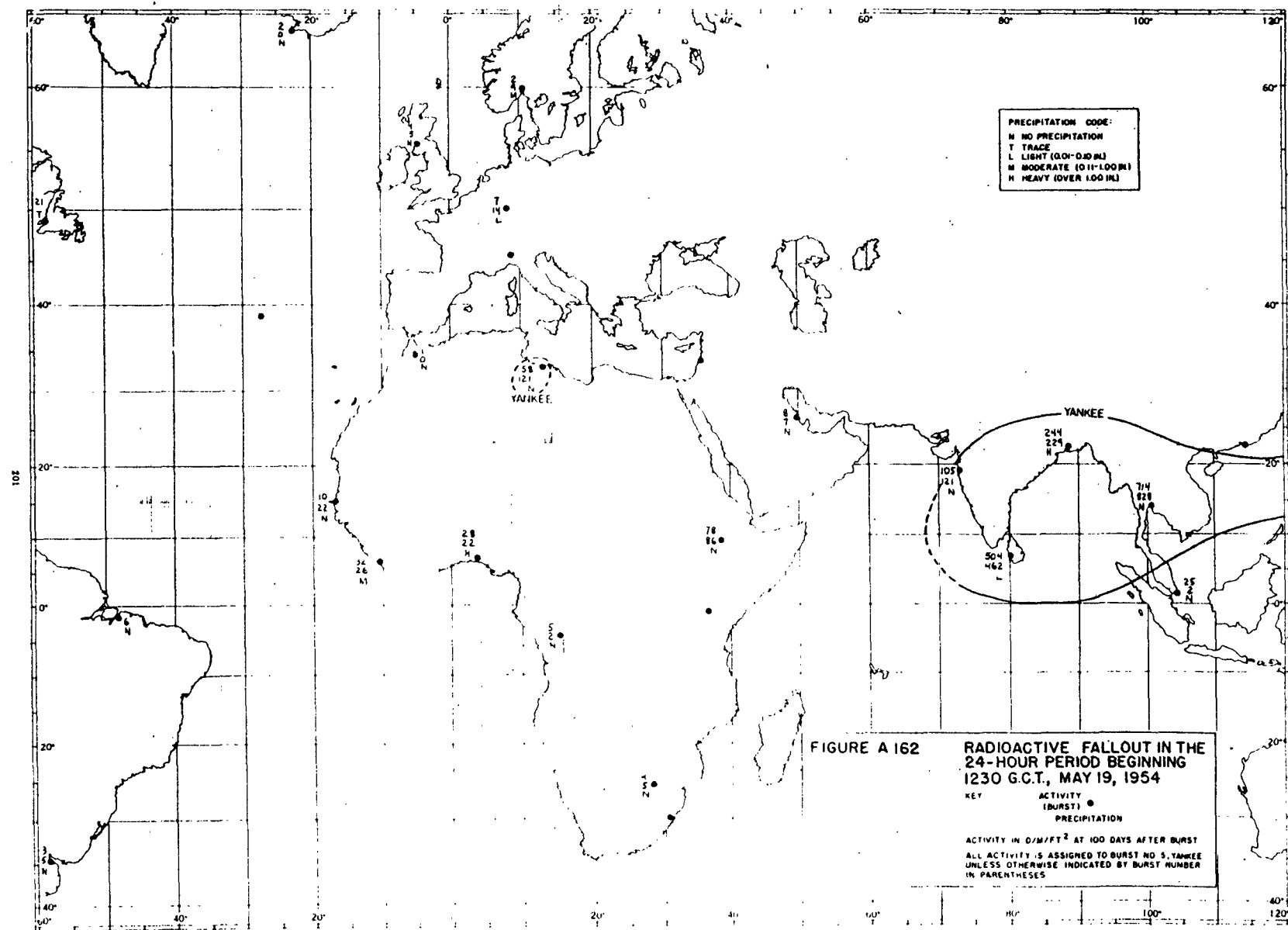












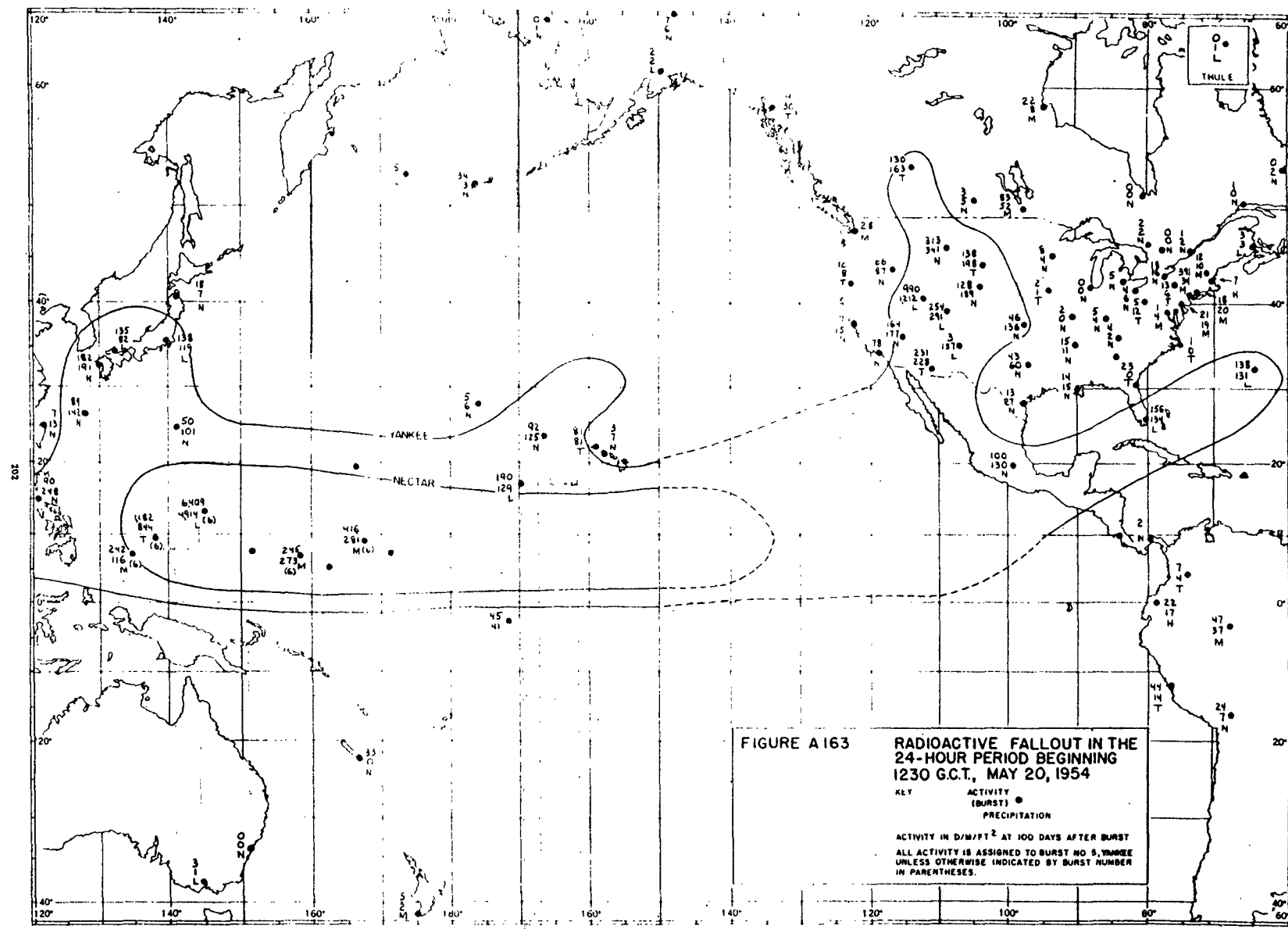
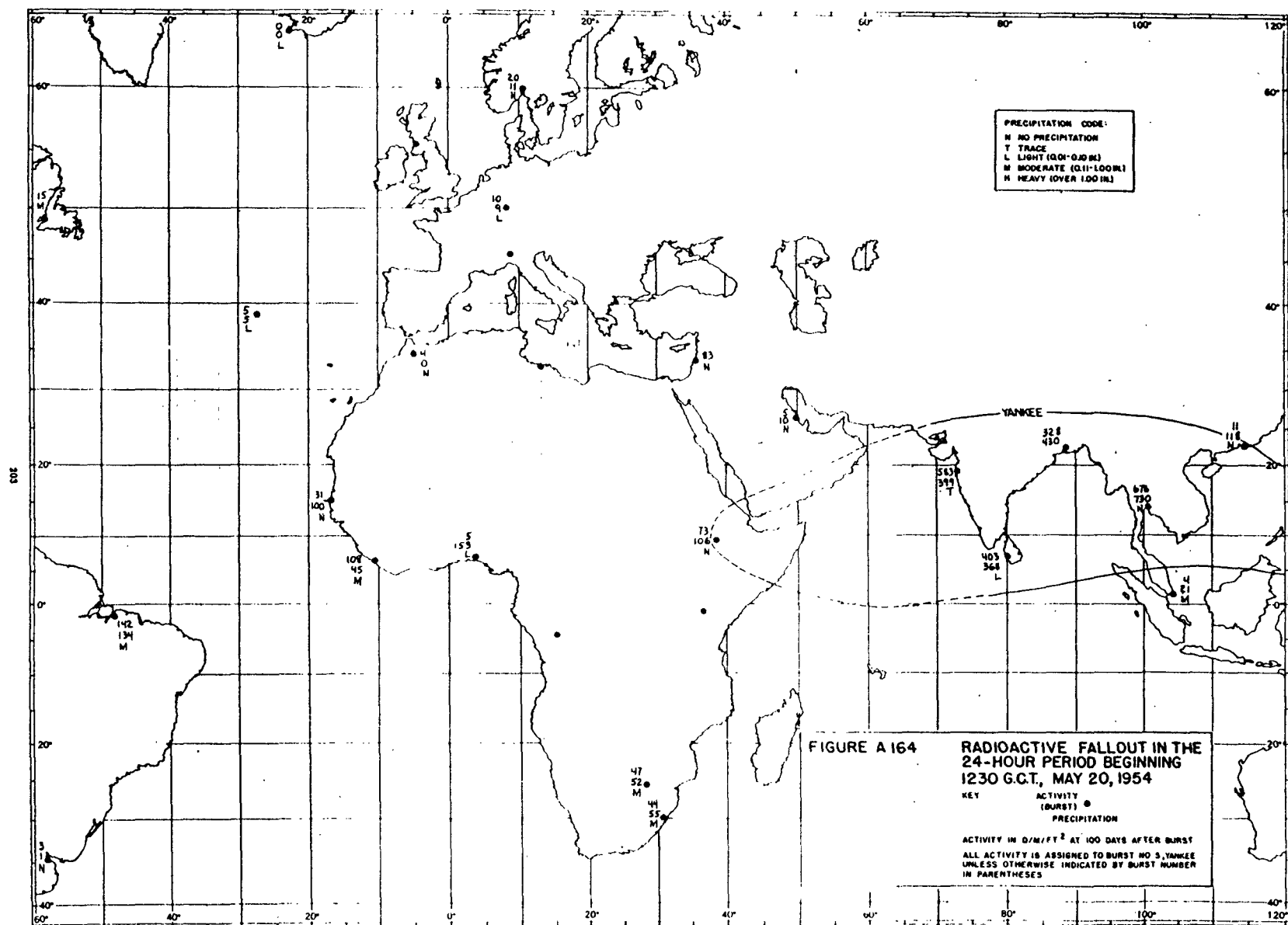


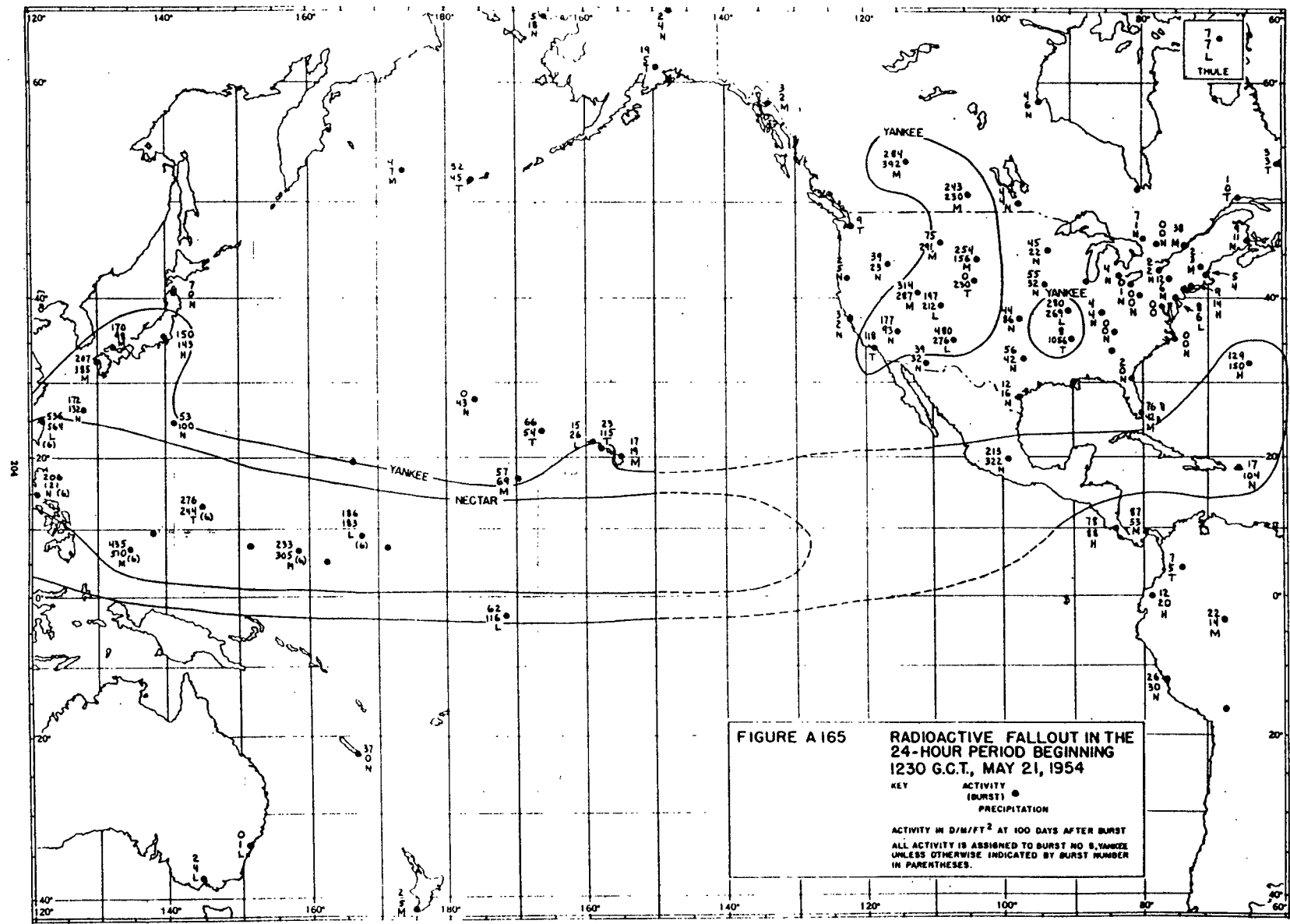
FIGURE A163

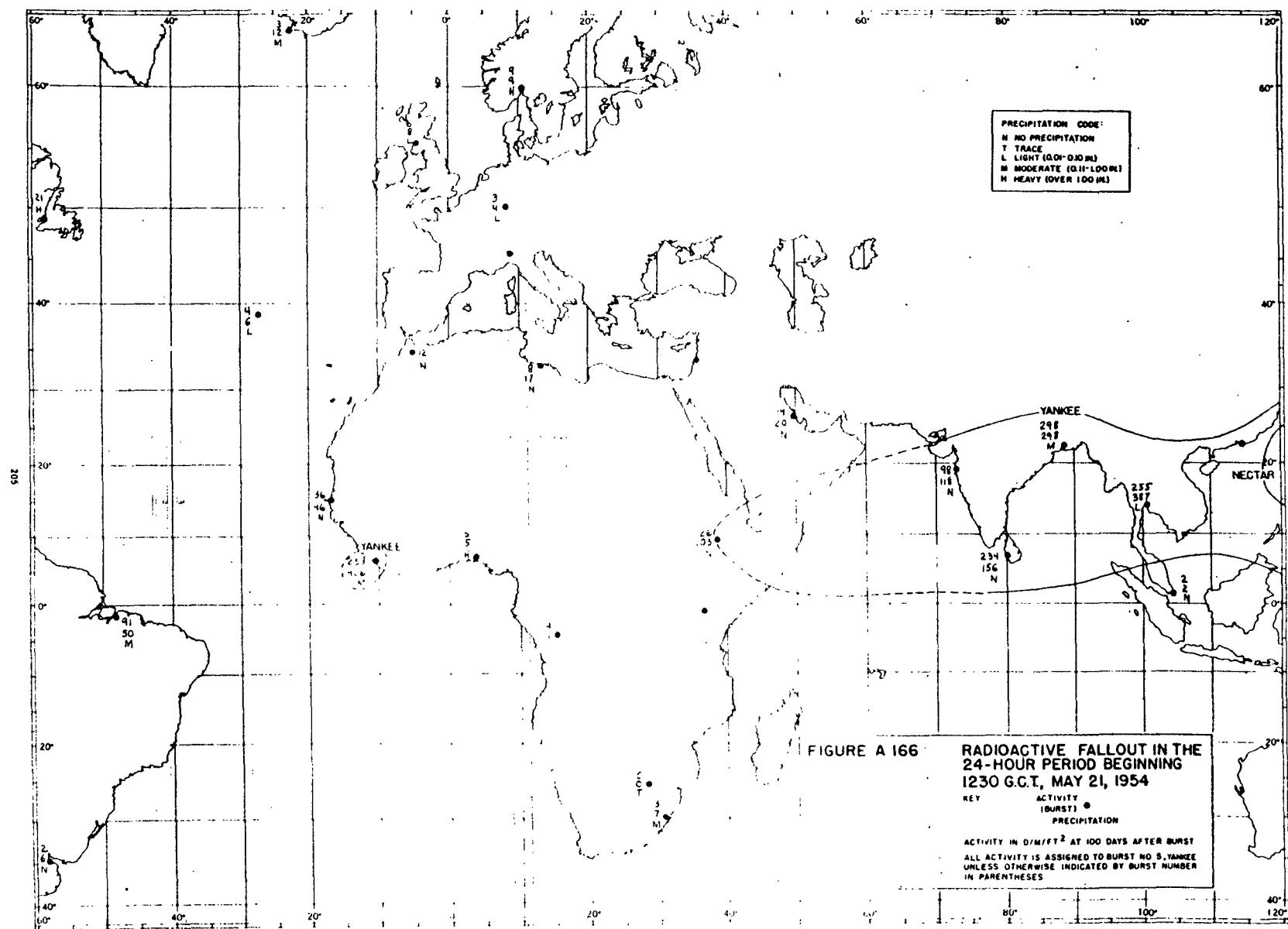
RADIOACTIVE FALLOUT IN THE
24-HOUR PERIOD BEGINNING
1230 G.C.T., MAY 20, 1954

KEY ACTIVITY (BURST) PRECIPITATION

ACTIVITY IN D/M²/FT² AT 100 DAYS AFTER BURST
ALL ACTIVITY IS ASSIGNED TO BURST NO 3, YANKEE
UNLESS OTHERWISE INDICATED BY BURST NUMBER
IN PARENTHESES.







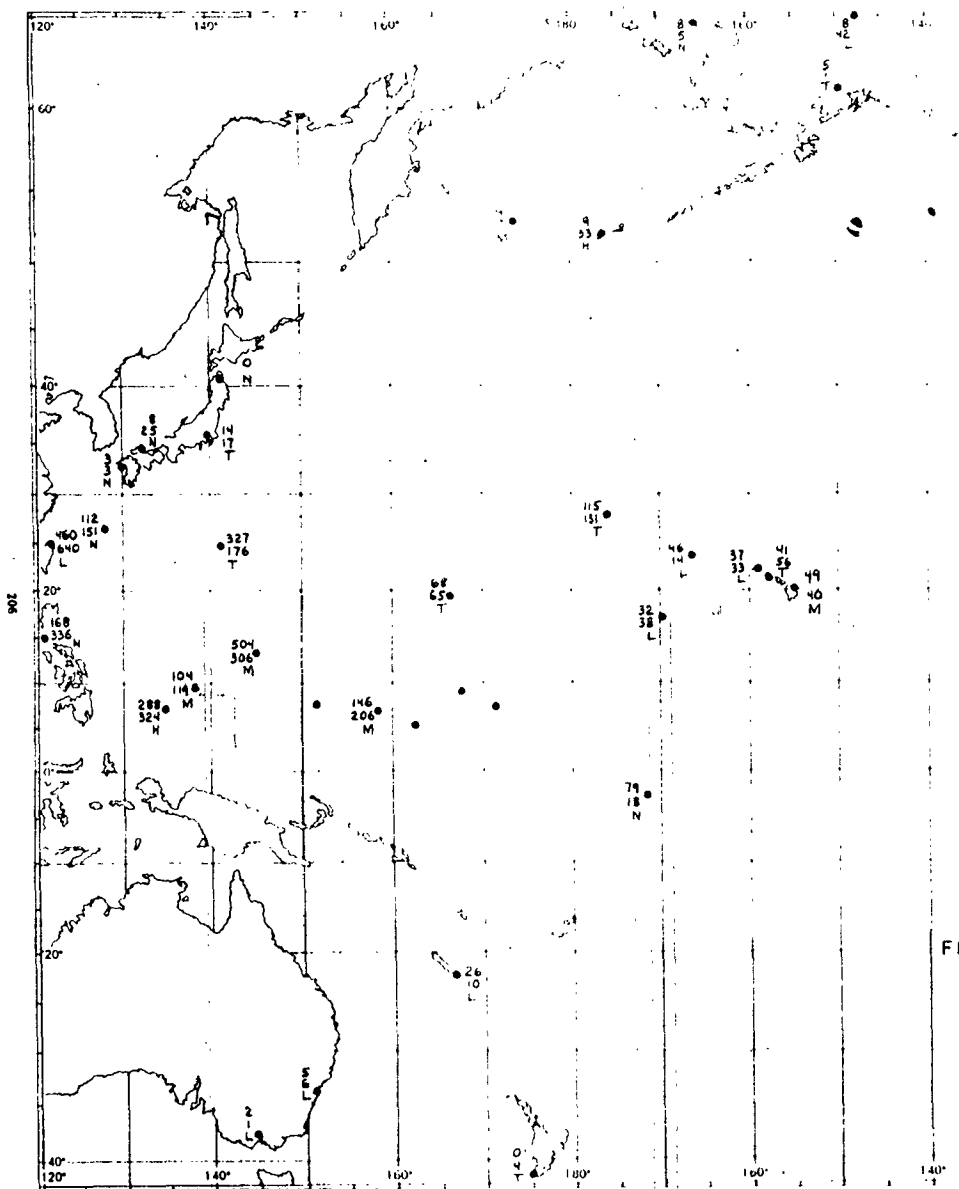
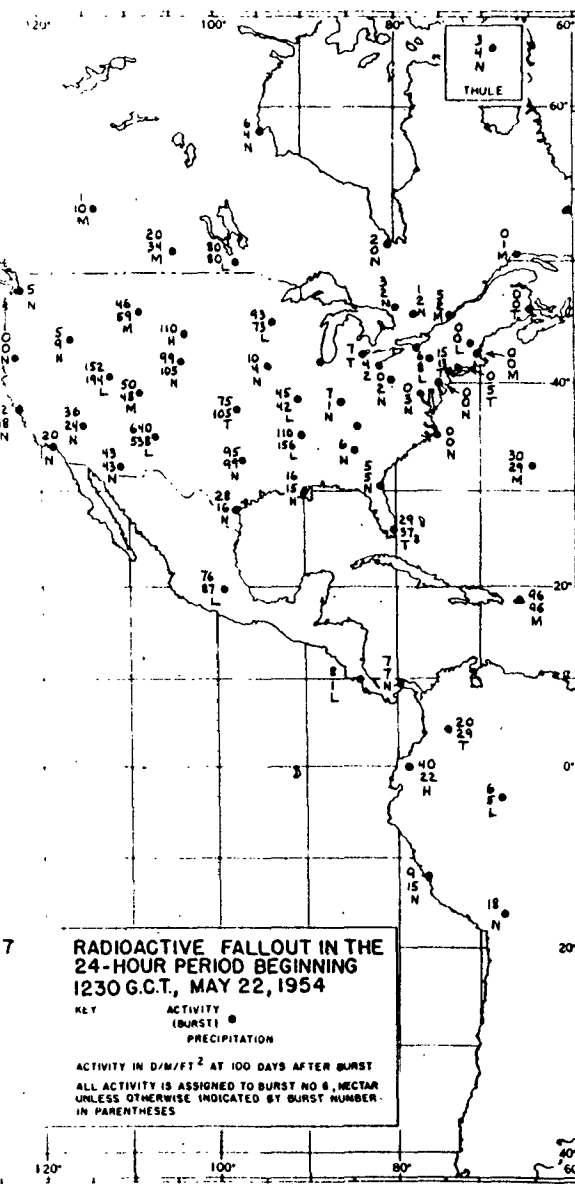
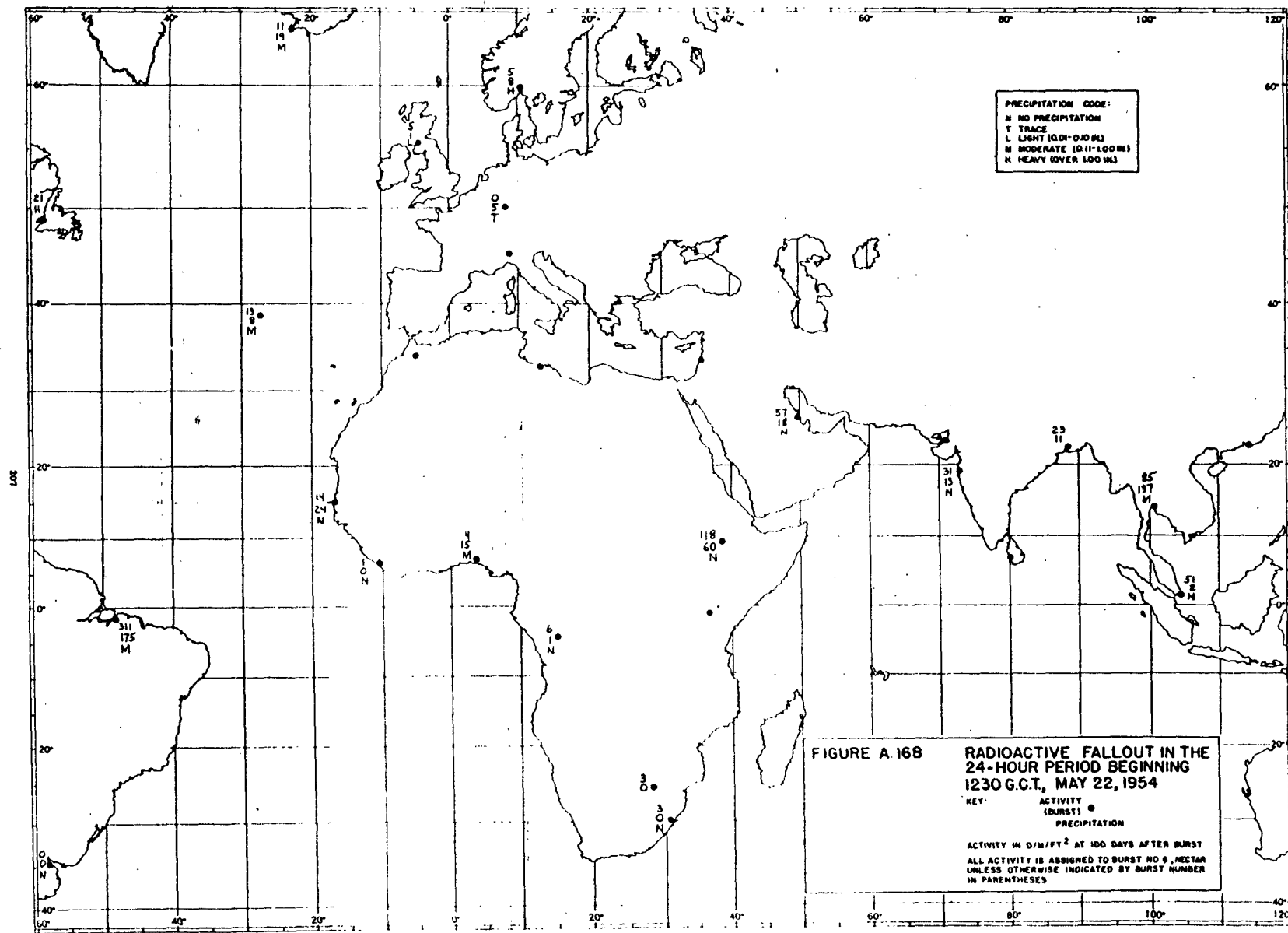
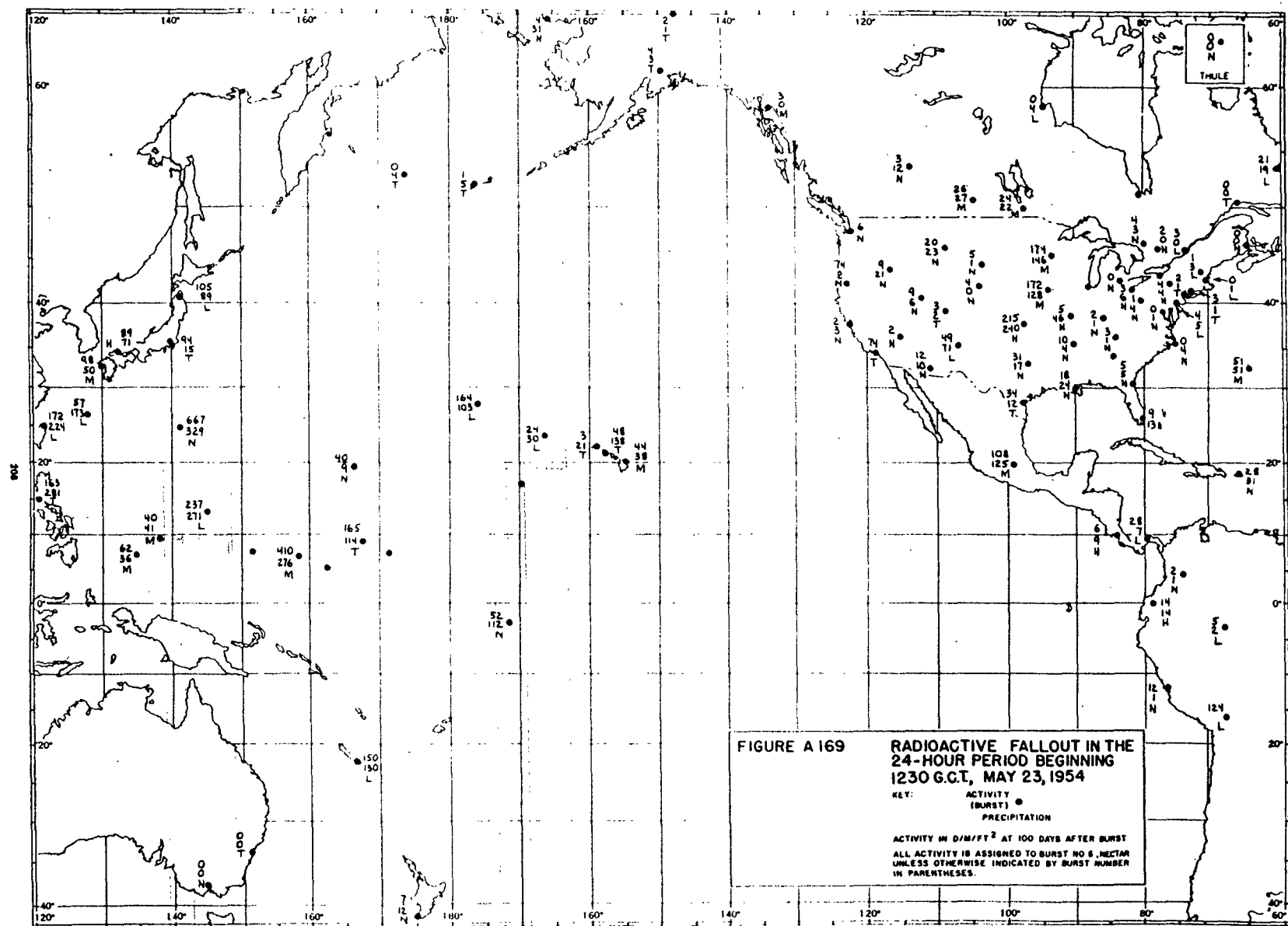


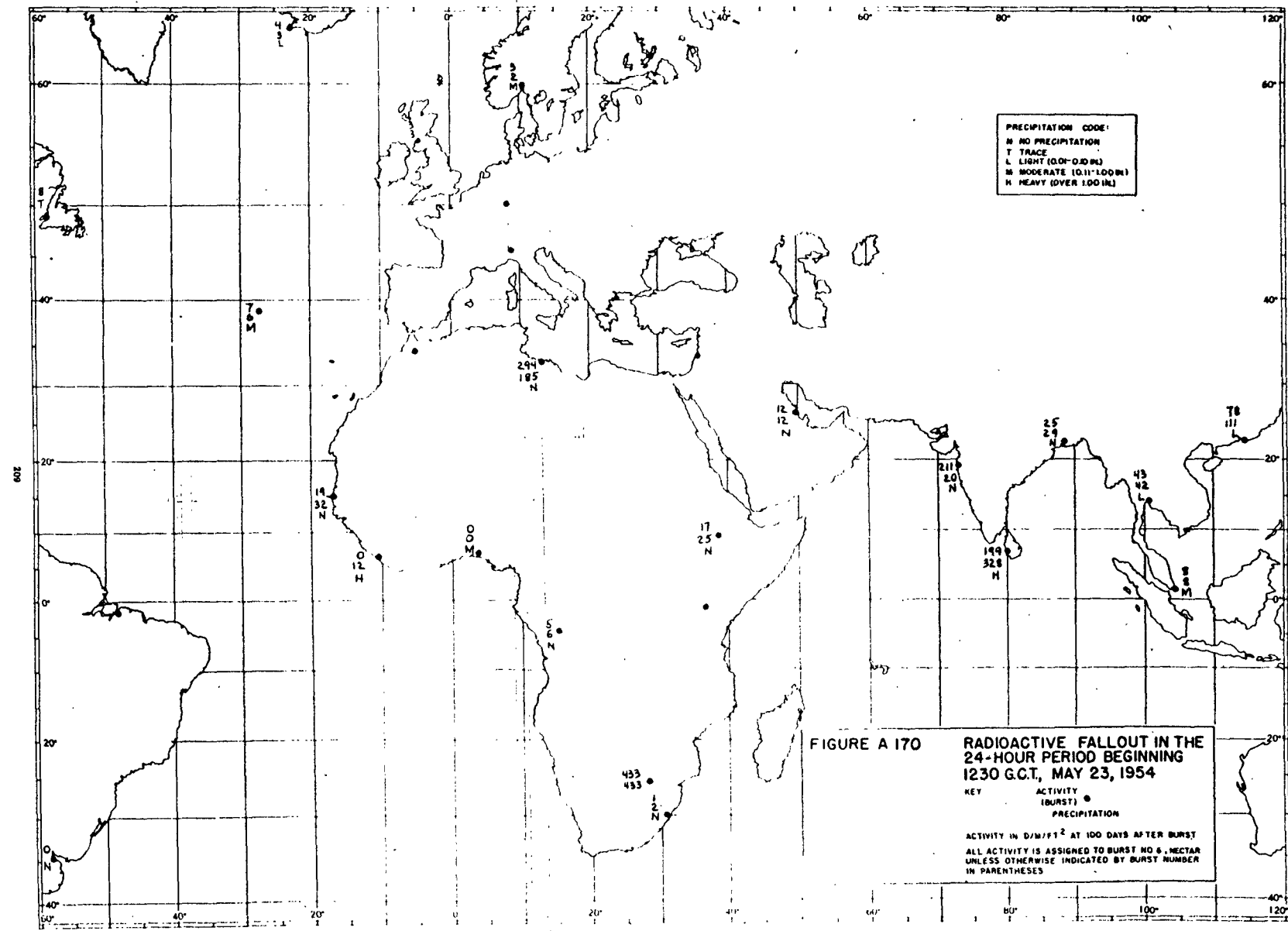
FIGURE A167

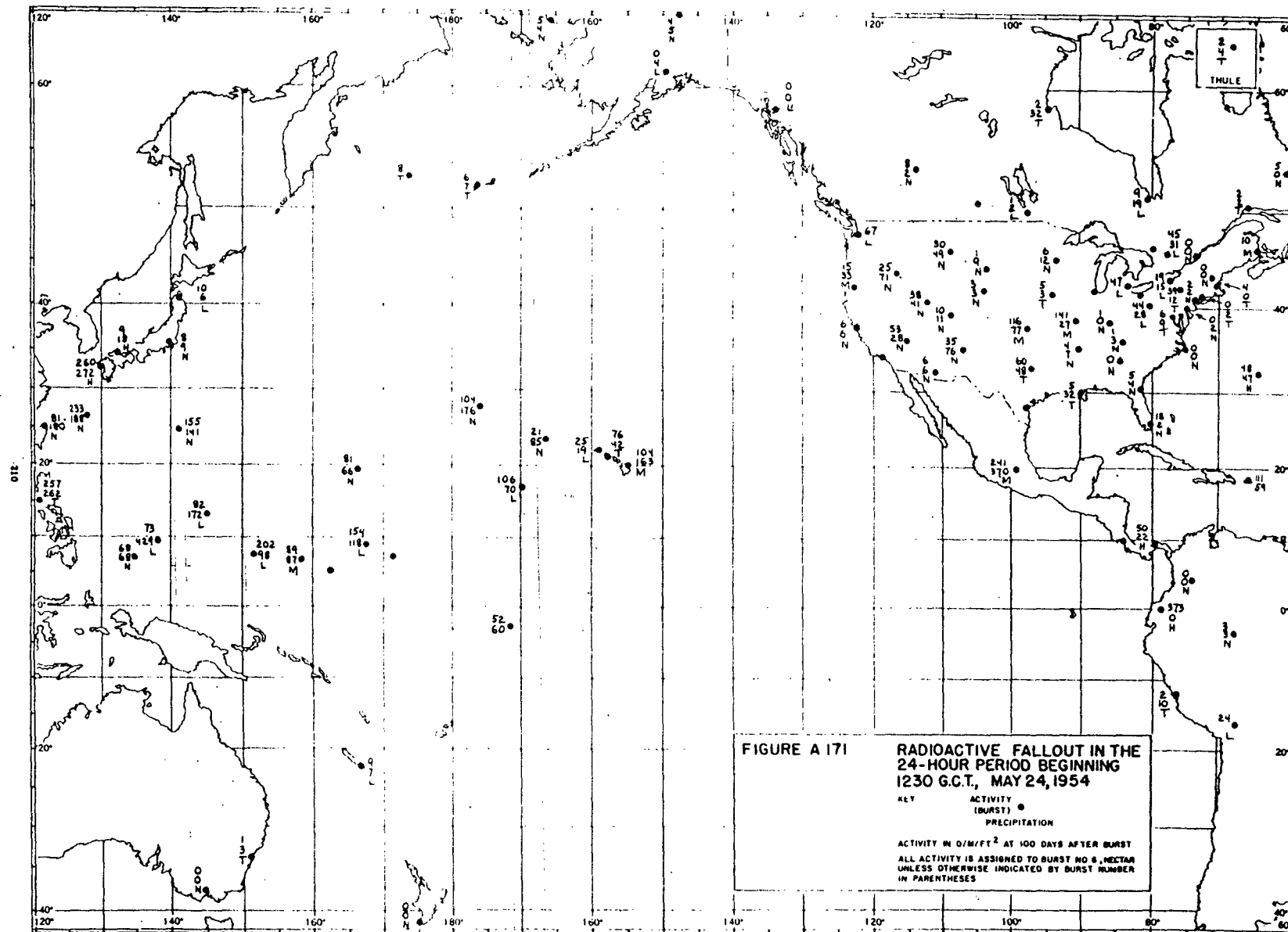


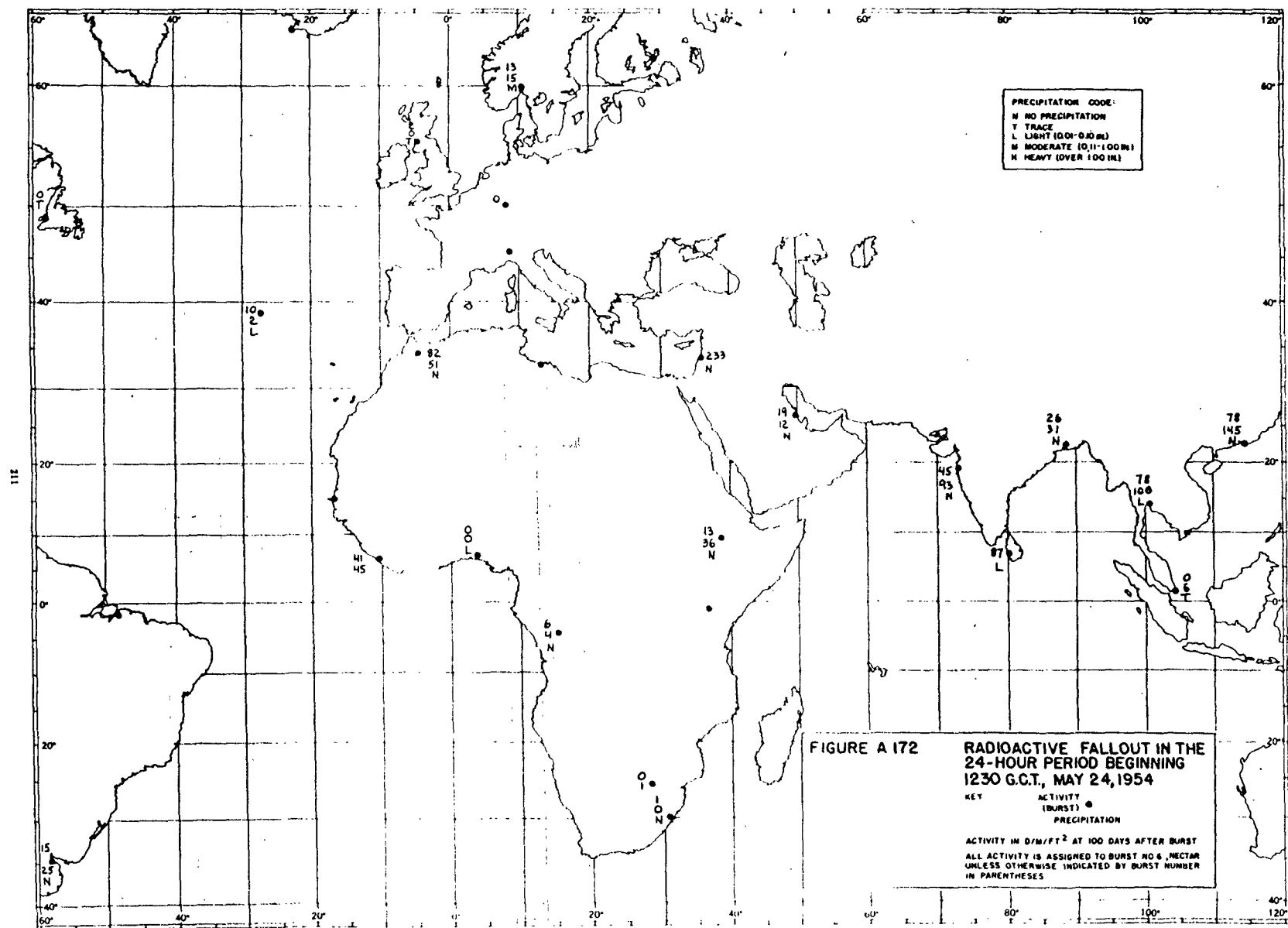


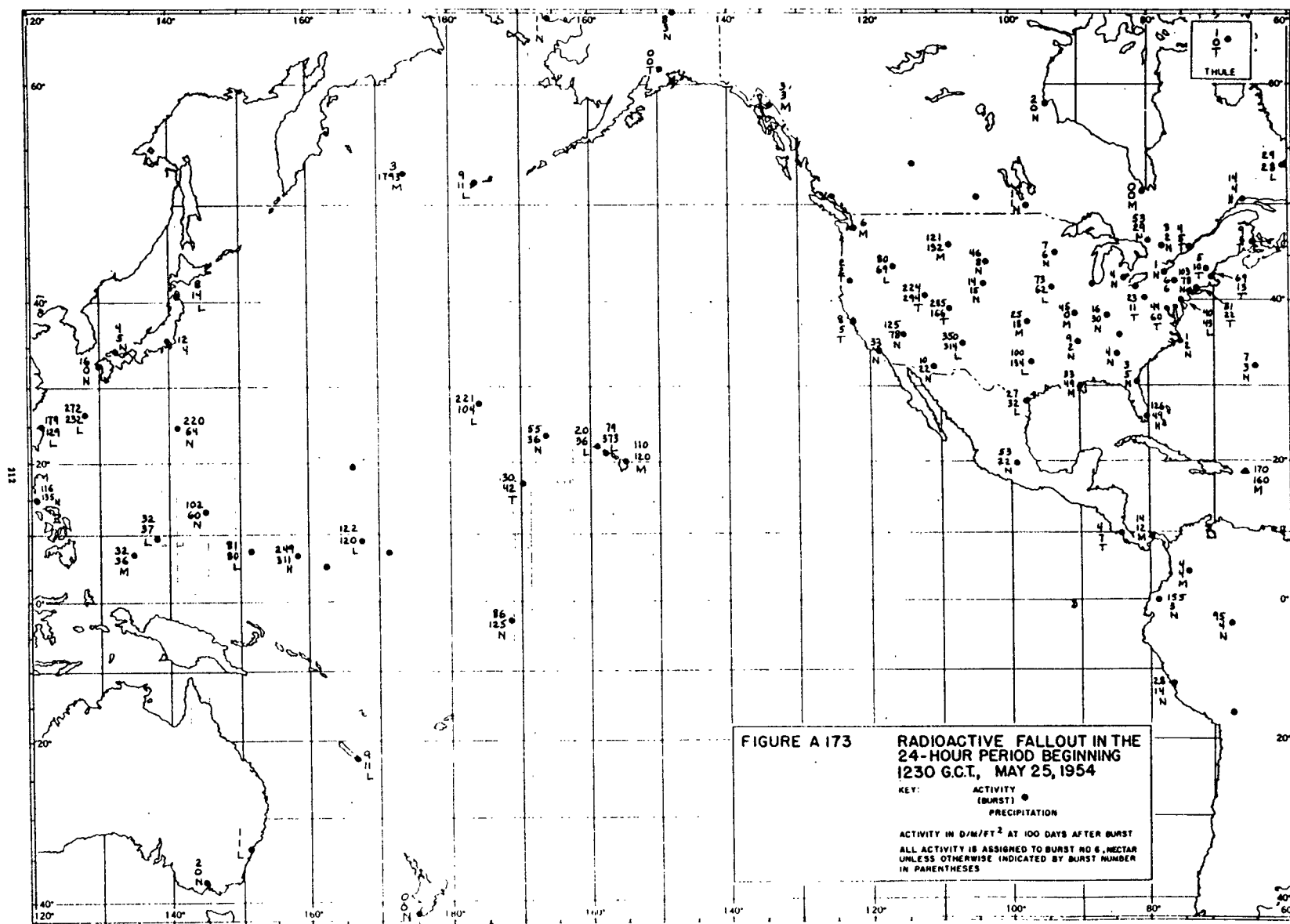
3

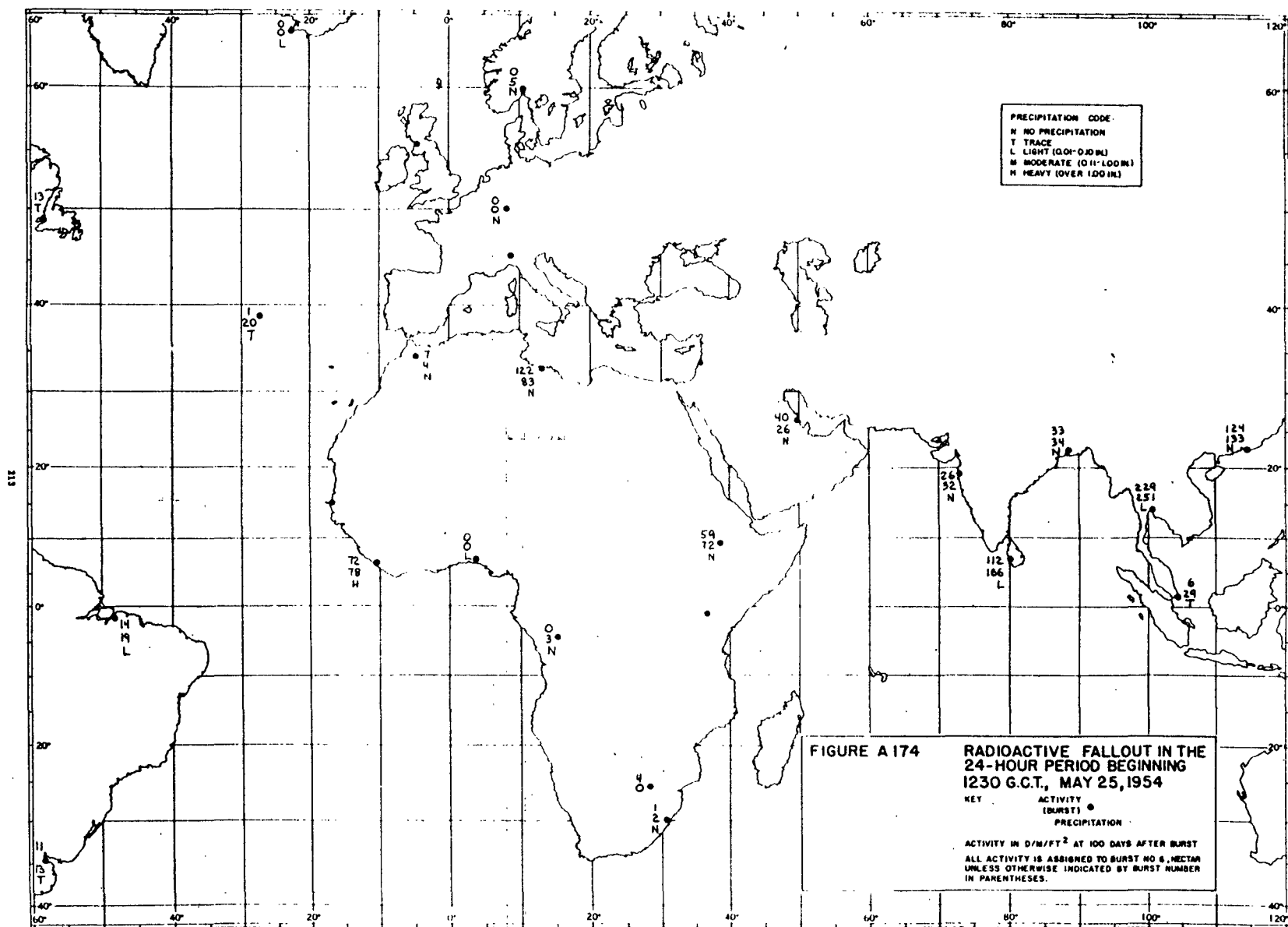












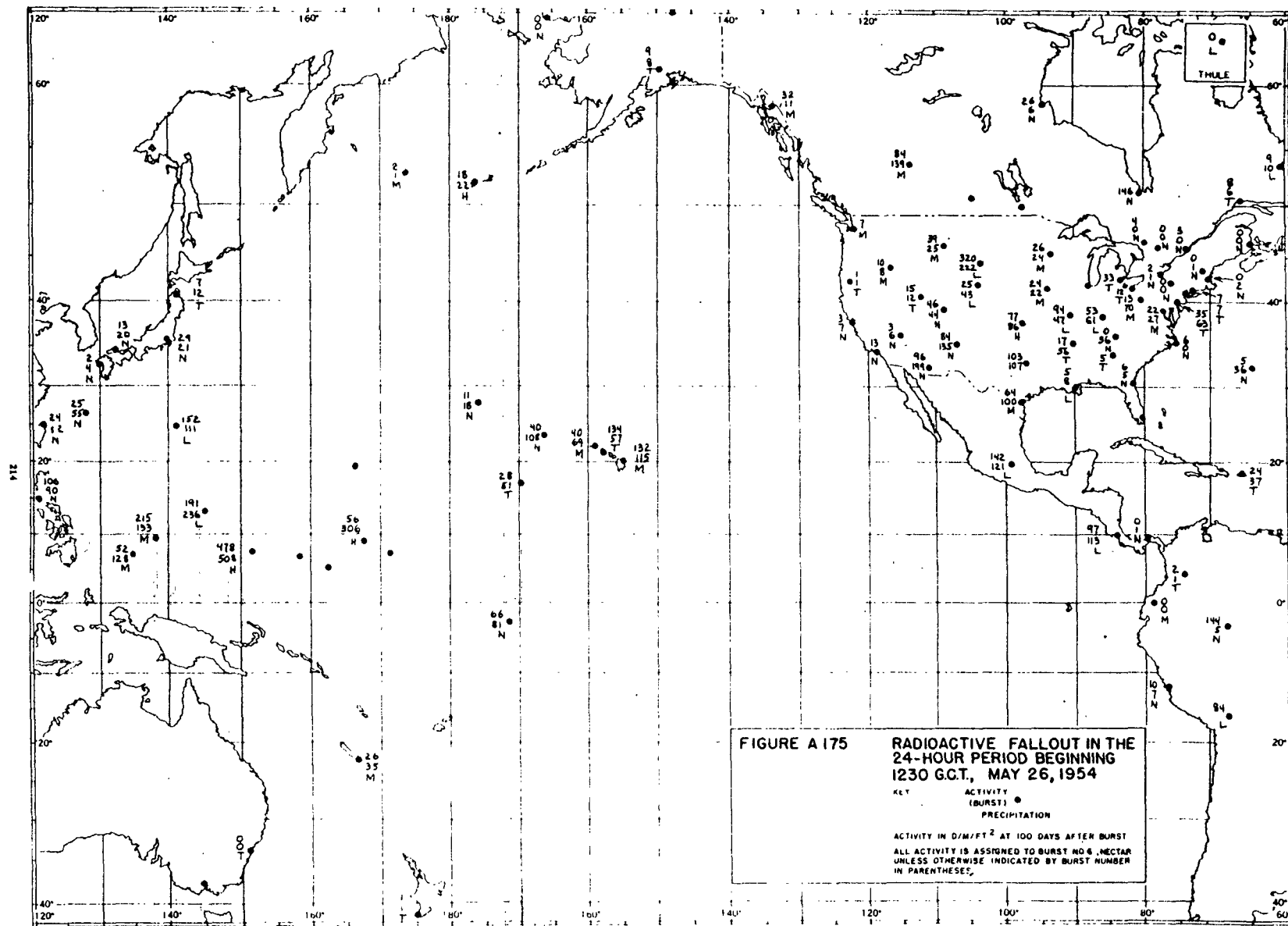
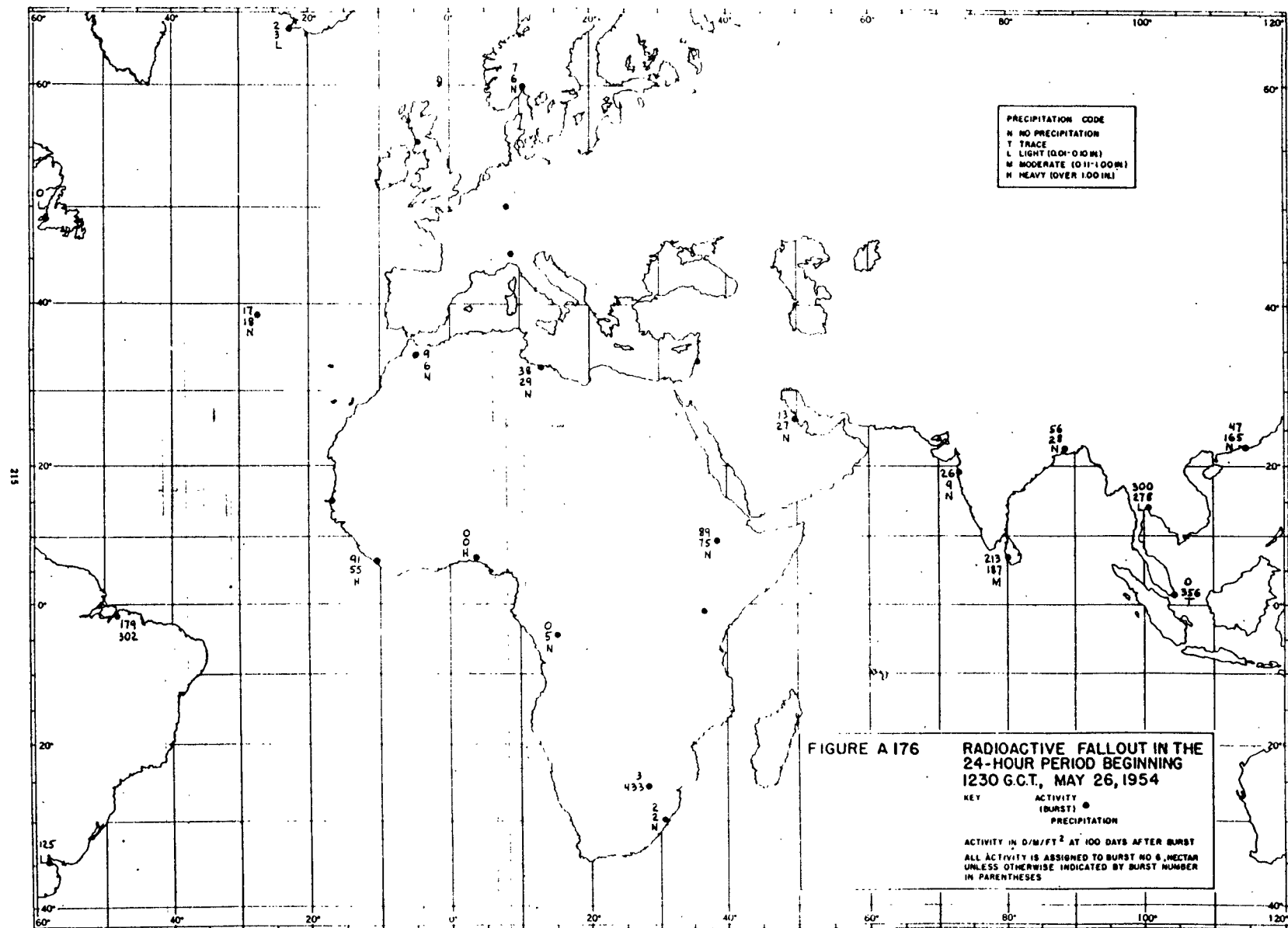
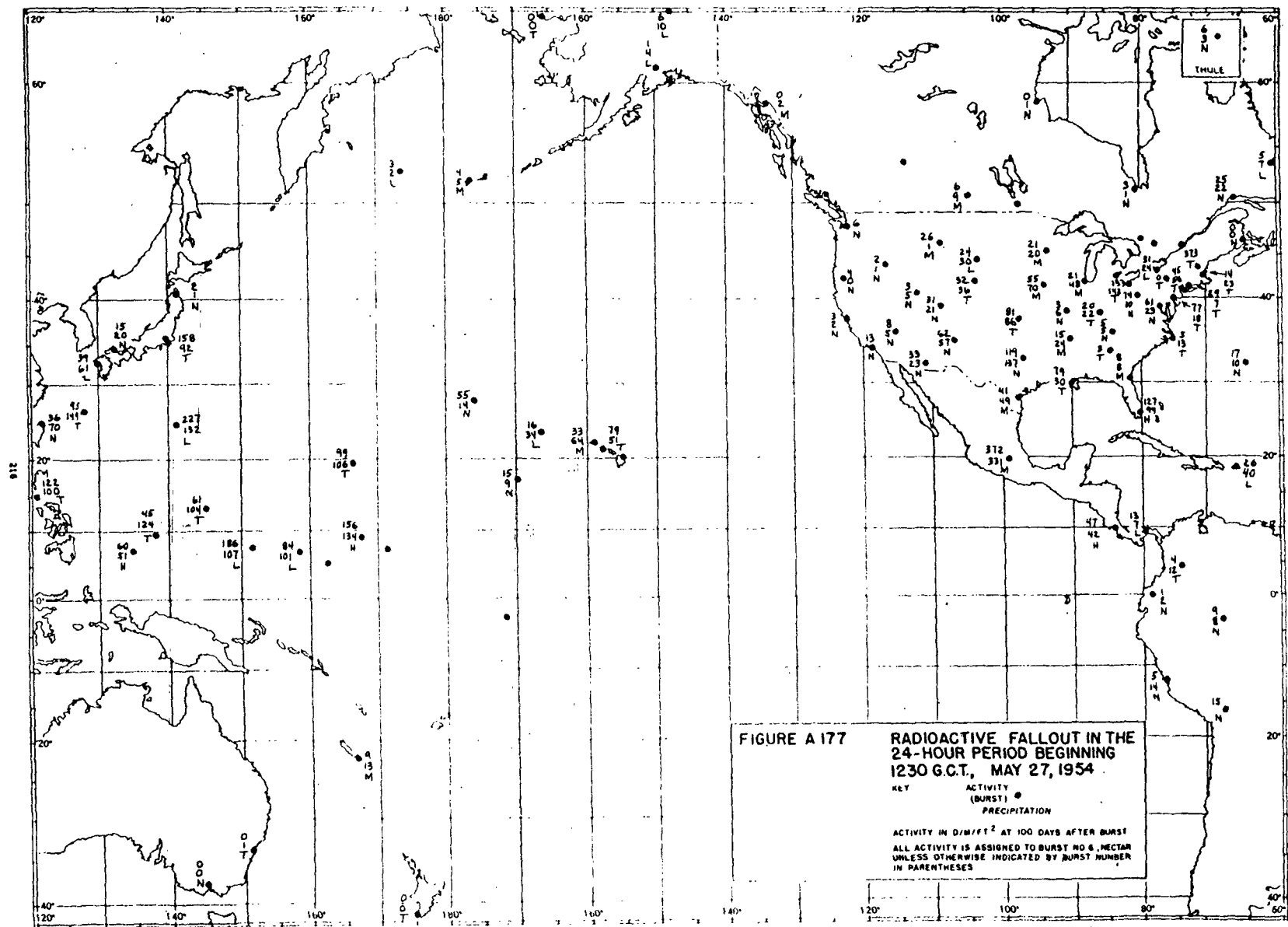
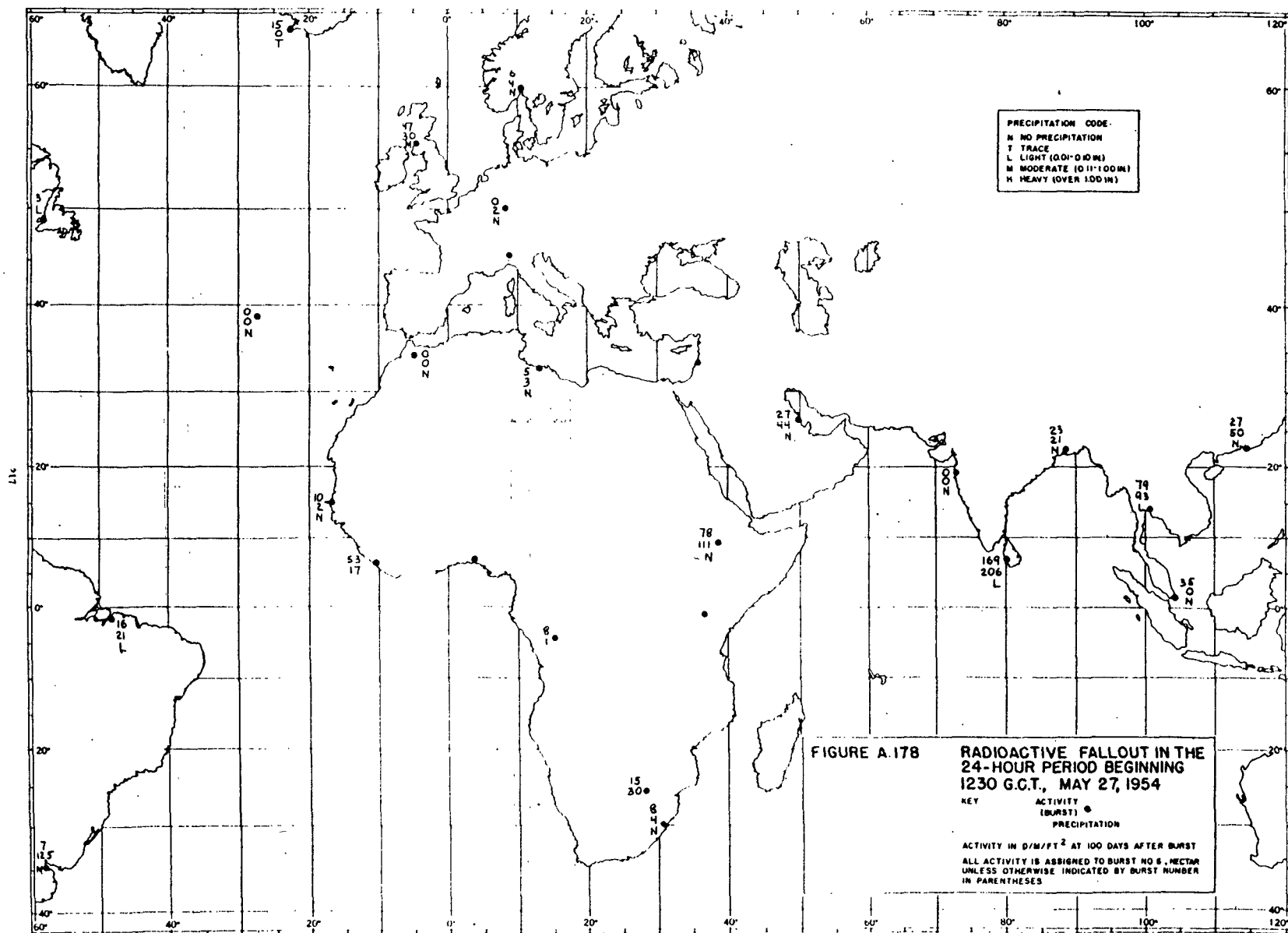


FIGURE A 175 **RADIOACTIVE FALLOUT IN THE
24-HOUR PERIOD BEGINNING
1230 G.C.T., MAY 26, 1954**







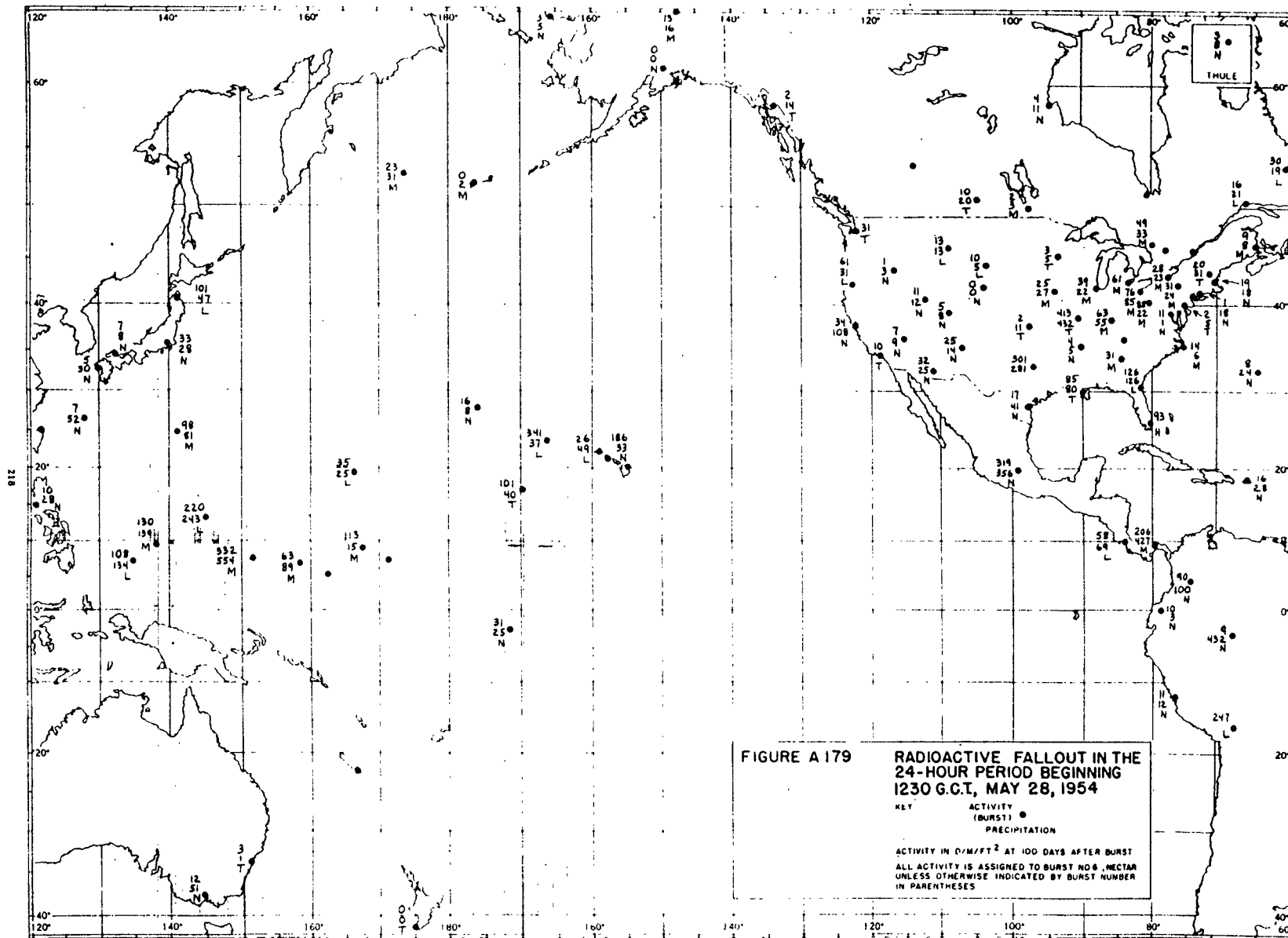
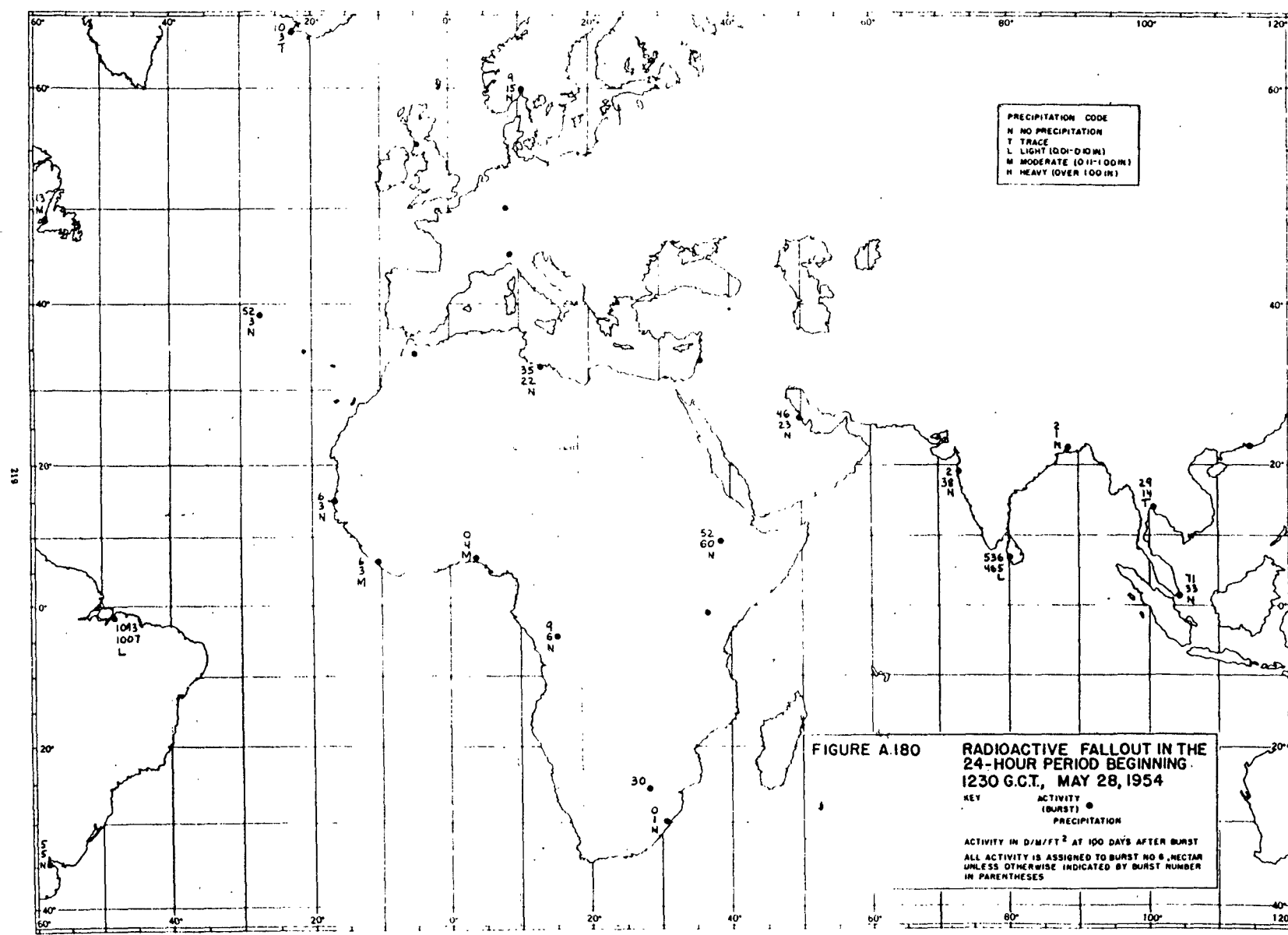


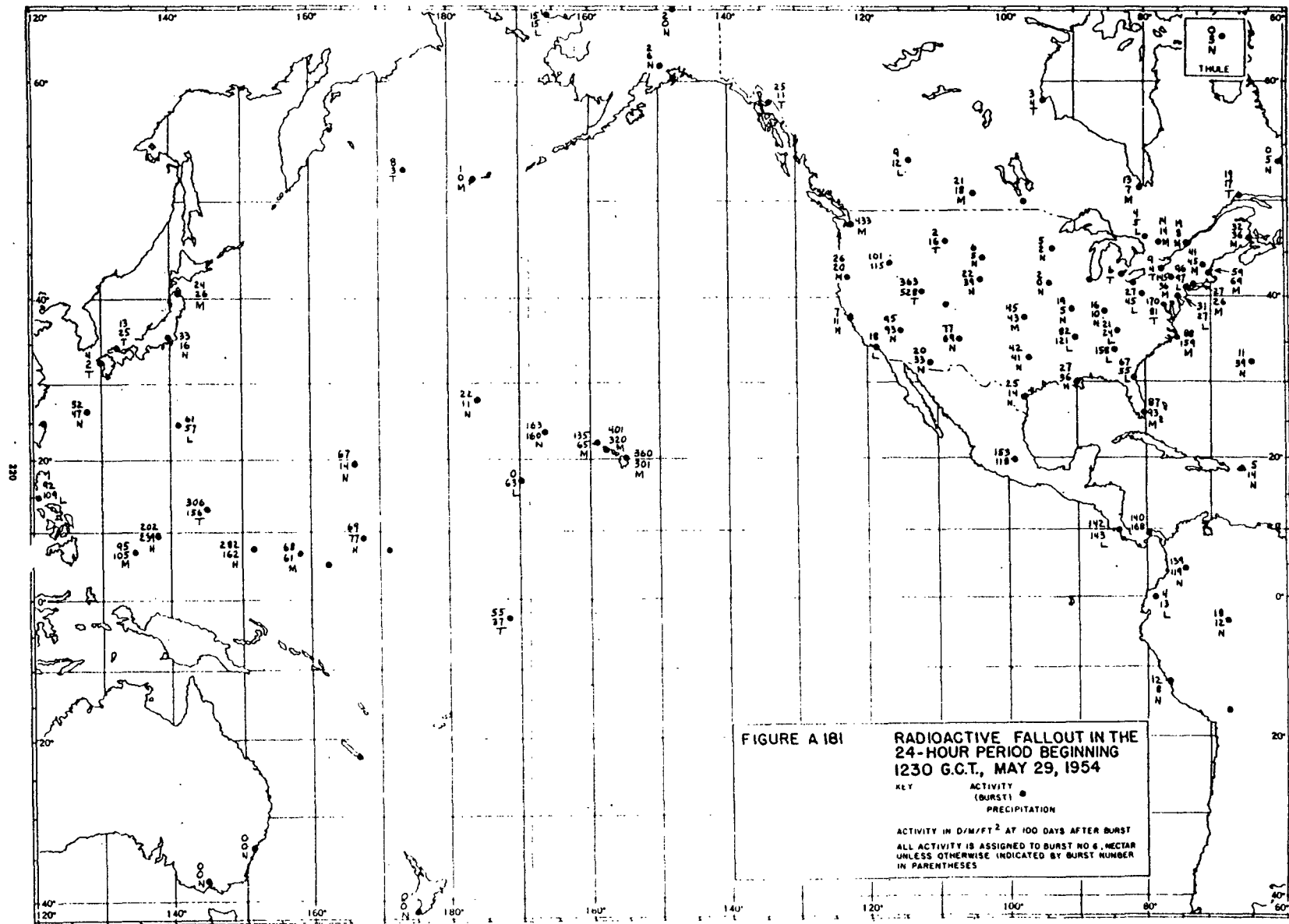
FIGURE A179

RADIOACTIVE FALLOUT IN THE
24-HOUR PERIOD BEGINNING
1230 G.C.T., MAY 28, 1954

KEY ACTIVITY
(BURST) ●
 PRECIPITATION

ACTIVITY IN $\mu\text{R}/\text{FT}^2$ AT 100 DAYS AFTER BURST
ALL ACTIVITY IS ASSIGNED TO BURST NO. 6, NECTAR
UNLESS OTHERWISE INDICATED BY BURST NUMBER
IN PARENTHESES





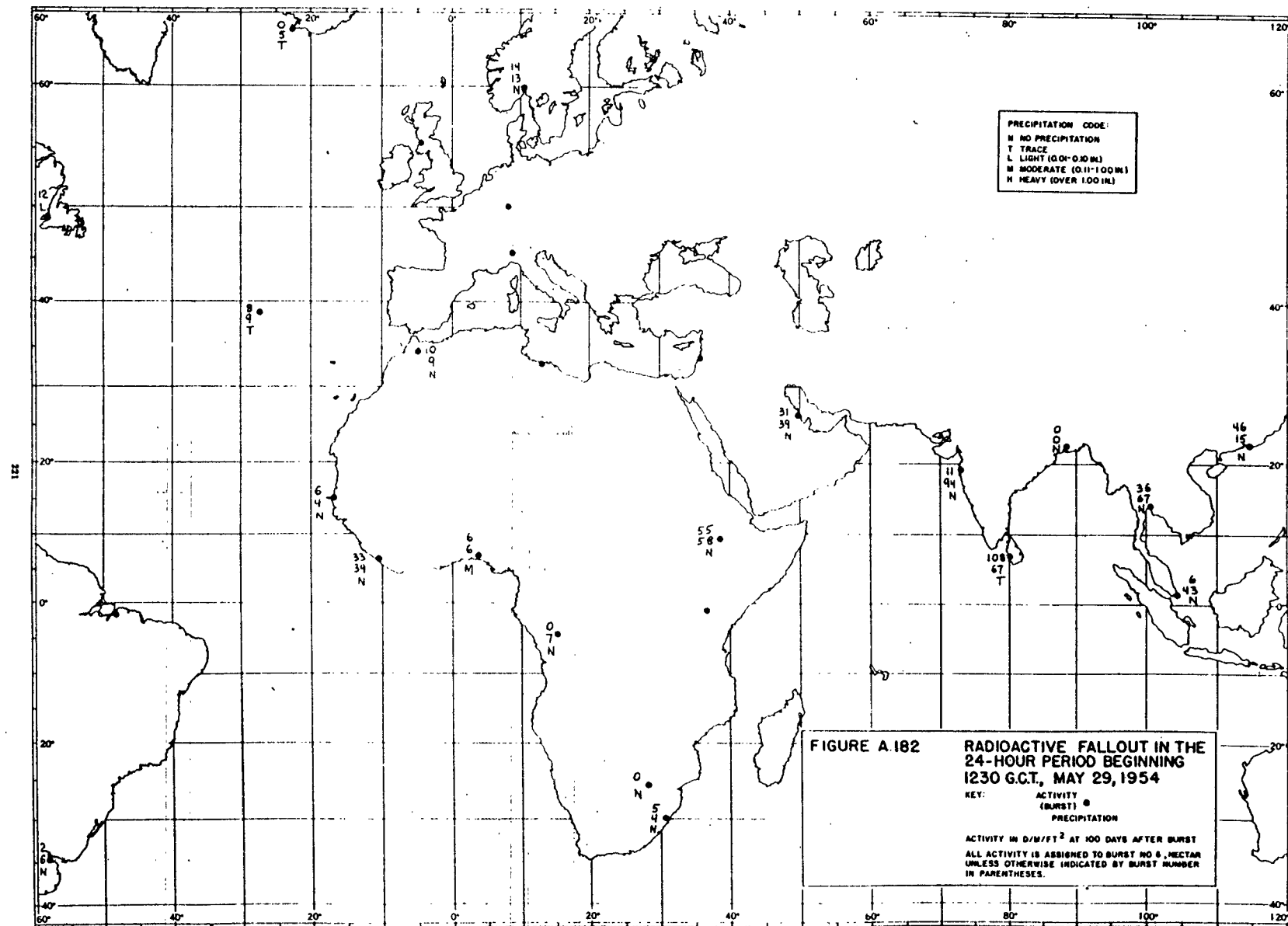
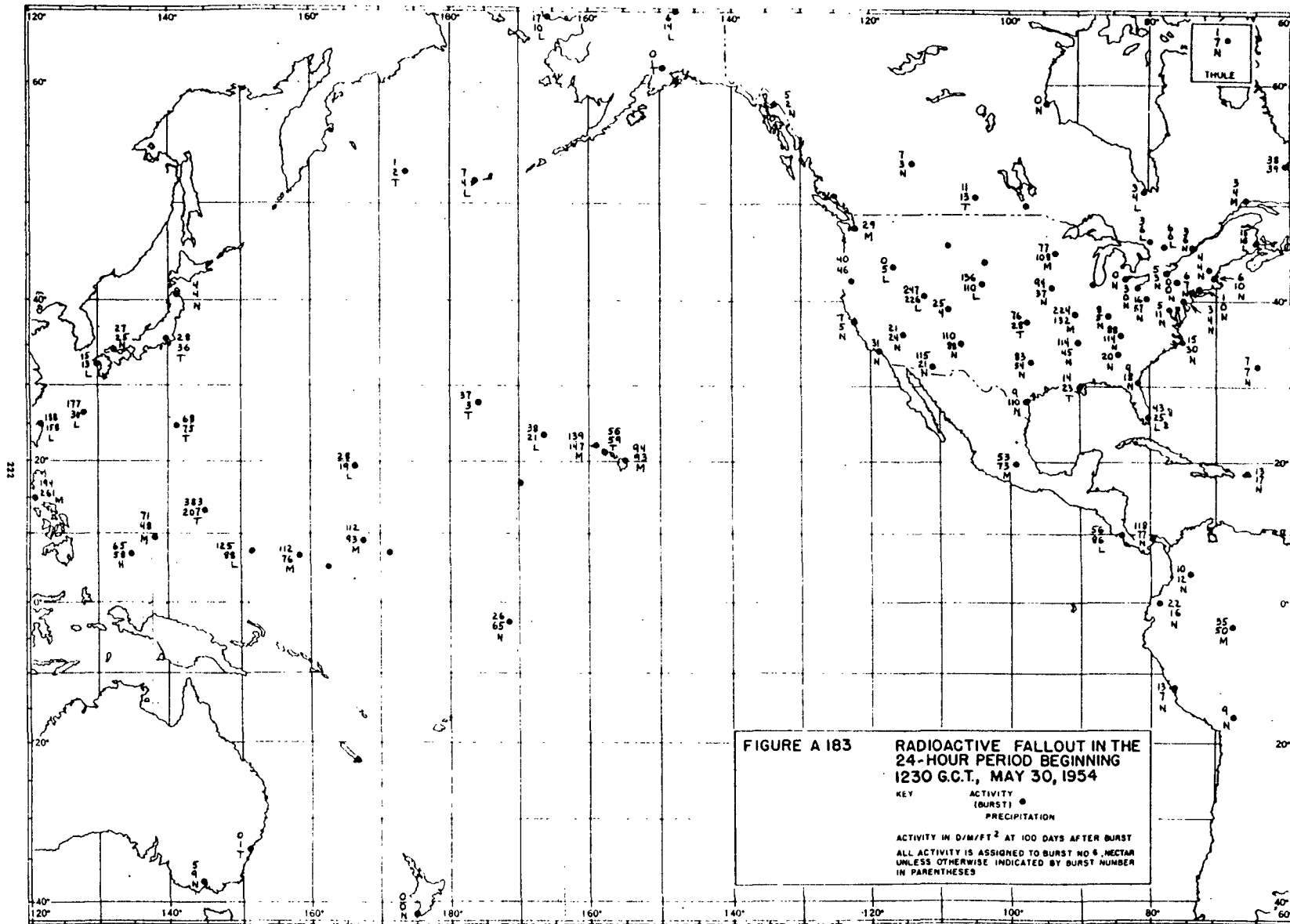
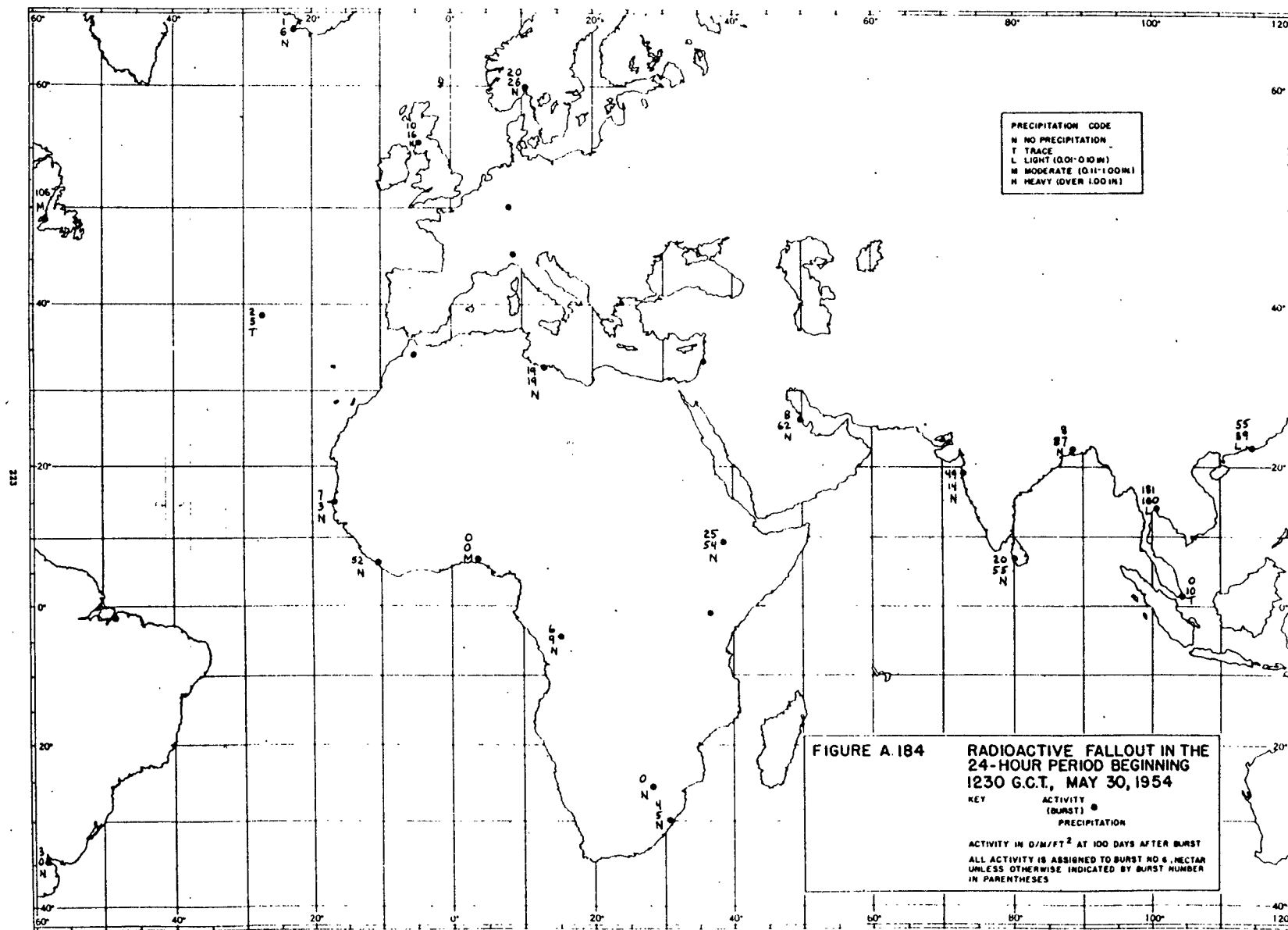
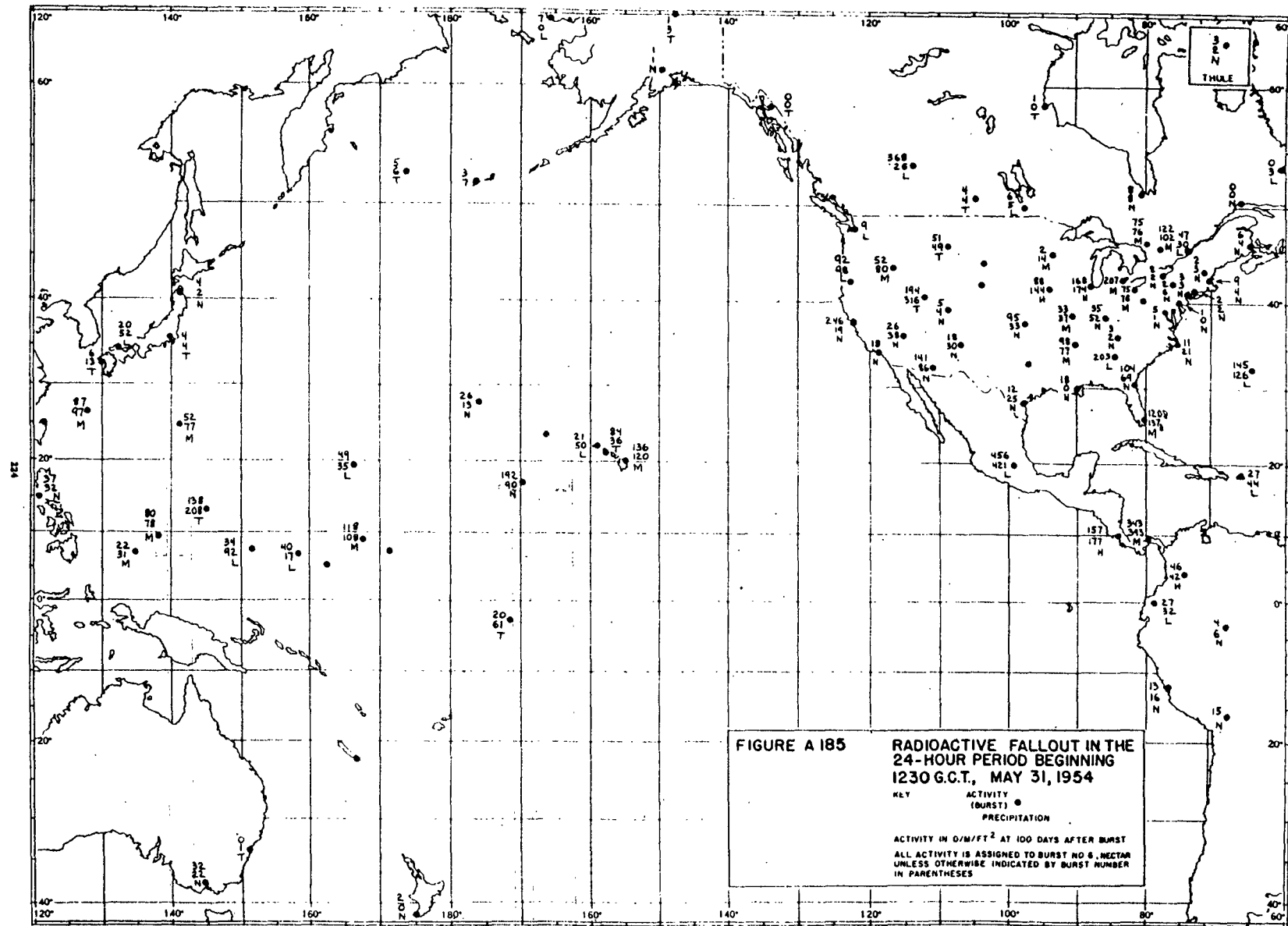
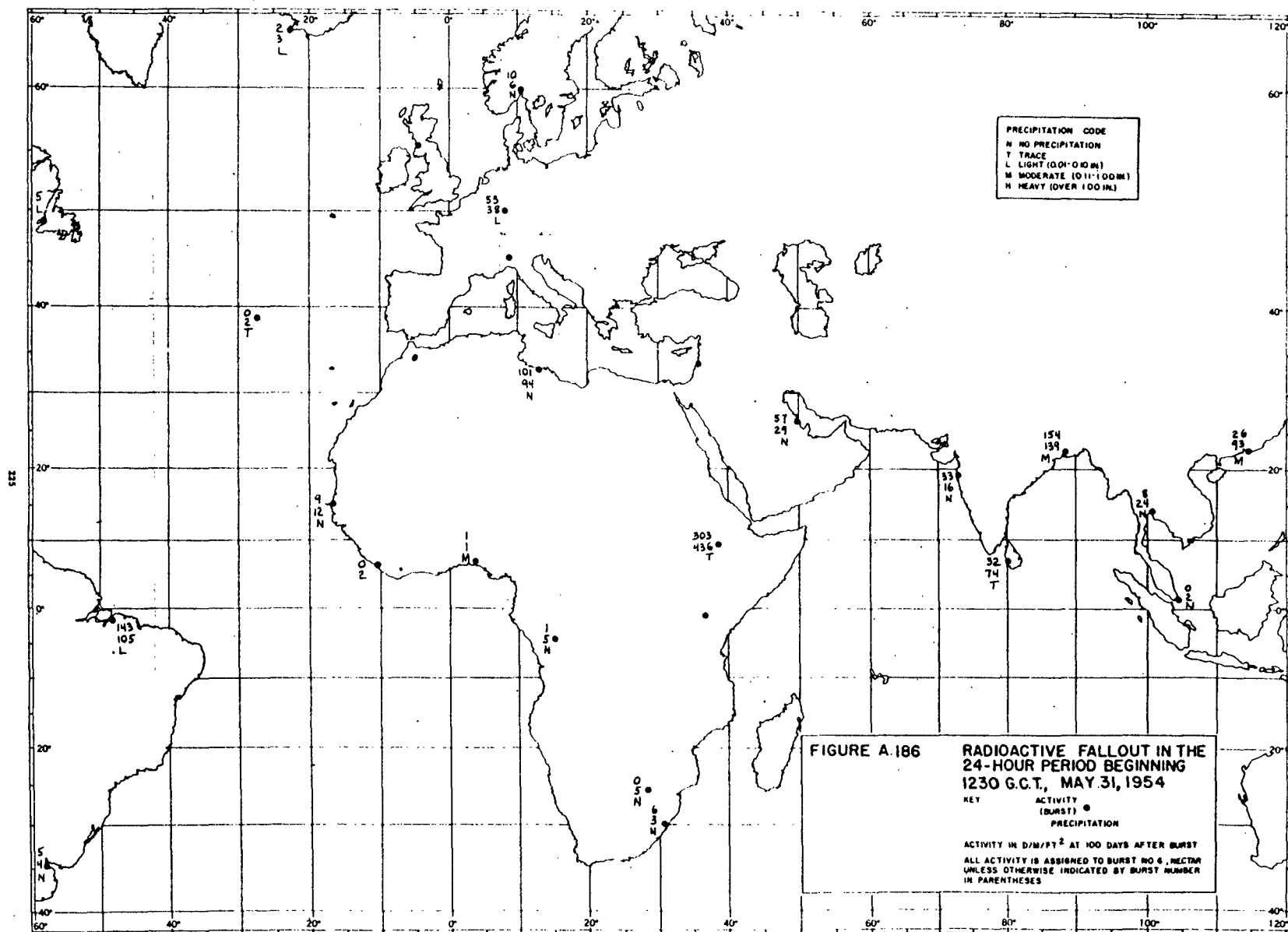


FIGURE A.182 **RADIOACTIVE FALLOUT IN THE
24-HOUR PERIOD BEGINNING
1230 G.C.T., MAY 29, 1954**









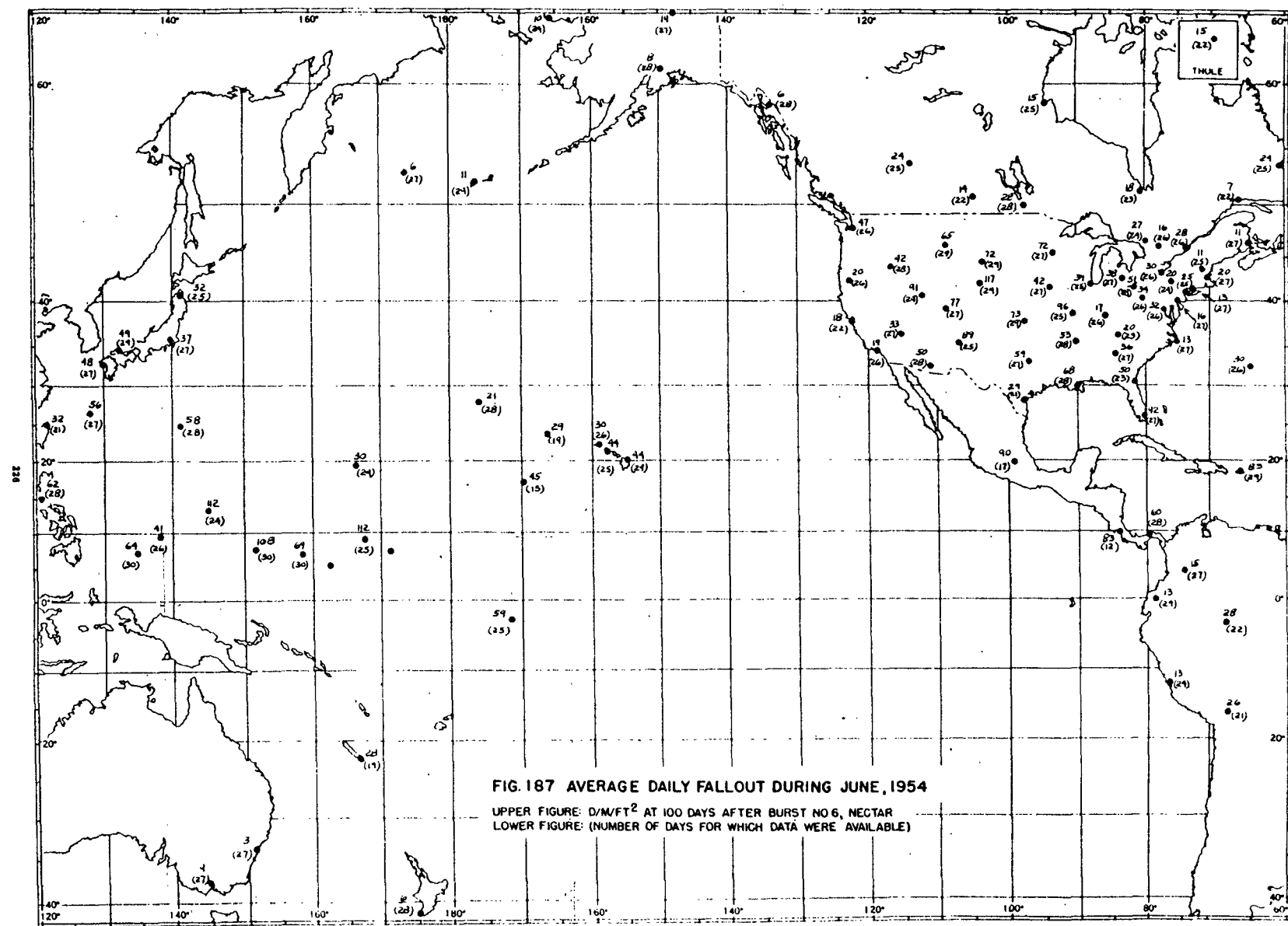
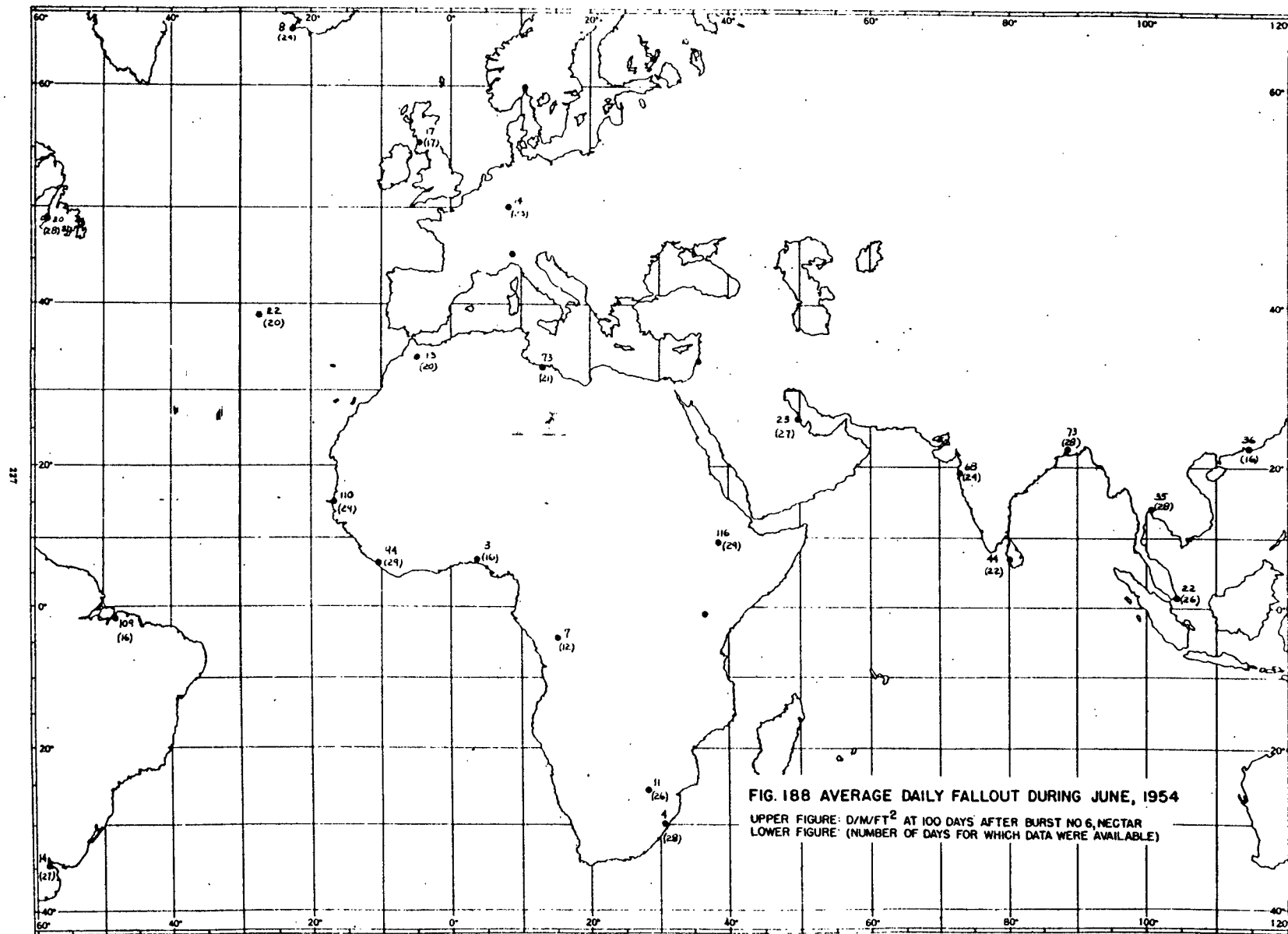


FIG. 187 AVERAGE DAILY FALLOUT DURING JUNE, 1954

UPPER FIGURE: D/M²/FT² AT 100 DAYS AFTER BURST NO 6, NECTAR
LOWER FIGURE: (NUMBER OF DAYS FOR WHICH DATA WERE AVAILABLE)



REFERENCES

1. List, R. J., Radioactive Debris From Operations Tumbler and Snapper, Part II. AEC, NYO-4512, February 25, 1953, (SECRET).
2. Hubert, L. F., et al, A Meteorological Analysis of the Transport of Debris from Operation Ivy, AEC, NYO-4555, October 30, 1953, (SECRET).
3. List, R. J., The Transport of Atomic Debris From Operation Upshot-Knothole, AEC, NYO-4602, June 25, 1954, (SECRET).
4. Los Alamos Scientific Laboratory, The Effects of Atomic Weapons, Washington, June 1950.